

<https://doi.org/10.15388/vu.thesis.799>

<https://orcid.org/0009-0001-7516-5307>

VILNIUS UNIVERSITY

Viktorija Preitakaite

# Exploration of Anticancer Compounds and Enzyme-Prodrug Systems

**DOCTORAL DISSERTATION**

Natural Sciences,  
Biochemistry (N 004)

VILNIUS 2025

The dissertation was prepared between 2020 and 2024 at the Department of Molecular Microbiology and Biotechnology, Institute of Biochemistry, Life Sciences Center, Vilnius University.

The research was supported by the Research Council of Lithuania.

**Academic supervisor –**

Prof. Dr. Rolandas Meškys (Vilnius University, Natural Sciences, Biochemistry – N 004).

**Dissertation Defence Panel:**

**Chairman** – Dr. Vytautas Smirnovas (Vilnius University, Natural Sciences, Biochemistry – N 004).

**Members:**

Prof. Dr. Daiva Baltriukienė (Vilnius University, Natural Sciences, Biochemistry – N 004),

Dr. Violeta Jonušienė (Vilnius University, Natural Sciences, Biochemistry – N 004),

Prof. Dr. Saulius Serva (Vilnius University, Natural Sciences, Biochemistry – N 004),

Dr. Ilma Tapio (Natural Resources Institute, Finland, Natural Sciences, Biochemistry – N 004).

The dissertation shall be defended at a public meeting of the Dissertation Defence Panel at 13:00 on 27 August 2025 in Room R401 of the Vilnius University Life Sciences Center.

Address: Saulėtekio Ave. 7, Vilnius, Lithuania

Tel. +37069667803; e-mail: viktorija.preitakaite@gmc.vu.lt

The text of this dissertation can be accessed at the library of Vilnius University, as well as on the website of Vilnius University:

[www.vu.lt/lt/naujienos/ivykiu-kalendorius](http://www.vu.lt/lt/naujienos/ivykiu-kalendorius)

<https://doi.org/10.15388/vu.thesis.799>

<https://orcid.org/0009-0001-7516-5307>

VILNIAUS UNIVERSITETAS

Viktorija Preitakaitė

# Priešvėžinių junginių ir fermento- provaisto sistemų tyrimas

**DAKTARO DISERTACIJA**

Gamtos mokslai,  
Biochemija (N 004)

VILNIUS 2025

Disertacija rengta 2020–2024 metais Vilniaus universiteto Gyvybės mokslų centro Biochemijos instituto Molekulinės mikrobiologijos ir biotechnologijos skyriuje.

Mokslinius tyrimus rėmė Lietuvos mokslo taryba.

**Mokslinis vadovas** – prof. dr. Rolandas Meškys (Vilniaus universitetas, gamtos mokslai, biochemija – N 004).

Gynimo taryba:

**Pirmininkas** – dr. Vytautas Smirnovas (Vilniaus universitetas, gamtos mokslai, biochemija – N 004).

**Nariai:**

prof. dr. Daiva Baltriukienė (Vilniaus universitetas, gamtos mokslai, biochemija – N 004),

dr. Violeta Jonušienė (Vilniaus universitetas, gamtos mokslai, biochemija – N 004),

prof. dr. Saulius Serva (Vilniaus universitetas, gamtos mokslai, biochemija – N 004),

dr. Ilma Tapio (Gamtos išteklių institutas, Suomija, gamtos mokslai, biochemija – N 004).

Disertacija ginama viešame Gynimo tarybos posėdyje 2025 m. rugpjūčio mėn. 27 d. 13:00 val. Vilniaus universiteto Gyvybės mokslų centro R401 auditorijoje. Adresas: Saulėtekio al. 7, R401, Vilnius, Lietuva, tel. +37069667803; el. paštas: viktorija.preitakaite@gmc.vu.lt

Disertaciją galima peržiūrėti Vilniaus universiteto bibliotekoje ir Vilniaus universiteto interneto svetainėje adresu: <https://www.vu.lt/naujienos/ivykiu-kalendorius>



## CONTENTS

ABBREVIATIONS.....	8
INTRODUCTION.....	11
SCIENTIFIC NOVELTY.....	12
MAJOR FINDINGS PRESENTED FOR DEFENCE OF THIS THESIS ...	14
1. LITERATURE OVERVIEW .....	15
1.1. Anticancer potential of indirubins.....	15
1.1.1. Medicinal value of indirubin and its derivatives .....	15
1.1.2. Molecular mechanisms underlying the anticancer activity of indirubins .....	16
1.2. Gene-directed enzyme prodrug therapy .....	20
1.2.1. Basic principles of GDEPT .....	20
1.2.2. The most extensively studied enzyme-prodrug strategies.....	22
1.2.3. Bystander effect .....	32
1.2.4. GDEPT delivery systems .....	33
1.2.5. Concluding remarks .....	40
1.3. Hydrolases and their applications .....	40
1.3.1. Introduction to hydrolases.....	41
1.3.2. Hydrolases in prodrug activation .....	41
1.3.3. Future perspectives of hydrolases in prodrug therapy .....	48
2. MATERIALS AND METHODS .....	50
2.1. Materials.....	50
2.1.1. Reagents .....	50
2.1.2. Nucleic acids .....	50
2.1.3. Bacteria.....	50
2.1.4. Cell lines.....	51
2.1.5. Plasmids .....	51
2.1.6. PCR primers .....	53
2.1.7. Recombinant proteins.....	55

2.1.8. Bacterial media.....	55
2.2. Methods.....	55
2.2.1. Bacterial growth conditions.....	55
2.2.2. Cell culturing.....	55
2.2.3. DNA manipulations.....	56
2.2.4. <i>E. coli</i> competent cell preparation and transformation.....	56
2.2.5. Overexpression of the recombinant 6×His-tagged proteins .....	57
2.2.6. Purification of 6×His-tagged proteins .....	57
2.2.7. SDS-PAGE.....	58
2.2.8. Enzymatic activity measurements and analysis of reaction mixtures	58
2.2.9. Generation of cell lines.....	59
2.2.10. Expression analysis of mRNA .....	60
2.2.11. Whole-cell extract preparation and Western blot analysis .....	60
2.2.12. Proteomic analysis.....	61
2.2.13. MTT assay.....	64
2.2.14. Statistical analysis .....	65
3. RESULTS.....	66
3.1. Screening of potential anticancer drug and prodrug candidates .....	66
3.1.1. Effects of water-soluble asymmetric indirubin carboxylic acids on cancer cell viability .....	66
3.1.2. Selection of cell lines potentially suitable for therapy .....	71
3.1.3. Effects of modified nucleosides and nucleobases on cancer cell viability .....	73
3.2. YqfB and D8_RL amidohydrolases as prodrug activating enzymes .	84
3.2.1. <i>In vitro</i> screening of potential prodrugs for YqfB and D8_RL amidohydrolases.....	85
3.2.2. Generation of stable cell lines expressing bacterial amidohydrolases	86
3.2.3. Hydrolysis of prodrugs in eukaryotic cells by YqfB and D8_RL enzymes.....	88
3.2.4. Effect of hydrolysis products derived from the complex prodrug 5-fluoro- <i>N</i> <sup>4</sup> -[3-indolepropionyl]cytidine on the viability of HCT116 cells.....	90

3.3. Cytidine deaminases CDA_EH, CDA_F14, and CDA_Lsp as prodrug activating enzymes .....	92
3.3.1. CDAs target various modified fluorinated pyrimidine nucleosides...	92
3.3.2. Bacterial CDA_Lsp activates $N^4$ -acyl-5-fluorocytidines in cancer cell lines .....	94
3.3.3. Bacterial CDA_EH, CDA_F14, and CDA_Lsp activate $S^4/O^4/N^4$ -substituted 5-fluoropyrimidines in cancer cell lines.....	97
3.3.4. Human-optimized versions of CDA_EH, CDA_F14, and CDA_Lsp provide improved activation of modified 5-fluoropyrimidines in cancer cells .....	99
3.3.5. CDA_Lsp activates $N^4/O^4$ -substituted fluorinated nucleosides in U87MG human glioblastoma cell line .....	103
4. DISCUSSION.....	105
CONCLUSIONS.....	112
REFERENCES.....	113
SUPPLEMENT .....	135
SANTRAUKA .....	152
ACKNOWLEDGEMENTS .....	179
LIST OF PUBLICATIONS.....	180
PATENT APPLICATIONS AND PATENTS .....	181
CONFERENCE PRESENTATIONS.....	181
CURRICULUM VITAE .....	183
NOTES.....	189

## ABBREVIATIONS

3BrPyrA	3-bromopyruvic acid
5FaCyd	5-fluoro- <i>N</i> <sup>4</sup> -acetylcytidine
5FbCyd	5-fluoro- <i>N</i> <sup>4</sup> -benzoylcytidine
5FC	5-fluorocytosine
5FCyd	5-fluorocytidine
5FCyd-C2	5-fluoro- <i>N</i> <sup>4</sup> -(C2-benzoyl-benzoyl)cytidine
5FCyd-C3	5-fluoro- <i>N</i> <sup>4</sup> -(C3-benzoyl-benzoyl)cytidine
5FCyd-C4	5-fluoro- <i>N</i> <sup>4</sup> -(C4-benzoyl-benzoyl)cytidine
5FdCyd	5-fluoro-2'-deoxycytidine
5FdCyd-Hex	5-fluoro- <i>N</i> <sup>4</sup> -hexanoyl-2'-deoxycytidine
5FiC	5-fluoroisocytosine
5FipCyd	5-fluoro- <i>N</i> <sup>4</sup> -[3-indolepropionyl]cytidine
5FpCyd	5-fluoro- <i>N</i> <sup>4</sup> -pivaloylcytidine
5FpiC	5-fluoro- <i>N</i> <sup>2</sup> -pivaloylisocytosine
5FU	5-fluorouracil
5FUDR	5-fluoro-2'-deoxyuridine
5FUDR-Mo	5-fluoro-4-(4-morpholinyl)-2'-deoxyuridine
5FUR	5-fluorouridine
5FUR-2isopr	5-fluoro-4-(2-isopropyl-5-methylphenoxy)-uridine
5FUR-5isopr	5-fluoro-4-(5-isopropyl-2-methylphenoxy)-uridine
5FUR-benz	5-fluoro-4-benzyloxyuridine
5FUR-but	5-fluoro-4-butoxyuridine
5FUR-buthio	5-fluoro-4-butylthiouridine
5FUR-eth	5-fluoro-4-ethoxyuridine
5FUR-eththio	5-fluoro-4-ethylthiouridine
5FUR-hexthio	5-fluoro-4-hexylthiouridine
5FUR-isobuthio	5-fluoro-4-isobutylthiouridine
5FUR-meth	5-fluoro-4-methoxyuridine
5FUR-meththio	5-fluoro-4-methylthiouridine
5FUR-octthio	5-fluoro-4-octylthiouridine
5FUR-phe	5-fluoro-4-phenoxyuridine
6BIO	6-bromoindirubin-3'-oxime
6MP	6-mercaptopurine
AAV	adeno-associated virus
ABC	ammonium bicarbonate
ADEPT	antibody-directed enzyme prodrug therapy
Amp	ampicillin
AP	alkaline phosphatase

CB1954	5-aziridiny1-2,4-dinitrobenzamide
CD	cytosine deaminase
CDA	cytidine deaminase
CDK	cyclin-dependent kinase
CE	carboxylesterase
CYP450	cytochrome P450
CPG2	carboxypeptidase G2
CPT-11	irinotecan
DMEM	Dulbecco's Modified Eagle Medium
DMSO	dimethyl sulfoxide
TMP	deoxythymidine monophosphate
E804	indirubin-3'-(2,3-dihydroxypropyl)-oximether
ECM	extracellular matrix
ESI	electrospray ionization
FAK	focal adhesion kinase
FASP	filter aided protein sample preparation
FBS	fetal bovine serum
FdUMP	fluorodeoxyuridine monophosphate
FdUTP	fluorodeoxyuridine triphosphate
FUTP	fluorouridine triphosphate
GCV	ganciclovir
GDEPT	gene-directed enzyme prodrug therapy
HEK	human embryonic kidney
HEPES	4-(2-hydroxyethyl)-1-piperazineethanesulfonic acid
HIV-1	human immunodeficiency virus type 1
HRP	horseradish peroxidase
HSV-TK	herpes simplex virus thymidine kinase
I3M	indirubin-3'-monoxime
IPTG	isopropyl $\beta$ -D-1-thiogalactopyranoside
ITRs	inverted terminal repeats
Kan	kanamycin
Kbp	kilobase pair
LB	lysogeny broth
MAPK	mitogen-activated protein kinase
MMP	matrix metalloproteinase
MSCs	mesenchymal stem cells
MTT	3-(4,5-dimethyl-2-thiazolyl)-2,5-diphenyl-2-H-tetrazolium bromide
MTX	methotrexate
NMR	nuclear magnetic resonance

Opti-MEM	reduced serum medium
PA	penicillin amidase
PBS	phosphate-buffered saline
PDAC	pancreatic ductal adenocarcinoma cells
PEI	polyethylenimine
PGA	penicillin G amidase
PNP	purine nucleoside phosphorylase
PSA	prostate-specific antigen
SDS-PAGE	sodium dodecyl sulfate–polyacrylamide gel electrophoresis
SOB	super optimal broth
SOC	super optimal broth with catabolite repression
STAT3	signal transducer and activator of transcription 3
TBS	tris-buffered saline
TNF	tumor necrosis factor
TRIS	tris(hydroxymethyl)aminomethane
TS	thymidylate synthase
UHPLC	ultra-high-performance liquid chromatography
UPRT	uracil phosphoribosyltransferase
VSV-G	vesicular stomatitis virus G glycoprotein

## INTRODUCTION

Cancer remains one of the leading causes of death worldwide and continues to pose a significant threat to human health. While existing treatments – such as chemotherapy, radiotherapy, and surgery – have advanced significantly, their long-term efficacy is often limited by drug resistance and systemic toxicity [1]. These limitations underscore the urgent need for novel anticancer agents with greater effectiveness and selectivity. Among the emerging candidates, indirubin and its derivatives have attracted considerable attention due to their promising anticancer properties. Despite its potential, indirubin's clinical use is restricted by poor water solubility, suboptimal pharmacokinetics, and limited therapeutic efficacy [2]. Various indirubin derivatives have been synthesized to address these limitations, exhibiting improved anticancer activity and more favorable drug-like characteristics [3]. Ongoing research into developing novel indirubin-based compounds may lead to more effective and selective therapeutic options for cancer treatment.

Targeted drug delivery and activation strategies are gaining interest in enhancing anticancer compounds' selectivity and therapeutic index. One such promising approach is gene-directed enzyme prodrug therapy (GDEPT). GDEPT utilizes a transgene that encodes an enzyme capable of converting a non-toxic prodrug into an active therapeutic metabolite, affecting cancer cells' viability [4]. GDEPT has several clear advantages over traditional cancer therapies: the active cytotoxic drug is produced only in the tumor tissue, which not only increases the success of the therapy but also induces fewer side effects; also, the prodrug can be administered many times with the same effect while the prodrug activating enzyme is still localized in the tumor, thus achieving complete death of the cancer cells [5]. Furthermore, the utilization of an exogenous enzyme offers the significant advantage of using a prodrug unrecognizable to human enzymes, thereby reducing off-target activity while maximizing toxicity in the tumor environment [6]. To date, several enzyme-prodrug combinations have been developed and shown to have great potential in both pre-clinical studies and early clinical trials, but none of them has reached the clinic due to several drawbacks [7]. Many strategies are hampered by the low specificity of the enzymes for the target prodrugs, high affinity for other natural substrates, limited prodrug uptake, poor pharmacokinetics, and activation of prodrugs by non-target enzymes [8,9]. The development of new enzyme-prodrug combinations with specific and precise effects is essential to bring GDEPT to the clinic.

One promising variant of enzymes that could be applied to GDEPT is hydrolases. These are a large class of enzymes that, in simple terms, catalyze the hydrolysis of chemical bonds in biomolecules by utilizing water as a hydroxyl group donor [10]. Due to their high stereo- and regioselectivity, hydrolases have a wide range of bio-applications in chemical synthesis, the food and cosmetic industry [11,12]. Meanwhile, this thesis focuses on demonstrating that hydrolases have the potential to be used for therapeutic purposes. Previously, the YqfB [13] and D8\_RL [14] proteins were described as small amidohydrolases active towards *N*<sup>4</sup>-acylated cytidines. In addition, CDA\_EH, CDA\_F14, and CDA\_Lsp enzymes were identified as cytidine deaminases active towards *S*<sup>4</sup>-/*N*<sup>4</sup>-/*O*<sup>4</sup>-modified pyrimidine nucleosides [15]. These enzymes offer some significant advantages, such as a broad spectrum of synthetic substrates, high catalytic activity, small size, and many others, which are usually highlighted in the development of therapeutic tools, making them a promising target for research.

The aim of this thesis was to develop and investigate novel anticancer compounds, with a particular focus on creating an enzyme toolbox for the activation of fluoropyrimidine-based prodrugs. To this end, the following objectives were undertaken:

1. To identify indirubin derivatives with cytotoxic activity against cancer cell lines.
2. To evaluate the potential of modified 5-fluoropyrimidine nucleosides as prodrugs for enzyme-prodrug therapy.
3. To investigate the applicability of YqfB and D8\_RL amidohydrolases in the activation of fluoropyrimidine-based prodrugs.
4. To assess the ability of cytidine deaminases CDA\_EH, CDA\_F14, and CDA\_Lsp to activate fluoropyrimidine prodrugs.

## SCIENTIFIC NOVELTY

Despite significant progress in cancer treatment, the effectiveness of current therapies remains limited by drug resistance and systemic toxicity, highlighting the need for novel anticancer agents with improved efficacy and selectivity. Indirubin and its derivatives have emerged as promising candidates due to their notable anticancer properties; however, poor water solubility has hindered their clinical application [2]. This thesis evaluated the potential toxicity of highly water-soluble monocarboxyindirubin derivatives, newly synthesized by our research group, to assess their suitability for further development. Several compounds exhibiting cytotoxic effects on cancer cells



were identified, expanding the current understanding of indirubin derivatives and highlighting their potential for therapeutic application. In parallel, prodrug technology has long been explored as a promising strategy for targeted cancer therapy. Although significant progress has been made in this field, prodrug technology still faces many drawbacks, such as limited prodrug uptake, poor pharmacokinetics, non-specific activation, and several others that limit their *in vivo* application [9]. In this thesis, a wide collection of modified 5-fluoropyrimidines was proposed as potential prodrugs. These compounds were offered in combination with enzymes capable of specifically activating them, increasing the likelihood of their application in further studies. Although several prodrugs based on the chemotherapeutic drug 5-fluorouracil are known [16], the modifications presented in this thesis were not previously demonstrated. It is known from previous studies that various amidohydrolases, due to their physicochemical properties, are attractive objects in many fields and have potential applications in food and pharmaceutical industries as well as in biotechnology [17–19]. In this work, it was demonstrated that amidohydrolases have the potential to be applied in GDEPT and used for therapeutic purposes. Previously, two small amidohydrolases, YqfB and D8\_RL, were identified with activity towards *N*<sup>4</sup>-acylcytidines [13,14]. This thesis showed that YqfB and D8\_RL can also catalyze the conversion of *N*<sup>4</sup>-acylated 5-fluorocytidines, resulting in the anticancer agent 5-fluorocytidine. Four novel synthetic compounds were suggested as suitable for the enzymatic hydrolysis mediated by YqfB and D8\_RL. Also, CDA\_EH, CDA\_F14, and CDA\_Lsp enzymes were identified previously as cytidine deaminases active towards *S*<sup>4</sup>-/*N*<sup>4</sup>-/*O*<sup>4</sup>-modified pyrimidine nucleosides [15]. In this thesis, it was demonstrated that CDA\_EH, CDA\_F14, and CDA\_Lsp can also activate *N*<sup>4</sup>-acyl/alkyl-5-fluorocytidines, 4-alkylthio-5-fluorouridines, 4-alkoxy-5-fluoro- and 4-alkoxy-5-fluoro-2'-deoxyuridines, resulting in the formation of the anticancer agents 5-fluorouridine or 5-fluoro-2'-deoxyuridine. Several novel prodrugs not described elsewhere were suggested as suitable candidates for activation by CDA\_EH, CDA\_F14, and CDA\_Lsp enzymes. Taken together, the results allowed us to propose several different enzyme-prodrug combinations based on five hydrolases and several variants of 5-fluoropyrimidine analogs. As none of these enzyme-prodrug strategies have been previously explored, this increases the possibility that at least one of the systems might be suitable for future applications in the clinic.

## MAJOR FINDINGS PRESENTED FOR DEFENCE OF THIS THESIS

1. Indirubin carboxylic acid and 2-indolinone derivatives are promising candidates for developing anticancer drugs.
2. Modified 5-fluoropyrimidine nucleosides show significant potential as prodrug candidates for targeted cancer therapy.
3. Combining YqfB and D8\_RL amidohydrolases with *N*<sup>4</sup>-acylated 5-fluorocytidine derivatives offers a novel enzyme-prodrug system for GDEPT.
4. The cytidine deaminases CDA\_EH, CDA\_F14, and CDA\_Lsp, together with *N*<sup>4</sup>-acyl/alkyl-5-fluorocytidines, 4-alkylthio-5-fluorouridines, 4-alkoxy-5-fluoro- and 4-alkoxy-5-fluoro-2'-deoxyuridines, have potential for application in enzyme-prodrug therapy.

## 1. LITERATURE OVERVIEW

### 1.1. Anticancer potential of indirubins

Cancer has emerged as one of the most significant threats to human life and health and is currently recognized as a leading cause of death worldwide. Despite advancements in treatment approaches such as chemotherapy, surgery, radiotherapy, and biotherapy, the persistent challenge of drug resistance remains a primary global concern [1]. Therefore, developing novel anticancer agents with improved efficacy and reduced toxicity is urgently needed. One promising group of such compounds is indirubin and its derivatives, whose therapeutic potential and anticancer mechanisms are discussed below.

#### 1.1.1. Medicinal value of indirubin and its derivatives

Indirubin (Fig. 1.1) is a purplish-red bisindole alkaloid recognized as the main bioactive component in several Traditional Chinese Medicine formulations, which have been employed for centuries in China, especially for treating chronic myelocytic leukemia [20]. Indirubin and its derivatives can be found in various natural sources, including plants [21], marine mollusks [22], bacteria [23], and human urine [24]. Recent studies have expanded the pharmacological profile of indirubin, revealing a broad spectrum of bioactivities beyond its anticancer properties. These include antipsoriatic [25], anti-Alzheimer's [26], anti-autoimmune [27], anti-inflammatory [28], and anti-influenza [29] effects.

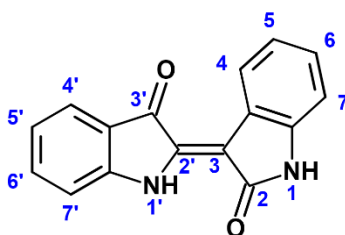


**Figure 1.1.** Structural formula and atom numbering of indirubin.

The crystal structure of indirubin was first characterized in the early 1960s, revealing one intramolecular hydrogen bond between the 2-C=O and N1-H groups, along with an intermolecular hydrogen bond between molecules. These interactions contribute to indirubin's physicochemical properties, including a highly planar structure, low solubility, and high melting point [2].

Although indirubin has been explored as an anticancer agent, its clinical potential has been limited by low water solubility, poor pharmacokinetics, and relatively low therapeutic efficacy. Various chemically modified indirubin derivatives have been developed to overcome these limitations, exhibiting enhanced anticancer activity and improved drug-like characteristics [3,30]. Consequently, indirubin-based compounds have emerged as promising candidates for developing novel anticancer therapies.

### 1.1.2. Molecular mechanisms underlying the anticancer activity of indirubins

Numerous studies have demonstrated that indirubin and its derivatives possess significant anticancer properties. These compounds inhibit cancer cell proliferation, induce apoptosis, suppress tumor angiogenesis, and cancer cell migration and invasion. Figure 1.2 illustrates the potential anticancer pathways of indirubins, several of which are discussed in more detail below.

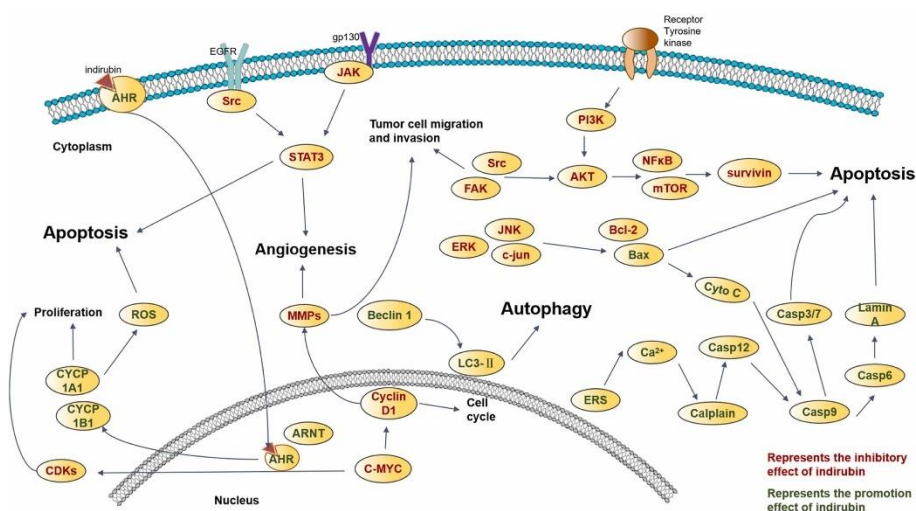


**Figure 1.2.** Schematic representation of key pathways involved in the anticancer mechanisms of indirubin and its derivatives [31].

### Inhibition of tumor cell proliferation

Cyclin-dependent kinases (CDKs) are a family of proteins that regulate cell cycle progression through cyclin activation. Dysregulation of CDK activity is a hallmark of many cancers, often driven by elevated cyclin levels, which lead to CDK overactivation and consequently, uncontrolled tumor cell proliferation [32,33]. Indirubin has been shown to inhibit the activity of

CDK1/cyclin B, CDK2/cyclin A, and CDK2/cyclin E in starfish oocytes [34]. It also reduces the expression of cyclin D1, a protein regulated by the NF- $\kappa$ B pathway and stimulated by tumor necrosis factor (TNF), leading to suppressed proliferation of KBM-5 chronic myeloid leukemia cells [35]. Compared to indirubin, its derivatives exhibit enhanced antiproliferative properties. For instance, indirubin-3'-monoxime (I3M) suppresses CDK2 expression, induces G2/M arrest in several cancer cell lines (including MCF-7, L1210, K-562, HL-60, and Jurkat), and effectively inhibits tumor cell proliferation [34]. I3M also inhibits MCF-7 cell growth by disrupting CDK1/cyclin B interactions and inducing cell cycle arrest at both G1/M and G2/S phases [36]. Furthermore, derivatives such as 5-nitro-5'-hydroxy-indirubin-3'-oxime and 5-nitro-5'-fluoro-indirubin-3'-oxime demonstrate strong CDK2 selectivity across multiple cancer cell lines, contributing to their potent antiproliferative activity [37].

C-MYC is a nuclear protein critical in promoting cell proliferation, dedifferentiation, transformation, and immortalization, thereby contributing significantly to tumor development [38]. Indirubin has been shown to inhibit C-MYC expression in prostate cancer PC-3 cells, potentially through modulation of the Wnt signaling pathway, leading to reduced cell proliferation [39]. Moreover, indirubin significantly downregulates C-MYC and cyclin D1 expression in human ovarian cancer cells. This antiproliferative effect appears to be associated with suppressing signal transducer and activator of transcription 3 (STAT3) phosphorylation [40].

Indirubin induces mitotic arrest in HeLa cells by disrupting the mitotic spindle [41]. It also enhances arsenic disulfide's antiproliferative and pro-apoptotic effects in diffuse large B-cell lymphoma cells [42]. I3M inhibits the proliferation of acute myeloid leukemia cells by downregulating the expression of the tyrosine kinase FGFR1 and suppresses fibroblast proliferation by inhibiting FGFR1 phosphorylation [43]. Additionally, I3M and 6-bromoindirubin-3'-oxime (6BIO) significantly reduce proliferation and induce cell death in various malignant lymphoid cell types, with 6BIO exhibiting particularly strong cytotoxic and antiproliferative effects [44].

### **Induction of tumor cell apoptosis**

STAT3 is an oncogenic transcription factor closely associated with cancer progression. Its activation occurs through phosphorylation, typically mediated by JAK and Src kinases [45]. Indirubin has been shown to dose-dependently inhibit STAT3 phosphorylation and promote apoptosis in human ovarian

cancer cells [40]. Additionally, indirubin derivatives demonstrate strong inhibitory activity on STAT3 signaling. For instance, indirubin-3'-(2,3-dihydroxypropyl)-oximether (E804) suppresses STAT3 activity in both breast cancer and glioblastoma cells by inhibiting the phosphorylation of JAK1, Src, and STAT3 [46,47]. Similarly, 6BIO interferes with the phosphorylation of JAKs, Src, and STAT3 in several human cancer cell types, contributing to decreased cell viability [48].

The PI3K/AKT/mTOR signaling pathway is frequently dysregulated in malignant tumors, playing a central role in promoting tumor development by modulating the activity of multiple downstream targets. This pathway is strongly associated with cancer cell proliferation, apoptosis resistance, survival, and migration [49]. Recent studies have highlighted the involvement of this signaling cascade in indirubin derivative-induced apoptosis. For instance, combining I3M and thymoquinone inhibits proliferation and migration while promoting apoptosis in A549 human non-small-cell lung cancer cells, accompanied by decreased levels of p-AKT, p-mTOR, p53, and NF- $\kappa$ B [50]. 6BIO has also been shown to suppress AKT phosphorylation and induce apoptosis in melanoma cells [51]. Additionally, I3M inhibits AKT phosphorylation and triggers apoptosis in pancreatic ductal adenocarcinoma (PDAC) cell lines [52].

Mitogen-activated protein kinases (MAPKs) are a group of serine/threonine kinases that play essential roles in regulating cell proliferation and apoptosis. The four major MAPK subfamilies – ERK, JNK, p38 MAPK, and ERK5 – can contribute to tumor progression and metastasis when abnormally activated, by promoting uncontrolled growth, apoptosis resistance, and invasiveness [53]. Several indirubin derivatives exert pro-apoptotic effects by modulating MAPK signaling pathways. I3M modulates phosphorylation of RAF/ERK, SAPK/JNK, and c-Jun, and downregulates caspase-3, -6, and -8 expression in PDAC cells [52]. I3M also suppresses ERK1/2 phosphorylation in myeloid leukemia cells and inhibits NIH/3T3 cell proliferation via the ERK1/2 and p38MAPK signaling pathways [43]. In melanoma cells, 6BIO modulates ERK1/2 phosphorylation, further contributing to apoptosis induction [51].

Bcl-2 family proteins are key regulators of apoptosis that act directly or indirectly on mitochondria. This family includes antiapoptotic proteins (e.g., Bcl-2, Bcl-XL, Mcl-1) and proapoptotic proteins (e.g., Bax, Bak, Bim). Their expression and regulation play a crucial role in controlling tumor cell apoptosis [54]. Indirubin induces apoptosis in human ovarian cancer cells by

downregulating Bcl-XL and upregulating Bax and caspase-3 [40]. In chronic myeloid leukemia cells, it promotes apoptosis by suppressing NF- $\kappa$ B-dependent expression of Survivin, Bcl-2, Bcl-XL, and TRAF1 [35]. The derivative E804 further enhances proapoptotic effects by reducing Mcl-1 levels in breast cancer and glioma cells and decreasing Bcl-XL expression in glioma cells [46,47].

### **Inhibition of tumor cell invasion and migration**

Matrix metalloproteinases (MMPs) are a family of proteases that degrade extracellular matrix components, disrupt tissue barriers, and facilitate tumor cell migration and invasion [55]. Indirubin suppresses the expression of MMP-9 and COX-2 in KBM-5 myeloid leukemia cells, thereby inhibiting cell invasion [35]. The derivative I3M reduces MMP-2 and MMP-9 levels in osteosarcoma cells, limiting their metastatic potential, and also downregulates MMP-2, MMP-7, and MMP-9 in PDAC cells to inhibit invasion [52,56]. Furthermore, 6BIO inhibits colorectal cancer cell migration and invasion by decreasing MMP-9 expression and increasing E-cadherin levels [57].

Focal adhesion kinase (FAK) is a central mediator of integrin-driven signaling pathways that facilitate tumor cell migration and invasion [58]. In head and neck cancer cells, the indirubin derivative 5'-nitro-indirubinoxime suppresses the integrin  $\beta$ 1/FAK/AKT pathway, inhibiting cell invasion, migration, VEGF expression, and tumor angiogenesis [59]. Similarly, I3M downregulates FAK expression and reduces the invasive potential of osteosarcoma cells [56].

### **Inhibition of angiogenesis**

In recent years, increasing attention has been given to the anti-angiogenic effects of indirubin and its derivatives. In tumor-derived endothelial cells, indirubin reduces the expression of angiogenesis-related markers TEM1 and TEM8, thereby inhibiting tumor angiogenesis [60]. It also suppresses VEGFR2 phosphorylation and disrupts the JAK/STAT3 signaling pathway, which collectively impairs endothelial cell migration, angiogenesis, and tube formation [61]. The indirubin derivative E804 blocks VEGF/VEGFR2 signaling in endothelial cells and inhibits STAT3 phosphorylation and Src activity, leading to anti-angiogenic effects [62]. Similarly, 5'-nitro-indirubinoxime downregulates VEGF expression and inhibits angiogenesis in head and neck cancer cells [59]. Additionally, I3M has been shown to downregulate VEGFR2 expression and significantly reduce microvessel density in newly forming vasculature [63].

## **Future perspectives on indirubin and its derivatives**

Indirubin and its derivatives have demonstrated antitumor activity against various malignancies, including leukemia, colorectal cancer, breast cancer, melanoma, glioma, and osteosarcoma. Their anticancer effects are primarily attributed to the inhibition of tumor cell proliferation, invasion, migration, and angiogenesis, as well as the induction of apoptosis. Nevertheless, concerns remain regarding their potential cytotoxicity to normal cells, sometimes exceeding that observed in tumor cells [64]. This observation highlights limitations in selectivity and suggests the involvement of complex and not yet fully characterized regulatory mechanisms. Therefore, further experimental studies are essential to clarify their mechanisms of action, assess safety profiles, and evaluate toxicity. Continued efforts in designing and synthesizing novel indirubin derivatives may help overcome current limitations and lead to more effective and selective anticancer agents.

### **1.2. Gene-directed enzyme prodrug therapy**

Gene-directed enzyme prodrug therapy (GDEPT) is an emerging strategy for cancer treatment based on the delivery of a gene that encodes an enzyme that is able to convert a prodrug into a potent cytotoxin exclusively in target cancer cells. More than 20 years of development later, several GDEPT systems have entered clinical trials. However, no GDEPT system has reached the market, which shows there are still challenges to overcome before GDEPT can be applied in the clinic. This literature review discusses the basics of the GDEPT strategy, examples of the most successful GDEPTs, the advantages and disadvantages of this therapeutic option, and several related issues, which will give an overall impression of where GDEPT currently stands and what is still lacking in the way of a full realization of this therapy.

#### **1.2.1. Basic principles of GDEPT**

Over the last few years, cancer therapy has increasingly focused on targeted approaches to maximize the effectiveness of treatment and minimize side effects. One such targeted strategy is gene-directed enzyme prodrug therapy, also known as suicide gene therapy. Although the concept of GDEPT has been around for more than 30 years, the clinical application of GDEPT has only become apparent in the last 10 years, when an increasing number of GDEPT systems have been introduced into clinical trials [7].



The simplified mechanism of GDEPT systems for cancer treatment is illustrated in Figure 1.3. GDEPT utilizes a transgene that encodes an enzyme capable of converting a non-toxic prodrug into an active therapeutic metabolite, affecting cancer cells' viability [4]. In this two-step strategy, the gene encoding the non-endogenous enzyme is initially directed toward the tumor tissue. Within the tumor, it undergoes transcription to form mRNA, from which subsequently the therapeutic enzyme is translated inside the cancer cells. This process is then followed by the systemic delivery of the prodrug, which undergoes selective activation into its active drug form only through the action of the foreign enzyme expressed within the cancer cells [6]. This approach relies on precisely targeting cancer cells while sparing healthy tissue. The therapeutic enzyme's gene specifically targets cancer cells using various viral vectors or alternative delivery methods [65,66]. Furthermore, tumor-specific promoters can regulate gene expression, enabling the enzyme and its associated enzymatic reaction to be exclusively targeted at tumor cells. This ensures that other cells remain unaffected even if they uptake the gene and prodrug [67]. The preferential prodrug conversion can potentially lead to a significantly higher therapeutic index in comparison to conventional cancer chemotherapy drugs.

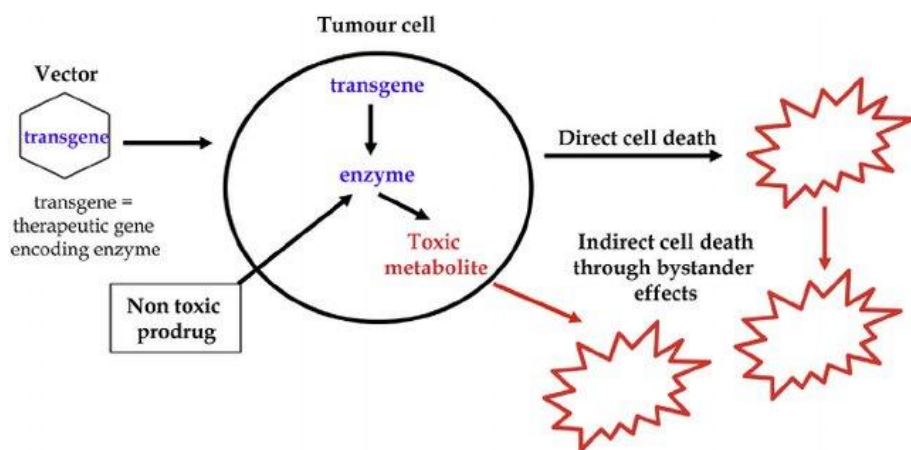


**Figure 1.3.** The principle mechanism of GDEPT systems [68].

The main requirements for GDEPT enzymes include exclusive or relatively high expression in tumor cells compared to healthy cells and high catalytic activity, enabling prodrug conversion even at low concentrations. The most commonly used GDEPT enzymes are of non-mammalian origin and are distinct from all circulating endogenous enzymes. This ensures that the enzyme will act in a targeted manner toward the prodrug used in the system

and not toward other endogenous compounds [69]. However, it should be kept in mind that, compared to mammalian enzymes, they have the disadvantage of being potentially immunogenic. The small size of the gene encoding the target enzyme can also be highlighted as a significant advantage, which allows the use of expression vectors in which the choice of transgene is size-restricted [70].

There are also several essential requirements for GDEPT prodrugs. First of all, prodrugs should be stable under physiological conditions and should be non-toxic or minimally toxic before activation but highly toxic after enzymatic activation [71]. In addition, prodrugs should be efficiently taken up by tumor cells and have a high affinity for the enzyme used in the system and a low affinity for endogenous enzymes [72]. The cytotoxic metabolite of the prodrug should also have a long half-life, which would ensure the efficacy of the therapy even without repeated administration of the prodrug. However, the half-life should not be too long to avoid off-target toxicity through drug diffusion to surrounding regions [70]. Since not all tumor cells carry the enzyme that activates the prodrug, prodrugs are expected to display a bystander effect, whereby the toxic form of the drug spreads from one tumor cell to another [73].

Finally, another important player in GDEPT is a carrier that can deliver the gene encoding the therapeutic enzyme to cancer cells or tumor tissue. The success of GDEPT depends significantly on the ability to safely introduce genetic material and achieve adequate expression of the desired gene product at a therapeutic level in specific cells or tissues [74]. An appropriate vector should have low cytotoxicity, high transfection efficiency, high tissue specificity, and low cost [75]. Many studies have focused on vector optimization and delivery methods, which deserve more attention and will be further discussed later.

#### 1.2.2. The most extensively studied enzyme-prodrug strategies

The literature provides a number of examples of widely studied enzyme-prodrug systems. Several pairs were effective in inducing tumor cell death and inhibiting cancer progression. Strategies that have received the most attention include herpes simplex virus thymidine kinase with ganciclovir, *Escherichia coli* cytosine deaminase with 5-fluorocytosine, cytochrome P450 with oxazaphosphorine, nitroreductase with CB1954, and a few others. The strengths and weaknesses of each system in terms of efficiency and safety are discussed below.

## Herpes simplex virus thymidine kinase/ganciclovir system

Transfection of the herpes simplex virus thymidine kinase (HSV-TK) gene into tumor cells, followed by ganciclovir (GCV) treatment, represents one of the most commonly used gene therapy models. The concept of the therapy relies on a viral thymidine kinase, synthesized through the expression of the inserted HSV-TK gene, converting GCV into GCV monophosphate, which is then converted by cellular kinases into a toxic GCV triphosphate (Fig 1.4). Cancer cell death is caused when GCV triphosphate, analogous to 2'-deoxyguanosine triphosphate, either inhibits DNA polymerase or is inserted into replicating DNA, thus inhibiting chain elongation and causing DNA breaks, ultimately leading to replication failure and apoptosis [76–78]. While human cells also express cytosolic and mitochondrial thymidine kinases, these endogenous enzymes have a much lower capability of converting ganciclovir compared to HSV-TK [79].

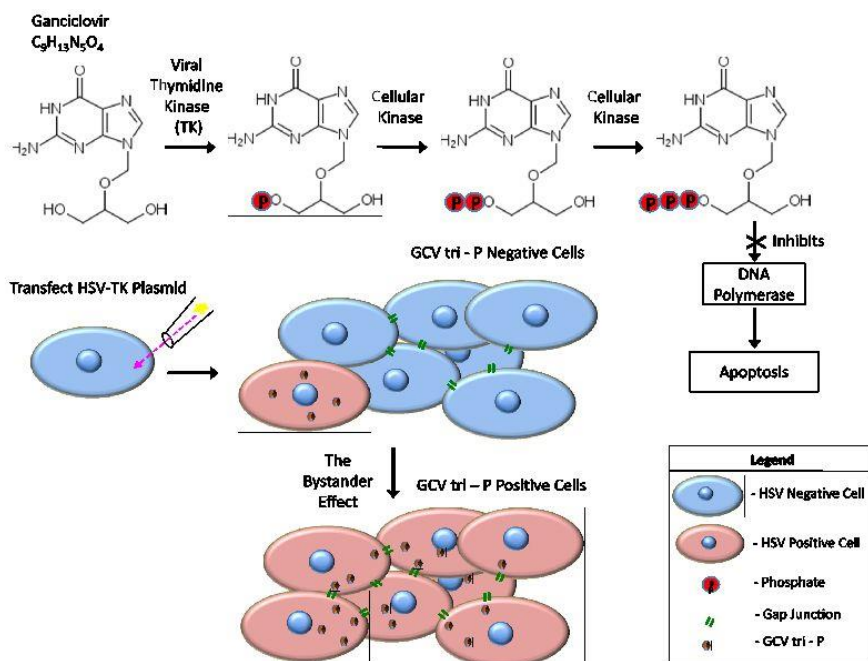


**Figure 1.4.** Conversion of ganciclovir to ganciclovir triphosphate by HSV-TK and cellular kinase [80].

The anticancer activity of the HSV-TK/GCV system has been proved *in vivo* using various animal tumor models, such as leukemia [81], liver cancer [82], glioma [83], bladder cancer [84], and others. The promising results of

preclinical studies have also led to clinical trials against various types of cancer [85–87]. Although encouraging results have been obtained, gene targeting and drug delivery to tumor cells remain challenging. Importantly, these are not the only problems associated with the HSV-TK/GCV strategy. Firstly, GCV-triphosphate, as an anti-tumor agent, can only affect dividing cells, which automatically reduces the system's versatility [88]. Also, GCV has a high diffusibility, limiting its concentration in tumor cells. This drawback can be overcome by increasing the GCV dose, but this is impossible in the clinic as high doses of GCV adversely affect non-target tissues such as bone marrow cells [89]. In addition, the active metabolite of GCV, GCV triphosphate, is membrane insoluble and has low diffusibility, which hinders the passive diffusion of GCV triphosphate into surrounding cells. Therefore, the only transport route for GCV triphosphate is through the gap junction, thereby limiting its bystander effect [90]. In addition, HSV-TK has a high affinity for its natural substrate, thymidine, which again requires a higher dose of GCV. Various attempts have been made to modify the active site of HSV-TK to increase its affinity for GCV, which may allow a lower dose of GCV administration to patients [91].

Due to the drawbacks of GCV, which limit the success of the therapy, other prodrugs are being investigated for possible activation by the HSV-TK. Alternatives showing promising results include acyclovir and valacyclovir. Acyclovir was found to have equal or more significant toxicity on ovarian cancer cell lines and a stronger bystander effect [92]. The L-valyl ester of acyclovir, valacyclovir, showed higher lipophilicity and increased bioavailability, making it possible to administer this prodrug orally [93]. Encouraging results have been obtained with the combination of HSV-TK/valacyclovir with surgery and accelerated radiation in patients with malignant gliomas [94]. On the other hand, HSV-TK/valacyclovir in the treatment of prostate cancer has met with limited success [95]. Nevertheless, the HSV-TK system is still of great interest. Several clinical trials are currently recruiting patients with glioblastoma (NCT03596086, NCT03603405, NCT06102525) and prostate cancer (NCT01913106).

### **Cytosine deaminase/5-fluorocytosine system**

Another well-studied GDEPT strategy combines cytosine deaminase (CD) and 5-fluorocytosine (5FC). The CD is an enzyme found only in bacteria and fungi that catalyzes cytosine deamination to uracil but is also capable of catalyzing the conversion of 5FC to 5-fluorouracil (5FU) [96]. While 5FU has been widely used for cancer chemotherapy, its therapeutic dose causes

significant side effects such as mucositis, dermatitis, and cardiac toxicity [97]. Therefore, interest has been shown in the possibility of using 5FU in the form of the prodrug 5FC, which is less toxic. In this way, the toxicity of 5FU can be directly targeted to CD-expressing cancer cells. Immediately after activation of prodrug 5FC by CD synthesized in cancer cells using the inserted gene, the resulting 5FU is further converted by endogenous enzymes into three main active metabolites: fluorodeoxyuridine monophosphate (FdUMP), fluorodeoxyuridine triphosphate (FdUTP) and fluorouridine triphosphate (FUTP) (Fig 1.5) [98]. FdUMP forms a stable complex with thymidylate synthase (TS) and, therefore, inhibits the production of deoxythymidine monophosphate (dTMP). dTMP is essential for DNA replication and repair, and deficiency of dTMP results in cytotoxicity. In addition, FdUTP and FUTP can be misincorporated into DNA and RNA molecules, respectively, leading to toxic effects [99]. As 5FU can reach neighboring cells independently of gap junctions and even cross the blood-brain barrier by diffusion, it exerts a significant bystander effect [100,101].

Due to its versatility, the CD/5FC system has been investigated for the treatment of various cancer types, such as colon cancer [103], glioma [104], and pancreatic cancer [105]. Also, combining the CD/5FC system with other treatment strategies has demonstrated promising results. One example was the CD/5FC system combined with radiotherapy, which worked synergistically due to the radiosensitising effect of 5FU on the treated cells [106,107]. Several modifications have also been made to the CD/5FC system to increase its therapeutic potential. One of the variations showing positive results was the co-insertion of *E. coli* uracil phosphoribosyltransferase (UPRT) along with CD into cancer cells. UPRT can directly convert 5FU to 5FdUMP, and its combination with CD may lead to stronger therapeutic effects [108,109]. It is also important to note that this strategy can overcome the problem of cellular resistance to 5FU, as it directly produces an active metabolite to which cancer cells usually remain sensitive even in the presence of 5FU resistance [110]. Finally, the CD/5FC system was more effective in many cancer types due to its stronger bystander effect compared to other GDEPT strategies, such as HSV-TK/GCV [111]. On the other hand, better therapeutic efficacy was achieved by combining CD/5FC and HSV-TK/GCV strategies [112].

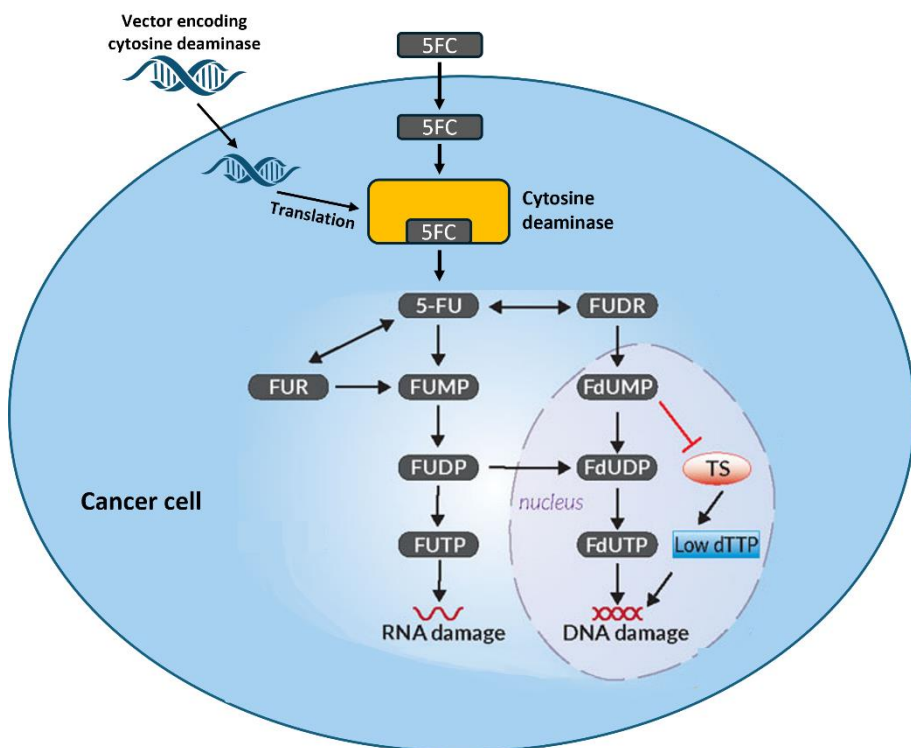


**Figure 1.5.** Schematic representation of the mechanism of action of the cytosine deaminase/5-fluorocytosine system. 5FC – 5-fluorocytosine; 5-FU – 5-fluorouracil; FUR – 5-fluorouridine; FUDR – 5-fluoro-2'-deoxyuridine; FUMP – 5-fluorouridine monophosphate; FUDP – 5-fluorouridine diphosphate; FUTP – 5-fluorouridine triphosphate; FdUMP – 5-fluoro-2'-deoxyuridine monophosphate; FdUDP – 5-fluoro-2'-deoxyuridine diphosphate; FdUTP – 5-fluoro-2'-deoxyuridine triphosphate; TS – thymidylate synthase; dTTP – deoxythymidine triphosphate. Modified according to Delma *et al.*, 2021 [102].

There have been some clinical trials using the CD/5FC system, but all with limited success. This may be due to several shortcomings of the CD/5FC that reduce its therapeutic potential. First, the short half-life of 5FC in the blood reduces the availability of 5FC at the tumor site [113]. Also, wild-type CD has poor activity against 5FC, which limits the overall therapeutic response [103]. This can be addressed by increasing the doses of 5FC, but this leads to undesirable side effects. The systemic toxicity to the body is linked to the normal gut microbiota, where bacteria can also synthesize CDs, converting 5-fluorocytosine to 5-fluorouracil in a non-targeted site, the intestine [8]. To avoid this, a strategy has been developed to use isocytosine deaminase, selected by screening environmental metagenomic libraries, and 5-

fluoroisocytosine to produce 5-fluorouracil. This strategy relies on the basis that the gut microbiota is unlikely to metabolize 5-fluoroisocytosine as extensively as 5FC [114]. Yeast CD has better catalytic properties for the conversion of 5FC compared to bacterial CD, but the application of yeast CD in therapy is limited by the poor thermostability of the enzyme [115]. Several groups have been developing bacterial CD mutants to improve their kinetic properties and yeast CD mutants to improve their stability [115,116]. Although the CD/5FC strategy continuously develops with some encouraging results, there are currently no active clinical trials based on this system.

### Cytochrome P450/oxazaphosphorine system

Cytochrome P450 (CYP450) enzymes are involved in the metabolism of xenobiotics and are responsible for deactivating toxic drugs in the liver. These enzymes can also activate oxazaphosphorine compounds, known as anticancer drugs, of which most studies have been carried out with cyclophosphamide and ifosfamide [117,118]. P450 class enzymes can metabolize these agents to yield 4-hydroxy derivatives followed by conversion to phosphoramidate or ifosfamide mustard and acrolein (Fig 1.6). Such compounds can form DNA cross-links that ultimately lead to cell death. As in the case of 5FU, the uptake of cytotoxic 4-hydroxy metabolites into the surrounding cells is independent of the gap junctions, giving them a strong bystander effect [119]. One of the main advantages of this system is the lower immunogenicity due to the naturally synthesized P450 enzymes in humans [120].

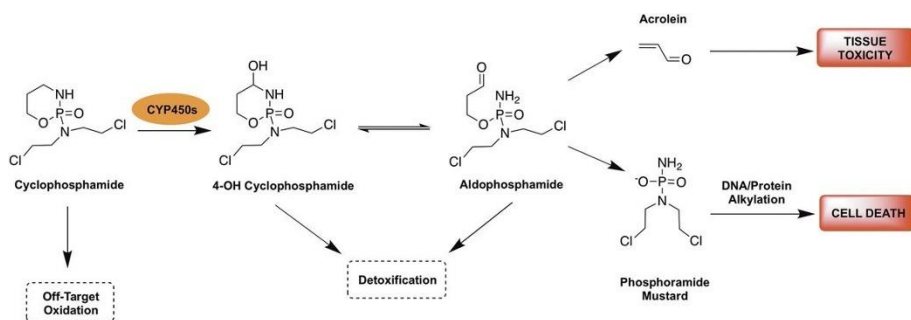


**Figure 1.6.** Schematic representation of cyclophosphamide biotransformation [121].

One of the main drawbacks of the CYP450/oxazaphosphorine system is the natural metabolism of prodrugs by liver P450 enzymes. This results in the formation of active toxic metabolites throughout the body, ultimately causing

various side effects, including cardiotoxicity, neurotoxicity, and nephrotoxicity [122]. Therefore, attempts are being made to inhibit the activity of P450 enzymes in the liver so that the prodrug can be activated only by the enzyme inserted into the cancer cells. One approach has been to use antithyroid drugs such as propylthiouracil and methimazole in parallel with the CYP450/oxazaphosphorine system to inhibit hepatic P450 reductase activity and to improve the activation of the prodrug in the tumor tissue [123]. Several clinical trials were carried out to demonstrate the therapeutic potential of the CYP450/oxazaphosphorine system [119]. However, despite the promising results, there are still serious concerns about the application of this system in cancer therapy, mainly due to the native activity of CYP450 in human cells and the difficulty of delivering the GDEPT elements to cancer cells without side effects on healthy cells [124].

### **Nitroreductase/CB1954 system**

Nitroreductases are flavin-associated oxidoreductases defined by their ability to reduce nitro substituents on aromatic rings. Type I nitroreductases are oxygen insensitive and can generate nitroso, hydroxylamine, and/or amine end-products in the presence of molecular oxygen, whereas type II nitroreductases are oxygen sensitive and can generate these products only in the absence of oxygen [125]. Type I nitroreductases have received the most attention in the GDEPT strategy, as they are predominantly found in bacteria and can catalyze the bioreductive activation of nitroaromatic prodrugs in both oxygenated and hypoxic tumor tissues [6]. Several different classes of prodrugs that nitroreductases could activate have been investigated, including dinitroaziridinybenzamides, dinitrobenzamide mustards, 4-nitrobenzyl carbamates, and nitroindolines. The dinitrobenzamide group prodrug 5-aziridiny-2,4-dinitrobenzamide (CB1954) has been the most successful in the GDEPT strategy for use in combination with nitroreductases [126]. CB1954 metabolites are powerful alkylating agents capable of cross-linking DNA, killing of both dividing and non-dividing tumor cells (Fig 1.7). This gives the strategy a significant advantage over some other GDEPT systems, which tend to target only dividing cells [127]. In addition, the metabolites of this prodrug diffuse easily into the surrounding cells, resulting in a strong bystander effect [128].



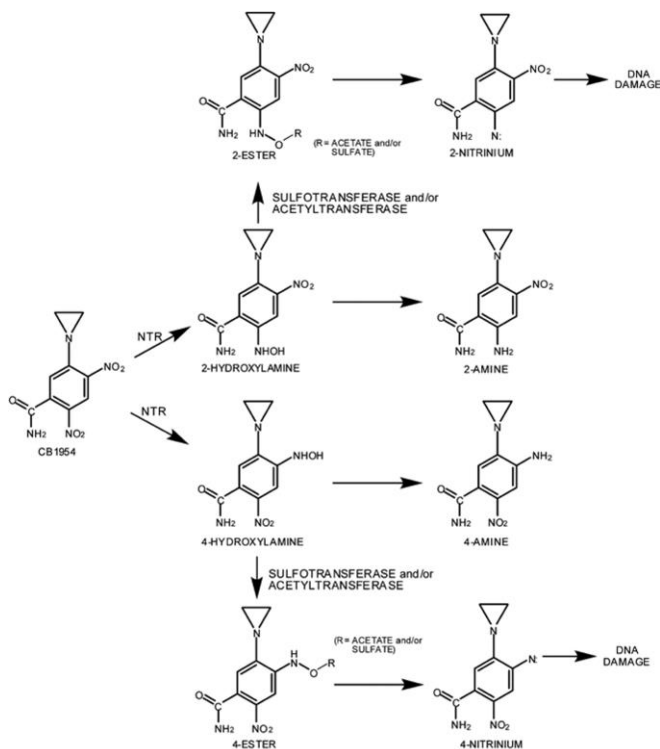


**Figure 1.7.** Metabolic activation pathway of CB1954 by nitroreductase [129].

The efficacy of the nitroreductase/CB1954 system in treating prostate and liver cancer has been demonstrated in clinical trials [130,131]. However, this system also has several significant drawbacks that limit its therapeutic potential. One of these is the low activation rate of CB1954. Alternatives to nitroreductases and better substrates for these enzymes have been explored, which retain at least a similar therapeutic effect as CB1954 on cancer cells [132,133]. Although promising results have been obtained *in vitro* and *in vivo*, a breakthrough for further clinical trials has not been achieved. Furthermore, the dose-dependent hepatotoxicity of CB1954 and the immunogenicity of bacterial nitroreductase also represent critical limitations of this GDEPT system [126,129].

### Purine nucleoside phosphorylase/6-methylpurine deoxyriboside system

The purine nucleoside phosphorylase (PNP)-based prodrug activation system relies on the use of *E. coli* PNP to convert prodrugs such as 6-methylpurine 2-deoxyriboside and fludarabine (Fig 1.8). These prodrugs are converted to 6-methylpurine or 2-fluoroadenine via PNP-catalyzed glycosidic bond cleavage. The resulting compounds are further converted by cellular enzymes into ATP

analogs, which are incorporated into RNA and inhibit both RNA and protein synthesis [134]. The main advantages of this system are the high bystander effect due to the gap junction-independent transport of activated drugs and the toxic effect on both proliferating and non-proliferating cells.

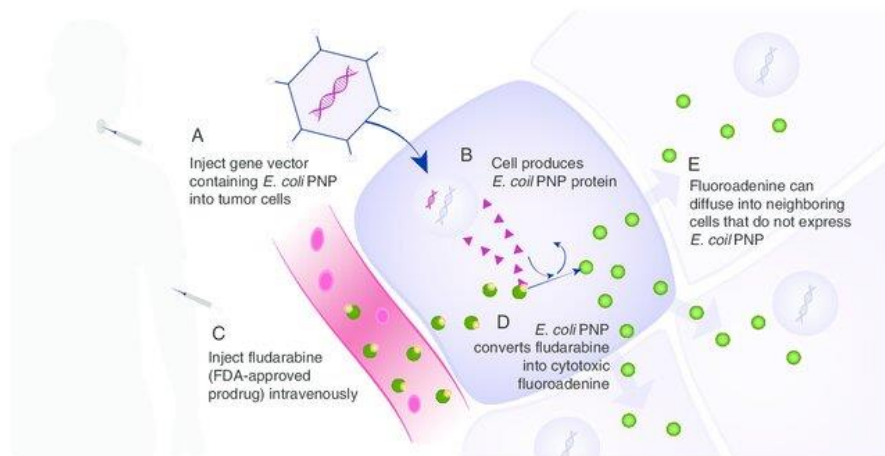


**Figure 1.8.** Mechanism of *E. coli* purine nucleoside phosphorylase prodrug activation using fludarabine [135].

The prodrugs used in this GDEPT system are only substrates for the *E. coli* PNPase, and human PNP does not carry out their conversion. For this reason, the toxic drug is only produced in targeted cells expressing bacterial PNP. Nevertheless, this limits the applicability of the therapy due to the potential of bacterial enzymes to induce host immune responses. To circumvent this issue, human PNP is being modified to recognize and catalyze the conversion of the prodrugs 6-methylpurine 2-deoxyriboside or fludarabine [136,137]. The *E. coli* PNP/fludarabine phosphate system was tested in the phase I clinical trial to assess its safety in head and neck cancer patients. Using this system, local production of 2-fluoroadenine in tumor tissues successfully killed tumors without any significant side toxicity [135]. These encouraging results allowed the study to move into the phase II clinical trial, which currently recruits patients with recurrent head and neck cancer (NCT03754933).

### Carboxylesterase/irinotecan system

Carboxylesterases are endogenous human enzymes capable of converting the less cytotoxic substrate irinotecan (CPT-11) into the highly toxic form SN-38. SN-38 inhibits topoisomerase I, disrupting the DNA relaxation machinery (Fig 1.9) [138]. This enzyme-prodrug system has been studied for the

treatment of colon cancer [139], glioma [140], and several other types of cancer [141,142]. Different isoforms of carboxylesterase have been used in the research. Carboxylesterase-1 (CE1), although abundantly localized in the liver, has a low catalytic efficiency, limiting the conversion rate of CPT-11 to SN-38. In contrast, CE2, which is predominantly expressed in the intestine, has a higher catalytic efficiency, but its application in treating different cancer types appeared to be more limited [143,144]. A rabbit analog of CE1 has also been developed to convert CPT-11 to SN-38. Although this isoform showed a higher catalytic efficiency compared to human CE1, it could induce an immune response in the human host [145]. To avoid this problem, a mutant CE1 was developed using a homology alignment of the human and rabbit versions of CE1, which helped to reduce the immunogenicity and increase the efficiency of the enzyme against CPT-11 [146].

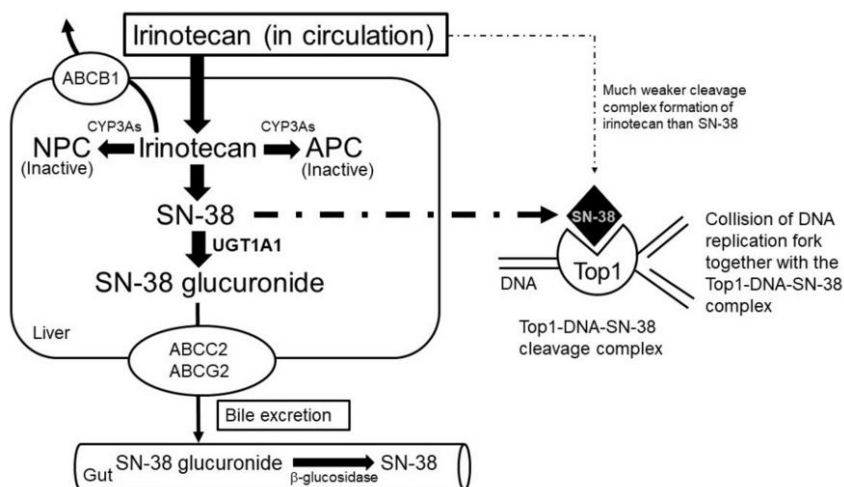


**Figure 1.9.** Metabolism of irinotecan. In the liver, irinotecan is activated to SN-38 by carboxylesterases. UDP-glucuronosyltransferase (UGT1A1) converts SN-38 to glucuronide. SN-38 glucuronide is hydrolysed in the intestine by β-glucosidase. In cancer cells, SN-38 inhibits topoisomerase I (Top1), which ultimately leads to lethal double-strand breaks [147].

SN-38 is poorly soluble in water, so its bystander effect may be lower [148]. To improve both the bystander effect and the overall anticancer efficacy, CE2 has been modified to obtain its secretory form [149]. This approach has shown promising success in several preclinical studies [150,151]. The CE/CPT-11 system has also been transferred to clinical trials. A phase I clinical trial for treating high-grade gliomas is currently active (NCT02192359). It analyses

the side effects and best dose of carboxylesterase-expressing neural stem cells in combination with irinotecan hydrochloride.

### 1.2.3. Bystander effect

Gene delivery to sufficient tumor cells to induce tumor regression remains a considerable weakness of the GDEPT strategy [152]. The efficiency of gene delivery to the target tissue is usually less than 10%, so the bystander effect is crucial for the success of GDEPT. The bystander effect is defined as the death of untransfected cells due to the indirect effect of neighboring transfected cells [73,153]. This can be achieved if the active metabolite exhibits diffusible characteristics or is actively transported to neighboring cells via gap junctions. In this way, the toxic effect of the drug can be intensified by several times.

The bystander effect can be classified into local and distant. The local effect leads to cell death and tumor regression, even though only a fraction of the cancer cell population expresses the gene encoding the enzyme that activates the prodrug. The distant effect is observed *in vivo* and is represented by the regression of tumor cells distant from the primary tumor expressing the transfected genes [154]. One good example of a local bystander effect is seen in the CD/5FC system, where the resulting toxic 5FU diffuses easily into the surrounding tissue. *In vitro* experiments showed that only 1-30% of CD-expressing cells are required to generate a sufficient amount of 5FU to inhibit the growth of neighboring non-transfected cells [153]. The local bystander effect of the HSV-TK/GCV system is another example, which is mediated through gap junctions since the active metabolite GCV-triphosphate is highly charged and cannot passively cross the cell membranes. However, it was observed that the expression of E-cadherin, involved in the formation and function of gap junctions, plays an important role in the HSV-TK/GCV bystander effect [155]. Meanwhile, the distant bystander effect is mainly attributed to the inflammation induced by GDEPT systems and the stimulation of systemic anti-cancer immune responses. This is particularly important in treating metastatic cancer, as the immune response can suppress tumor cells outside the primary tumor. The distant bystander effect of both the CD/5FC and HSV-TK/GCV systems has been proposed to be explained by the immune system's involvement in the killing of cancer cells [154,156,157].

It is important to note that bystander effects are not always associated only with a positive outcome. Although it enhances the effects of a toxic drug, it can also lead to harmful effects on normal healthy cells, limiting the clinical applicability of GDEPT [158]. Cell cycle-independent GDEPT systems have

higher off-target toxicity compared to GDEPT systems that only affect actively dividing cells. However, in most cases, the bystander effect is insufficient, and efforts are being made to increase it. One possibility is to modulate the host's immune response, thereby increasing the bystander effect and the overall toxicity of the system. Cancer antigens released from dying cells affected by GDEPT can stimulate the immune system, which in turn helps to eliminate more distant cells [159]. Also, co-expression of immunomodulators such as IL-2, IL-12, IFN- $\gamma$ , and TNF- $\alpha$  with a suicide gene has been used to enhance the bystander effect [70]. While the off-target toxicity of bystander effects is not usually of concern, the risks associated with the modulation of the immune response should be evaluated.

#### 1.2.4. GDEPT delivery systems

One of the significant challenges in GDEPT is the development of efficient gene delivery systems to enhance enzyme expression and improve therapeutic efficacy. Viral and non-viral vectors have been investigated for targeted gene delivery to tumor cells. Among viral vectors, adenoviruses, adeno-associated viruses, lentiviruses, retroviruses, and herpes simplex virus are commonly employed in GDEPT applications [65]. Non-viral delivery systems include liposomes, polymers, and genetically engineered cells capable of expressing prodrug-converting enzymes [66]. While non-viral vectors offer notable safety advantages, particularly for clinical use, viral vectors remain superior regarding gene transfer efficiency. Several of the most extensively studied gene delivery systems for GDEPT, as well as their advantages and limitations, are discussed below.

##### **Adenovirus vectors**

Adenoviruses possess a 36-kilobase pair (kbp) linear double-stranded DNA genome comprising over 30 genes, flanked by inverted terminal repeats (ITRs) and a packaging signal sequence ( $\psi$ ) [160]. Adenoviral vectors are engineered by deleting key regulatory genes, depending on the desired transgene size and application (Fig. 1.10). In first-generation adenoviral vectors, the essential early genes E1A and E1B are replaced with a constitutively active expression cassette carrying the therapeutic transgene. Additional deletions of E2, E3, and E4 genes allow for the insertion of larger transgene cassettes (up to ~10 kbp) and can further enhance vector performance. The modified adenoviral genome is introduced into the human embryonic kidney (HEK) 293 cells for viral particle production, which

provides the necessary E1, E2, and E4 gene products in trans. Adenoviral vectors exhibit broad tropism and, importantly, do not integrate into the host genome – the delivered transgene remains episomal, reducing the risk of insertional mutagenesis [161,162].

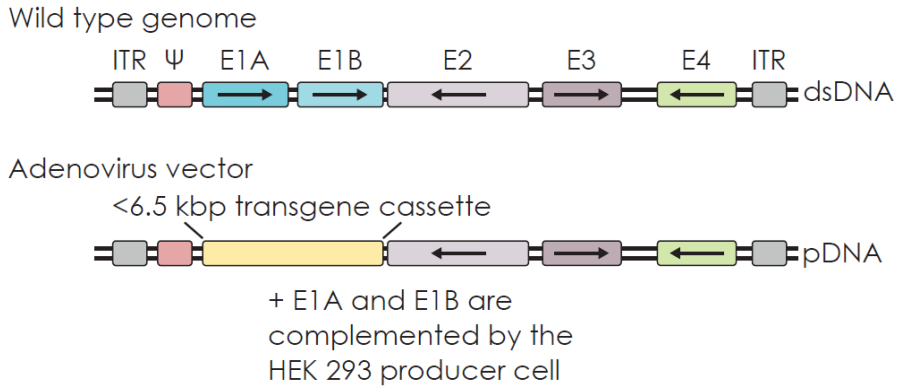


**Figure 1.10.** Schematic representation of the wild-type adenovirus genome and the first-generation adenoviral vector plasmid. Adapted from Bezeljak, 2022 [163].

In gene delivery applications, innate and adaptive immune responses directed against adenoviral vectors represent significant challenges limiting their therapeutic potential. Adenoviral capsid proteins and nucleic acids are recognized by complement system components and pattern recognition receptors, such as Toll-like receptors, triggering inflammatory responses. These immunostimulatory properties raise safety concerns and reduce the efficacy of systemic adenoviral gene delivery *in vivo*. Nevertheless, this inherent immunogenicity of adenoviral vectors can be advantageous in local cancer therapy, where immune activation may contribute to enhanced anti-tumor responses [164]. Adenoviral vectors have been widely employed for the delivery of suicide genes encoding prodrug-converting enzymes in cancer therapy. Notable examples include the transfer of genes encoding CD, PNP, and TK to tumor cells, enabling localized activation of prodrugs [161].

### Adeno-associated virus vectors

Adeno-associated viruses (AAVs) show considerable promise in gene therapy applications. AAVs are non-replicative, do not cause human disease, and exhibit broad tissue tropism. These viruses contain a single-stranded DNA genome, which naturally lacks key regulatory genes necessary for replication and expression. These missing genes are typically provided by adenoviral co-

infection of the host cell, though helper functions can also be supplied by herpes simplex virus or baculovirus. For gene delivery, the AAV genome is "guttled" – devoid of its viral genes – and replaced with a transgene expression cassette (Fig. 1.11). However, a significant limitation of AAV vectors is their relatively low transgene capacity, accommodating only up to 4.7 kbp of genetic material, which can be restrictive for some applications [165]. Therapeutic AAV particles are typically produced in HEK 293 cells through the co-transfection of three plasmid constructs [166].

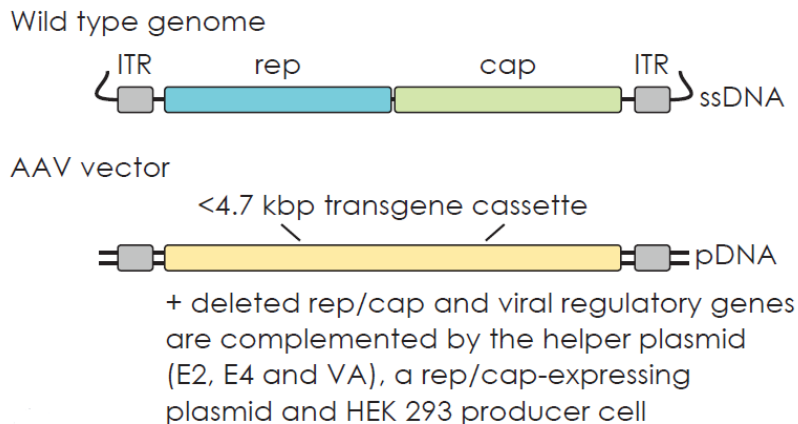


**Figure 1.11.** Schematic representation of the wild-type AAV genome and the AAV vector plasmid containing the transgene expression cassette. Adapted from Bezeljak, 2022 [163].

While AAV-based cancer therapies are still in the early stages of development, the inherent properties of AAV vectors offer promising strategies for targeted gene delivery [167]. For example, AAVs that can cross the blood-brain barrier and specifically target the central nervous system show potential for treating invasive glioblastoma [168]. To enhance cancer specificity, wild-type AAV capsids can be engineered to target tumor-specific cell surface antigens [169,170]. For example, AAV2 was modified to bind the HER2 receptor, enabling the selective delivery of the HSV-TK suicide gene in a mouse xenograft model. A single systemic injection of the HER2-targeted AAV vector, combined with GCV, significantly reduced tumor mass [171,172]. AAV particles are generally less immunogenic than other vector types, though many adults have pre-existing neutralizing antibodies, which can reduce the efficiency of AAV-based gene therapy [173]. Additionally, AAVs are considered highly safe due to their non-toxic nature and the low risk of

genome integration. The versatility of AAVs makes them a promising option for *in vivo* gene delivery [174].

### **Retrovirus vectors**

While adenovirus and AAV vectors are predominantly used for *in vivo* gene delivery, retroviral vectors, such as lentiviruses and gammaretroviruses, are the most commonly employed for the *ex vivo* transformation of patient-derived cells. Lentiviral vectors derived from human immunodeficiency virus type 1 (HIV-1) have been modified to prevent disease and express vesicular stomatitis virus G glycoprotein (VSV-G) instead of the native HIV-1 envelope (env) protein. Pseudotyping lentiviral particles with VSV-G enhances vector productivity, stability, and infectivity while expanding their tropism to various cell types and tissues [175,176]. Most of the HIV-1 RNA genome is deleted to ensure safety, leaving only three essential structural and regulatory genes: gag, pol, and rev. The removal of viral accessory proteins further eliminates the risk of pathogenicity. Moreover, the gag/pol, rev, VSV-G, and transgene (< 9 kbp) are expressed from separate plasmids in producer cell lines, preventing the formation of replication-competent viruses through recombination (Fig. 1.12) [177]. This ensures that only the transgene is included in the lentiviral particles, while other viral elements are excluded. Lentiviral vectors cannot replicate and deliver therapeutic genes with high efficiency [178]. Upon transduction, the expression cassette is integrated into the genome of the target cells, providing stable, long-term expression in both dividing and non-dividing cells. Alternatively, non-integrating lentiviral vectors have been developed to persist as episomal DNA, bypassing the oncogenic risks of integration [179].

Gammaretrovirus vectors, derived from murine leukemia virus, represent another class of retroviral vectors. Unlike lentiviral vectors, gammaretrovirus vectors can only infect actively dividing cells and are more likely to integrate into gene regulatory regions, raising concerns about insertional oncogenesis [176]. An example of a gammaretroviral therapeutic is vocimagene amiretrorepvec (Toca 511), which encodes yeast CD to convert the prodrug 5FC into the toxic compound 5FU in glioma cells [180]. While promising results were observed in mouse brain tumor models, a phase 2/3 clinical trial did not demonstrate improved patient survival after Toca 511 injection compared to standard treatment [181]. Lentiviral and gammaretroviral vectors will likely remain the *ex vivo* stable cell transduction methods.



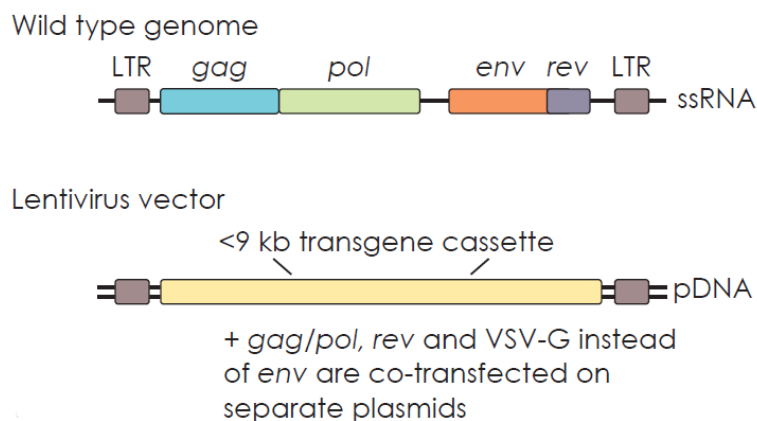


**Figure 1.12.** Schematic representation of the wild-type lentivirus genome and the lentiviral vector plasmid containing the transgene expression cassette. Adapted from Bezeljak, 2022 [163].

### Herpes simplex virus vectors

Herpes simplex virus (HSV) is one of the largest DNA viruses, with a linear double-stranded genome that includes essential and accessory genes. Accessory genes can be deleted individually without significantly affecting viral replication, whereas deletion of any essential gene completely blocks productive virus infection [182]. The ability to manipulate these genes has led to developing three types of HSV vectors: replication-defective recombinant vectors, replication-competent recombinant vectors, and amplicon vectors. Replication-defective recombinant HSV vectors are engineered by mutating or deleting the essential genes required for viral replication. Despite their inability to replicate, these vectors retain many advantageous properties of wild-type HSV-1. HSV-1 naturally exhibits neurotropism but can also infect a broad range of dividing and non-dividing cell types [183]. These vectors are non-toxic to host cells and are highly efficient gene delivery tools that do not integrate into the host cell genome [184]. In contrast, replication-competent recombinant vectors retain the ability to replicate due to the deletion of only non-essential genes. This allows gene delivery to an initial population of target cells, with subsequent spread of the therapeutic gene to neighboring cells through viral replication [185]. Amplicon vectors' genome lacks all HSV-1 genes except for a single origin of replication and a packaging signal necessary for encapsidation [186]. These vectors can accommodate large DNA inserts compared to other viral systems. However, their application in gene therapy is limited by challenges in producing helper virus-free vector stocks, as

contamination with helper virus poses risks of cytotoxicity and undesired immune responses [187]. Due to its natural neurotropism, HSV-1 is a particularly promising vector for brain cancer therapy. Additionally, HSV-1 encodes TK, making it particularly attractive for TK-mediated GDEPT. Replication-defective HSV vectors expressing TK have demonstrated therapeutic efficacy in glioma models [188]. Furthermore, HSV vectors co-expressing both TK and CD have been developed for double suicide gene therapy in a gliosarcoma model [189]. Nevertheless, the clinical application of HSV vectors remains limited by potential cytotoxicity and insufficient persistence in dividing cells [190].

## Liposomes

Among non-viral vectors, liposomes based on cationic lipids represent the most widely used gene delivery systems and have attracted considerable attention as non-viral delivery vehicles [191]. Liposomes are synthetic lipid vesicles composed of fatty acids or polymers, typically forming one or more bilayer membrane structures surrounding an aqueous core, enabling the encapsulation of small molecules (Fig. 1.13). Liposomes offer distinct advantages due to their biocompatibility, biodegradability, and low toxicity, as they are composed of naturally occurring substances. They provide stable encapsulation of various molecules, including nucleic acids, thereby protecting DNA from enzymatic degradation and facilitating cellular uptake and endosomal escape, ultimately resulting in effective gene transfer.

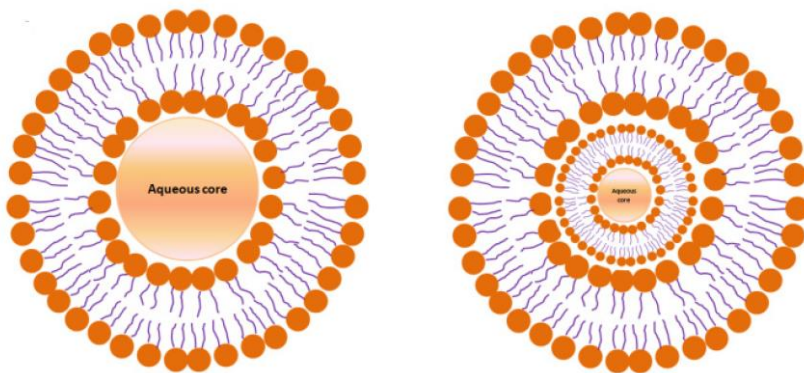


**Figure 1.13.** Schematic representation of the structure of liposomes. Adapted from Jin *et al.*, 2014 [192].

In addition to their excellent biocompatibility and low immunogenicity, liposomes can deliver large DNA fragments with well-defined

physicochemical properties and ease of preparation and handling. Furthermore, they exhibit potential for transfection across various tissues and cell types [193]. Liposomes as carriers for suicide genes have been investigated in clinical trials for the treatment of glioblastoma [194]. However, due to their positive surface charge, cationic liposomes may interact non-specifically with negatively charged cellular components such as serum proteins and enzymes, which can lead to reduced cellular adhesion, hemolysis, and decreased transfection efficiency [195]. Moreover, the preparation of liposomes often involves organic solvents such as ethyl ether or chloroform, which may be harmful to cells and tissues.

## **Polymers**

Various cationized biodegradable and non-biodegradable polymers have been extensively studied for their ability to deliver DNA into target cells. These include poly-L-lysine, poly-L-ornithine, polyethylenimine (PEI), chitosan, dendrimers, and others [196]. These polymers possess a positive charge, allowing them to condense negatively charged DNA molecules into nanoparticles typically smaller than 200 nm, thereby facilitating cellular uptake and promoting endosomal escape [197]. In particular, PEI has attracted considerable attention as one of the most effective non-viral gene delivery vectors. Its advantages include high DNA condensation ability and the so-called "proton sponge effect", which facilitates gene release into the cytoplasm by inducing endosomal swelling and rupture [198]. PEI-based systems have been applied for gene delivery to various tumor tissues [199]. Moreover, PEI can be chemically modified or conjugated with targeting ligands to enhance specificity by directing gene transfer to cells expressing the corresponding receptors. However, despite its promising properties, the clinical translation of PEI remains limited due to several drawbacks, including cytotoxicity, low transfection efficiency *in vivo*, and poor stability of PEI/DNA complexes in physiological conditions.

## **Mesenchymal stem cells**

Mesenchymal stem cells (MSCs) have emerged as efficient carriers for targeted gene delivery in cancer gene therapy. MSCs can be efficiently transduced with viral and non-viral vectors encoding therapeutic genes. Among these, retroviral vectors have been most frequently employed, particularly for the delivery of suicide genes such as CD and HSV-TK [200]. MSCs possess several advantageous features for targeted gene delivery,

including their immunoprivileged status – due to low expression of major histocompatibility complex (MHC) class I and absence of MHC class II – allowing them to evade host immune responses and avoid rejection following allogeneic transplantation. Moreover, their inherent tumor-tropic properties enable MSCs to selectively migrate toward tumors and metastatic sites, facilitating localized gene delivery [201]. Despite these promising characteristics, several critical considerations regarding using MSCs as gene delivery vehicles exist. First, MSCs are metabolically active cells capable of secreting a broad spectrum of bioactive molecules, including growth factors, cytokines, and chemokines, which could potentially promote tumor growth and metastasis. Second, the tumor microenvironment may induce malignant transformation of the administered MSCs. Third, important parameters such as the optimal number of MSCs required for therapeutic efficacy, the timing, and the route of administration remain to be fully elucidated [200]. Therefore, a deeper understanding of MSC biology within the tumor microenvironment and comprehensive studies investigating their homing mechanisms are essential to advancing MSC-based delivery vectors' safety and efficacy.

#### 1.2.5. Concluding remarks

Over the last three decades, numerous preclinical studies have been developed on gene-directed enzyme-prodrug therapy for cancer treatment. Many clinical trials have been performed based on preclinical data. Although significant progress has been made, none of the GDEPT systems have been approved for clinical use. Important challenges that remain to be addressed include the development of efficient vectors for effective and targeted gene transfer into tumor cells, the development of prodrugs that can be efficiently converted into active drugs having a strong bystander effect, and the engineering of enzymes with low immunogenicity and high affinity for prodrugs. Overcoming these obstacles may lead to more effective cancer treatments based on GDEPT technology.

### 1.3. Hydrolases and their applications

Hydrolases represent a class of hydrolytic enzymes that function as biochemical catalysts, utilizing water as a hydroxyl group donor during the substrate breakdown. Hydrolytic enzymes play crucial roles in various cellular processes and have numerous commercial applications. In the context of this thesis, particular attention is given to hydrolases for their role towards prodrug

to drug metabolism for cancer treatment. This literature review outlines the different types of hydrolases, focusing on their therapeutic potential.

### 1.3.1. Introduction to hydrolases

Hydrolases are enzymes that catalyze the hydrolysis of chemical bonds within biomolecules, resulting in the breakdown of large molecules into smaller fragments (Fig. 1.14). Hydrolases represent one of the largest and most diverse enzyme families, with over 200 distinct enzymes capable of catalyzing the hydrolysis of a wide range of chemical bonds, including carbon-oxygen (C–O), carbon-nitrogen (C–N), carbon-carbon (C–C), and phosphorus-nitrogen (P–N) bonds. Some common examples of hydrolases include esterases, glycosidases, amidases, deaminases, and lipases, among many others [10].

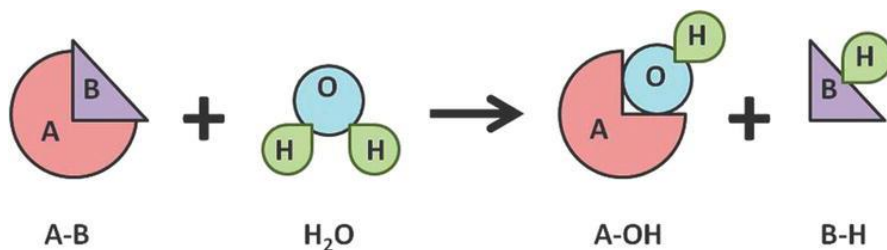


**Figure 1.14.** Schematic representation of the reaction catalysed by hydrolases [10].

Hydrolases play a crucial role in various degradative reactions within the body. These enzymes break down large molecules into smaller fragments, which are then utilized for synthesis, waste excretion, or as carbon sources for energy production. Hydrolases are involved in essential biological processes such as digestion, transport, excretion, regulation, and signaling [202]. Industrially, hydrolases are the most widely used enzyme class, comprising about 75% of all enzymes utilized in industrial applications. Among these, carbohydrases, proteases, and lipases dominate the market, accounting for over 70% of enzyme sales. Hydrolases are critical in various industries, including detergent, leather, textiles, paper, food, dairy, biofuels, and waste treatment [203].

### 1.3.2. Hydrolases in prodrug activation

Prodrug design represents a crucial aspect of modern drug discovery. Prodrugs can provide numerous advantages over their parent compounds, including increased solubility, enhanced chemical stability, improved bioavailability,

reduced side effects, and greater selectivity. They have been successfully applied across various therapeutic areas, such as antiviral, antihypertensive, antibiotic, anticoagulant, anti-inflammatory, antifungal, anesthetic, and anticancer therapies. A fundamental consideration in prodrug design is incorporating an efficient and/or controlled activation mechanism capable of converting the prodrug into its active form to fulfill the requirements of a specific medical application. Enzyme-mediated activation is widely utilized, with hydrolases playing a crucial role in this process [204,205].

Hydrolases, classified as class 3 enzymes according to the Enzyme Commission (EC) classification, play a crucial role in drug metabolism, particularly in the context of cancer treatment. These enzymes facilitate the metabolic activation of prodrugs, enabling their selective targeting and enhanced therapeutic efficacy against cancer cells. In prodrug design, the prodrug is specifically engineered to serve as a substrate for a selected enzyme. Numerous prodrugs have been developed that are converted into active anticancer agents by hydrolytic enzymes of both mammalian and non-mammalian origin [206]. The following sections discuss several hydrolases that play a significant role in the enzymatic conversion of prodrugs into their active drug forms.

### **Carboxylesterase**

Carboxylesterases (CEs), classified under EC 3.1.1.1, are ubiquitous enzymes primarily responsible for detoxifying ester-containing xenobiotics. Their catalytic activity involves hydrolysis reactions that generate the corresponding carboxylic acid and alcohol. CEs serve as an important biological barrier by restricting the distribution of potentially toxic compounds and promoting their elimination through conversion into more polar metabolites [207]. CEs are capable of cleaving ester bonds in a wide range of clinically relevant drugs, including heroin, cocaine, meperidine, and lidocaine [208]. In addition to their role in drug metabolism, CEs participate in other critical biological processes and prodrug activation.

CEs exhibit variable activity and substrate specificity depending on species and tissue localization. They are widely distributed throughout the body, including the intestines, blood, brain, skin, and tumors. Biochemical studies have shown that CEs efficiently hydrolyze small molecular substrates; however, their activity differs considerably with larger substrates. Structural analyses of CEs have revealed that their substrate specificity is influenced by the size and accessibility of the enzyme's active site [209]. Several

representative esterase-activated prodrugs have been reported. Temocapril, a long-acting angiotensin-converting enzyme inhibitor, is rapidly hydrolyzed to its active dicarboxylic acid form [210]. Dipivefrin, administered as an ophthalmic solution for the treatment of glaucoma, is hydrolyzed to epinephrine upon corneal penetration [211]. Lovastatin and simvastatin, used for lowering cholesterol in patients with hypercholesterolemia, are hydrolyzed by human CE1 to their respective hydroxy acid forms, which inhibit HMG-CoA reductase activity [212]. Irinotecan (CPT-11) is converted by carboxylesterases into its active metabolite, a potent inhibitor of topoisomerase I [213]. Pharmacokinetic studies demonstrated that four- to five-fold higher doses of CPT-11 were required to induce tumor regression in human rhabdomyosarcoma xenografts grown in esterase-deficient mice compared to xenografts grown in mice with functional esterases [214]. These findings indicate the critical role of carboxylesterase-mediated activation in the antitumor activity of CPT-11.

### **Matrix metalloproteinase**

Matrix metalloproteinases (MMPs; EC 3.4 subtypes) are zinc-dependent endopeptidases comprising more than 25 family members, classified based on their domain structure and substrate specificity. These enzymes play a critical role in the degradation of extracellular matrix (ECM) components, including collagen, laminin, fibronectin, and elastin. In addition to ECM remodeling, MMPs are capable of cleaving various non-matrix proteins, such as growth factor receptors and cell adhesion molecules, thereby contributing to processes essential for tumor growth, survival, and metastasis. Owing to their significant involvement in tumor angiogenesis, invasion, and metastasis, MMPs have been investigated as therapeutic targets in several pathological conditions, including cancer, arthritis, glomerulonephritis, periodontal disease, and ulcers [215].

Among the MMP family, MMP-2 and MMP-9 have been extensively utilized for the targeted activation of prodrugs. Model prodrugs have been developed that release anthraquinone-type cytotoxic agents upon activation by MMP-9; these agents are often employed in combination with conventional therapies for treating multiple myeloma [216]. The selective delivery of doxorubicin to tumor tissues has been explored through the design of its peptide conjugates, which function as prodrugs activated by the combined proteolytic action of MMP-2, MMP-9, and MMP-14. Doxorubicin is a potent anthracycline widely used in cancer therapy, exerting its cytotoxic effect via topoisomerase II-mediated DNA damage. Conjugation of doxorubicin to MMP-cleavable

peptides has generated a series of prodrugs susceptible to cleavage by MMP-2, MMP-9, and MMP-14. Evaluating these prodrugs in the fibrosarcoma cell line HT1080, which expresses multiple MMPs, and in HT1080 xenografts in mice demonstrated selective conversion of the prodrug to free doxorubicin [217]. Furthermore, the prodrug exhibited a 10-fold increase in the tumor-to-heart distribution ratio, enhanced antitumor efficacy, and reduced toxicity compared to free doxorubicin.

### **Alkaline phosphatase**

Alkaline phosphatase (AP; EC 3.1.3.1) is a metalloenzyme containing zinc and magnesium ions, characterized by broad substrate specificity. It catalyzes the hydrolytic removal of phosphate groups from various molecules, including nucleotides, proteins, and alkaloids. AP is ubiquitously expressed in numerous tissues, with the highest expression levels observed in the liver. Notably, the differential expression of AP isozymes, particularly in liver and bone tissues, has been employed as a diagnostic biomarker for various malignancies and renal dysfunctions [218]. AP has been implicated in the activation of several clinically utilized phosphate prodrugs, such as fosfluconazole, fosphenytoin, fosprepitant, amifostine, clindamycin phosphate, estramustine phosphate, and etoposide phosphate. The primary rationale for developing these prodrugs has been to improve the aqueous solubility of their parent compounds, thereby enhancing their suitability for parenteral administration. In addition, certain phosphate prodrugs have been specifically designed for targeted cancer therapy [207].

Many conventional chemotherapeutic agents have been modified through phosphorylation to generate less active or inactive prodrugs that AP can subsequently reactivate via hydrolytic removal of the phosphate group. One of the earliest examples is the phosphorylated derivative of etoposide, which exhibits over 100-fold reduced cytotoxicity against human carcinoma cell lines compared to the parent drug [206]. AP derived from the calf intestine has been utilized to convert etoposide phosphate into the clinically approved anticancer drug etoposide. The reduced cytotoxicity of the phosphorylated etoposide is attributed to its inability to readily permeate cell membranes, thereby limiting its activity against cancer cells. Targeted delivery of AP to tumor cells using the tumor-specific monoclonal antibody L6 has demonstrated significant immunospecific antitumor activity both *in vitro* and *in vivo*. These findings suggest that the L6-AP conjugate can efficiently convert non-toxic phosphorylated prodrugs into potent cytotoxic anticancer agents at the tumor site.



## **β-Glucuronidase**

Human β-glucuronidase (EC 3.2.1.31) is a lysosomal enzyme that plays a critical role in the degradation of glucuronic acid-containing glycosaminoglycans, such as heparan sulfate, chondroitin sulfate, and dermatan sulfate [219]. The proper function of β-glucuronidase is essential for remodeling extracellular matrix components. Mutations in the β-glucuronidase gene have been associated with mucopolysaccharidosis type VII (Sly syndrome), a rare lysosomal storage disorder [220]. Due to the high levels of endogenous extracellular β-glucuronidase found in necrotic regions of tumors, glucuronide-based prodrugs have potential utility as therapeutic agents. In non-necrotic tumor regions, where endogenous enzyme levels are insufficient, exogenous β-glucuronidase can be delivered using GDEPT strategies [221]. Elevated expression of β-glucuronidase has been observed in various tumors, including breast, lung, gastrointestinal tract carcinomas, and melanomas, compared to normal tissues.

Exploiting tumor-specific enzyme distribution, several glucuronide prodrugs have been developed for selective activation in cancer tissues, taking advantage of the fact that β-glucuronidase is mainly absent from systemic circulation. BHAMG, a synthetic glucuronide prodrug of aniline mustard, can be enzymatically activated by *Escherichia coli* β-glucuronidase [222]. Pyrrolo[2,1-c][1,4]-benzodiazepine-β-glucuronide, a prodrug of a DNA minor groove binder, has similarly been shown to be activated by β-glucuronidase [223]. Another notable example is HMR1826, a glucuronide-conjugated prodrug of doxorubicin (Fig. 1.15) [219]. Upon hydrolysis by β-glucuronidase, the resulting 4-hydroxybenzyl carbamate-doxorubicin intermediate undergoes a self-immolative 1,6-elimination reaction to release the active doxorubicin molecule.

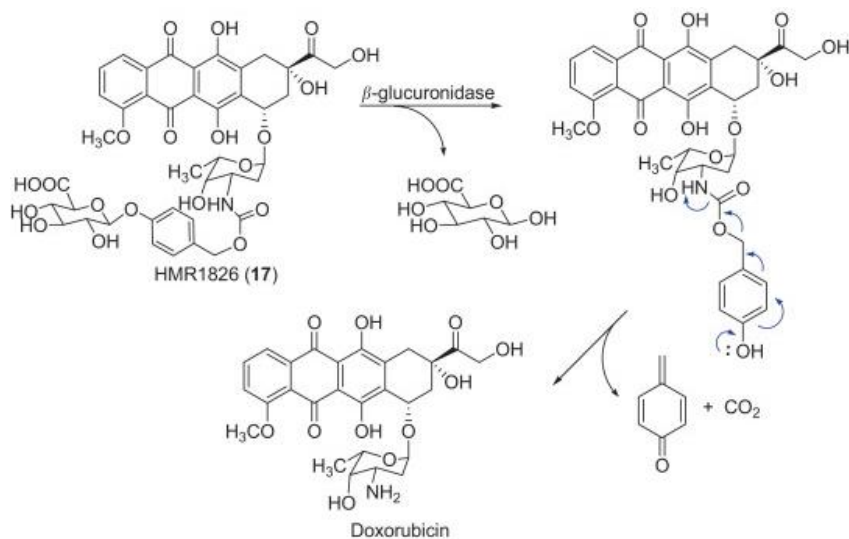


**Figure 1.15.** Activation of doxorubicin–glucuronide conjugate (HMR1826) by  $\beta$ -glucuronidase followed by 1,6-elimination of the self-immolative linker. Adapted from Yang *et al.*, 2011 [207].

### Prostate-specific antigen

Prostate-specific antigen (PSA, EC 3.4.21.77) is a glycoprotein composed of a single polypeptide chain with a molecular weight of approximately 33–34 kDa, containing around 7% carbohydrate. PSA is primarily synthesized by the prostate's ductal and acinar epithelial cells and is secreted into the glandular lumen, where it cleaves semenogelin I and II in the seminal coagulum. Intracellular PSA remains enzymatically inactive due to high concentrations of zinc ions. However, elevated serum PSA levels are commonly observed in prostate cancer patients, likely resulting from the disruption of the basement membrane barrier, which typically prevents PSA from leaking into the surrounding stroma [224]. Several characteristics make PSA an attractive candidate for targeted prodrug activation: its specific expression in prostate tissue, the enzymatic activity of the extracellular form, the inactivity of PSA in serum and intracellular compartments, and its elevated levels in malignant prostate cancer cells. These properties support using PSA as a prodrug-converting enzyme to selectively activate anticancer agents in prostate-derived malignancies.

Peptide-based prodrugs incorporating PSA-cleavable substrate sequences have been developed to achieve site-specific drug release. Upon proteolytic cleavage by PSA, the conjugated anticancer agent is liberated locally within

the tumor microenvironment. This mechanism enables selective cytotoxicity toward PSA-expressing cancer cells. Several PSA-specific substrate sequences have been identified, including Ser–Lys–Leu–Gln–, His–Ser–Ser–Lys–Leu–Gln–, and glutaryl–Hyp–Ala–Ser–Chg–Gln–, all of which share a unique glutamine residue at the P1 position [225]. These peptide sequences are often linked to cytotoxic agents through dipeptides such as Ser–Leu or Leu to enhance PSA-mediated cleavage. The resulting peptide–drug conjugates have demonstrated an increased therapeutic index in preclinical models of prostate cancer, supporting the feasibility of PSA-targeted prodrug therapy [226]. Various anticancer agents have been incorporated into PSA-activated prodrugs, including doxorubicin, thapsigargin, vinblastine, 5-fluoro-2'-deoxyuridine, diazeniumdiolate, protoxin, and paclitaxel [227–230]. Notably, a peptide–doxorubicin conjugate has progressed to phase I clinical trials [226].

### Carboxypeptidase

Carboxypeptidases (EC 3.4.16–3.4.18) are proteolytic enzymes that catalyze the hydrolysis of peptide bonds at the C-terminal end of proteins and peptides, releasing single amino acids and truncated peptides. Among them, carboxypeptidase G2 (CPG2), a 42 kDa exopeptidase derived from *Pseudomonas* sp. strain RS-16, belongs to the aminoacylase-1/M20 family and is absent in mammalian systems. While the natural substrate of CPG2 is folic acid, the enzyme exhibits broader specificity and can hydrolyze glutamate from amidic, urethanic, and ureidic bonds [231]. This enzymatic versatility allows CPG2 to serve as an effective prodrug-converting enzyme in GDEPT. A series of CPG2-activated nitrogen mustard prodrugs have been developed, featuring cytotoxic nitrogen mustard moieties conjugated directly to glutamate or via self-immolative linkers (Fig. 1.16) [232,233]. Upon enzymatic activation by CPG2, these prodrugs are hydrolyzed to release glutamic acid and the parent cytotoxins, including benzoic acid nitrogen mustards, aniline nitrogen mustards, and phenol nitrogen mustards.

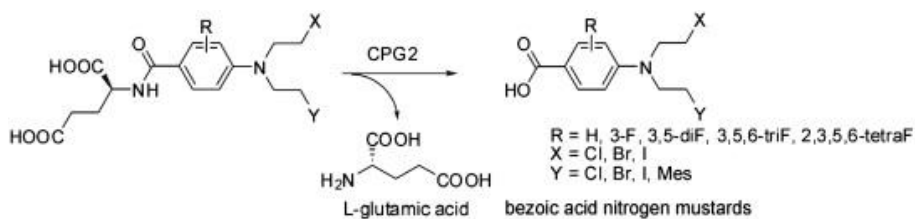


**Figure 1.16.** The mechanism of mustard prodrugs activated by CPG2 [207].

Methotrexate (MTX) has also been modified into prodrug forms by covalently linking amino acids or peptides to its  $\alpha$ -carboxyl group, rendering the conjugates less cytotoxic until activated by CPG2 [234]. *In vitro* studies using the UCLA-P3 human lung carcinoma cell line demonstrated that methotrexate–amino acid conjugates displayed significantly reduced cytotoxicity in the absence of CPG2, with  $IC_{50}$  values in the micromolar range ( $\sim 7.0 \mu\text{mol/L}$ ), compared to the nanomolar  $IC_{50}$  value of free MTX (28 nmol/L). However, when cells were treated with the KS1/4–CPG2 conjugate – a carcinoma-specific monoclonal antibody fused to CPG2 – the MTX–Phe exhibited an  $IC_{50}$  of 63 nmol/L. Neither the KS1/4–CPG2 conjugate alone nor the MTX–Phe prodrug alone produced significant cytotoxicity, supporting the enzyme-specific and tumor-targeted activation strategy [235].

### **Penicillin amidase**

Penicillin amidase (PA), also known as penicillin acylase, is widely expressed in various microorganisms, including yeasts, fungi, and bacteria. It belongs to the N-terminal nucleophile hydrolase family, a class of enzymes characterized by a conserved structural fold near the active site and a nucleophilic residue at the N-terminus. Penicillin G amidase (PGA, Type II), which uses penicillin G as a substrate, is notable for its broad substrate specificity. Several prodrugs have been designed for targeted activation by PGA, particularly within the context of antibody-directed enzyme prodrug therapy (ADEPT) [236]. One such example involves the development of a palytoxin-based prodrug, N-(4'-hydroxyphenylacetyl)palytoxin (NHPAP), in which the highly potent cytotoxin palytoxin is conjugated to a cleavable N-acyl moiety for selective activation by PGA. Palytoxin exerts cytotoxic effects across various cell types, including fibroblasts, lymphocytes, erythrocytes, and epithelial cells. PGA was covalently attached to the tumor-specific monoclonal antibody L6 (L6–PGA) to minimize systemic toxicity and enhance tumor selectivity. The prodrug NHPAP exhibited over 1000-fold reduced cytotoxicity in carcinoma and lymphoma cells lacking PGA expression. In contrast, efficient enzymatic conversion of NHPAP to active palytoxin was observed in H2981 cells expressing the L6 antigen, resulting in cytotoxic effects comparable to free palytoxin.

#### **1.3.3. Future perspectives of hydrolases in prodrug therapy**

Prodrugs have demonstrated considerable efficacy in overcoming challenges associated with parent drug molecules by improving key properties such as

oral bioavailability, pharmacokinetic profiles, patient acceptability, and target specificity. Several prodrugs are already in clinical use, showcasing the potential of this strategy [237]. While some prodrugs can be activated through chemical processes independent of enzymes, many require enzymatic activation [238,239]. As the discovery of promising compounds with suboptimal pharmaceutical characteristics continues, prodrug strategies have become increasingly essential for optimizing therapeutic efficacy. Understanding the enzymes involved in prodrug activation is crucial for the strategic design of future prodrug-based therapies.

Hydrolases continue to show great potential in targeted cancer therapy, especially in the activation of prodrugs [207]. These enzymes offer the benefit of catalyzing selective transformations under physiological conditions, allowing for site-specific drug release and reduced systemic toxicity. Endogenous hydrolases are commonly employed for prodrug activation, and with the recent focus on delivering active drug molecules to specific tissues or organs, non-endogenous hydrolases have been introduced for targeted prodrug activation. Approaches such as ADEPT or GDEPT are leading strategies in cancer treatment, employing different hydrolytic enzymes to activate prodrugs selectively within the tumor microenvironment [71]. While these approaches hold great promise, they also come with challenges, and many obstacles remain to be addressed (see chapter 1.2.2.). As our understanding of enzyme-substrate specificity, tissue-specific expression patterns, and structural factors influencing catalytic activity deepens, designing more efficient and tumor-selective hydrolase-prodrug systems is becoming increasingly achievable. Protein engineering and directed evolution also present opportunities to create hydrolase variants with improved activity, stability, and substrate selectivity. Future research is likely to explore novel hydrolases and incorporate them into innovative delivery platforms like GDEPT. With the continued advancement of technology, these strategies are expected to become powerful tools for treating various diseases.

## 2. MATERIALS AND METHODS

### 2.1. Materials

#### 2.1.1. Reagents

Indirubin carboxylic acid and 2-indolinone derivatives (dr. Mikas Sadauskas), *N*<sup>4</sup>-acyl-5-fluorocytidines (dr. Martyna Koplūnaitė), *N*<sup>4</sup>-alkyl-5-fluorocytidines (PhD student Kamilė Butkutė), as well as 4-alkylthio-5-fluorouridines and 4-alkoxy-5-fluoro(-2'-deoxy)uridines (dr. Ringailė Lapinskaitė) were synthesized and purified by the respective contributors, who also performed compound purity analyses. All remaining reagents, chemicals, and kits used in this work are of the highest commercially available quality.

#### 2.1.2. Nucleic acids

The oligonucleotide primers listed in Table 2.2. were purchased from Azenta, Germany. Plasmid vectors encoding human-optimized genes were obtained from Thermo Fisher Scientific, Lithuania.

#### 2.1.3. Bacteria

- ***E. coli* DH5α:** F<sup>-</sup> *endA1 glnV44 thi-1 recA1 relA1 gyrA96 deoR nupG purB20* φ80d*lacZ*ΔM15 Δ(*lacZYAargF*)U169, *hsdR17*(r<sub>K</sub><sup>-</sup>m<sub>K</sub><sup>+</sup>), λ<sup>-</sup> (Pharmacia, USA)
- ***E. coli* HMS174 Δ*pyrF* Δ*yqfB*:** construction was carried out at the Department of Molecular Microbiology and Biotechnology on the basis of HMS174 (F<sup>-</sup> *recA1 hsdR* (rK12<sup>-</sup>mK12<sup>+</sup>) (DE3) (Rif R) (Novagen)
- ***E. coli* HMS174 Δ*pyrF* Δ*cdd*:** construction was carried out at the Department of Molecular Microbiology and Biotechnology on the basis of HMS174
- ***E. coli* KRX Δ*cdd*:** construction was carried out at the Department of Molecular Microbiology and Biotechnology on the basis of KRX (F<sup>-</sup>, *traD36*, Δ*ompP*, proA<sup>+</sup>B<sup>+</sup>, *lacIq*, Δ(*lacZ*)M15] Δ*ompT*, *endA1*, *recA1*, *gyrA96* (Nal<sup>r</sup>), *thi-1*, *hsdR17* (r<sub>K</sub><sup>-</sup>, m<sub>K</sub><sup>+</sup>), e14<sup>-</sup> (McrA<sup>-</sup>), *relA1*, *supE44*, Δ(*lac-proAB*), Δ(*rhaBAD*)):T7 RNA polymerase (Promega)

### 2.1.4. Cell lines

- **HCT116:** human colon cancer cell line (gift from Dr. Daiva Baltriukienė, Life Sciences Center, Vilnius University, Vilnius, Lithuania)
- **MCF7:** human breast cancer cell line (gift from Dr. Daiva Baltriukienė, Life Sciences Center, Vilnius University, Vilnius, Lithuania)
- **A549:** human lung adenocarcinoma cell line (gift from Dr. Daiva Baltriukienė, Life Sciences Center, Vilnius University, Vilnius, Lithuania)
- **MH22a:** murine liver tumor cell line (gift from Dr. Daiva Baltriukienė, Life Sciences Center, Vilnius University, Vilnius, Lithuania)
- **293FT:** human embryonal kidney-derived cell line (Invitrogen, USA)
- **U87MG:** human glioblastoma cell line (ECACC, UK)

### 2.1.5. Plasmids

**Table 2.1.** Plasmid vectors used in this study.

Plasmid	Notes	Source
pBABE-Puro	Retroviral vector for cloning and expressing a gene of interest. Puromycin selection. Amp <sup>R</sup> , Puro <sup>R</sup>	Cell Biolabs, Inc., USA
pBABE-YqfB_His	The <i>yqfB</i> gene was amplified by PCR using primers <i>YqfB BamHI FW</i> and <i>YqfB H Eco105I RV</i> , digested with <i>BamHI</i> and <i>Eco105I</i> and cloned into the corresponding site of pBABE-Puro vector. 6×His encoding sequence added to the 3' end.	This study
pBABE-D8_RL_His	The <i>D8_RL</i> gene was amplified by PCR using primers <i>D8 BamHI FW</i> and <i>D8 H Eco105I RV</i> , digested with <i>BamHI</i> and <i>Eco105I</i> and cloned into the corresponding site of pBABE-Puro vector. 6×His encoding sequence added to the 3' end.	This study
pBABE-CDA_EH_His	The <i>cda_eh</i> gene was amplified by PCR using primers <i>EH BamHI FW</i> and <i>CDA Eco105I RV</i> , digested with <i>BamHI</i> and <i>Eco105I</i> and cloned into the corresponding site of pBABE-Puro vector. 6×His encoding sequence added to the 3' end.	This study
pBABE-CDA_F14_His	The <i>cda_f14</i> gene was amplified by PCR using primers <i>F14 BamHI FW</i> and <i>CDA</i>	This study

	<i>Eco105I</i> <i>RV</i> , digested with <i>Bam</i> HI and <i>Eco105I</i> and cloned into the corresponding site of pBABE-Puro vector. 6×His encoding sequence added to the 3' end.	
pBABE-CDA_Lsp_His	The <i>cda_lsp</i> gene was amplified by PCR using primers <i>Lsp Bam</i> HI <i>FW</i> and <i>CDA Eco105I RV</i> , digested with <i>Bam</i> HI and <i>Eco105I</i> and cloned into the corresponding site of pBABE-Puro vector. 6×His encoding sequence added to the 3' end.	This study
pMA-RQ-CDA_EH_Flag	Vector encoding C-terminally FLAG-tagged human codon-optimized CDA_EH sequence.	Thermo Fisher Scientific, Lithuania
pMA-RQ-CDA_F14_Flag	Vector encoding C-terminally FLAG-tagged human codon-optimized CDA_F14 sequence.	Thermo Fisher Scientific, Lithuania
pMA-RQ-CDA_Lsp_Flag	Vector encoding C-terminally FLAG-tagged human codon-optimized CDA_Lsp sequence.	Thermo Fisher Scientific, Lithuania
pBABE-CDA_EH_Flag	<i>Bam</i> HI – <i>Eco105I</i> DNA fragment from pMA-RQ-CDA_EH_Flag were subcloned into the pBABE-Puro vector using <i>Bam</i> HI and <i>Eco105I</i> restriction sites.	This study
pBABE-CDA_F14_Flag	<i>Bam</i> HI – <i>Eco105I</i> DNA fragment from pMA-RQ-CDA_F14_Flag were subcloned into the pBABE-Puro vector using <i>Bam</i> HI and <i>Eco105I</i> restriction sites.	This study
pBABE-CDA_Lsp_Flag	<i>Bam</i> HI – <i>Eco105I</i> DNA fragment from pMA-RQ-CDA_Lsp_Flag were subcloned into the pBABE-Puro vector using <i>Bam</i> HI and <i>Eco105I</i> restriction sites.	This study
pTO-CDA_Lsp_Flag	<i>Bam</i> HI – <i>Not</i> I DNA fragment from pMA-RQ-CDA_Lsp_Flag were subcloned into the pcDNA4/TO vector using <i>Bam</i> HI and <i>Not</i> I restriction sites.	Dr. Arūnas Kazlauskas
pET21b	Vector for inducible expression of C-terminally 6×His-tagged proteins. Amp <sup>R</sup>	Novagen, Germany
pET21b-YqfB	The <i>yqfB</i> gene was amplified by PCR using primers <i>YqfB Nde</i> I <i>FW</i> and <i>YqfB Xho</i> I <i>RV</i> ,	This study



	digested with <i>NdeI</i> and <i>XhoI</i> and cloned into the corresponding site of pET21b vector.	
pET28a	Vector for inducible expression of C-terminally 6×His-tagged proteins. Kan <sup>R</sup>	Novagen, Germany
pET28a-D8_RL	The <i>D8_RL</i> gene was amplified by PCR using primers <i>D8 NcoI FW</i> and <i>D8 XhoI RV</i> , digested with <i>NcoI</i> and <i>XhoI</i> and cloned into the corresponding site of pET28a vector.	This study
pCMV-gag-pol	Vector for the expression of retroviral structural proteins under the control of the CMV immediate early promoter. The gag region encodes genes that comprise capsid proteins; the pol region encodes reverse transcriptase and integrase proteins. Amp <sup>R</sup>	Cell Biolabs, Inc., USA
pCMV-VSV-G	Vector for the expression of envelope protein (glycoprotein G) for the production of retroviral particles. Amp <sup>R</sup>	Cell Biolabs, Inc., USA

#### 2.1.6. PCR primers

**Table 2.2.** Oligonucleotide primers used in this study.

Primer name	Sequence 5'→3'	Purpose of use
YqfB BamHI FW	TGACGGATCCATGCAGCCA AACGA	Cloning of <i>yqfB</i> gene into pBABE-Puro vector
YqfB H Eco105I RV	TGACTACGTATCAGTGGTG GTGGTGGTG	
D8 BamHI FW	TGACCGGATCCATGGAAC AATTAAAATTTC	Cloning of <i>D8_RL</i> gene into pBABE-Puro vector
D8 H Eco105I RV	TGACTACGTATTAGCCGTG GTGGTGATG	
EH BamHI FW	TGACGGATCCATGAAGGA AACACTTTG	Cloning of <i>cda_eh</i> gene into pBABE-Puro vector
CDA Eco105I RV	TGACTACGTATTAGCCGTG GTGGTGATG	
F14 BamHI FW	TGACGGATCCATGAACAA GGAAGATT	Cloning of <i>cda_f14</i> gene into pBABE-Puro vector
CDA Eco105I RV	TGACTACGTATTAGCCGTG GTGGTGATG	
Lsp BamHI FW	TGACGGATCCATGCGTGAC AAACTGA	

CDA Eco105I RV	TGACTACGTATTAGCCGTG GTGGTGATG	Cloning of <i>cda_lsp</i> gene into pBABE- Puro vector
pBABE 5N	CCTTGAACCTCCTCTTTC	Sequencing primers for pBABE-Puro vector
pBABE 3N	GGACTTTCCACACCCTA	
YqfB NdeI FW	TATACATATGCAGCCAAAC GACATC	Cloning of <i>yqfB</i> gene into pET21b vector
YqfB XhoI RV	TTAACTCGAGAAGACATTT AAATTCAATCAC	
D8 NcoI FW	TGACATGGAACAATTAAA ATTTCAAAGAATTGGAAC AAT	Cloning of <i>D8_RL</i> gene into pET28a vector
D8 XhoI RV	TGACCTCGAGGCCATCGTG TGCTGGT	
T7 promoter	TAATACGACTCACTATAGG G	Sequencing primers for pET vectors
T7 terminator	GCTAGTTATTGCTCAGCGG	
YqfB qPCR FW	ACATTCTGGCTGGGCGTAA A	Verification of successfully modified genome by RT- qPCR analysis
YqfB qPCR RV	ATCCAGCGTTACGGTTGAG G	
D8 qPCR FW	GGTCCGAAGTACACGGTTG G	
D8 qPCR RV	AGGCGACTGATCCATTCGT T	
EH qPCR FW	ATGCCTACTGCCCCGTATTC C	
EH qPCR RV	CTTAAAGATGGCCGTCCGC T	
F14 qPCR FW	GCCTATGCCCCGTATTCCA A	
F14 qPCR RV	TGCAGCGAAAATGGCACTT C	
Lsp qPCR FW	GGTGCGGACGGTGTTATCT A	
Lsp qPCR RV	TTACCGTTGCAAACAACCG C	
EH Hopt qPCR FW	GCTGCAACATCGAGAACA CC	
EH Hopt qPCR RV	AAGGGGCACCATCAGCTTC	
F14 Hopt qPCR FW	CCGATGATATCGAGGCCCT G	

F14 Hopt qPCR RV	CAGTGTCTCTTTGCCGTTG C	
Lsp Hopt qPCR FW	CCTGTGGGAGCTGCTGTTA T	
Lsp Hopt qPCR RV	GTATAGGTCTGGCAGCCGT G	

### 2.1.7. Recombinant proteins

**Table 2.3.** Recombinant proteins used in this study.

Name	Theoretical mass, kDa	Tag
YqfB	11.9	C-terminal 6×His
D8_RL	14.9	C-terminal 6×His
CDA_EH	16	C-terminal 6×His
CDA_F14	15.4	C-terminal 6×His
CDA_Lsp	15.3	C-terminal 6×His

### 2.1.8. Bacterial media

- **LB:** 1% tryptone, 0.5% yeast extract, 0.05% NaCl
- **LB agar:** LB + 1.5% agar
- **SOB:** 2% tryptone, 0.5% yeast extract, 10 mM NaCl, 2.5 mM KCl, 10 mM MgCl<sub>2</sub>, 10 mM MgSO<sub>4</sub> (added separately from 1 M stock solution)
- **SOC:** SOB + 20 mM glucose

All media and stock solutions were autoclaved at 121 °C for 20 minutes. Antibiotics were sterilized using filtration.

## 2.2. Methods

### 2.2.1. Bacterial growth conditions

Bacteria in LB, LB agar, or SOC media were cultured at 37 °C or 30 °C for 18 hours or as required. Standard concentrations of antibiotics were used: 100 mg/L ampicillin (Amp) and 50 mg/L kanamycin (Kan).

### 2.2.2. Cell culturing

All procedures were performed under aseptic conditions, adhering to biological safety requirements. 293FT cells were cultured in DMEM (Gibco,

USA) supplemented with 10% fetal bovine serum (FBS, Gibco, USA), 0.1 mM MEM Non-Essential Amino Acids (NEAA, Gibco, USA), 6 mM L-glutamine (Gibco, USA), 1 mM MEM sodium pyruvate (Gibco, USA), 100 U/mL penicillin, 0.1 mg/mL streptomycin (Gibco, USA), and 0.5 mg/mL geneticin (Gibco, USA). HCT116, MCF7, and U87MG cell lines were maintained in DMEM with 10% FBS, 100 U/mL penicillin, and 0.1 mg/mL streptomycin. Cells were incubated at 37 °C with 5% CO<sub>2</sub> in a water-saturated incubator. For passaging, cells were detached using trypsin/EDTA (Gibco, USA) at 37 °C.

### 2.2.3. DNA manipulations

DNA manipulations were performed using standard molecular cloning techniques [240]. PCR reactions were carried out using an Eppendorf Mastercycler ep Gradient S thermocycler. DNA electrophoresis was conducted in TAE buffer (40 mM TRIS, 20 mM acetic acid, 1 mM EDTA) using a voltage range of 4–10 V/cm. Thermo Scientific™ TopVision Agarose gels at 1% concentration (or 0.8% for fragment extraction) with 0.5 µg/mL ethidium bromide were utilized and visualized under a UV transilluminator. The length of DNA fragments was determined using the Thermo Scientific™ GeneRuler DNA Ladder Mix and the concentration was measured using a nanophotometer. Plasmid DNA was isolated using the Thermo Scientific™ GeneJET Plasmid Miniprep Kit, and DNA fragments were purified from PCR products, enzymatic reaction mixtures, and agarose gels using the Thermo Scientific™ GeneJET Gel Extraction and DNA Cleanup Micro Kit, all according to the manufacturer's protocols. Various enzymes and reagents, including DNA restriction endonucleases, T4 ligase, Phusion High-Fidelity PCR Master Mix, and DreamTaq Green PCR Master Mix, were obtained from Thermo Scientific™ and used as recommended. The nucleotide sequences of the cloned DNA fragments were validated by sequencing at Azenta, Germany. All DNA sequences were analysed using Benchling [241], ApE [242] and BLAST [243] platforms.

### 2.2.4. *E. coli* competent cell preparation and transformation

For the routine transformation of *E. coli* with plasmid or ligation mix, competent cells were prepared using the calcium chloride transformation method. A colony from a fresh LB agar plate of the *E. coli* strain was inoculated into LB broth and grown at 37 °C with aeration until the culture reached an OD<sub>600</sub> of 0.5–0.7. From this point, the bacteria were kept on ice.

For each transformation, cells from 1.5 mL of the culture were collected and resuspended in 750  $\mu$ L of sterile 0.1 M  $\text{CaCl}_2$ . After incubating on ice for 20 minutes, the cells were collected again and resuspended in 100  $\mu$ L of 0.1 M  $\text{CaCl}_2$ . Up to 1  $\mu$ g of plasmid DNA or ligation mix was added to the competent cells, followed by 20 minutes incubation on ice. The cells were then heat-shocked in an Eppendorf Thermomixer at 42 °C for 1.5 minutes. Immediately after the heat shock, the cells were placed on ice for 3 minutes. Subsequently, 900  $\mu$ L of SOC medium was added, and the cells were incubated at 37 °C for 1 hour. After incubation, the cells were collected by centrifugation at 10,000  $\times g$  for 1 minute, resuspended in 100  $\mu$ L of LB medium, and plated on agar plates. The plates were then incubated overnight (or as needed) at 37 °C or 30 °C.

#### 2.2.5. Overexpression of the recombinant 6 $\times$ His-tagged proteins

The genes of interest were cloned into pET28a or pET21b vectors and then transformed into HMS174  $\Delta pyrF \Delta yqfB$  or KRX  $\Delta cdd$  cells. These transformed bacteria were cultured in LB medium supplemented with 50 mg/L Kan (for pET28a) or 100 mg/L Amp (for pET21b). The cultures were incubated at 37 °C until reaching an  $\text{OD}_{600}$  of 0.5–0.6. Subsequently, they were cooled on ice, and IPTG was added at varying final concentrations between 0.1 and 1 mM. The induced cultures were then incubated at different temperatures for either 4 hours or 18 hours. Optimal conditions for producing the highest amounts of soluble proteins were identified: 0.5 mM IPTG with 18 hours of incubation at 30 °C for YqfB, and 0.5 mM IPTG with 18 hours of incubation at 20 °C for D8\_RL. Following induction, the cells were harvested by centrifugation, resuspended in TRIS buffer (25 mM TRIS-HCl, pH 8.0, 200 mM NaCl) for YqfB, or HEPES buffer (20 mM HEPES, pH 7.5, 300 mM NaCl) for D8\_RL, and then disrupted by sonication at 750 W for 1 minute using a VC-750 ultrasound processor (Sonics & Materials, Inc.). Cell debris was removed by centrifugation at 16,000  $\times g$  for 10 minutes, yielding the cleared *E. coli* cell lysates. All procedures related to the overexpression of recombinant CDA\_EH, CDA\_F14, and CDA\_Lsp 6 $\times$ His-tagged proteins were performed by Dr. Nina Urbelienė according to previously developed protocol [15].

#### 2.2.6. Purification of 6 $\times$ His-tagged proteins

The cleared *E. coli* cell lysates, prepared as described in Chapter 2.2.5, were loaded onto a Ni-NTA column (GE Healthcare) pre-equilibrated with either

TRIS or HEPES buffer, depending on the protein of interest (specified in Chapter 2.2.5). The adsorbed proteins were then eluted using a linear gradient of 0–500 mM imidazole. Fractions containing the proteins were pooled and desalted by dialysis with TRIS or HEPES buffer. The purity of the recombinant proteins was verified by electrophoresis, and their concentrations were determined using the Lowry method [244] with bovine serum albumin as the standard.

#### 2.2.7. SDS-PAGE

Protein separation was carried out using sodium dodecyl sulfate–polyacrylamide gel electrophoresis (SDS-PAGE) according to standard methods [245]. A 4.5% stacking gel and a 14% separating gel were employed. Proteins were stained with Coomassie Brilliant Blue R-250, and the gels were subsequently destained in a warm water bath. The PageRuler™ Prestained Protein Ladder (Thermo Scientific™) was used as a molecular weight marker.

#### 2.2.8. Enzymatic activity measurements and analysis of reaction mixtures

For YqfB and D8\_RL, the enzymatic reaction mixtures contained a final 5  $\mu\text{M}$  concentration of  $N^4$ -acyl-fluorocytidines and a final 1  $\mu\text{M}$  concentration of the recombinant protein in 25 mM TRIS-HCl pH 8.0 buffer. Reactions were incubated at 37 °C for 12 hours. For CDA\_EH, CDA\_F14, and CDA\_Lsp, enzymatic reactions were carried out in a reaction buffer consisting of 10 mM Tris-HCl (pH 7.5).  $N^4$ -alkyl-fluorocytidines, 4-alkylthio-fluorouridines, and 4-alkoxy-fluoro(-2'-deoxy)uridines were prepared at a final concentration of 200  $\mu\text{M}$ . The reactions included the enzymes CDA\_EH, CDA\_F14, and CDA\_Lsp, each at a final concentration of 2  $\mu\text{M}$ . When de-acetylation was required, Grul1 esterase [246] was added to the reaction mixture to achieve a final concentration of 10  $\mu\text{M}$ . All reactions were incubated at 37 °C for 1 hour. To terminate the reactions, the mixtures were combined with an equal volume of acetonitrile and centrifuged at 30000  $\times g$  for 10 minutes.

Further procedures were carried out by dr. Agota Aučynaitė. 1–3  $\mu\text{L}$  of the prepared reaction mixtures were analyzed using liquid chromatography–tandem mass spectrometry (LC-MS). The analysis was conducted on a Nexera X2 UHPLC system coupled with an LCMS-8050 mass spectrometer (Shimadzu, Japan), equipped with an electrospray ionization (ESI) source operating in both negative and positive ionization modes. Chromatographic separation was performed using a 3  $\times$  150 mm YMC-Triart C18 column with a particle size of 3  $\mu\text{m}$  (YMC, Japan) at 40 °C. The mobile phase consisted of

0.1% formic acid (solvent A) and acetonitrile (solvent B), delivered in gradient elution mode at a flow rate of 0.45 ml/min. The following gradient program was used: 0 to 1 min, 5% solvent B; 1 to 5 min, 95% solvent B; 5 to 7 min, 95% solvent B; 7 to 8 min, 5% solvent B; 8 to 12 min, 5% solvent B. Mass scans were recorded from  $m/z$  50 to  $m/z$  750, with an interface temperature of 300 °C and a desolvation line temperature of 250 °C. Nitrogen (N<sub>2</sub>) was used as the nebulizing gas at 3 L/min and drying gas at 10 L/min, while dry air was used as the heating gas at 10 L/min. Data analysis was performed using LabSolutions LCMS software (Shimadzu).

#### 2.2.9. Generation of cell lines

Retroviral pBABE-Puro vector encoding the desired construct (1066.6 ng) were co-transfected with pCMV-gag-pol (355.6 ng) and pCMV-VSV-G (177.8 ng) (Cell Biolabs, Inc., USA) into 4 cm<sup>2</sup> size dish of ~70% confluent 293FT cells. 100 µL Opti-MEM medium (Gibco, USA) was mixed with 4 µL Lipofectamine 2000 reagent (Invitrogen, USA) and incubated for 5 minutes at room temperature. Then, plasmids diluted in 100 µL Opti-MEM medium were added to the diluted Lipofectamine 2000. Following a gentle mix and incubation at room temperature for 20 minutes, the transfection mix was added dropwise to 293FT cells. 16 hours post-transfection, fresh medium was added to the cells. 24 hours later, the retroviral medium was collected and passed through 0.45 µm sterile syringe filters. Target HCT116 and MCF7 cells (~60% confluent) were transduced with the optimized titre of the retroviral medium diluted in fresh medium (typically 1:1–1:10) containing 8 µg/mL polybrene (Sigma-Aldrich, USA) for 24 hours. The retroviral medium was then replaced with fresh medium, and 24 hours later, the medium was again replaced with fresh medium containing 2 µg/mL puromycin (Sigma-Aldrich, USA) for selection of cells which had integrated the construct. A pool of transduced cells was utilized for subsequent experiments following complete death of non-transduced cells placed under selection in parallel.

All procedures related to U87MG cells was performed by dr. Arūnas Kazlauskas. U87-CDA\_Lsp cell line, which stably expressed CDA\_Lsp, was generated by transfecting U87MG cells with linearized (*ScaI* restriction) vector pTO-CDA\_Lsp\_Flag and performing multiple rounds of selection of cells that were resistant to zeocin (500 µg/ml; Gibco, USA). At the final selection stage, cells were propagated and examined for the expression of CDA\_Lsp by Western blot analysis, as described below in this section.

## 2.2.10. Expression analysis of mRNA

Total RNA was extracted from transduced HCT116 and MCF7 cell lines using TRIzol Reagent (Thermo Scientific™) and the cDNA synthesis was performed with Maxima H Minus First Strand cDNA Synthesis Kit with dsDNase (Thermo Scientific™), according to the manufacturer's instructions. The mRNA expressions of *yqfB*, *D8\_RL*, *cda\_ah*, *cda\_f14*, and *cda\_lsp* were analyzed by Real-Time Quantitative PCR (RT-qPCR) using Luminaris Color HiGreen High ROX kit (Thermo Scientific™). The primers for the bacterial genes included: YqfB\_qPCR\_FW, YqfB\_qPCR\_RV for *yqfB* (149 bp amplicon size), D8\_qPCR\_FW, D8\_qPCR\_RV for *D8\_RL* (137 bp amplicon size), EH\_qPCR\_FW, EH\_qPCR\_RV for *cda\_ah* (137 bp amplicon size), F14\_qPCR\_FW, F14\_qPCR\_RV for *cda\_f14* (138 bp amplicon size), and Lsp\_qPCR\_FW, Lsp\_qPCR\_RV for *cda\_lsp* (146 bp amplicon size). The primers for human-optimized genes were used as follows: EH\_Hopt\_qPCR\_FW, EH\_Hopt\_qPCR\_RV for *cda\_ah* (138 bp amplicon size), F14\_Hopt\_qPCR\_FW, F14\_Hopt\_qPCR\_RV for *cda\_f14* (137 bp amplicon size), and Lsp\_Hopt\_qPCR\_FW, Lsp\_Hopt\_qPCR\_RV for *cda\_lsp* (140 bp amplicon size). In each set of RT-qPCR analyses, two negative controls were used: nuclease-free water and cells expressing "empty control" vector pBABE-Puro. Amplification parameters for all genes were those offered by the manufacturer.

## 2.2.11. Whole-cell extract preparation and Western blot analysis

Whole-cell extracts of HCT116 and MCF7 cell lines expressing YqfB, D8\_RL, CDA\_EH, CDA\_F14 or CDA\_Lsp were prepared by resuspending the cell pellet in RIPA lysis buffer (50 mM TRIS-HCl; 1.5 M NaCl, pH 7.6; 1% Triton X-100; 5 mM sodium dodecyl sulphate; 25 mM sodium deoxycholate; 1% phenylmethylsulfonyl fluoride, 0.2% aprotinin, 0.2% sodium orthovanadate). The extracts were cleared by centrifugation for 15 min at 12000 ×g at 4 °C. Subsequently, total extract proteins were fractionated by SDS-PAGE and transferred onto the 0.2 µm polyvinylidene fluoride (PVDF) membrane (PVDF Western Blotting Membranes 0.2 µm, Merck). After the blocking for 1 hour in 2% bovine serum albumin dissolved in Tris-buffered saline (TBS), the immobilized proteins were incubated overnight at 4 °C with the primary mouse monoclonal antibody against 6×His Tag (Thermo Scientific™; catalog No. MA1-21315, dilution 1:1000) or the primary rabbit monoclonal antibody against FLAG epitope Tag (DYKDDDDK Tag, Thermo Scientific™; catalog No. 701629, dilution 1:250) in blocking solution. After



extensive washing in TBS-T buffer (TBS supplemented with 0.05% Tween-20), membranes were incubated with the horseradish peroxidase- (HRP-) conjugated anti-mouse (Carl Roth, Germany; catalog No. 4759, dilution 1:10000) or anti-rabbit (Elabscience, USA; catalog No. E-AB-1003, dilution 1:10000) secondary antibody for 1 hour at 22 °C. Immunocomplexes were visualized using an enhanced chemiluminescence substrate (Pierce ECL Western Blotting Substrate, Thermo Scientific™) and documented by Uvitec Alliance imaging system (Uvitec Cambridge, United Kingdom).

Whole-cell extracts of U87MG cells (negative control) and U87-CDA\_Lsp cells expressing FLAG-tagged protein CDA\_Lsp were routinely prepared by resuspending the cell pellet in modified RIPA lysis buffer (50 mM Tris-HCl, pH 7.5, 150 mM NaCl, 1% Igepal CA-630, 0.5% sodium deoxycholate, 0.1% SDS) supplemented with a protease inhibitor cocktail (Sigma-Aldrich). Subsequently, the extracts were cleared by centrifugation for 30 min at 13000 ×g at 4 °C. 60 µg of the total extract protein was fractionated by 15% SDS-PAGE and transferred onto the 0.1 µm nitrocellulose membrane (Amersham Protran Sandwich 0.1 µm, Merck). After the blocking overnight in 5% nonfat milk dissolved in phosphate-buffered saline (PBS), the immobilized proteins were incubated for 3 h at 25 °C with the primary rabbit monoclonal antibody against FLAG epitope tag, diluted as 1:500 in blocking solution. After extensive washing in PBS-T buffer (PBS supplemented with 0.5% Tween-20), membranes were incubated with the horseradish peroxidase- (HRP-) conjugated anti-rabbit secondary antibody (Invitrogen, catalog No. 65-6120, dilution 1:2000) for 40 min at 25 °C. Immunocomplexes were visualized using a chromogenic substrate 3,3',5,5'-tetramethylbenzidine (TMB, Sigma-Aldrich) and documented by an image scanner.

#### 2.2.12. Proteomic analysis

- Preparation of cell extracts for proteomic analysis and enrichment of recombinant protein.

Whole-cell extracts of HCT116 and MCF7 cell lines stably expressing YqfB or D8\_RL amidohydrolases were prepared by resuspending the cell pellet in Urea lysis buffer (7 M Urea; 2 M Thiourea; 100 mM Dithiothreitol (DTT); 50 mM TRIS-HCl, pH 7.4; 1% phenylmethylsulfonyl fluoride, 0.2% aprotinin, 0.2% sodium orthovanadate). The extracts were cleared by centrifugation for 15 min at 12000 ×g at 4 °C. The protein concentration was estimated using Pierce Coomassie (Bradford) Protein Assay Kit (Thermo Scientific™). Cell extract was enriched for 6×His-tagged proteins 8-fold using

HisPur Ni-NTA spin column (Thermo Scientific™). Urea lysis buffer containing 10 mM imidazole was used as equilibration buffer, Urea lysis buffer containing 25 mM imidazole was used as wash buffer and Urea lysis buffer containing 250 mM imidazole was used as elution buffer. Purification procedure was performed according to manufacturer recommendations.

Further procedures were carried out by PhD student Gediminas Plakys.

- Filter aided protein sample preparation (FASP) for mass spectrometry analysis

FASP of protein samples was performed using Nanosep®, MWCO 3 kDa ultrafiltration centrifugal units (Pall Corporation, New York, NY, USA) at 13500 ×g and tryptic digestion were performed according to a modified FASP method described earlier [247]. Cell extract in lysis buffer or enriched fraction in elution buffer were loaded on centrifugal unit to result in up to 200 µg of protein. Sample buffers was exchanged with 200 µL denaturing buffer (8 M urea, 100 mM ammonium bicarbonate (ABC), pH 8.0). Denaturing buffer was exchanged for 100 µL reducing buffer (10 mM DTT in denaturing buffer). The sample in reducing buffer was incubated in an Eppendorf Thermomixer C at 37 °C 600 rpm for 60 min. After incubation, 200 µL of denaturing buffer were added to centrifugal units, after centrifugation, flowthrough was discarded. 100 µL of alkylation buffer (50 mM iodoacetamide in denaturing buffer) were added and centrifugal units were incubated at 37 °C 600 rpm for 60 min. DTT was added to yield a final concentration of 50 mM to deactivate residual iodoacetamide. Alkylation reagents were removed by centrifugation, flowthrough was discarded. Centrifugal units were washed once with 200 µL denaturing buffer, flowthrough was discarded. Three more buffer exchanges were made to FASP digestion buffer (50 mM ABC), 200 µL of FASP digestion buffer were used each time. Proteins were digested overnight in 100 µL FASP digestion buffer with a 1:50 enzyme-to-sample (w/w) ratio using Pierce, trypsin protease MS-grade (Thermo Scientific™). Centrifugal units with digestion reaction mixture were incubated in a 37 °C water bath Sub36 (Grant Instruments, Shepreth, UK) for 16 h. After digestion, the flowthrough was collected into new collection tubes, the centrifugal filter units were rinsed twice with 50 µL FASP digestion buffer, the flowthrough was collected. The solvent from the recovered peptide fraction was evaporated using a vacuum dryer Speed Vac SC110 (Thermo Savant, Waltham, MA, USA). In order to remove volatile salts, dried peptides were resuspended in 100 µL 50% methanol and vacuum dried, procedure was repeated once to remove volatile salts. Dried peptides were redissolved in 35 µL 0.1% formic acid with of 0.2

pmol/ $\mu$ L Hi3 PhosB standard peptide mixture (Waters Corporation, Milford, MA, USA). Prepared samples were analyzed by LC-MS/MS.

- Liquid chromatography and mass spectrometry

Liquid chromatography (LC) separation of trypsin cleaved peptides was performed with ACQUITY UPLC I-Class System (Waters Corporation, Milford, MA, USA). Peptides were separated on a reversed-phase analytical column ACQUITY UPLC Peptide BEH C18 Column 300 Å, 1.7  $\mu$ m, 2.1 mm  $\times$  150 mm (Waters Corporation, Milford, MA, USA) at a flow rate of 40  $\mu$ L/min, 5% solvent B was set until 2.5 min, then a linear gradient from 5% to 35% solvent B was set until 50 min, followed by a linear gradient from 35% to 85% solvent B until 51 min, 85% solvent B until 53 min, linear gradient from 85% to 5% solvent B until 53.5 min, 5% solvent B until 60 min (solvent A: 0.1% formic acid, solvent B: 100% acetonitrile and 0.1% formic acid). The analytical column temperature was set to 40 °C and injection volume was set to 10  $\mu$ L. The LC was coupled online through an ESI ionization source with Synapt G2 mass spectrometer (Waters Corporation, Milford, MA, USA). Data was acquired using MassLynx version 4.2 software (Waters Corporation, Milford, MA, USA) in positive ion mode. LC-MS data was collected using data-independent acquisition (DIA) mode MSE for 55 minutes. The source/TOF conditions were set as follows: resolution mode, capillary voltage 2.6 kV, sampling cone voltage 40 V, extraction cone voltage 4 V, source temperature 120 °C, desolvation gas flow 800 l/h at 450 °C. During spectral data acquisition, the trap collision energy of the mass spectrometer was ramped from 18 to 35 eV for high-energy scans in MSE mode, for low-energy scans collision energy was disabled. The mass range was set to 50–2000 Da with a scan time set to 0.5 s. A reference compound (2 ng/ $\mu$ L in 50% acetonitrile, 0.1% formic acid) leucine enkephalin (Waters Corporation, Milford, MA, USA) was co-infused continuously at a 8  $\mu$ L/min flow rate and scanned every 45 s as a reference for accurate mass measurements (reference mass: m/z 556.2771).

- Data processing and protein identification

For peptide and protein identification raw data files were processed using ProteinLynx Global SERVER (PLGS) version 3.0.3 (Waters Corporation, Milford, MA, USA). The following parameters were used to generate peak lists: low and elevated energy thresholds, 135 and 20 counts, respectively; reference mass correction window, 0.25 Da at 556.2771 Da/e. Processed data was analyzed using the following parameters: trypsin was selected as a primary digest reagent, one missed cleavage was permitted,

carbamidomethylation of cysteines was set as a fixed modification, deamidation of asparagine and glutamine, oxidation of methionine and carbamylation of lysine were set as variable modifications. Minimal identification criteria included 3 fragment ions per peptide, 7 fragment ions per protein and a minimum of 1 peptide per protein. The false discovery rate (FDR) was set to 4%. LC-MS proteomics data were searched against a database of 82,681 protein sequences. The protein sequence database was constructed using sequences obtained from UniProt database ([www.uniprot.org](http://www.uniprot.org)): the reference human proteome (UniProt ID: UP000005640), rabbit muscle glycogen phosphorylase (UniProt ID: P00489) and sequences of recombinant proteins YqfB [13] and D8\_RL [14].

### 2.2.13. MTT assay

The viability of cells treated with different compounds in 96 well plates was examined by a 3-(4,5-dimethyl-2-thiazolyl)-2,5-diphenyl-2-H-tetrazolium bromide (MTT) assay. Solutions of all tested compounds were prepared fresh for each experiment in DMSO diluted in the complete culture medium and added to HCT116, MCF7, or U87MG cells to a final concentration of 1–100  $\mu$ M. The concentration of DMSO in the assay never exceeded 0.02% and had no influence on cell growth. HCT116 and MCF7 cells were cultured on 96-well plates at a density of 4000 cells/well. The cells were incubated for 24 hours to allow cells to attach to the culture vessel before they were exposed to several concentrations of prodrugs for 24–48 hours. After that, culture medium was carefully removed and 100  $\mu$ L of the MTT solution (0.5 mg/mL MTT reagent (Merck, Germany) in PBS) was added to each well. The metabolically active cells reduced MTT to blue formazan crystals. After 1 hour of incubation at 37 °C, MTT-formazan crystals were dissolved in 120  $\mu$ L DMSO, 100  $\mu$ L of which was transferred to new 96-well plate suitable for optical measurements. The absorbance of the colored formazan product was measured at 540 and 650 nm by Varioskan Flash Spectrophotometer (Thermo Scientific™). The untreated cells served as negative control group. Prior to performing statistical analysis, the obtained data was processed in three steps: first, the 650 nm measurements (background) were subtracted from each individual 540 nm measurement; the mean measurement value obtained from the samples treated with DMSO was subtracted from the control group and each test cell sample group treated with different compounds; cell viability was then evaluated by comparing test samples to the negative control, with the viability of untreated cells normalized to 1. Each test group was tested in eight replicates.

The MTT assay for U87MG cells was performed as described below. U87MG (control) and U87-Lsp cells were seeded onto 96-well plates (2500 cells per well). The next day, cell culture media was replaced with media containing different concentrations of chemicals or DMSO as vehicle control. After 72 h of incubation, cells were washed with PBS, and 80  $\mu$ L of the MTT/cell medium mixture (0.5  $\mu$ g/mL of the final MTT reagent concentration) was added to each well. After 3 h of incubation at 37°C, this mixture was replaced by 100  $\mu$ L DMSO. The intensity (absorbance) of the colored formazan product was measured at 550 and 620 nm by Multiskan GO Microplate Spectrophotometer (Thermo Scientific™). The obtained data was processed as described previously in this chapter.

#### 2.2.14. Statistical analysis

All grouped MTT analysis data was presented as mean with 95% confidence interval. Comparisons between groups were made by the one-tailed Welch's t test for independent samples or one-way ANOVA followed by Tukey's multiple comparison test. The Shapiro-Wilk test was performed to evaluate deviation from normality. The significance level was chosen at  $\alpha = 0.05$  for all criteria used. Data were plotted and statistical analysis was performed using RStudio version 1.3.1073.

### 3. RESULTS

The results presented in this thesis are organized into three main sections: (1) screening of potential anticancer drug and prodrug candidates; (2) evaluation of the bacterial amidohydrolases YqfB and D8\_RL for their ability to activate prodrugs; and (3) investigation of the bacterial cytidine deaminases CDA\_EH, CDA\_F14, and CDA\_Lsp for prodrug activation.

#### 3.1. Screening of potential anticancer drug and prodrug candidates

##### 3.1.1. Effects of water-soluble asymmetric indirubin carboxylic acids on cancer cell viability

Despite ongoing advancements in cancer treatment, drug resistance and systemic toxicity remain significant barriers to effective therapy, underscoring the need for novel anticancer agents with enhanced efficacy and selectivity. Indirubin and its derivatives have emerged as promising candidates due to their established anticancer properties, which appear to be influenced by their solubility in water [2]. In earlier work, Dr. Mikas Sadauskas synthesized and purified several water-soluble 2-indolinone and indirubin carboxylic acid derivatives [254]. Building on this, the present study aimed to evaluate the anticancer activity of these newly synthesized compounds. The structures of all tested compounds are shown in Figure 3.1.

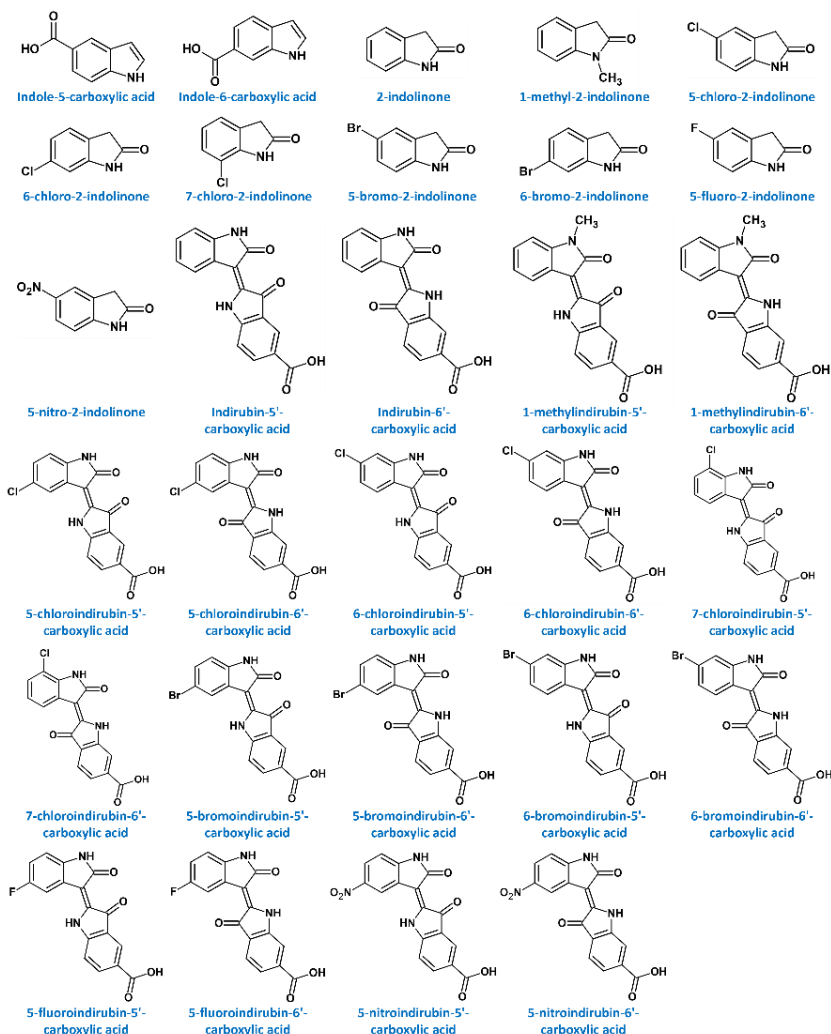


**Figure 3.1.** Indirubin carboxylic acid and 2-indolinone derivatives used in this study.

The HCT116 and MCF7 cell lines were used to test the toxicity of the selected compounds. Cells were exposed to different concentrations of the purified monocarboxyindirubins for 48 h, and viability was measured using the MTT assay (Fig 3.2). The MTT assay indirectly estimates cell viability by measuring cellular metabolic activity. It relies on reducing yellow tetrazolium salt (MTT) to purple formazan crystals, a process primarily mediated by mitochondrial dehydrogenases in metabolically active cells. Since only viable cells maintain sufficient metabolic function to catalyze this reaction, the amount of formazan formed serves as an indirect but widely accepted indicator of viable cell number. All compounds tested showed a statistically

significant reduction in cell viability. While 1-methylindirubin-5'-carboxylic acid displayed the highest cytotoxic effect for both cell lines, 5-bromoindirubin-5'-carboxylic acid and 5-nitroindirubin-6'-carboxylic acid showed high cytotoxicity for the HCT116 cell line only. Interestingly, substrates for the synthesis of monocarboxyindirubins (indole-5-carboxylic acid, indole-6-carboxylic acid, and 2-indolinone) all exhibited potent activity against the MCF7 cell line but not against HCT116 cells.

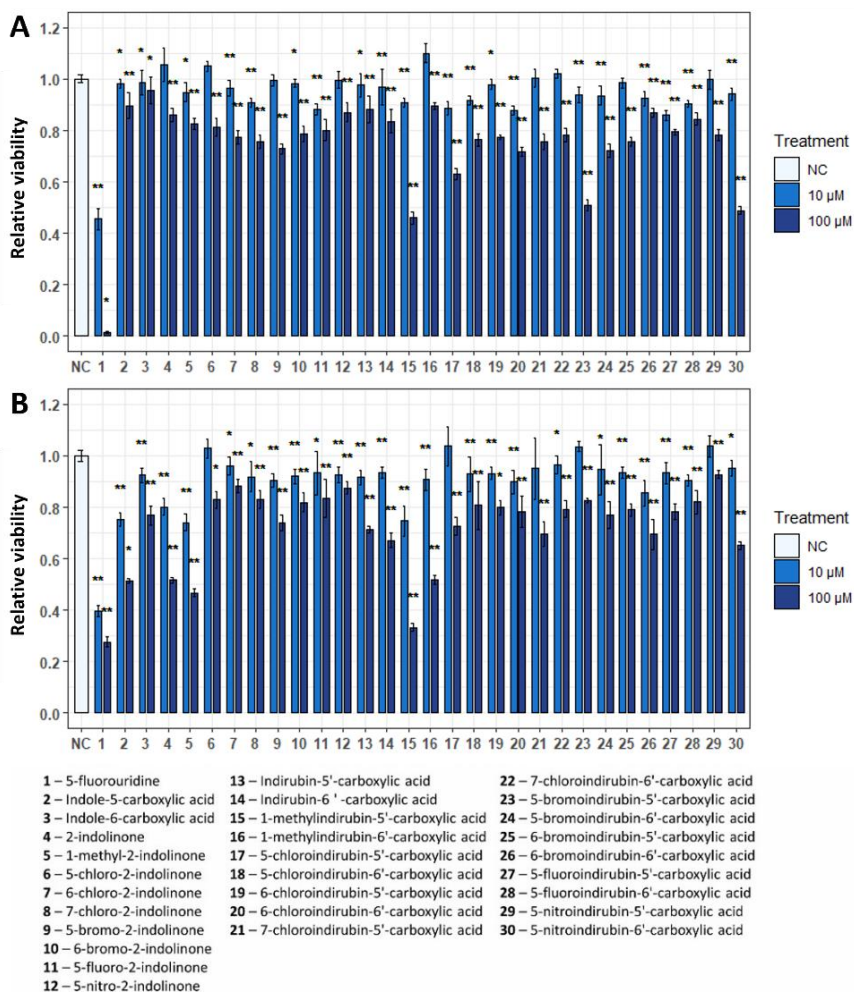


**Figure 3.2.** Cytotoxic activity of 2-indolinone and indirubin carboxylic acid derivatives against different cell lines: A – HCT116 cell line, B – MCF7 cell line. Both cell lines were treated with 10 µM and 100 µM of different indirubin carboxylic acids for 48 h. 5-fluorouridine was used as a positive control. Statistical significance is indicated by *p*-values, where the symbol \* designates *p* < 0.05, whereas the symbol \*\* designates *p* < 0.01 for untreated cells – negative control (NC).



Taken together, these data indicated that different cell lines might be differently affected by water-soluble indirubins and that certain monocarboxyindirubin, namely 1-methylindirubin-5'-carboxylic acid, represented a suitable lead compound for the development of monocarboxyindirubin-based anticancer agents. Following the results obtained, several analog compounds were synthesized and tested. This included modified 1-methylindirubin-5'-carboxylic acid derivatives and several new related agents (Fig 3.3).

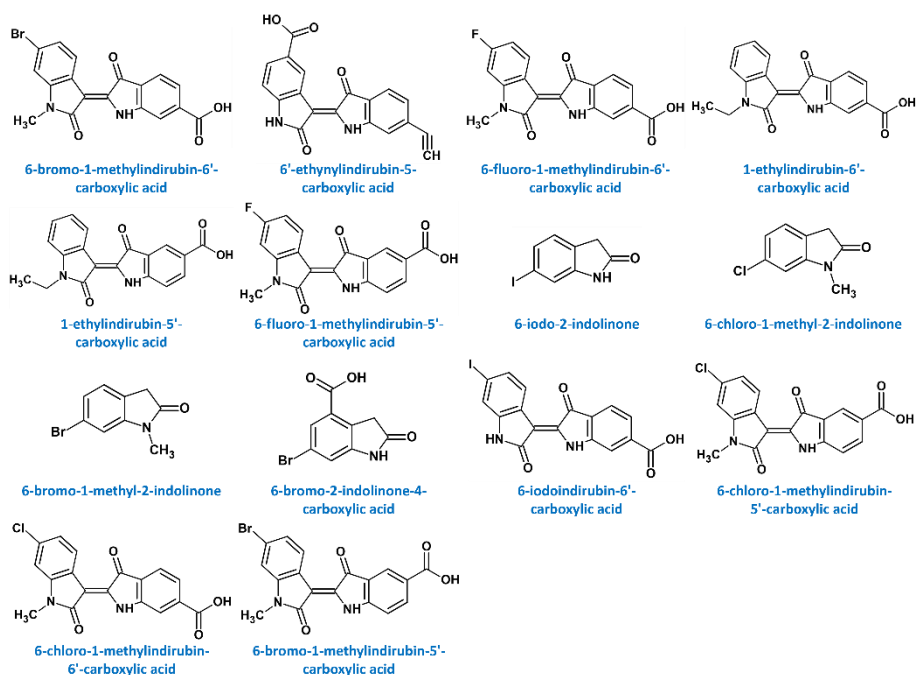


**Figure 3.3.** Modified 2-indolinones and indirubin carboxylic acids used in this study.

HCT116 and MCF7 cell lines were treated with the selected compounds, and their viability was assessed by MTT 48 hours after exposure (Fig 3.4). All compounds again resulted in a statistically significant decrease in cell viability. 6-bromo-1-methylindirubin-6'-carboxylic acid, 6-chloro-1-methylindirubin-5'-carboxylic acid, and 6-chloro-1-methylindirubin-6'-carboxylic acid displayed the highest toxicity for both cell lines tested. This indicated that not only 1-methylindirubin-5'-carboxylic acid but also its various derivatives or derivatives of 1-methylindirubin-6'-carboxylic acid could affect cancer cells in a similar or even more toxic manner. Another promising compound was 6'-ethynylindirubin-5-carboxylic acid, which was toxic to both cell lines even at lower concentration. The data provided further

evidence that monocarboxyindirubins are promising compounds for developing anticancer agents.

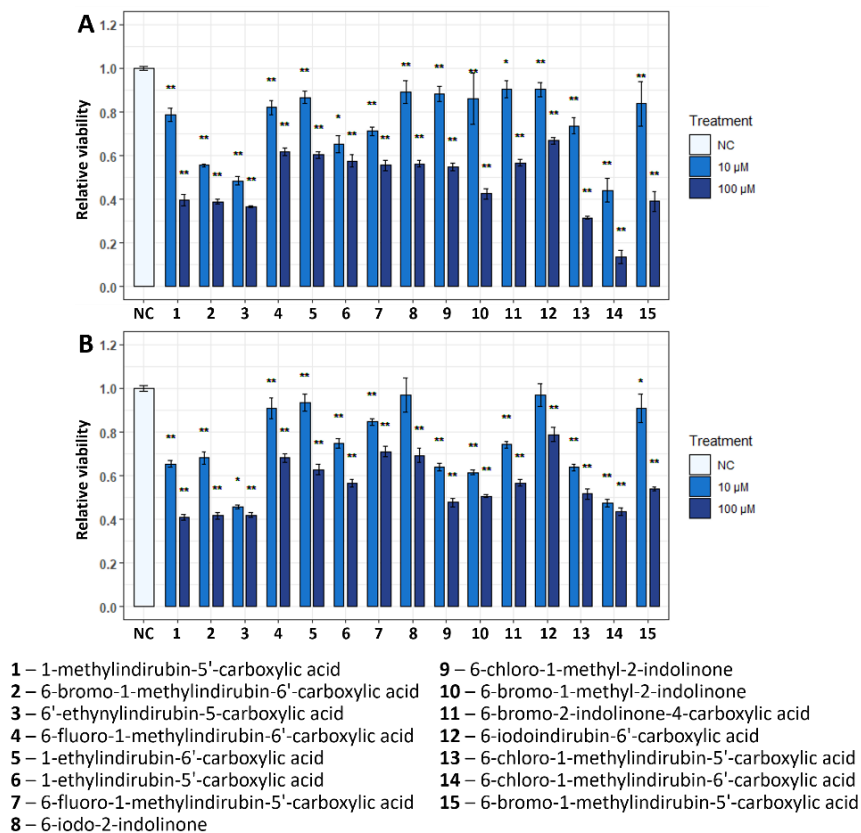


**Figure 3.4.** Cytotoxic activity of modified 2-indolinones and indirubin carboxylic acids against different cell lines: A – HCT116 cell line, B – MCF7 cell line. Both cell lines were treated with 10 µM and 100 µM of different compounds for 48 h. Statistical significance is indicated by *p*-values, where the symbol \* designates  $p < 0.05$ , whereas the symbol \*\* designates  $p < 0.01$  for untreated cells – negative control (NC).

In summary, novel compounds possessing anticancer activity were explored to offer alternatives to currently existing enzyme-prodrug strategies. Various derivatives of 2-indolinone and indirubin carboxylic acids were screened for their effects on cancer cells. Several compounds were identified as having a biologically significant adverse impact on the viability of the cancer cell lines tested. These could be the basis for developing novel prodrugs, thus contributing to improving enzyme-prodrug therapy.

### 3.1.2. Selection of cell lines potentially suitable for therapy

One of the most successful compounds with toxic activity against cancer cells is 5-fluorouracil (5FU). It is a well-known chemotherapeutic drug widely used in the treatment of a variety of cancers, including colorectal cancer and breast cancer [98]. Once inside the cells, 5FU is metabolized to 5-fluorouridine (5FUR) and 5-fluoro-2'-deoxyuridine (5FdUR), resulting in several active metabolites that inhibit the activity of thymidylate synthase and cause DNA and RNA damage (Fig 3.5). Because the mechanism of action of 5FU is well understood, we decided to look for new prodrug options targeting metabolites of this compound.

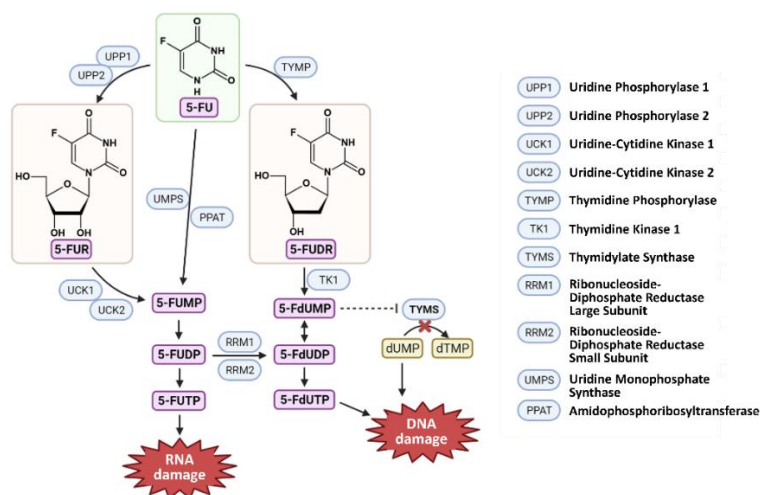


**Figure 3.5.** Mechanism of action of 5-fluorouracil. 5-FU – 5-fluorouracil; 5-FUR – 5-fluorouridine; 5-FdUR – 5-fluoro-2'-deoxyuridine; 5-FUMP – 5-fluorouridine monophosphate; 5-FUDP – 5-fluorouridine diphosphate; 5-FUTP – 5-fluorouridine triphosphate; 5-FdUMP – 5-fluoro-2'-deoxyuridine monophosphate; 5-FdUDP – 5-fluoro-2'-deoxyuridine diphosphate; 5-FdUTP – 5-fluoro-2'-deoxyuridine triphosphate; dUMP – deoxyuridine monophosphate; dTMP – deoxythymidine monophosphate. Modified according to Longley *et al.*, 2003 [98].

Cancer cells are known to exhibit innate or acquired resistance to 5FU and its metabolites [248]; therefore, several cell lines were screened for potential resistance to 5FUR to identify suitable models for further studies. The group of cells tested included immortalized human embryonic kidney cell line HEK293T, human colorectal carcinoma cell line HCT116, human breast cancer cell line MCF7, human lung adenocarcinoma cell line A549, and murine liver tumor cell line MH22a. The choice of these different cell lines

was based on the following: the HEK293T cell line acts as a gold standard in cell-based assays, which would allow rapid testing of different compounds due to its ease of manipulation; the mouse cell line was chosen to determine whether successful enzyme-prodrug pairs can be more easily transferred to animal models in the future; and the human cancer cell lines were selected in the hope of offering a targeted enzyme-prodrug pair for future use. The selected cell lines were exposed to several different concentrations of 5FUR for 24 hours, followed by viability assessment using the MTT method (Fig 3.6). As expected, the response of different cells to the same compound varies.

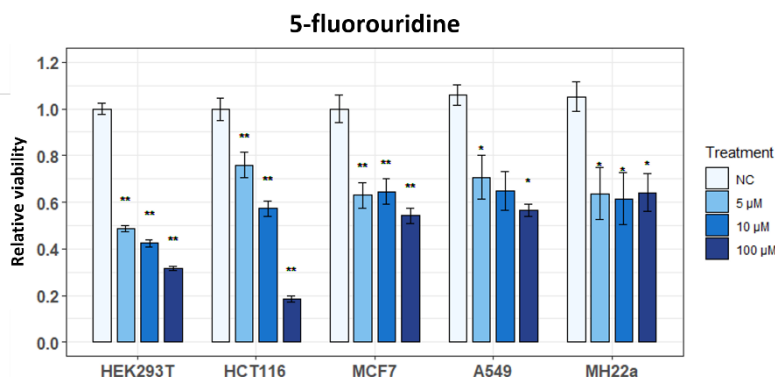


**Figure 3.6.** MTT assay of different cell lines following treatment of 5-fluorouridine (5FUR). All cell lines were exposed to concentrations of 5 μM, 10 μM, and 100 μM of the 5FUR for 24 hours. Statistical significance indicated by  $p$ -values, where the symbol \* designates  $p < 0.05$ , whereas the symbol \*\* designates  $p < 0.01$  with respect to untreated cells (negative control (NC)).

Treatment of cells with lower concentrations of 5FUR (5 μM and 10 μM) resulted in the most pronounced decrease in cell viability of HEK293T cells. This indicated the high potential of these cells for assessing the stability of prodrugs in the cellular environment, as even a random conversion from prodrug to toxic drug should be easily detected. However, it was observed that these cells were not optimal tools for the MTT assay due to their inherent property of maintaining a weak interaction with the surface of the culture plate wells. The most promising results were obtained when assessing the effect of 5FUR on the HCT116 cell line, as a concentration-dependent decrease in cell viability was observed. The other cell lines studied showed similar behavior in response to 5FUR, with a comparable level of cell viability (around 60 %) at all concentrations tested. The MCF7 cell line showed a slightly greater decrease in viability compared to A549 and MH22a, and the dispersion of the results was slightly lower. Considering the results overall, it was decided not

to exclude either cell line as a tool for screening potential prodrugs. Still, to simplify the design of the experiments, the HCT116 and MCF7 cell lines were preferred for further studies.

### 3.1.3. Effects of modified nucleosides and nucleobases on cancer cell viability

Further screening of various compounds as potential prodrugs was performed using the selected cell lines. The aim was to identify compounds that would ideally be sufficiently stable in the cellular environment to avoid the formation of a toxic drug at an off-target location and time. A suitable prodrug should be converted to a toxic drug only following bioconversion mediated by the target prodrug-activating enzyme and should have no or only minimal effect on cell viability.

To extend the sample size of the compounds to be tested, it was decided to analyze not only derivatives of 5FUR but also those of 5-fluorocytidine (5FCyd). This idea was based on the fact that cytidine deaminase is synthesized in human cells and catalyzes the conversion of 5FCyd into 5FUR [249]. To test whether 5FCyd has a similar effect on cancer cells as 5FUR, the HCT116 and MCF7 cell lines were treated with these compounds for 24 hours, followed by an MTT assay to assess cell viability (Fig 3.7). The concentrations of the compounds were chosen to range from 1 to 100  $\mu$ M.

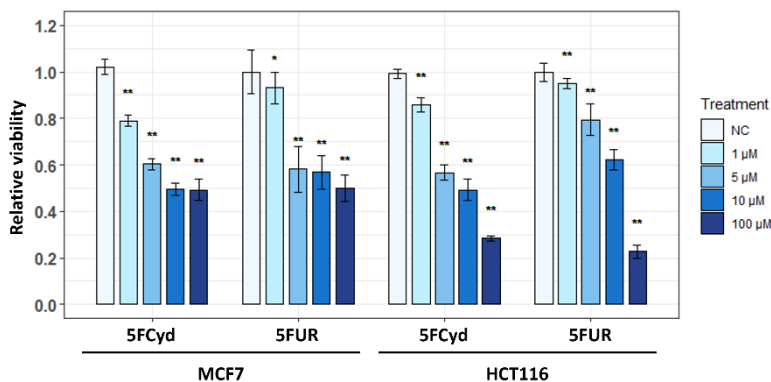


**Figure 3.7.** MTT assay of MCF7 and HCT116 cell lines following treatment of 5-fluorocytidine (5FCyd) and 5-fluorouridine (5FUR). Both cell lines were exposed to concentrations of 1–100  $\mu$ M of the target compounds for 24 hours. Statistical significance indicated by *p*-values, where the symbol \* designates  $p < 0.05$ , whereas the symbol \*\* designates  $p < 0.01$  with respect to untreated cells (negative control (NC)).

The results showed that the effects of 5FCyd and 5FUR on cell viability were highly similar for both cell lines tested. This supports the idea of using not only 5FUR but also 5FCyd derivatives for selecting prodrugs. Several 5FCyd derivatives modified at the  $N^4$  position were firstly selected, which included the 5-fluoro- $N^4$ -acetylcytidine (5FaCyd), 5-fluoro- $N^4$ -benzoylcytidine (5FbCyd), 5-fluoro- $N^4$ -pivaloylcytidine (5FpCyd), and 5-fluoro- $N^4$ -[3-indolepropionyl]cytidine (5FipCyd) (Fig 3.8), all of which were synthesized at the Department of Molecular Microbiology and Biotechnology (see chapter 2.1.1). These prodrugs could possibly be activated by enzymes possessing amidohydrolase activity.

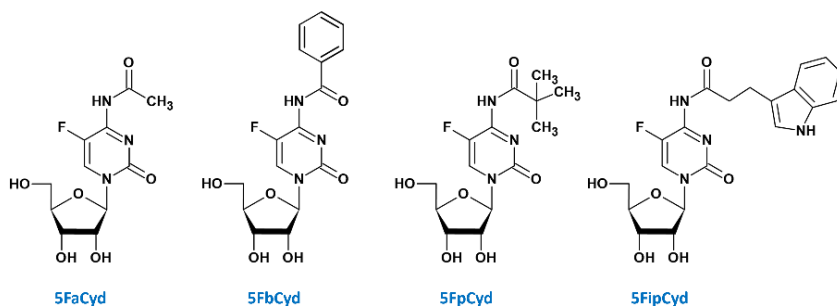


**Figure 3.8.** 5-fluorocytidine derivatives selected as potential prodrugs. 5FaCyd – 5-fluoro- $N^4$ -acetylcytidine, 5FbCyd – 5-fluoro- $N^4$ -benzoylcytidine, 5FpCyd – 5-fluoro- $N^4$ -pivaloylcytidine, 5FipCyd – 5-fluoro- $N^4$ -[3-indolepropionyl]cytidine.

To investigate whether the selected prodrugs do not exert toxic effects on eukaryotic cells prior to their activation, HCT116 and MCF7 cancer cell lines were treated with several concentrations of the target compounds (Fig 3.9). Cell viability was assessed by MTT assay 24 hours after the exposure. At lower concentrations of all tested prodrugs (1–10  $\mu$ M), the viability of HCT116 cells was not biologically significantly different compared to untreated control cells. However, cell viability was significantly reduced at a concentration of 100  $\mu$ M, and further studies should avoid concentrations above 10  $\mu$ M for these cells. MCF7 cells highlighted a slightly different response. Each prodrug individually showed a similar decrease in cell viability across the range of concentrations tested. 5FpCyd and 5FipCyd showed higher toxicity to MCF7 cells compared to 5FaCyd and 5FbCyd. However, the different results obtained between the different cell lines suggest that all the selected prodrugs should be studied further.

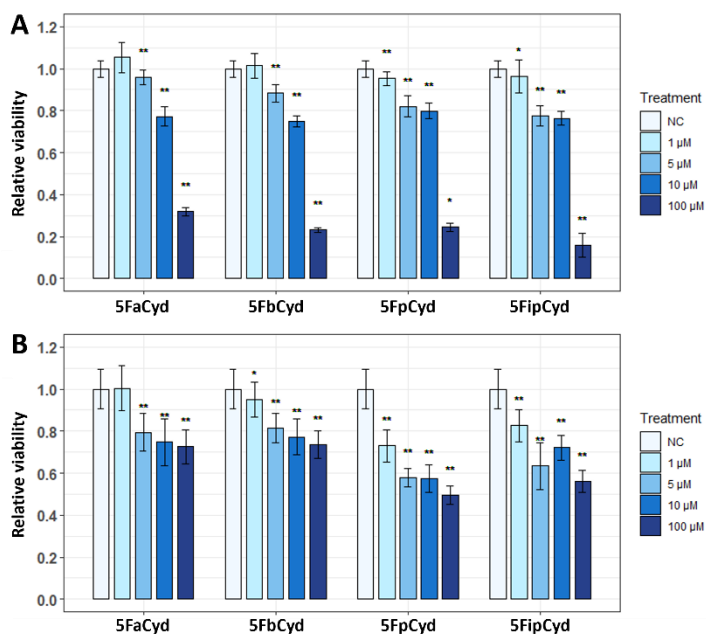


**Figure 3.9.** MTT assay of HCT116 (A) and MCF7 (B) cell lines following treatment of prodrugs. Both cell lines were exposed to concentrations of 1–100  $\mu\text{M}$  of the target prodrugs for 24 hours. 5FaCyd – 5-fluoro- $N^4$ -acetylcytidine, 5FbCyd – 5-fluoro- $N^4$ -benzoylcytidine, 5FpCyd – 5-fluoro- $N^4$ -pivaloylcytidine, 5FipCyd – 5-fluoro- $N^4$ -[3-indolepropionyl]cytidine. Statistical significance indicated by  $p$ -values, where the symbol \* designates  $p < 0.05$ , whereas the symbol \*\* designates  $p < 0.01$  with respect to untreated cells (negative control (NC)).

Other 5-fluorocytidines modified at the  $N^4$  position were also examined. This included compounds modified with larger moieties, such as C2, C3, and C4-benzoyl-benzoyl groups (Fig 3.10). It was expected that more specific enzymes could be used for the bioconversion of such derivatives, as not all enzymes are likely capable of interacting with the site required for hydrolysis. HCT116 and MCF7 cell lines were treated with 5-fluoro- $N^4$ -(C2-benzoyl-benzoyl)cytidine (5FCyd-C2), 5-fluoro- $N^4$ -(C3-benzoyl-benzoyl)cytidine (5FCyd-C3) and 5-fluoro- $N^4$ -(C4-benzoyl-benzoyl)cytidine (5FCyd-C4) at concentrations ranging from 1 to 100  $\mu\text{M}$ . After 24 hours, cell viability was evaluated by MTT (Fig 3.11). All compounds tested were non-toxic to the HCT116 cell line, except the 100  $\mu\text{M}$  concentration at which the compounds significantly reduced cell viability. For the MCF7 cell line, all tested compounds were generally more toxic compared to the HCT116 cell line, but no significant differences between the various concentrations were recorded. 5FCyd-C4 appeared to be the preferred choice for both cell lines as their

viability remained almost unchanged after exposure to this compound. Altogether, all agents were promising for further studies.

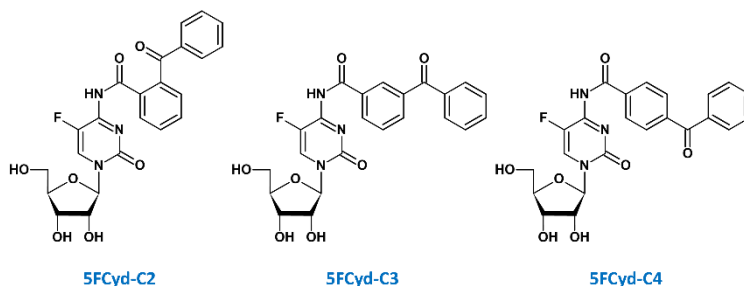


**Figure 3.10.** 5-fluoro-*N*<sup>4</sup>-(C2-benzoyl-benzoyl)cytidine (5FCyd-C2), 5-fluoro-*N*<sup>4</sup>-(C3-benzoyl-benzoyl)cytidine (5FCyd-C3) and 5-fluoro-*N*<sup>4</sup>-(C4-benzoyl-benzoyl)cytidine (5FCyd-C4) as potential prodrugs investigated in this study.

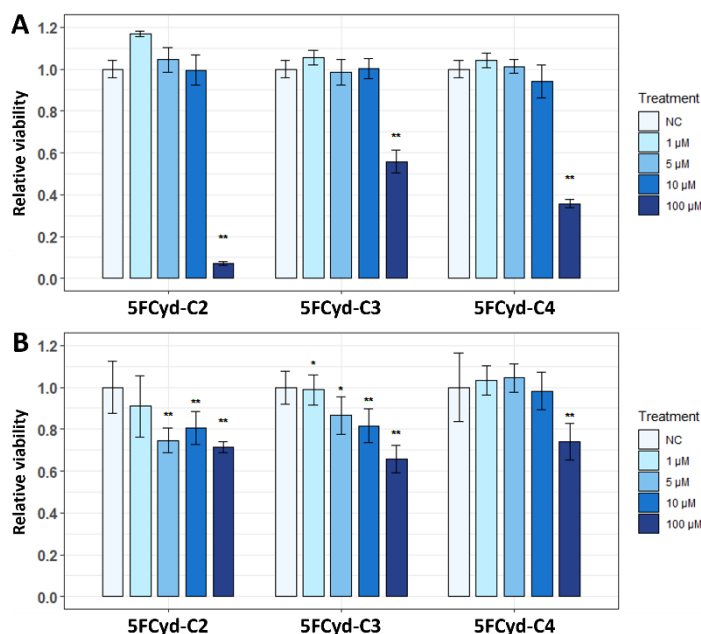


**Figure 3.11.** MTT assay of HCT116 (A) and MCF7 (B) cell lines following treatment of 5-fluoro-*N*<sup>4</sup>-(C2-benzoyl-benzoyl)cytidine (5FCyd-C2), 5-fluoro-*N*<sup>4</sup>-(C3-benzoyl-benzoyl)cytidine (5FCyd-C3) and 5-fluoro-*N*<sup>4</sup>-(C4-benzoyl-benzoyl)cytidine (5FCyd-C4). Both cell lines were exposed to concentrations of 1–100 μM of the target prodrugs for 24 hours. Statistical significance indicated by *p*-values, where the symbol \* designates *p* < 0.05, whereas the symbol \*\* designates *p* < 0.01 with respect to untreated cells (negative control (NC)).



The effect of 5-fluoroisocytosine (5FiC) and its derivative 5-fluoro-*N*<sup>2</sup>-pivaloylisocytosine (5FpiC) on cell viability was further tested (Fig 3.12). Compounds of this type can be activated by the action of isocytosine deaminase and, in the case of 5FpiC, additionally by an enzyme with amidohydrolase activity. As a result, 5FU would be obtained.

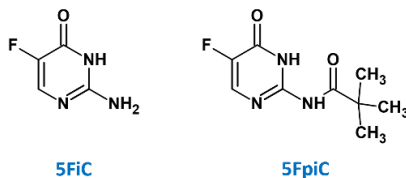


**Figure 3.12.** 5-fluoroisocytosine (5FiC) and its derivative 5-fluoro-*N*<sup>2</sup>-pivaloylisocytosine (5FpiC) selected as potential prodrugs.

HCT116 and MCF7 cell lines were treated with 5FiC and 5FpiC for 24 hours, followed by an assessment of their viability by MTT (Fig 3.13). For both cell lines examined, none of the concentrations of the compounds tested (within a range of 1 to 100  $\mu$ M) had a biologically significant effect on their viability. Identifying isocytosine deaminases and amidohydrolases suitable for activating 5FiC and 5FpiC could be promising for further studies.

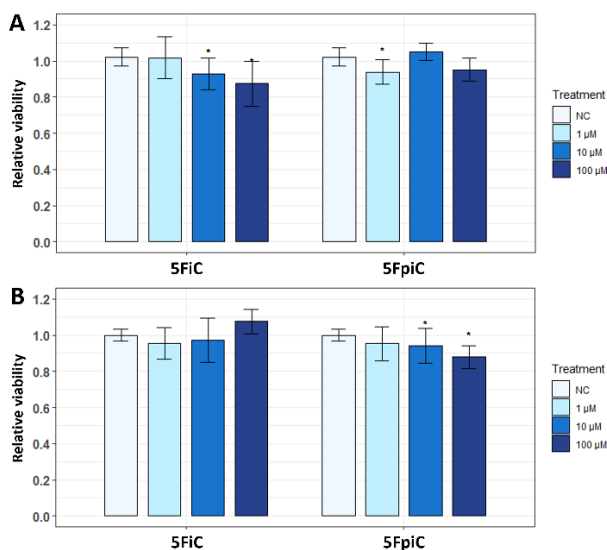


**Figure 3.13.** MTT assay of HCT116 (A) and MCF7 (B) cell lines following treatment of 5-fluoroisocytosine (5FiC) and 5-fluoro-*N*<sup>2</sup>-pivaloylisocytosine (5FpiC). Both cell lines were exposed to concentrations of 1–100  $\mu$ M of the target prodrugs for 24 hours. Statistical significance indicated by *p*-values, where the symbol \* designates *p* < 0.05, whereas the symbol \*\* designates *p* < 0.01 with respect to untreated cells (negative control (NC)).

Compounds based on 5-fluoro-2'-deoxycytidine/uridine were further tested. One such agent was 5-fluoro-4-(4-morpholinyl)-2'-deoxyuridine (5FUDR-Mo) (Fig 3.14), which, after bioconversion, would produce not only 5FUDR but also morpholine, another compound with well-known anticancer activity [250]. This choice was based on the possibility of two toxic drugs being formed from one non-toxic prodrug, which could potentially enhance the effect of the therapy. Similarly, the other compound chosen was 5-fluoro-*N*<sup>4</sup>-hexanoyl-2'-deoxycytidine (5FdCyd-Hex) (Fig 3.14), the bioconversion of which would lead to the production of 5-fluoro-2'-deoxycytidine (5FdCyd) and another anticancer compound, caproic acid [251].

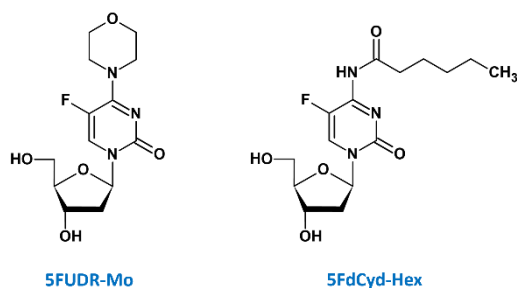


**Figure 3.14.** 5-fluoro-4-(4-morpholinyl)-2'-deoxyuridine (5FUDR-Mo) and 5-fluoro-*N*<sup>4</sup>-hexanoyl-2'-deoxycytidine (5FdCyd-Hex) used in this study.

HCT116 and MCF7 cell lines were treated with 5FUDR-Mo and 5FdCyd-Hex. After 24 hours, their viability was assessed by MTT (Fig 3.15). 5FUDR-Mo was slightly less toxic to both cell lines compared to 5FdCyd-Hex. Cell viability was approximately 85% and 70% after exposure to the highest concentration tested (100  $\mu$ M) of 5FUDR-Mo and 5FdCyd-Hex, respectively. These compounds were reasonable candidates for further studies, but the need for other options remained.

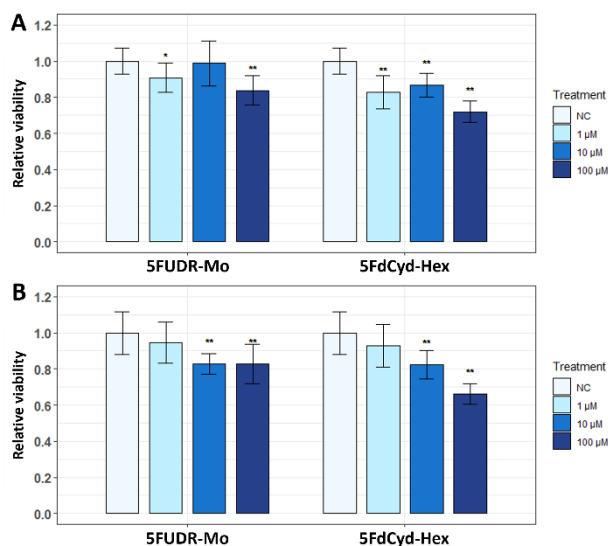


**Figure 3.15.** MTT assay of HCT116 (A) and MCF7 (B) cell lines following treatment of 5-fluoro-4-(4-morpholinyl)-2'-deoxyuridine (5FUDR-Mo) and 5-fluoro-*N*<sup>4</sup>-hexanoyl-2'-deoxycytidine (5FdCyd-Hex). Both cell lines were exposed to concentrations of 1  $\mu$ M, 10  $\mu$ M, and 100  $\mu$ M of the target prodrugs for 24 hours. Statistical significance indicated by *p*-values, where the symbol \* designates *p* < 0.05, the symbol \*\* designates *p* < 0.01, and the symbol \*\*\* designates *p* < 0.001 with respect to untreated cells (negative control (NC)).

To follow up on the idea of using a prodrug whose bioconversion would lead to the formation of two toxic drugs, several toxic compounds were further investigated in combination. The aim was to assess the potential of a combination of two drugs before synthesizing the prodrugs on their basis. A couple of such combinations were 5FCyd and 3-bromopyruvic acid (3BrPyrA) as well as 5FUR and 6-mercaptopurine (6MP) (Fig 3.16). For both 3BrPyrA and 6MP, the anticancer activity of these compounds was reported for several different cancer types [252,253].

HCT116 and MCF7 cell lines were first exposed to 5FCyd, 3BrPyrA, and a combination of these compounds. After 24 hours, cell viability was assessed by MTT (Fig 3.17). It was observed that 3BrPyrA slightly reduced cell viability for both lines tested. However, no significant changes in cell viability were observed when evaluating the effect of 5FCyd alone and in combination with 3BrPyrA. The toxic effects of 3BrPyrA on these cells were possibly insufficient to observe significant changes in cell viability when combined with 5FCyd.

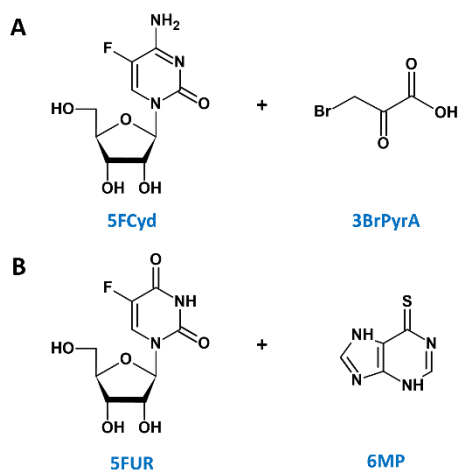


**Figure 3.16.** Drug combinations used in this study. A – 5-fluorocytidine (5FCyd) in combination with 3-bromopyruvic acid (3BrPyrA); B – 5-fluorouridine (5FUR) in combination with 6-mercaptopurine (6MP).

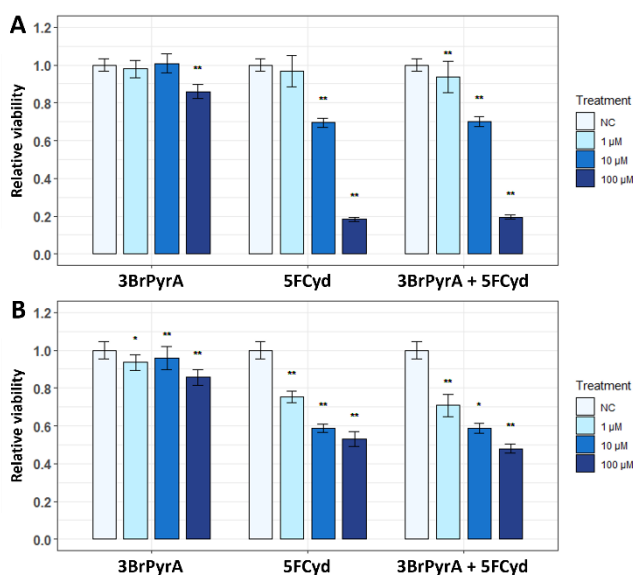


**Figure 3.17.** MTT assay of HCT116 (A) and MCF7 (B) cell lines following treatment of 3-bromopyruvic acid (3BrPyrA), 5-fluorocytidine (5FCyd), and a combination of these two compounds. Both cell lines were exposed to concentrations of 1–100  $\mu$ M of the target compounds for 24 hours. Statistical significance indicated by *p*-values, where the symbol \* designates *p* < 0.05, whereas the symbol \*\* designates *p* < 0.01 with respect to untreated cells (negative control (NC)).

Subsequently, the MCF7 cell line was exposed to 5FUR, 6MP, and a combination of these compounds. Cell viability was assessed by MTT after 24 and 48 hours (Fig 3.18). Similar results were observed at both time points. Although 6MP significantly reduces MCF7 cell viability, no significant differences were observed when comparing the effects of 5FUR alone and 5FUR in combination with 6MP. This implied that further investigation for toxic compounds that could potentiate each other's effects on cancer cells was needed.

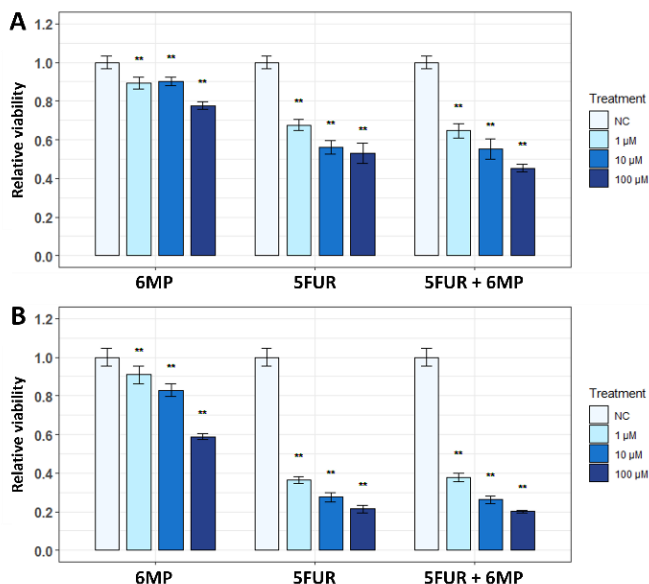


**Figure 3.18.** MTT assay of MCF7 cell line following treatment of 6-mercaptopurine (6MP), 5-fluorouridine (5FUR), and a combination of these two compounds. Cells were exposed to concentrations of 1–100  $\mu$ M of the target compounds for 24 (A) and 48 (B) hours. Statistical significance indicated by *p*-values, where the symbol \* designates  $p < 0.05$ , whereas the symbol \*\* designates  $p < 0.01$  with respect to untreated cells (negative control (NC)).

Finally, several modified 5-fluorouridines were also analyzed. The derivatives modified at the  $O^4/S^4$ -position were selected, such as 5-fluoro-4-benzoyloxyuridine (5FUR-benz), 5-fluoro-4-butoxyuridine (5FUR-but), 5-fluoro-4-methoxyuridine (5FUR-meth), 5-fluoro-4-methylthiouridine (5FUR-meththio), and 5-fluoro-4-ethylthiouridine (5FUR-eththio) (Fig 3.19). Bioconversion of these compounds by enzymes possessing amidohydrolase activity would lead directly to the formation of toxic 5FUR.

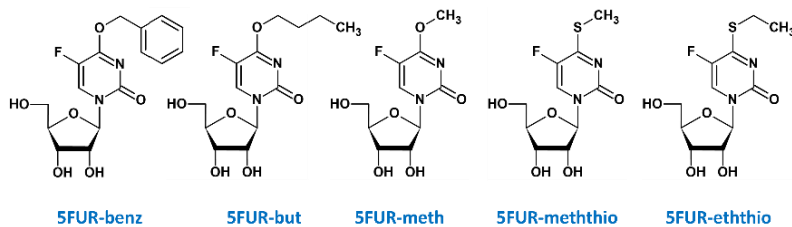


**Figure 3.19.** 5-fluorouridine derivatives selected as potential prodrugs. 5FUR-benz – 5-fluoro-4-benzyloxyuridine, 5FUR-but – 5-fluoro-4-butoxyuridine, 5FUR-meth – 5-fluoro-4-methoxyuridine, 5FUR-meththio – 5-fluoro-4-methylthiouridine, 5FUR-eththio – 5-fluoro-4-ethylthiouridine.

The HCT116 cell line was exposed to 5FUR-benz, 5FUR-but, 5FUR-meth, 5FUR-meththio, and 5FUR-eththio at several concentrations (1–100  $\mu$ M). After 24 hours, cell viability was evaluated by MTT (Fig 3.20). The results showed that 5FUR-benz and 5FUR-but did not exert a significant toxic effect on HCT116 cells at any of the concentrations tested. 5FUR-meth reduced cell viability to approximately 75% only when exposed to the highest concentration examined (100  $\mu$ M). 5FUR-meththio and 5FUR-eththio showed slightly higher toxicity to the cells tested compared to the other compounds; however, their use in further studies was not excluded. To sum up, the 5FUR derivatives investigated showed great potential to be further analyzed as candidate prodrugs.

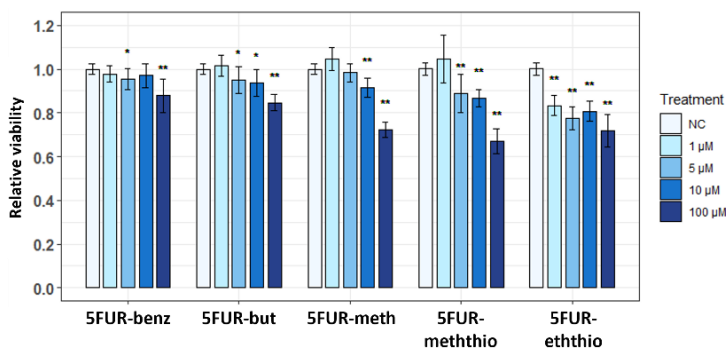


**Figure 3.20.** MTT assay of HCT116 cell line following treatment of 5-fluoro-4-benzyloxyuridine (5FUR-benz), 5-fluoro-4-butoxyuridine (5FUR-but), 5-fluoro-4-methoxyuridine (5FUR-meth), 5-fluoro-4-methylthiouridine (5FUR-meththio), and 5-fluoro-4-ethylthiouridine (5FUR-eththio). Cells were exposed to concentrations of 1–100  $\mu$ M of the target compounds for 24 hours. Statistical significance indicated by *p*-values, where the symbol \* designates *p* < 0.05, whereas the symbol \*\* designates *p* < 0.01 with respect to untreated cells (negative control (NC)).

Based on the promising results obtained in screening 5FUR derivatives as potential prodrugs, other 4-alkoxy-5-fluorouridines were also analyzed. The list of agents was expanded to include 5-fluoro-4-ethoxyuridine (5FUR-eth), 5-fluoro-4-phenoxyuridine (5FUR-phe), 5-fluoro-4-(5-isopropyl-2-methylphenoxy)-uridine (5FUR-5isopr), and 5-fluoro-4-(2-isopropyl-5-methylphenoxy)-uridine (5FUR-2isopr) (Fig 3.21).

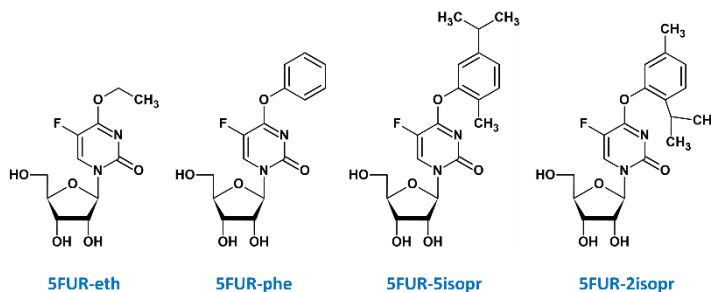


**Figure 3.21.** Modified 5-fluorouridines selected as potential prodrugs. 5FUR-eth – 5-fluoro-4-ethoxyuridine, 5FUR-phe – 5-fluoro-4-phenoxyuridine, 5FUR-5isopr – 5-fluoro-4-(5-isopropyl-2-methylphenoxy)-uridine, 5FUR-2isopr – 5-fluoro-4-(2-isopropyl-5-methylphenoxy)-uridine.

The HCT116 cell line was exposed to different concentrations of 5FUR-eth, 5FUR-phe, 5FUR-5isopr, and 5FUR-2isopr, and their viability was assessed after 24 hours by MTT (Fig 3.22). All compounds tested did not exert biologically significant toxic effects on HCT116 cells. Considering the toxicity of the potential prodrugs to cancer cells, these compounds were among the most promising options for further studies.

To summarise the results, the effects of various modified nucleosides and nucleobases on cancer cells were evaluated. The candidate prodrugs included modified 5-fluorocytidines, 5-fluoro-2'-deoxycytidines, 5-fluoroisocytosines, 5-fluorouridines, and 5-fluoro-2'-deoxyuridines. Most of these compounds showed minimal or no cytotoxicity on their own – an advantageous feature for prodrug design. Bioconversion of these compounds is expected to yield cytotoxic metabolites such as 5FU, 5FUR, or 5FUDR, whose anticancer activity and mechanisms are well established. Although identifying a suitable activating enzyme for each compound may not always be feasible, the comparative analysis of different compound classes provides valuable insights into future compound synthesis and selection directions.

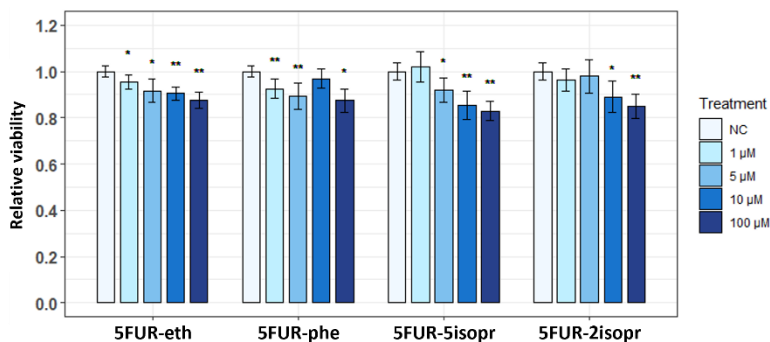


**Figure 3.22.** MTT assay of HCT116 cell line following treatment of 5-fluoro-4-ethoxyuridine (5FUR-eth), 5-fluoro-4-phenoxyuridine (5FUR-phe), 5-fluoro-4-(5-isopropyl-2-methylphenoxy)-uridine (5FUR-5isopr), and 5-fluoro-4-(2-isopropyl-5-methylphenoxy)-uridine (5FUR-2isopr). Cells were exposed to concentrations of 1–100  $\mu$ M of the target compounds for 24 hours. Statistical significance indicated by  $p$ -values, where the symbol \* designates  $p < 0.05$ , whereas the symbol \*\* designates  $p < 0.01$  with respect to untreated cells (negative control (NC)).

### 3.2. YqfB and D8\_RL amidohydrolases as prodrug activating enzymes

Optimal functioning of the enzyme-prodrug strategy is ensured by designing a non-toxic prodrug for the cells before activation and selecting an enzyme that can activate such a prodrug. The suitable enzyme should be able to activate the prodrug efficiently and in a highly specific manner. The hypothesis was that YqfB and D8\_RL amidohydrolases could possess such properties. Previously, the YqfB [15] and D8\_RL [16] proteins were described as small amidohydrolases (103 aa and 128 aa, respectively) active towards  $N^4$ -acylated cytidines, e.g.,  $N^4$ -acetylcytidine [15–17]. YqfB is the product of the *yqfB* gene in *Escherichia coli*, while D8\_RL was isolated from metagenomic libraries. Both of these enzymes are unique monomeric amidohydrolases belonging to human activating signal cointegrator homology (ASCH) domain-containing proteins, which are widespread and diverse, but so far, most of them do not have a confirmed function [18]. Although both YqfB and D8\_RL can catalyze the conversion of  $N^4$ -acylated cytidines, their structural and catalytic properties are different [16], which makes both enzymes equally interesting objects for this study. This thesis describes the potential of YqfB and D8\_RL amidohydrolases to be used as prodrug-activating enzymes.



### 3.2.1. *In vitro* screening of potential prodrugs for YqfB and D8\_RL amidohydrolases

This study investigated which prodrugs are potential substrates for YqfB and D8\_RL amidohydrolases. Several  $N^4$ -acylated 5-fluorocytidine derivatives, including 5-fluoro- $N^4$ -acetylcytidine, 5-fluoro- $N^4$ -benzoylcytidine, 5-fluoro- $N^4$ -pivaloylcytidine, and 5-fluoro- $N^4$ -[3-indolepropionyl]cytidine (see Fig 3.8), were incubated with purified enzymes and, after 12 hours of incubation, samples were analyzed by LC-MS. As expected, both YqfB and D8\_RL amidohydrolases were able to hydrolyze 5-fluoro- $N^4$ -acetylcytidine to 5-fluorocytidine (Fig 3.23) since  $N^4$ -acetylcytidine is their primary substrate. In addition, the enzymes were active towards all other substrates tested: 5-fluoro- $N^4$ -benzoylcytidine, 5-fluoro- $N^4$ -pivaloylcytidine and 5-fluoro- $N^4$ -[3-indolepropionyl]cytidine.

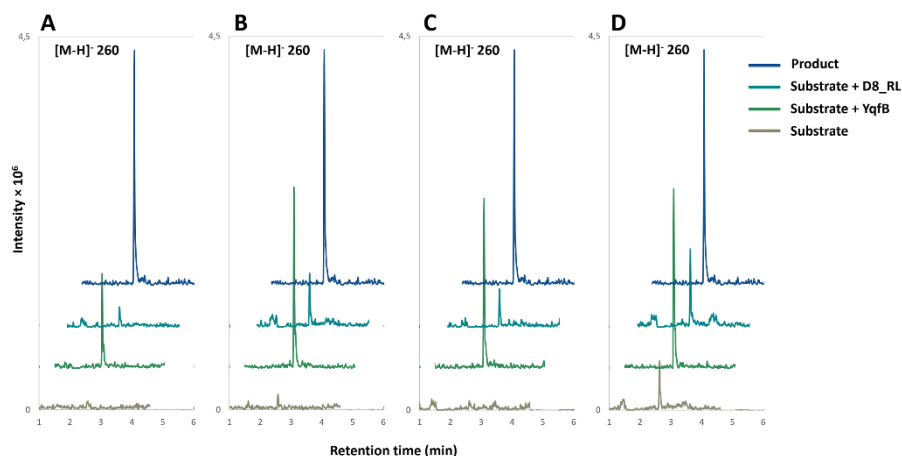


**Figure 3.23.** Substrate specificity of YqfB and D8\_RL amidohydrolases. The graphs show mass traces of the 5-fluorocytidine ( $m/z$  [M-H]<sup>+</sup> 260) in the samples from the enzymatic reactions. YqfB and D8\_RL amidohydrolases were incubated with (A) 5-fluoro- $N^4$ -acetylcytidine, (B) 5-fluoro- $N^4$ -benzoylcytidine, (C) 5-fluoro- $N^4$ -pivaloylcytidine, and (D) 5-fluoro- $N^4$ -[3-indolepropionyl]cytidine. The product 5-fluorocytidine was used as a positive control (highlighted in dark blue).

The recombinant D8\_RL enzyme displayed a lower *in vitro* efficiency than the recombinant YqfB enzyme, which needed to be considered in further studies regarding the design of experimental conditions. However, both enzymes were suitable for further analysis as even lower amounts of the product generated can lead to biologically significant changes in cell viability.

### 3.2.2. Generation of stable cell lines expressing bacterial amidohydrolases

Further, we aimed to determine whether bacterial amidohydrolases can activate prodrugs in eukaryotic cells. Cell lines stably expressing YqfB or D8\_RL amidohydrolases were generated for this purpose. Genes encoding YqfB and D8\_RL enzymes were inserted into the genome of both HCT116 and MCF7 cancer cell lines by retroviral transduction. The expression of the inserted genes in the generated cell lines was confirmed by real-time PCR (Fig 3.24).

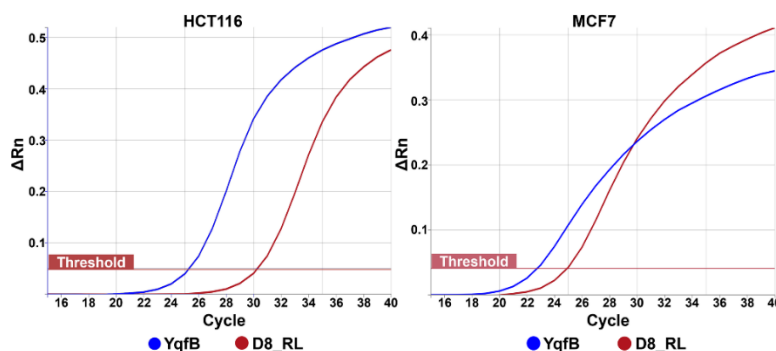


**Figure 3.24.** Confirmation of *yqfB* and *D8\_RL* expression in HCT116 and MCF7 cells by real time PCR. Amplification plots for different transduced cell lines displayed (y axis ( $\Delta Rn$ ) – normalized fluorescence of SYBR Green probe, x axis – PCR cycle number). Exponential increase of fluorescence with values crossing the threshold confirm the presence of *yqfB* and *D8\_RL* mRNA in the corresponding transduced cell lines.

To confirm YqfB and D8\_RL gene expression at the protein level, Western blot analysis was performed on protein extracts prepared from both cell lines expressing YqfB and D8\_RL amidohydrolases. No bands showing protein expression were detected. It was hypothesized that the level of these proteins in the cells is too low for detection using this method. The minimum threshold detected via Western blotting with the primary antibodies against 6×His Tag is 25 ng of protein per sample (Fig 3.25).



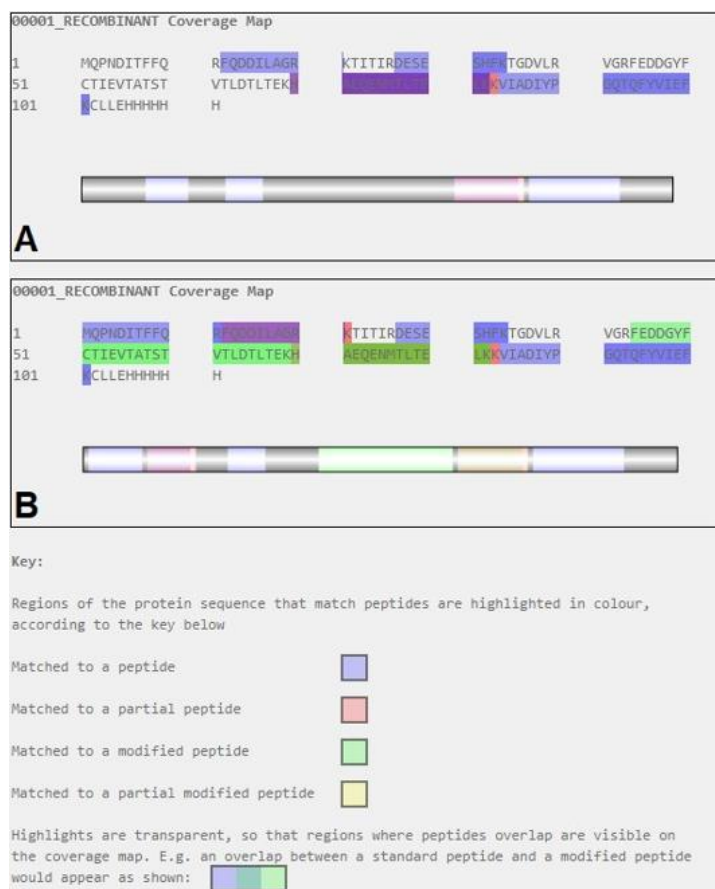


**Figure 3.26.** The graphical representation of YqfB sequence coverage obtained after tryptic digestion. A–YqfB sequence coverage (44 %) result received after replicate “HCT116\_YqfB\_Ni-NTA\_10ul” analysis; B–YqfB sequence coverage (78 %) result received after replicate “HCT116\_YqfB\_Ni-NTA\_10ul\_2” analysis. The mass spectrometry proteomics data have been deposited to the ProteomeXchange Consortium via the PRIDE partner repository with the dataset identifier PXD045918. The dataset contains database search result files. In these result files, the YqfB protein has manually assigned “00001\_RECOMBINANT” protein.Entry identifier.

### 3.2.3.Hydrolysis of prodrugs in eukaryotic cells by YqfB and D8\_RL enzymes

It was aimed to assess whether the bacterial amidohydrolases YqfB and D8\_RL have the potential to be used in enzyme-prodrug therapy. To achieve this, it was analyzed whether the target enzymes could activate prodrugs inside the cancer cells, leading to a decrease in their viability. The HCT116 and the MCF7 cell lines stably expressing YqfB or D8\_RL amidohydrolases were

treated with several different concentrations of the selected prodrugs (1–10  $\mu$ M for HCT116 and 1–100  $\mu$ M for MCF7). Cell viability was assessed by MTT assay 24 hours after the exposure and compared to control cells transduced with a vector without any gene insert (Fig 3.27).

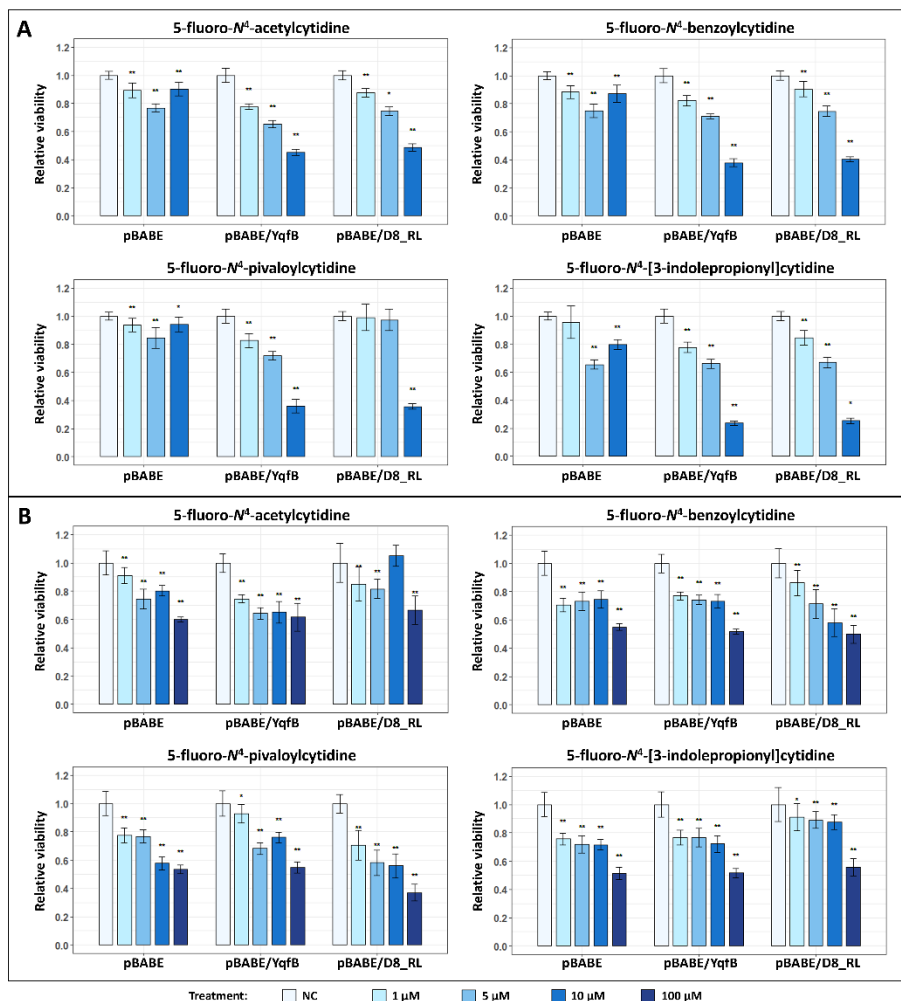


**Figure 3.27.** MTT assay of cell lines expressing YqfB and D8\_RL following treatment of prodrugs. HCT116 (A) and MCF7 (B) cell lines transduced with YqfB-encoding vector pBABE/YqfB, D8\_RL-encoding vector pBABE/D8\_RL or control vector pBABE-Puro (designated as pBABE) were exposed to several different concentrations (1–10  $\mu$ M for HCT116 and 1–100  $\mu$ M for MCF7) of prodrug 5-fluoro-*N*<sup>4</sup>-acetylcytidine, 5-fluoro-*N*<sup>4</sup>-benzoylcytidine, 5-fluoro-*N*<sup>4</sup>-pivaloylcytidine, and 5-fluoro-*N*<sup>4</sup>-[3-indolepropionyl]cytidine for the 24 hours. Statistical significance indicated by *p*-values, where the symbol \* designates *p* < 0.05, whereas the symbol \*\* designates *p* < 0.01 with respect to untreated cells (negative control (NC)).

The viability of HCT116 cell lines expressing the YqfB or D8\_RL amidohydrolase genes was significantly reduced after exposure to all tested prodrugs. Differences in cell viability between amidohydrolase-expressing and control cells were most clearly observed when cells were exposed to 10  $\mu$ M of the prodrugs. These results indicate that bacterial amidohydrolases convert the non-toxic prodrugs into the therapeutic agent 5-fluorouridine in the HCT116 cell line when acting together with cellular cytidine deaminase. These results are supported by the fact that cell viability is similarly reduced by 5-fluorocytidine and 5-fluorouridine (see Fig 3.7). However, the viability of MCF7 cell lines with inserted YqfB or D8\_RL genes did not differ from the control cells for all prodrugs tested. This suggests that although YqfB and D8\_RL amidohydrolases in combination with modified cytidine-based prodrugs could serve as novel enzyme-prodrug systems, the success of the therapy may depend on the type and/or origin of the cancer cells.

#### 3.2.4. Effect of hydrolysis products derived from the complex prodrug 5-fluoro- $N^4$ -[3-indolepropionyl]cytidine on the viability of HCT116 cells

While analyzing the effects of the activated prodrugs on the viability of the HCT116 cell line, differences in toxicity were observed, even though the cells were treated with the same concentrations of the tested compounds. YqfB and D8\_RL amidohydrolase-expressing HCT116 cells showed the most significant decrease in viability after exposure to 5-fluoro- $N^4$ -[3-indolepropionyl]cytidine (Fig 3.28). This led to the analysis of possible factors contributing to the higher toxicity of this substrate.

Hydrolysis of 5-fluoro- $N^4$ -[3-indolepropionyl]cytidine by YqfB or D8\_RL enzyme produces not only 5-fluorocytidine but also a second product – 3-indolepropionic acid. It was hypothesized that it might have an additional toxic effect on cancer cells. 3-Indolepropionic acid was shown to have cytostatic and antineoplastic properties in breast cancer [255], hence it was decided to test whether a similar effect could be observed in the target cells. HCT116 cells were treated with different concentrations of 3-indolepropionic acid, 5-fluorocytidine, and a mixture of these compounds, and cell viability was assessed by MTT after 24 hours (Fig 3.29).

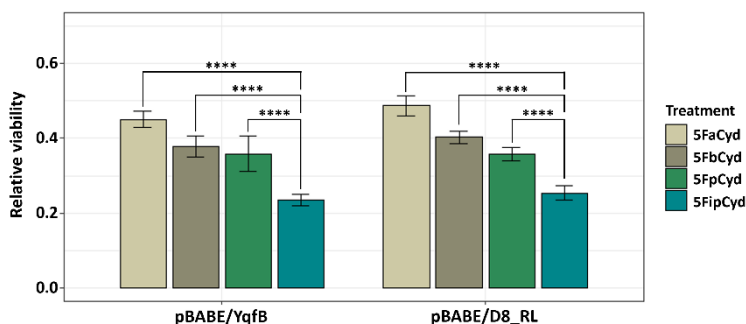


**Figure 3.28.** MTT assay of the HCT116 cell lines expressing YqfB or D8\_RL after exposure to 10  $\mu$ M of prodrugs. The HCT116 cell line transduced with a YqfB-encoding vector is designated as pBABE/YqfB and the one transduced with a D8-encoding vector is designated as pBABE/D8\_RL. 5FaCyd – 5-fluoro- $N^4$ -acetylcytidine, 5FbCyd – 5-fluoro- $N^4$ -benzoylcytidine, 5FpCyd – 5-fluoro- $N^4$ -pivaloylcytidine, 5FipCyd – 5-fluoro- $N^4$ -[3-indolepropionyl]-cytidine. Significant differences in cell viability were obtained between cells treated with different prodrugs when one-way ANOVA test (Tukey's multiple comparison) was performed (\*\*\*\* $p < 0.0001$ ).

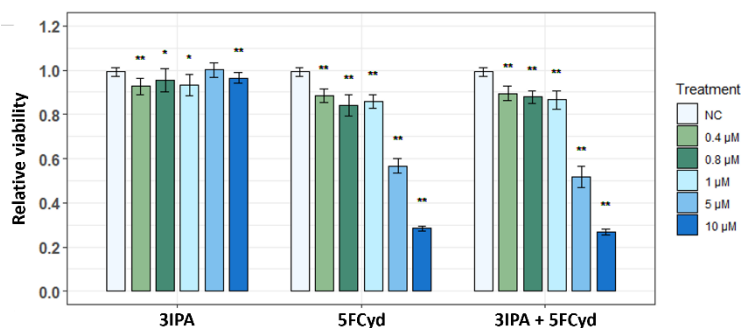


**Figure 3.29.** MTT assay of HCT116 cell line following treatment of hydrolysis products derived from the complex prodrug 5-fluoro- $N^4$ -[3-indolepropionyl]cytidine. The HCT116 cell line was exposed to concentrations of 0.4–10  $\mu$ M of 3-indolepropionic acid (3IPA), 5-fluorocytidine (5FCyd), and a mixture of these two compounds for 24 hours. Statistical significance indicated by  $p$ -values, where the symbol \* designates  $p < 0.05$ , whereas the symbol \*\* designates  $p < 0.01$  with respect to untreated cells (negative control (NC)).

The results showed that a combination of 5-fluorocytidine and 3-indolepropionic acid had nearly the same toxic effect on HCT116 cells as 5-fluorocytidine alone. No biologically significant effect of 3-indolepropionic acid on cell viability was observed. Although the literature suggests that 3-

indolepropionic acid has anticancer properties, no similar results were obtained. The origin of the cells used in this study differs from the previously described breast cancer cells, which may have contributed to the fact that the same result was not observed. 5-fluoro- $N^4$ -[3-indolepropionyl]cytidine may have higher toxicity due to any number of factors that would be worth investigating. Testing the effects of this prodrug on multiple cancer cell lines could be a starting point for further research. Another important consideration is that the hydrolysis of this substrate produces two products in equal proportions, and further studies should, therefore, consider which concentrations of both products are appropriate to achieve the maximum toxic effect on cancer cell lines.

### 3.3. Cytidine deaminases CDA\_EH, CDA\_F14, and CDA\_Lsp as prodrug activating enzymes

Recent studies by Urbelienė and colleagues have identified several prokaryotic homo-tetrameric cytidine deaminases (CDAs) capable of converting  $S^4$ -/ $N^4$ -/ $O^4$ -modified pyrimidine nucleosides, as well as 5-fluoropyrimidines directly into uridine derivatives [15]. These enzymes present advantages over conventional human CDA, as they directly generate toxic metabolites without requiring additional enzymes, such as esterases, and possess a broad substrate spectrum. These characteristics highlight the potential of newly identified CDAs in developing novel enzyme-prodrug strategies for cancer therapy. Based on this hypothesis the study was therefore focused on examining the ability of prokaryotic CDAs to activate prodrugs based on modified fluorinated nucleosides.

#### 3.3.1. CDAs target various modified fluorinated pyrimidine nucleosides

A select set of modified fluorinated pyrimidine nucleosides were synthesized to investigate their potential to be used as enzymatically activated prodrugs (Fig. 3.30). This substrate collection included control toxic compounds (**1–3**),  $N^4$ -acyl-5-fluorocytidines (**4–7**), 4-alkylthio-5-fluorouridines (**8–17**) (in both acetylated and deacetylated forms),  $N^4$ -alkyl-5-fluorocytidines (**18–24**), 4-alkoxy- and 4-aryloxy-5-fluorouridines (**25–41**) (in both acetylated and deacetylated forms), and 4-alkoxy-5-fluoro-2'-deoxyuridines (**42–49**) (in both acetylated and deacetylated forms).



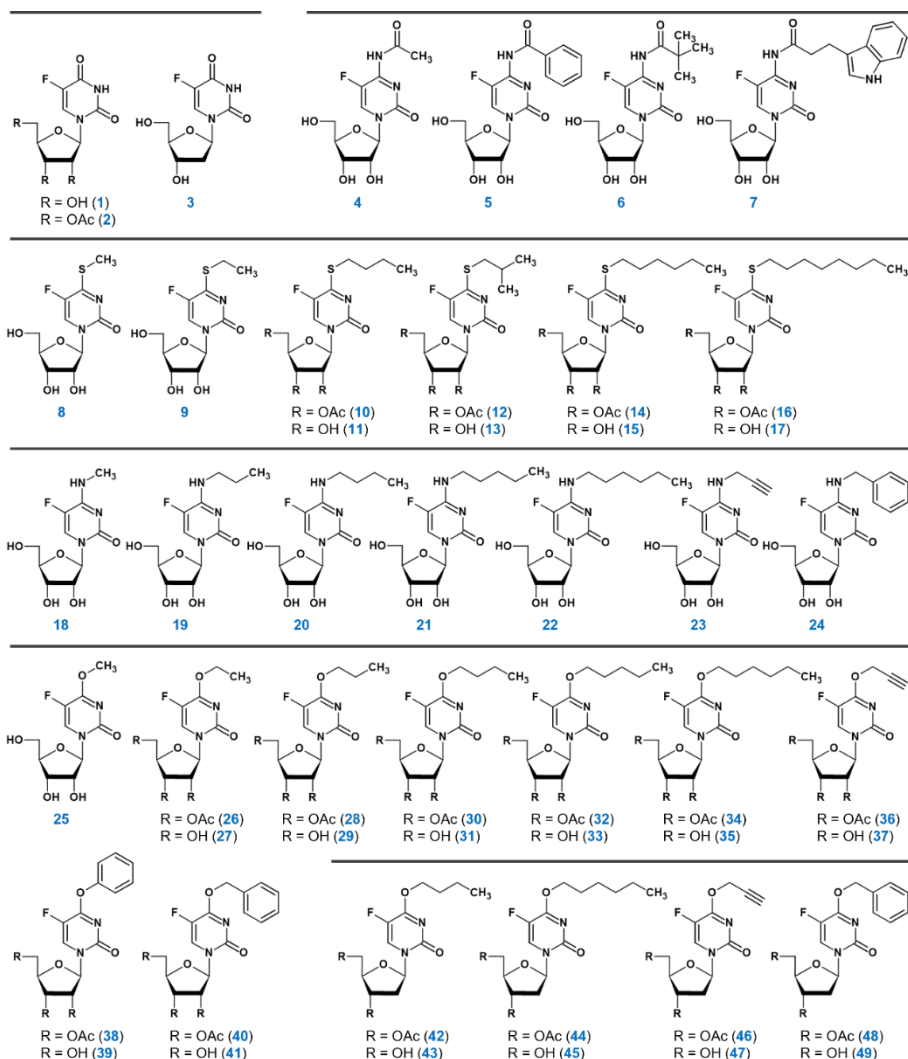


**Figure 3.30.** Structural overview of modified fluorinated pyrimidine nucleosides utilized in this study.

The synthesized substrates were evaluated for their *in vitro* enzymatic activation into toxic compounds. Three CDAs, namely CDA\_EH, CDA\_F14, and CDA\_Lsp, were selected for this analysis. Based on previously reported findings that these CDAs exhibit a broad substrate spectrum [15], they were hypothesized to activate at least some of the selected modified 5-fluoropyrimidines. Recombinant CDA\_EH, CDA\_F14, and CDA\_Lsp were overexpressed in *E. coli* HMS174 $\Delta$ pyrF $\Delta$ cdd cells and purified following previously established protocol [15]. Enzymatic activity toward the target

substrates was assessed using LC-MS, a representative chromatogram illustrating this analysis is provided in Figure 3.31.

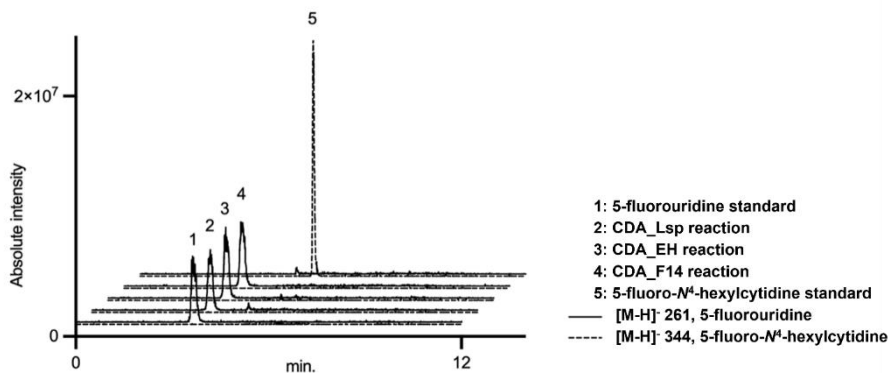


**Figure 3.31.** Representative assessment of enzymatic activity of CDA\_EH, CDA\_F14, and CDA\_Lsp towards 5-fluoro-*N*<sup>4</sup>-hexylcytidine (**22**) using LC-MS. The graph displays mass traces of 5-fluorouridine ( $m/z$  [M-H]<sup>-</sup> 261, solid lines) and 5-fluoro-*N*<sup>4</sup>-hexylcytidine ( $m/z$  [M-H]<sup>-</sup> 344, dashed lines) from enzymatic reaction samples (2, 3, 4), along with product (1) and substrate (5) standards. The analysis was performed in the same manner for all tested substrates using LabSolutions LCMS software (Shimadzu).

No conversion was detected for the acetylated substrates (**10**, **12**, **14**, **16**, **26**, **28**, **32**, **34**, **36**, **38**, **42**, **44**, **46**, **48**), indicating that CDA\_EH, CDA\_F14, and CDA\_Lsp do not accept acetylated compounds as substrates. In contrast, substrates with free ribose moiety (**11**, **13**, **15**, **17–24**, **27**, **29**, **33**, **35**, **37**, **39**, **43**, **45**, **47**, **49**) were accepted by the enzymes, with two exceptions: CDA\_EH showed only minimal activity towards 5-fluoro-*N*<sup>4</sup>-methylcytidine (**18**), producing only trace amounts of product after 1 hour; and CDA\_F14 showed no activity towards 5-fluoro-4-octylthiouridine (**17**), with no product formation detected after 1 hour. These findings highlight the ability of the evaluated CDAs to activate 5-fluoropyrimidines with diverse modifications and allow for further exploration of novel enzyme-prodrug systems in cancer cell lines.

### 3.3.2. Bacterial CDA\_Lsp activates *N*<sup>4</sup>-acyl-5-fluorocytidines in cancer cell lines

CDA\_EH, CDA\_F14, and CDA\_Lsp efficiently converted 5-fluoropyrimidine analogs *in vitro*. Therefore, we analyzed the ability of CDAs to activate modified 5-fluoropyrimidines in cancer cells. HCT116 and MCF7

cell lines were engineered to express bacterial CDAs. The genes encoding bacterial CDA\_EH, CDA\_F14, and CDA\_Lsp were individually integrated into the genomes of HCT116 and MCF7 cells via retroviral transduction. Gene expression in generated cell lines was confirmed by real-time PCR (Fig. 3.32).

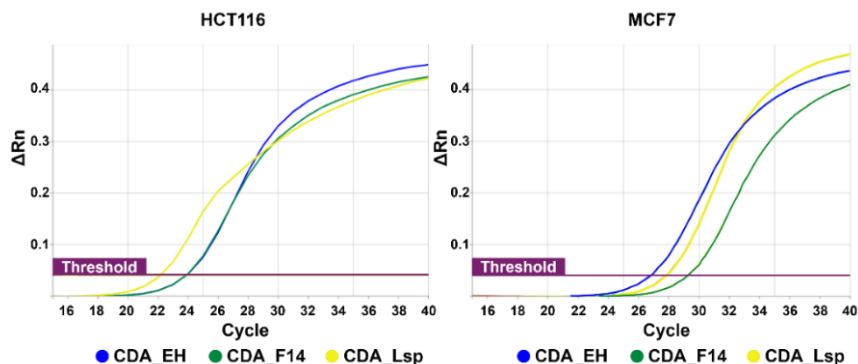


**Figure 3.32.** Confirmation of *cda\_eh*, *cda\_f14*, and *cda\_lsp* expression in HCT116 and MCF7 cells by real-time PCR. Amplification plots for different transduced cell lines displayed (y-axis ( $\Delta Rn$ ) – normalized fluorescence of SYBR Green probe, x-axis – PCR cycle number). Exponential increase of fluorescence with values crossing the threshold confirms the presence of *cda\_eh*, *cda\_f14*, and *cda\_lsp* mRNA in the corresponding transduced cell lines.

Western blot analysis was performed to assess the expression of bacterial CDAs at the protein level. Protein bands corresponding to CDA\_EH, CDA\_F14, and CDA\_Lsp were undetected in the HCT116 and MCF7 cell samples. These results align with our previous findings, where the biosynthesis of bacterial YqfB and D8\_RL enzymes in eukaryotic cells did not reach the detection threshold of the Western blot method (see chapter 3.2.2.). However, despite the low YqfB and D8\_RL expression levels, enzymatic activity was still detectable, and treatment with different prodrugs led to biologically significant viability changes in the cancer cell lines. Therefore, further investigation was undertaken to determine whether the bacterial CDAs could activate modified 5-fluoropyrimidines inside the cancer cells. The activity of CDA\_Lsp towards *N*<sup>4</sup>-acyl-5-fluorocytidines (**4–7**) was evaluated first. HCT116 and MCF7 cell lines expressing CDA\_Lsp were treated with **4–7**, with concentration ranges (1–10  $\mu$ M for HCT116 and 10–100  $\mu$ M for MCF7) selected based on our previous work (chapter 3.1.3.). Cell viability was assessed by MTT assay 24 hours post-exposure, and results were compared to control cells transduced with a vector lacking the gene insert (Fig. 3.33).

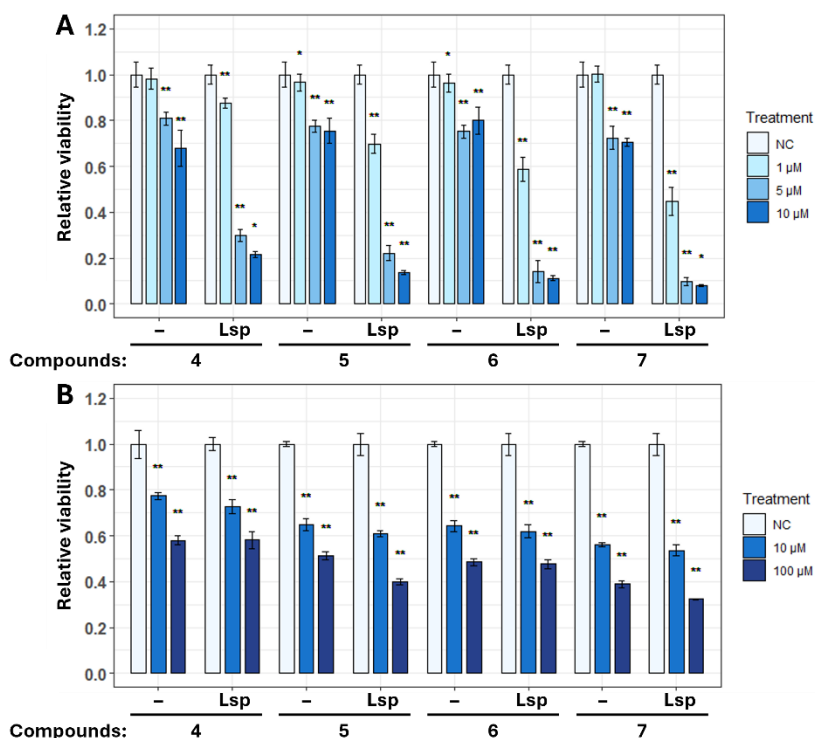


**Figure 3.33.** MTT assay of HCT116 (A) and MCF7 (B) cell lines expressing CDA\_Lsp following treatment with compounds 4–7. Cell lines transduced with CDA\_Lsp-encoding vector pBABE-CDA\_Lsp (designated as Lsp) or control vector pBABE-Puro (designated as symbol –) were exposed to several different concentrations (1–10  $\mu$ M for HCT116; 10–100  $\mu$ M for MCF7) of compounds for the 24 hours. Statistical significance is indicated by *p*-values, where the symbol \* designates *p* < 0.05, whereas the symbol \*\* designates *p* < 0.01 with respect to untreated cells (negative control (NC)).

The viability of HCT116 cells expressing CDA\_Lsp was significantly reduced following exposure to all *N*<sup>4</sup>-acyl-5-fluorocytidines tested. Notably, the most pronounced differences in viability between control and the cells expressing CDA\_Lsp were observed after treatment with 5  $\mu$ M and 10  $\mu$ M concentrations of compounds. These findings suggest CDA\_Lsp effectively activates *N*<sup>4</sup>-acyl-5-fluorocytidines within cancer cells, forming a toxic metabolite that reduces cell viability. In contrast, no significant difference in viability was observed between control and CDA\_Lsp-expressing MCF7 cells, suggesting a cell line-specific response to *N*<sup>4</sup>-acyl-5-fluorocytidines. Additionally, issues related to the stability of the compounds were noted during this study, which may have influenced the results. These observations underscore the need for

further research into modified 5-fluoropyrimidines to develop chemically stable and broadly effective compound variants.

### 3.3.3. Bacterial CDA\_EH, CDA\_F14, and CDA\_Lsp activate $S^4/O^4/N^4$ -substituted 5-fluoropyrimidines in cancer cell lines

The enzymatic activity of bacterial CDAs in catalyzing the conversion of  $S^4/O^4/N^4$ -substituted 5-fluoropyrimidines within cancer cells was further examined. HCT116 and MCF7 cell lines expressing bacterial CDA\_EH, CDA\_F14, and CDA\_Lsp were treated with 4-alkylthio-5-fluorouridines (**8**, **9**),  $N^4$ -alkyl-5-fluorocytidines (**22**, **23**), and 4-alkoxy-5-fluorouridines (**25**, **27**, **30**, **31**, **41**). Cells were exposed to the target substrates at concentrations of 5  $\mu$ M, 10  $\mu$ M, and 100  $\mu$ M for 48 hours, followed by evaluation of cell viability via MTT assay (Fig. 3.34). Detailed graphs illustrating changes in cell viability are provided in Supplement (Section S1).

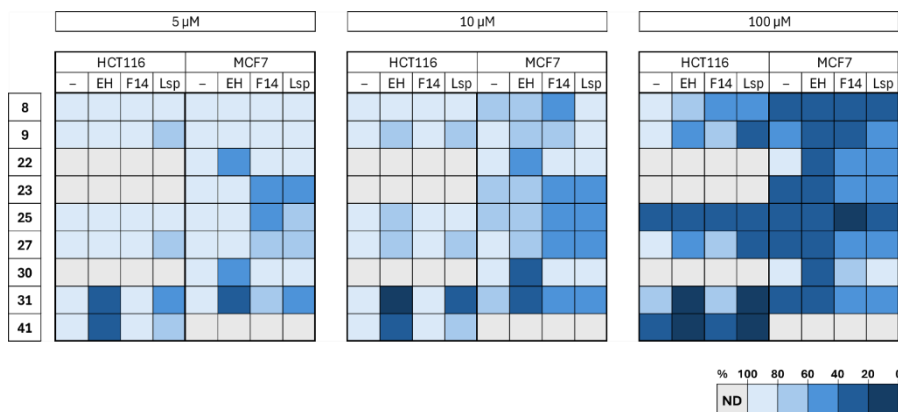


**Figure 3.34.** Graphical representation of viability changes in HCT116 and MCF7 cell lines expressing bacterial CDA\_EH, CDA\_F14, and CDA\_Lsp following exposure to  $S^4/O^4/N^4$ -substituted 5-fluoropyrimidines. Cell lines transduced with CDA\_EH-encoding vector pBABE-CDA\_EH (designated as EH), CDA\_F14-encoding vector pBABE-CDA\_F14 (designated as F14), CDA\_Lsp-encoding vector pBABE-CDA\_Lsp (designated as Lsp) or control vector pBABE-Puro (designated as symbol “-”) were exposed to 5  $\mu$ M, 10  $\mu$ M, and 100  $\mu$ M concentrations of compounds for 48 hours. ND – not determined.

The cell viability results revealed notable variations in the prodrug-activating enzymes and the cell lines. Exposure to 4-methylthio-5-fluorouridine (**8**) at the highest concentration (100  $\mu$ M) demonstrated a viability decrease of the HCT116 cell line, where more efficient conversion was observed in cells expressing CDA\_F14 and CDA\_Lsp. In contrast, compound **8** was highly

toxic to MCF7 cells, and no significant differences in cell viability were observed between control cells and those expressing the CDAs. Higher concentrations of 4-ethylthio-5-fluorouridine (**9**) effectively reduced the viability of HCT116 cells expressing CDAs, with the CDA\_Lsp enzyme showing the most efficient conversion. In MCF7 cells, CDA\_EH and CDA\_F14 were more effective; however, at higher concentrations compound **9** exhibited toxicity in control cells. The treatment of MCF7 cells with both *N*<sup>4</sup>-hexyl- and *N*<sup>4</sup>-propargyl-5-fluorocytidines (**22** and **23**) displayed differences in cell viability between CDA-expressing and control cells, even at the lowest concentration of 5  $\mu$ M. Compound **22** was more efficiently activated by CDA\_EH, whereas **23** showed greater activation by CDA\_F14 and CDA\_Lsp. Unlike **23**, compound **22** did not cause toxicity in control cells, even at a concentration of 100  $\mu$ M. The 4-alkoxy-5-fluorouridines (**25**, **27**, **30**, **31**, **41**) also produced variable results in cell viability. 4-Methoxy-5-fluorouridine (**25**) was highly toxic to both HCT116 and MCF7 cells, while 4-ethoxy-5-fluorouridine (**27**) significantly reduced cell viability in CDA\_EH and CDA\_Lsp-expressing HCT116 cells at a concentration of 100  $\mu$ M. Although 100  $\mu$ M concentration of **27** was toxic to MCF7 cells, treatment with 10  $\mu$ M of **27** in CDA\_F14 and CDA\_Lsp-expressing MCF7 cells significantly reduced cell viability. We also included acetylated derivatives in our analysis to assess the impact of ribose hydroxyl group protection on compound behavior. This approach evaluated whether acetylation enhances chemical stability and reduces cytotoxicity in control cells while enabling activation in CDA-expressing cells via intracellular esterases. 5-Fluoropyrimidines with 4-butoxy group **30** and **31** reduced the viability of CDA\_EH-expressing MCF7 cells even at 5  $\mu$ M concentration, although the conversion of these compounds was less effective in CDA\_F14 and CDA\_Lsp-expressing cells. Compound **30**, unlike **31**, did not exhibit toxic effects to control cells even at high concentrations. Since **30** is an acetylated derivative of **31**, these results suggest that the acetylated compounds may be better tolerated by the cells while still undergoing conversion in CDA-expressing cell lines. This implies that further research could directly explore using acetylated compounds without removal of protecting group prior to the cell treatment. 4-Benzoyloxy-5-fluorouridine (**41**) effectively reduced the viability of CDA\_EH-expressing HCT116 cells at concentrations of 5  $\mu$ M and 10  $\mu$ M. However, higher concentration was toxic to control cells. 5-Fluorouridines with 4-butylthio, 4-isobutylthio, 4-hexylthio and 4-octylthio substituents (**11**, **13**, **15**, **17**) and 4-phenoxy-5-fluorouridine (**39**) were also tested for their potential activation in the HCT116 cell line expressing bacterial CDA\_Lsp. While these compounds demonstrated chemical stability and had minimal impact on the viability of

control cells, no significant differences in cell viability were observed between control and CDA\_Lsp-expressing cells (Fig. S1 in Supplement Section S1). In summary, bacterial CDA\_EH, CDA\_F14, and CDA\_Lsp were capable of activating select 4-alkylthio-5-fluorouridines, *N*<sup>4</sup>-alkyl-5-fluorocytidines, and 4-alkoxy-5-fluorouridines in HCT116 and MCF7 cancer cells. Although these bacterial CDAs exhibited similar enzymatic activity, cell viability after prodrug treatment varied depending on the specific CDA expressed. Most prodrugs showed higher toxicity to control MCF7 cells than the control HCT116 cells. *N*<sup>4</sup>-alkyl-5-fluorocytidines and 4-alkoxy-5-fluorouridines offered advantages over 4-alkylthio-5-fluorouridines in reducing cell viability at lower concentrations while causing minimal toxicity to control cells. However, the observed differences between the prodrugs within the same groups underscore the importance of evaluating the effects of each compound on cancer cells individually.

#### 3.3.4. Human-optimized versions of CDA\_EH, CDA\_F14, and CDA\_Lsp provide improved activation of modified 5-fluoropyrimidines in cancer cells

The analysis of bacterial CDAs' ability to activate modified 5-fluoropyrimidines in cancer cell lines yielded mixed results. This variability may be attributed to the limited biosynthesis of bacterial enzymes in eukaryotic cells. Therefore, human codon-optimized variants of CDA\_EH, CDA\_F14, and CDA\_Lsp were developed and integrated into the genomes of HCT116 and MCF7 cells. The expression of the optimized variants in the cell lines, both at the gene and protein levels, was confirmed through real-time PCR (Fig. 3.35A) and Western blot analysis (Fig. 3.35B).

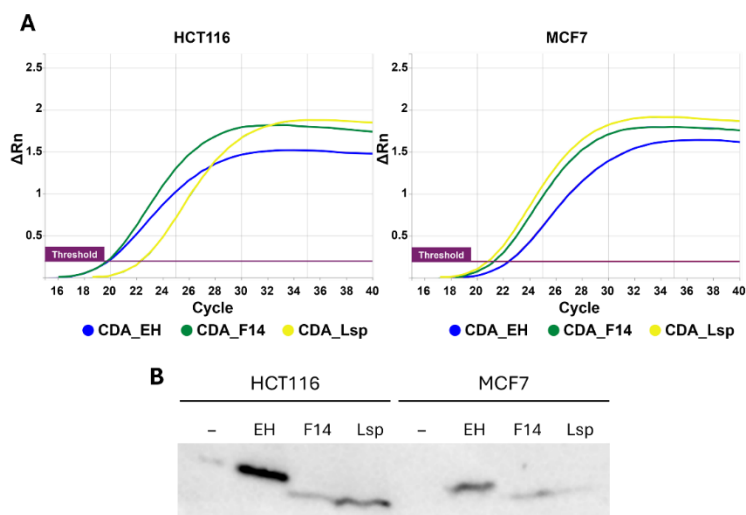


**Figure 3.35.** Expression of human codon-optimized CDA\_EH, CDA\_F14, and CDA\_Lsp in HCT116 and MCF7 cell lines at the gene (A) and protein (B) level. Amplification plots for different transduced cell lines displayed (y-axis ( $\Delta Rn$ ) – normalized fluorescence of SYBR Green probe, x-axis – PCR cycle number). Exponential increase of fluorescence with values crossing the threshold confirms the human-optimized version of *cda\_eh*, *cda\_f14*, and *cda\_lsp* mRNA in the corresponding transduced cell lines. Whole-cell extracts of HCT116 and MCF7 cell lines expressing CDA\_EH (designated as EH), CDA\_F14 (designated as F14), CDA\_Lsp (designated as Lsp) or control cells (designated as symbol –) were loaded into a gel and protein bands were detected using antibody against FLAG epitope Tag.

The conversion of modified 5-fluoropyrimidines by human codon-optimized CDAs in cancer cell lines was further examined. HCT116 and MCF7 cells expressing human-optimized CDA\_EH, CDA\_F14, and CDA\_Lsp were exposed to various compounds, including 4-alkylthio-5-fluorouridines (**8**, **9**), *N*<sup>4</sup>-alkyl-5-fluorocytidines (**18–24**), 4-alkoxy-5-fluorouridines (**25**, **27**, **28**, **30**, **31**, **32**, **34**, **36**, **40**, **41**), and 4-alkoxy-5-fluoro-2'-deoxyuridines (**42**, **44**, **46**, **48**). Two pairs of 4-alkoxy-5-fluorouridines were evaluated in both acetylated and deacetylated forms (**30** and **31**; **40** and **41**), whereas the remaining compounds were analyzed in either the acetylated or deacetylated form only. Cell viability was assessed using the MTT assay 48 hours after exposure (Fig. 3.36). Detailed graphs illustrating the changes in cell viability are provided in Supplement (Section S2).



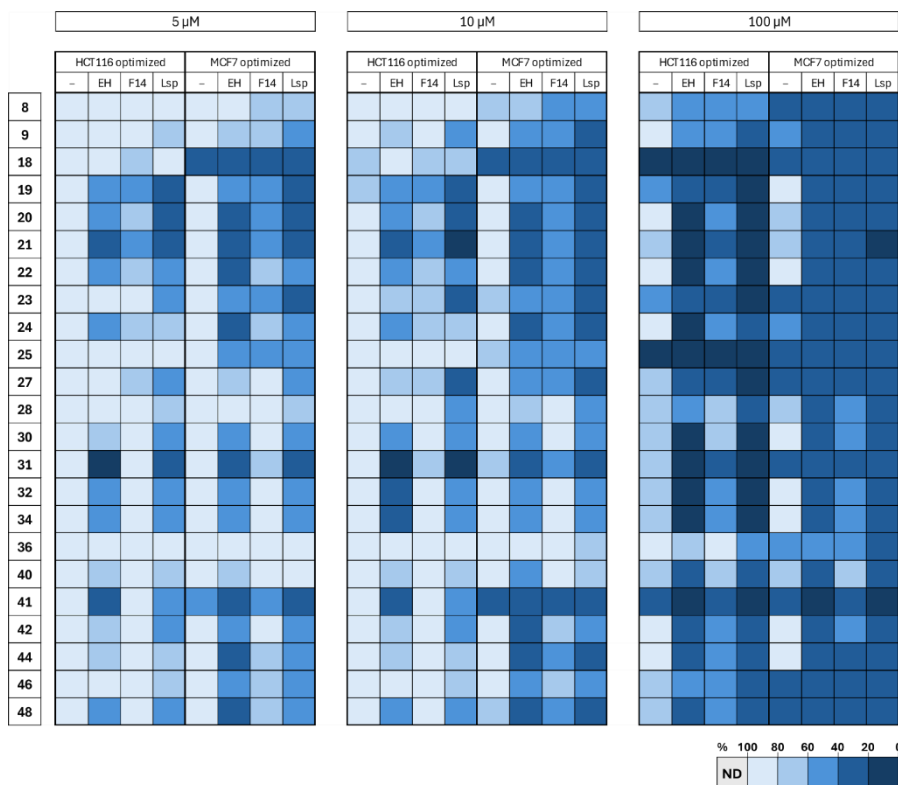


**Figure 3.36.** Graphical representation of viability changes in HCT116 and MCF7 cell lines expressing human codon-optimized CDA\_EH, CDA\_F14, and CDA\_Lsp following exposure to  $S^4/N^4/O^4$ -substituted 5-fluoropyrimidines. The cell lines were transduced with vectors encoding human-optimized CDA variants: pBABE-CDA\_EH (designated as EH), pBABE-CDA\_F14 (designated as F14), pBABE-CDA\_Lsp (designated as Lsp), or the control vector pBABE-Puro (designated as symbol “-”). Cells were exposed to 5 μM, 10 μM, and 100 μM concentrations of the selected compounds for 48 hours. ND – not determined.

None of the potential prodrugs tested exhibited intrinsic toxicity to HCT116 control cells at a concentration of 5 μM. Only minimal toxicity was observed for  $N^4$ -methyl- and  $N^4$ -propyl-5-fluorocytidines (**18** and **19**) when exposed to HCT116 control cells at 10 μM. The lowest concentrations of the tested compounds also did not induce toxicity in control MCF7 cells, with the exceptions of **18** and **41** (4-benzyloxy-5-fluorouridine). Although, **18** did not appear to be a suitable prodrug for the HCT116 cells, as no significant difference in viability was observed between control and CDA-expressing cells. In contrast, **41** significantly reduced the viability of HCT116 cells expressing CDA\_EH and CDA\_Lsp. When comparing the 4-alkylthio-5-

fluorouridines, a more pronounced effect on cell viability was observed with 4-ethylthio-substituted uridine **9** than with 4-methylthio group bearing compound **8**. Additionally, **9** activation in human codon-optimized CDA-expressing cells was more efficient than in bacterial CDA-expressing cells (see Fig. 3.34). *N*<sup>4</sup>-alkyl-5-fluorocytidines demonstrated considerable potential as prodrugs, primarily due to their efficient activation in CDA-expressing cell lines and the minimal toxicity to control cells across a wide range of concentrations. Cytidines with longer alkyl moiety (**20**, **21**, **22**, and **24**) induced significant decreases in viability in CDA-expressing HCT116 cell lines, while all of these, along with *N*<sup>4</sup>-propyl-5-fluorocytidine (**19**), also showed similar effects in CDA-expressing MCF7 cell lines. Notably, compounds **22** and **23** were more efficiently activated in human-optimized CDA-expressing cell lines compared to bacterial CDA-expressing cell lines (see Fig. 3.34). However, despite codon optimization, differences in cell viability after exposure to prodrugs between CDA\_EH, CDA\_F14, or CDA\_Lsp-expressing cell lines remained, indicating that CDAs exhibited varying preferences for different prodrugs. Most of the 4-alkoxy-5-fluorouridines tested showed potential as candidates for prodrug therapy. Compounds **27**, **30**, **31**, **32**, **34**, and **41** significantly reduced the viability of CDA-expressing HCT116 cells at the lowest concentrations tested, with similar effects observed in MCF7 cell lines for these compounds, as well as compound **25**. Compounds **25**, **27**, **30**, **31**, and **41** were more efficiently activated in human-optimized CDA-expressing cells than in bacterial CDA-expressing cells (see Fig. 3.34). The activity of different CDAs towards 4-alkoxy-5-fluorouridines in cancer cells was variable, with the most efficient conversion of prodrugs to toxic metabolites occurring in CDA\_EH and CDA\_Lsp-expressing cell lines. Acetylated 4-butoxy- and 4-benzyloxy-5-fluorouridines **30** and **40** were better tolerated by control cells at higher concentrations than their deacetylated derivatives, **31** and **41**, respectively. However, **31** and **41** were more effective than **30** and **40** in reducing the viability of CDA-expressing cells at lower concentrations. Therefore, specific experimental design should guide the choice between acetylated and deacetylated compounds for further studies. Treatment of cells with acetylated 4-alkoxy-5-fluoro-2'-deoxyuridines (**42**, **44**, **46**, **48**) produced promising results. They significantly reduced the viability of CDA\_EH- and CDA\_Lsp-expressing MCF7 cell lines when treated with 5  $\mu$ M, with similar effects observed for 2'-deoxyuridines **42** and **48** in HCT116 cell lines. A pronounced decrease in the viability of CDA-expressing cells was also noted after exposure to 100  $\mu$ M concentrations of **42** and **44**, whereas the viability of control cells remained unaffected. In summary, the results highlighted several

compounds for further evaluation, demonstrating their potential for prodrug development based on their chemical stability and effectiveness in reducing the viability of cancer cells. The varying substrate preferences of different CDAs were also observed, facilitating the selection of the most appropriate enzyme-prodrug pair for specific applications.

### 3.3.5. CDA\_Lsp activates $N^4/O^4$ -substituted fluorinated nucleosides in U87MG human glioblastoma cell line

Several compounds that effectively reduced the viability of CDA-expressing HCT116 and MCF7 cells were selected for further analysis. The human glioblastoma U87MG cell line was chosen to evaluate the versatility of the CDA-modified 5-fluoropyrimidine enzyme-prodrug system. The gene encoding human codon-optimized CDA\_Lsp was integrated into the genome of U87MG cells. The expression of CDA\_Lsp in the generated cell line was confirmed through Western blot analysis (Fig. S2 in Supplement Section S2). Next, the ability of CDA\_Lsp to activate prodrugs within U87MG cells was investigated. For this purpose,  $N^4$ -propyl- and  $N^4$ -pentyl-5-fluorocytidines (**19**, **21**), and acetylated 4-butoxy-5-fluorouridine **30**, which exhibited high efficacy in earlier experiments, were selected. The CDA\_Lsp-expressing U87MG cells were treated with **19**, **21**, and **30** for 72 hours, after which cell viability was assessed using the MTT assay (Fig. 3.37).

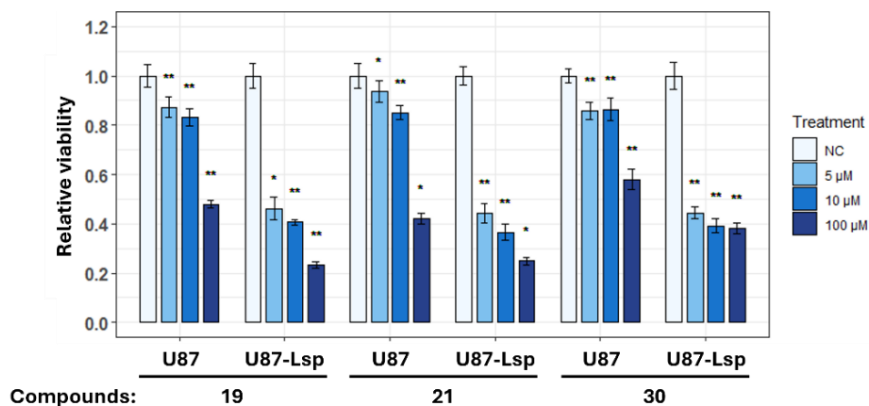


**Figure 3.37.** MTT assay of U87MG cell line expressing CDA\_Lsp following treatment of  $N^4/O^4$ -substituted 5-fluoropyrimidines. U87MG cell line expressing CDA\_Lsp (designated as U87-Lsp) or control cell line (designated as U87) were exposed to three different concentrations (5  $\mu$ M, 10  $\mu$ M, and 100  $\mu$ M) of compounds **19**, **21**, and **30** for 72 hours. Statistical significance is indicated by  $p$ -values, where the symbol \* designates  $p < 0.05$ , whereas the symbol \*\* designates  $p < 0.01$  with respect to untreated cells (negative control (NC)).

The results demonstrated a significant decrease in the viability of CDA\_Lsp-expressing U87MG cells following exposure to all tested prodrugs. While the compounds exhibited toxicity to control cells at 100  $\mu$ M, pronounced differences between control and CDA\_Lsp-expressing cells were evident at prodrug concentrations of 5  $\mu$ M and 10  $\mu$ M, thereby obviating the necessity for higher doses. These results confirm the efficacy of the CDA\_Lsp-**19/21/30** enzyme-prodrug systems in reducing the viability of U87MG cancer cells and highlight the system's versatility across various cancer cell lines.

## 4. DISCUSSION

In this thesis, a set of candidate compounds with potential for therapeutic application was identified and evaluated. The compounds investigated fall into two main categories. The first group includes 2-indolinone and indirubin carboxylic acid derivatives. Given the established anticancer activity of indirubin [2], these derivatives were assessed for their cytotoxic potential in cancer cell lines. The strategy focused on identifying novel cytotoxic compounds that could serve as alternative anticancer drug candidates for further investigation. Several derivatives significantly reduced cancer cell viability, highlighting their potential as lead compounds for future drug development and the advancement of anticancer therapies. The second group comprises analogs of 5-fluoropyrimidines that can undergo hydrolytic activation to yield the cytotoxic metabolites 5FUR and 5FUDR. This approach relied on these metabolites' well-characterized mechanisms of action *in vivo* [98], allowing the experimental focus to remain on evaluating the prodrug properties without additional mechanistic studies on their activated forms. Most of the tested 5-fluoropyrimidine analogs exhibited low or no intrinsic cytotoxicity – an advantageous property in prodrug development. These findings directed further research toward identifying selective and efficient prodrug-activating enzymes.

It is known from previous studies that various amidohydrolases, due to their physicochemical properties, are attractive objects in many fields and have potential applications in food and pharmaceutical industries as well as in biotechnology [17–19]. Here, we have demonstrated that amidohydrolases have the potential to be applied in GDEPT and used for therapeutic purposes. We also suggest four novel prodrug variants suitable for hydrolysis by the YqfB and D8\_RL enzymes, which indicates that these amidohydrolases could be used with an even wider range of potential prodrugs. This allows for the design of several enzyme-prodrug combinations, which increases the chances that at least one of the systems will be suitable for future use in the clinic. While analyzing the toxicity of our prodrugs towards various cancer cells, we found that some of these compounds were slightly toxic to the MCF7 breast cancer cell line. Advantageously, the broad range of amidohydrolase substrates will allow us to search for alternative options and reduce the likelihood of toxicity of the prodrugs prior to their activation. In addition, the YqfB and D8\_RL enzymes are relatively small (12 kDa and 15 kDa, respectively), which may be particularly useful for clinical applications, especially considering the transfer of DNA fragments. To the best of our knowledge, some of the most efficient gene transfer systems are still virus-

based, and one of the main drawbacks of this strategy is the limited packaging capacity [256]. Nevertheless, this should not affect the transfer of genes encoding YqfB and/or D8\_RL (312 bp and 387 bp, respectively). Moreover, the halotolerance of these enzymes opens up the possibility of delivering them into the tumor microenvironment as a protein likely to remain stable and active even in biological fluids such as blood. In a recent study, analogs of YqfB amidohydrolase found in other microorganisms showed better catalytic efficiency compared to YqfB for the primary substrate *N*<sup>4</sup>-acetylcytidine [257]. This suggests that more studies may lead to even better amidohydrolase enzyme-prodrug combinations to achieve the highest therapeutic efficacy.

In the present work, HCT116 and MCF7 cancer cell lines stably expressing YqfB and D8\_RL amidohydrolases were generated. Previous studies have used genes encoding human-optimized versions of bacterial enzymes [114], but we have shown here that the expression of non-optimized genes of the bacterial amidohydrolases occurs in eukaryotic cells. In HCT116 cells expressing both YqfB and D8\_RL, we observed a statistically significant decrease in cell viability when exposed to selected prodrugs, indicating that these cells synthesize active amidohydrolases capable of converting the target compounds to 5-fluorocytidine, which is subsequently converted by a cellular cytidine deaminase into its toxic form. This demonstrates that YqfB and D8\_RL amidohydrolases, in combination with *N*<sup>4</sup>-acylated 5-fluorocytidine derivatives, could be applied as novel enzyme-prodrug systems in GDEPT. To further confirm this, future studies should assess the success of the suggested enzyme-prodrug combinations using more complex systems, e.g., organotypic cultures.

We also report data showing that the viability of amidohydrolase-encoding MCF7 cells after exposure to all the tested prodrugs did not differ from that of control cells. There may be two reasons for this: either the proteins synthesized in the cells are inactive, or the prodrugs tested are excessively toxic to the MCF7 cell line, and we could no longer observe a difference between the control and the amidohydrolase-encoding cells. There is also the possibility that the selected enzyme-prodrug pairs may not be suitable for breast cancer therapy. Studies have already shown that different characteristics of cancer cell lines lead to differences in sensitivity to specific therapeutic agents [258]. These results highlight the need for further studies using other cancer cell lines to analyze the success of amidohydrolase-based enzyme-prodrug therapy under different conditions. This would also provide a better understanding of whether the system we propose is universal or could only be applied to treating a specific cancer type.

Ultimately, the enzyme-prodrug system we present has the advantage of versatile prodrug design, which could allow the production of two separate toxic compounds right after the hydrolysis of one substrate. This feature, with the appropriate combination of compounds, would reduce the concentration of the prodrug administered into the body while achieving the same or even more significant toxic effect, thus increasing the therapeutic applicability of the system. Several examples in the literature exist where a single prodrug can produce two toxic compounds that act synergistically or even have different biological effects [259,260]. One of the four prodrugs we have investigated, 5-fluoro-*N*<sup>4</sup>-[3-indolepropionyl]cytidine, also has this characteristic: both products obtained after hydrolysis – 5-fluorocytidine and 3-indolepropionic acid – are potential anticancer agents [255]. We aimed to show that their cumulative toxicity on cancer cells is greater than that of each of them individually; however, the results obtained using the HCT116 cells showed that 3-indolepropionic acid does not affect the viability of this cell line and the cumulative effect of the compounds is approximately the same as that of 5-fluorocytidine alone. Nevertheless, the possibility of masking the effect of the two compounds in a single prodrug in our proposed system remains and may be one of the most desirable features for future studies using different cancer cell lines.

In this study, we explored the ability of CDAs to activate prodrugs based on modified 5-fluoropyrimidine nucleosides. Three CDAs were selected for this investigation: CDA\_EH and CDA\_F14, which were identified in previous research through the analysis of metagenomic libraries, and CDA\_Lsp, which was detected in the intestinal microbiota [15]. Due to its ability to catalyze the conversion of a broad spectrum of substrates, CDA\_EH, CDA\_F14, and CDA\_Lsp were considered as promising candidates for prodrug activation studies. Notably, these enzymes catalyze the conversion of *S*<sup>4</sup>/*N*<sup>4</sup>/*O*<sup>4</sup>-substituted pyrimidine nucleosides to uridine derivatives. We demonstrated that the substrate specificity of these CDAs can be significantly extended to include 5-fluoropyrimidine nucleosides with different modifications at the *S*<sup>4</sup>/*N*<sup>4</sup>/*O*<sup>4</sup> positions. This enzymatic activity offers potential applications in therapies that rely on forming toxic 5FU or its nucleoside derivatives [261]. Several enzyme-prodrug therapies have been developed utilizing human CDA. For instance, the prodrug capecitabine is converted into 5FU via a three-enzyme cascade, which includes human CDA [262]. Another example is the enzyme-prodrug system involving amidohydrolases and acylated 5-fluorocytidines, developed in our previous study, which produces 5-fluorocytidine [263]. This compound is then converted to the toxic 5-

fluorouridine within cells, a process also reliant on human CDA. While these systems have demonstrated promising results, it is well known that the activity of human CDA can vary among individuals, reducing the general applicability of these therapies [264,265]. Additionally, the substrate specificity of human CDA is restricted, limiting the range of prodrugs that can be utilized [266]. In contrast, the CDAs examined in this study can directly convert modified 5-fluorocytidines into 5-fluorouridines, bypassing the need for additional enzymes, such as esterases or human CDA, in the prodrug activation process.

A range of modified 5-fluoropyrimidine nucleosides were evaluated as potential prodrugs, including  $N^4$ -acyl-5-fluorocytidines (**4–7**), 4-alkylthio-5-fluorouridines (**8–17**),  $N^4$ -alkyl-5-fluorocytidines (**18–24**), 4-alkoxy- and 4-aryloxy-5-fluorouridines (**25–41**), and 4-alkoxy-5-fluoro-2'-deoxyuridines (**42–49**). The broad selection of substrates was driven by the hypothesis that some might be activated by the investigated CDAs. Our results demonstrate that all analyzed nucleoside analogs, except for their acetylated forms, were converted to 5-fluorouridine or 5-fluoro-2'-deoxyuridine by CDA\_EH, CDA\_F14, and CDA\_Lsp *in vitro*, with the exceptions of CDA\_EH, which exhibited minimal activity toward 5-fluoro- $N^4$ -methylcytidine (**18**), and CDA\_F14 which showed no activity toward 5-fluoro-4-octylthiouridine (**17**). These findings suggest the potential for further expansion of the compound library, allowing for additional modifications at  $S^4/N^4/O^4$  positions and variations between ribonucleosides and deoxyribonucleosides. Prior studies have examined collections of pyrimidine analogs with various modifications, assessing their potential for anti-cancer activity [267–269]. In contrast, our study provides a platform for screening modified nucleoside-based prodrugs using enzymes known to activate them. This approach establishes a systematic framework for evaluating new modified pyrimidine nucleosides as potential prodrug candidates.

We further demonstrated that the investigated compounds can be activated in cancer cell lines expressing bacterial CDA\_EH, CDA\_F14, and CDA\_Lsp. Activation of  $N^4$ -acyl-5-fluorocytidines was successfully observed in the CDA\_Lsp-expressing HCT116 cell line. In contrast, no significant differences between control and CDA\_Lsp-expressing MCF7 cells were detected. These results align with the data from our previous study in which  $N^4$ -acyl-5-fluorocytidines were activated in HCT116, but not in MCF7 cell lines expressing bacterial amidohydrolases, suggesting cell type-specific response to  $N^4$ -acyl-5-fluorocytidines [263]. Furthermore, issues related to the chemical stability of  $N^4$ -acyl-5-fluorocytidines were noted during the experiments. Since prodrug strategies rely on the chemical stability of compounds [270], it



was essential to continue research to identify compounds with more favorable prodrug properties. In this context, 4-alkylthio-5-fluorouridines exhibited greater chemical stability than *N*<sup>4</sup>-acyl-5-fluorocytidines, though cell-specific responses were still observed. While no significant effects on MCF7 cell viability were noted, 4-alkylthio-5-fluorouridines significantly reduced the viability of bacterial CDA-expressing HCT116 cells, but only at the highest concentrations tested. This observation raises concerns for future studies, as anticancer agents are typically utilized at lower concentrations within the therapeutic window to avoid off-target toxicity [271]. Among the compounds tested, *N*<sup>4</sup>-alkyl-5-fluorocytidines and 4-alkoxy-5-fluorouridines demonstrated the most significant potential as prodrugs. These compounds exhibited non-toxic effects on control cells even at higher concentrations and effectively reduced the viability of CDA-expressing cells at lower concentrations. However, each compound must be evaluated individually when analyzing the viability of bacterial CDA-expressing cells.

We established that the prodrugs were activated with varying efficiencies across different bacterial CDA-expressing cell lines. This variability can be attributed to the hypothesis that the synthesis of bacterial enzymes in eukaryotic cells is hindered by differences in codon usage and tRNA abundance between organisms [272]. The expression of recombinant bacterial enzymes in mammalian cells can be enhanced through codon optimization, which resolves the expression limitations associated with codon usage and maximizes protein expression [273,274]. Consequently, human codon-optimized variants of CDA\_EH, CDA\_F14, and CDA\_Lsp were generated and integrated into the genomes of HCT116 and MCF7 cancer cell lines. The results indicated that codon optimization not only preserved the activity of the enzymes but also improved the prodrug conversion efficiency. However, differences in cell viability among the CDA\_EH, CDA\_F14, and CDA\_Lsp-expressing cell lines after prodrug treatment remained, indicating that CDAs from different bacterial sources exhibit distinct substrate preferences. Nevertheless, the platform established in this study provides an efficient method for selecting the most suitable enzyme for activating specific prodrugs while also allowing for the integration of additional CDAs into the assays as necessary.

Potential activation of 23 modified 5-fluoropyrimidine nucleosides in HCT116 and MCF7 cancer cell lines expressing human-optimized CDA variants was investigated. All prodrugs tested demonstrated greater efficacy in cell lines expressing human-optimized CDAs than in those expressing bacterial CDAs. The previously observed tendency, wherein *N*<sup>4</sup>-alkyl-5-

fluorocytidines and 4-alkoxy-5-fluorouridines exhibit greater potential as prodrugs than 4-alkylthio-5-fluorouridines, was also evident in these experimental conditions. This outcome can be attributed to two possible factors. First, CDA\_EH, CDA\_F14, and CDA\_Lsp activate 5-fluoropyrimidines with different modifications at varying efficiencies [15], leading to differences in the formation of toxic metabolites within the cells. Second, nucleoside analogs are transported across the cell membrane with varying efficiencies [275], which may limit the entry of specific prodrugs, thus restricting their conversion to toxic metabolites. The analysis of acetylated and deacetylated variants of modified 5-fluoropyrimidines revealed notable differences in efficacy and toxicity to control cells. Acetylated 5-fluoropyrimidines at the 2', 3', and 5' positions were better tolerated at higher concentrations than their deacetylated analogs. This increased tolerance may be attributed to the stability of the compounds, as the presence of additional acetyl groups limits spontaneous transformation into toxic metabolites. The conversion of acetylated prodrugs to 5-fluorouridine or 5-fluoro-2'-deoxyuridine in cells expressing CDAs requires the involvement of intracellular esterases [276], enhancing the precision of the activation mechanism. When comparing free nucleosides **31** and **41** with their acetylated counterparts **30** and **40**, exposure to low concentrations of deacetylated analogs resulted in a more significant decrease in cell viability of CDA-expressing cells, likely due to the more rapid conversion to toxic metabolites. However, the relative non-toxicity of acetylated prodrugs to control cells makes them more promising candidates for further studies. Acetylated prodrugs are also preferred over their deacetylated counterparts because acetylation often enhances the bioavailability and transport of nucleosides across cell membranes, increasing their therapeutic potential [277]. Additionally, we found decreased cell viability in CDA-expressing cells upon exposure to 4-alkoxy-5-fluoro-2'-deoxyuridines tested. Given the distinct mechanisms of toxicity associated with 5-fluorouridine and 5-fluoro-2'-deoxyuridine [248], our findings suggest a possibility to expand the range of prodrugs tested by synthesizing both modified ribonucleoside and deoxyribonucleoside variants. This approach offers a significant advantage in addressing cellular resistance to anticancer agents, as once resistance to a specific ribonucleoside analog is observed, the platform facilitates the rapid selection and testing of its deoxyribonucleoside analog, or vice versa.

Finally, we evaluated the versatility of potential enzyme-prodrug combinations in other systems. Several compounds that demonstrated the most effective decrease in viability of CDA-expressing HCT116 and MCF7

cell lines were subsequently tested in the CDA\_Lsp-expressing U87MG human glioblastoma cell line. Glioblastoma, known for its aggressive nature and resistance to many conventional chemotherapeutic agents, presents a significant challenge in cancer treatment [278]. The successful application of the enzyme-prodrug systems investigated in this study within glioblastoma cells would offer new opportunities for difficult-to-treat cancer research. The results indicated that exposure of *N*<sup>4</sup>-propyl-5-fluorocytidine (**19**), *N*<sup>4</sup>-pentyl-5-fluorocytidine (**21**), and acetylated 4-butoxy-5-fluorouridine (**30**) to CDA\_Lsp-expressing U87MG cells effectively reduced cell viability. This finding highlights the efficacy of the CDA\_Lsp-**19/21/30** combinations across different cell line origins. Ultimately, this platform could be translated into clinical settings through targeted gene delivery strategies, enabling tumor-specific expression of selected CDAs to locally activate 5-fluoropyrimidine prodrugs and reduce systemic toxicity. However, further studies are required to validate the broader applicability of these strategies, including testing in additional cancer cell lines and more complex experimental models.

In conclusion, this study introduced a platform designed to efficiently screen modified 5-fluoropyrimidine nucleosides as potential prodrugs, utilizing CDAs of bacterial origin. We identified several enzyme-prodrug combinations that effectively reduced cancer cell viability. Additionally, we demonstrated the potential of *N*<sup>4</sup>-alkyl-5-fluorocytidines and 4-alkoxy-5-fluorouridines as prodrugs. Finally, our platform supports a wide range of 5-fluoropyrimidine analogs and diverse activating enzymes, making it a flexible and effective tool for rapidly identifying and evaluating new targets for further studies.

## CONCLUSIONS

1. Derivatives of 2-indolinone and indirubin carboxylic acid exhibited significant cytotoxicity against HCT116 and MCF7 cancer cell lines, supporting their potential as candidates for anticancer drug development.
2. A diverse range of modified 5-fluoropyrimidine nucleosides showed minimal intrinsic cytotoxicity across cancer cell lines, confirming their suitability as prodrugs for targeted cancer therapy.
3. Bacterial amidohydrolases YqfB and D8\_RL effectively activated *N*<sup>4</sup>-acylated 5-fluorocytidine-based prodrugs, significantly reducing cancer cell viability and demonstrating their potential as prodrug-activating enzymes.
4. Bacterial cytidine deaminases CDA\_EH, CDA\_F14, and CDA\_Lsp efficiently activated a broad range of 5-fluoropyrimidine prodrugs, with *N*<sup>4</sup>-alkyl-5-fluorocytidines and 4-alkoxy-5-fluorouridines exhibiting significant, selective cytotoxicity in CDA-expressing cells, supporting their potential for use in targeted cancer therapy.

## REFERENCES

- 1 Dallavalle S, Dobričić V, Lazzarato L, *et al.* Improvement of conventional anti-cancer drugs as new tools against multidrug resistant tumors. *Drug Resist Updat.* 2020;50:100682. doi: 10.1016/j.drug.2020.100682
- 2 Wang H, Wang Z, Wei C, *et al.* Anticancer potential of indirubins in medicinal chemistry: Biological activity, structural modification, and structure-activity relationship. *Eur J Med Chem.* 2021;223:113652. doi: 10.1016/j.ejmech.2021.113652
- 3 Schäfer M, Semmler ML, Bernhardt T, *et al.* Small Molecules in the Treatment of Squamous Cell Carcinomas: Focus on Indirubins. *Cancers.* 2021;13:1770. doi: 10.3390/cancers13081770
- 4 Zhang J, Kale V, Chen M. Gene-Directed Enzyme Prodrug Therapy. *AAPS J.* 2014;17:102–10. doi: 10.1208/s12248-014-9675-7
- 5 Schellmann N, Deckert PM, Bachran D, *et al.* Targeted enzyme prodrug therapies. *Mini Rev Med Chem.* 2010;10:887–904. doi: 10.2174/138955710792007196
- 6 Williams EM, Little RF, Mowday AM, *et al.* Nitroreductase gene-directed enzyme prodrug therapy: insights and advances toward clinical utility. *Biochem J.* 2015;471:131–53. doi: 10.1042/BJ20150650
- 7 Malekshah OM, Chen X, Nomani A, *et al.* Enzyme/Prodrug Systems for Cancer Gene Therapy. *Curr Pharmacol Rep.* 2016;2:299–308. doi: 10.1007/s40495-016-0073-y
- 8 Karjoo Z, Chen X, Hatefi A. Progress and Problems with the Use of Suicide Genes for Targeted Cancer Therapy. *Adv Drug Deliv Rev.* 2016;99:113–28. doi: 10.1016/j.addr.2015.05.009
- 9 Souza C, Pellosi DS, Tedesco AC. Prodrugs for targeted cancer therapy. *Expert Rev Anticancer Ther.* 2019;19:483–502. doi: 10.1080/14737140.2019.1615890
- 10 Bendre A, Shukla E, Gaikwad S. Hydrolases: The Most Diverse Class of Enzymes. 2022.
- 11 Martinkova L, Křen V. Nitrile and Amide-converting Microbial Enzymes: Stereo, Regio- and Chemoselectivity. *Biocatal Biotransformation - BIOCATAL BIOTRANSFORM.* 2002;20:73–93. doi: 10.1080/10242420290018069
- 12 Patel NY, Baria DM, Yagnik SM, *et al.* Bio-prospecting the future in perspective of amidohydrolase L-glutaminase from marine habitats. *Appl Microbiol Biotechnol.* 2021;105:5325–40. doi: 10.1007/s00253-021-11416-6
- 13 Stanislauskienė R, Laurynėnas A, Rutkienė R, *et al.* YqfB protein from *Escherichia coli*: an atypical amidohydrolase active towards N4-acylcytosine derivatives. *Sci Rep.* 2020;10:788. doi: 10.1038/s41598-020-57664-w

- 14 Urbelienė N, Meškienė R, Tiškus M, *et al.* A Rapid Method for the Selection of Amidohydrolases from Metagenomic Libraries by Applying Synthetic Nucleosides and a Uridine Auxotrophic Host. *Catalysts*. 2020;10:445. doi: 10.3390/catal10040445
- 15 Urbelienė N, Tiškus M, Tamulaitienė G, *et al.* Cytidine deaminases catalyze the conversion of N(S,O)4-substituted pyrimidine nucleosides. *Sci Adv*. 2023;9:eade4361. doi: 10.1126/sciadv.ade4361
- 16 Malet-Martino M, Jolimaitre P, Martino R. The prodrugs of 5-fluorouracil. *Curr Med Chem Anti-Cancer Agents*. 2002;2:267–310. doi: 10.2174/1568011023354146
- 17 Martínez-Gómez AI, Martínez-Rodríguez S, Pozo-Dengra J, *et al.* Potential Application of N-Carbamoyl- $\beta$ -Alanine Amidohydrolase from *Agrobacterium tumefaciens* C58 for  $\beta$ -Amino Acid Production. *Appl Environ Microbiol*. 2009;75:514–20. doi: 10.1128/AEM.01128-08
- 18 Nandakumar R, Yoshimune K, Wakayama M, *et al.* Microbial glutaminase: biochemistry, molecular approaches and applications in the food industry. *J Mol Catal B Enzym*. 2003;23:87–100. doi: 10.1016/S1381-1177(03)00075-4
- 19 Bellini RG, Coronado MA, Paschoal AR, *et al.* Structural analysis of a novel N-carbamoyl-d-amino acid amidohydrolase from a Brazilian *Bradyrhizobium japonicum* strain: *In silico* insights by molecular modelling, docking and molecular dynamics. *J Mol Graph Model*. 2019;86:35–42. doi: 10.1016/j.jmgm.2018.10.005
- 20 Qi-yue Y, Ting Z, Ya-nan H, *et al.* From natural dye to herbal medicine: a systematic review of chemical constituents, pharmacological effects and clinical applications of indigo naturalis. *Chin Med*. 2020;15:127. doi: 10.1186/s13020-020-00406-x
- 21 Maugard T, Enaud E, Choisy P, *et al.* Identification of an indigo precursor from leaves of *Isatis tinctoria* (Woad). *Phytochemistry*. 2001;58:897–904. doi: 10.1016/S0031-9422(01)00335-1
- 22 Vougiotiannopoulou K, Skaltsounis A-L. From Tyrian Purple to Kinase Modulators: Naturally Halogenated Indirubins and Synthetic Analogues. *Planta Med*. 2012;78:1515–28. doi: 10.1055/s-0032-1315261
- 23 MacNeil IA, Tiong CL, Minor C, *et al.* Expression and isolation of antimicrobial small molecules from soil DNA libraries. *J Mol Microbiol Biotechnol*. 2001;3:301–8.
- 24 Adachi J, Mori Y, Matsui S, *et al.* Indirubin and Indigo Are Potent Aryl Hydrocarbon Receptor Ligands Present in Human Urine \*. *J Biol Chem*. 2001;276:31475–8. doi: 10.1074/jbc.C100238200
- 25 Hsieh W-L, Lin Y-K, Tsai C-N, *et al.* Indirubin, an acting component of indigo naturalis, inhibits EGFR activation and EGF-induced CDC25B gene expression in epidermal keratinocytes. *J Dermatol Sci*. 2012;67:140–6. doi: 10.1016/j.jdermsci.2012.05.008

- 26 Leclerc S, Garnier M, Hoessel R, *et al.* Indirubins Inhibit Glycogen Synthase Kinase-3 $\beta$  and CDK5/P25, Two Protein Kinases Involved in Abnormal Tau Phosphorylation in Alzheimer's Disease: A PROPERTY COMMON TO MOST CYCLIN-DEPENDENT KINASE INHIBITORS? \* 210. *J Biol Chem.* 2001;276:251–60. doi: 10.1074/jbc.M002466200
- 27 Zhang A, Qu Y, Zhang B, *et al.* The different effects of indirubin on effector and CD4+CD25+ regulatory T cells in mice: potential implication for the treatment of autoimmune diseases. *J Mol Med.* 2007;85:1263–70. doi: 10.1007/s00109-007-0235-9
- 28 Kunikata T, Tatefuji T, Aga H, *et al.* Indirubin inhibits inflammatory reactions in delayed-type hypersensitivity. *Eur J Pharmacol.* 2000;410:93–100. doi: 10.1016/S0014-2999(00)00879-7
- 29 Mak N-K, Leung C-Y, Wei X-Y, *et al.* Inhibition of RANTES expression by indirubin in influenza virus-infected human bronchial epithelial cells. *Biochem Pharmacol.* 2004;67:167–74. doi: 10.1016/j.bcp.2003.08.020
- 30 Eisenbrand G, Hippe F, Jakobs S, *et al.* Molecular mechanisms of indirubin and its derivatives: novel anticancer molecules with their origin in traditional Chinese phytomedicine. *J Cancer Res Clin Oncol.* 2004;130:627–35. doi: 10.1007/s00432-004-0579-2
- 31 Yang L, Li X, Huang W, *et al.* Pharmacological properties of indirubin and its derivatives. *Biomed Pharmacother.* 2022;151:113112. doi: 10.1016/j.biopha.2022.113112
- 32 Asghar U, Witkiewicz AK, Turner NC, *et al.* The history and future of targeting cyclin-dependent kinases in cancer therapy. *Nat Rev Drug Discov.* 2015;14:130–46. doi: 10.1038/nrd4504
- 33 Heptinstall AB, Adiyasa ,IWS, Cano ,Céline, *et al.* Recent Advances in CDK Inhibitors for Cancer Therapy. *Future Med Chem.* 2018;10:1369–88. doi: 10.4155/fmc-2017-0246
- 34 Hoessel R, Leclerc S, Endicott JA, *et al.* Indirubin, the active constituent of a Chinese antileukaemia medicine, inhibits cyclin-dependent kinases. *Nat Cell Biol.* 1999;1:60–7. doi: 10.1038/9035
- 35 Sethi G, Ahn KS, Sandur SK, *et al.* Indirubin Enhances Tumor Necrosis Factor-induced Apoptosis through Modulation of Nuclear Factor- $\kappa$ B Signaling Pathway \*. *J Biol Chem.* 2006;281:23425–35. doi: 10.1074/jbc.M602627200
- 36 Marko D, Schätzle S, Friedel A, *et al.* Inhibition of cyclin-dependent kinase 1 (CDK1) by indirubin derivatives in human tumour cells. *Br J Cancer.* 2001;84:283–9. doi: 10.1054/bjoc.2000.1546
- 37 Choi S-J, Lee J-E, Jeong S-Y, *et al.* 5,5'-Substituted Indirubin-3'-oxime Derivatives as Potent Cyclin-Dependent Kinase Inhibitors with Anticancer Activity. *J Med Chem.* 2010;53:3696–706. doi: 10.1021/jm100080z

- 38 Stoezel T, Schwarb P, Trumpp A, *et al.* c-Myc affects mRNA translation, cell proliferation and progenitor cell function in the mammary gland. *BMC Biol.* 2009;7:63. doi: 10.1186/1741-7007-7-63
- 39 Wei Y, Su J, Deng Z, *et al.* [Indirubin inhibits the proliferation of prostate cancer PC-3 cells]. *Zhonghua Nan Ke Xue Natl J Androl.* 2015;21:788–91.
- 40 Chen L, Wang Jinhua, Wu Jianbo, *et al.* Indirubin suppresses ovarian cancer cell viabilities through the STAT3 signaling pathway. *Drug Des Devel Ther.* 2018;12:3335–42. doi: 10.2147/DDDT.S174613
- 41 Mohan L, Raghav D, Ashraf SM, *et al.* Indirubin, a bis-indole alkaloid binds to tubulin and exhibits antimitotic activity against HeLa cells in synergism with vinblastine. *Biomed Pharmacother.* 2018;105:506–17. doi: 10.1016/j.biopha.2018.05.127
- 42 Wang L, Li X, Liu X, *et al.* Enhancing effects of indirubin on the arsenic disulfide-induced apoptosis of human diffuse large B-cell lymphoma cells. *Oncol Lett.* 2015;9:1940–6. doi: 10.3892/ol.2015.2941
- 43 Zhen Y, Sørensen V, Jin Y, *et al.* Indirubin-3'-monoxime inhibits autophosphorylation of FGFR1 and stimulates ERK1/2 activity via p38 MAPK. *Oncogene.* 2007;26:6372–85. doi: 10.1038/sj.onc.1210473
- 44 Chebel A, Kagialis-Girard Sandrine, Catallo Regine, *et al.* Indirubin derivatives inhibit malignant lymphoid cell proliferation. *Leuk Lymphoma.* 2009;50:2049–60. doi: 10.3109/10428190903288449
- 45 Groner B, Lucks P, Borghouts C. The function of Stat3 in tumor cells and their microenvironment. *Semin Cell Dev Biol.* 2008;19:341–50. doi: 10.1016/j.semcdb.2008.06.005
- 46 Nam S, Buettner R, Turkson J, *et al.* Indirubin derivatives inhibit Stat3 signaling and induce apoptosis in human cancer cells. *Proc Natl Acad Sci.* 2005;102:5998–6003. doi: 10.1073/pnas.0409467102
- 47 Zhang Y, Du Z, Zhuang Z, *et al.* E804 induces growth arrest, differentiation and apoptosis of glioblastoma cells by blocking Stat3 signaling. *J Neurooncol.* 2015;125:265–75. doi: 10.1007/s11060-015-1917-8
- 48 Liu L, Gaboriaud Nicolas, Vougloukianopoulou Konstantina, *et al.* MLS-2384, a new 6-bromoindirubin derivative with dual JAK/Src kinase inhibitory activity, suppresses growth of diverse cancer cells. *Cancer Biol Ther.* 2014;15:178–84. doi: 10.4161/cbt.26721
- 49 Aoki M, Fujishita T. Oncogenic Roles of the PI3K/AKT/mTOR Axis. In: Hunter E, Bister K, eds. *Viruses, Genes, and Cancer.* Cham: Springer International Publishing 2017:153–89.
- 50 Dera AA, Rajagopalan P, Al Fayi M, *et al.* Indirubin-3-monoxime and thymoquinone exhibit synergistic efficacy as therapeutic combination in in-vitro and in-vivo models of Lung cancer. *Arch Pharm Res.* 2020;43:655–65. doi: 10.1007/s12272-020-01241-2



- 51 Liu L, Nam S, Tian Y, *et al.* 6-Bromindirubin-3'-oxime inhibits JAK/STAT3 signaling and induces apoptosis of human melanoma cells. *Cancer Res.* 2011;71:3972–9. doi: 10.1158/0008-5472.CAN-10-3852
- 52 Ichimaru Y, Sano M, Kajiwaru I, *et al.* Indirubin 3'-Oxime Inhibits Migration, Invasion, and Metastasis In Vivo in Mice Bearing Spontaneously Occurring Pancreatic Cancer via Blocking the RAF/ERK, AKT, and SAPK/JNK Pathways. *Transl Oncol.* 2019;12:1574–82. doi: 10.1016/j.tranon.2019.08.010
- 53 Braicu C, Buse M, Busuioc C, *et al.* A Comprehensive Review on MAPK: A Promising Therapeutic Target in Cancer. *Cancers.* 2019;11:1618. doi: 10.3390/cancers11101618
- 54 Kelly PN, Strasser A. The role of Bcl-2 and its pro-survival relatives in tumorigenesis and cancer therapy. *Cell Death Differ.* 2011;18:1414–24. doi: 10.1038/cdd.2011.17
- 55 Singh S, Barrett J, Sakata K, *et al.* ETS Proteins and MMPs: Partners in Invasion and Metastasis. *Curr Drug Targets.* 2002;3:359–67. doi: 10.2174/1389450023347489
- 56 Zhang Y, Song L, Li J, *et al.* Inhibitory effects of indirubin-3'-monoxime against human osteosarcoma. *IUBMB Life.* 2019;71:1465–74. doi: 10.1002/iub.2058
- 57 Liu K, Li J, Wu X, *et al.* GSK-3 $\beta$  inhibitor 6-bromo-indirubin-3'-oxime promotes both adhesive activity and drug resistance in colorectal cancer cells. *Int J Oncol.* 2017;51:1821–30. doi: 10.3892/ijo.2017.4163
- 58 Wang C, Jiang K, Gao D, *et al.* Clusterin Protects Hepatocellular Carcinoma Cells from Endoplasmic Reticulum Stress Induced Apoptosis through GRP78. *PLOS ONE.* 2013;8:e55981. doi: 10.1371/journal.pone.0055981
- 59 Kim S-A, Kwon S-M, Kim J-A, *et al.* 5'-Nitro-indirubinoxime, an indirubin derivative, suppresses metastatic ability of human head and neck cancer cells through the inhibition of Integrin  $\beta$ 1/FAK/Akt signaling. *Cancer Lett.* 2011;306:197–204. doi: 10.1016/j.canlet.2011.03.006
- 60 Li Z, Zhu ,Chaofu, An ,Baiping, *et al.* Indirubin inhibits cell proliferation, migration, invasion and angiogenesis in tumor-derived endothelial cells. *OncoTargets Ther.* 2018;11:2937–44. doi: 10.2147/OTT.S157949
- 61 Zhang X, Song Y, Wu Y, *et al.* Indirubin inhibits tumor growth by antitumor angiogenesis via blocking VEGFR2-mediated JAK/STAT3 signaling in endothelial cell. *Int J Cancer.* 2011;129:2502–11. doi: 10.1002/ijc.25909
- 62 Shin E-K, Kim J-K. Indirubin derivative E804 inhibits angiogenesis. *BMC Cancer.* 2012;12:164. doi: 10.1186/1471-2407-12-164
- 63 Kim J-K, Shin EK, Kang Y-H, *et al.* Indirubin-3'-monoxime, a derivative of a chinese antileukemia medicine, inhibits angiogenesis. *J Cell Biochem.* 2011;112:1384–91. doi: 10.1002/jcb.23055

- 64 Fogaça MV, Cândido-Bacani ,Priscila de Matos, Benicio ,Lucas Milanez, *et al.* Effects of indirubin and isatin on cell viability, mutagenicity, genotoxicity and BAX/ERCC1 gene expression. *Pharm Biol.* 2017;55:2005–14. doi: 10.1080/13880209.2017.1354387
- 65 Schepelmann S, Springer CJ. Viral vectors for gene-directed enzyme prodrug therapy. *Curr Gene Ther.* 2006;6:647–70. doi: 10.2174/156652306779010679
- 66 Wang C, Pan C, Yong H, *et al.* Emerging non-viral vectors for gene delivery. *J Nanobiotechnology.* 2023;21:272. doi: 10.1186/s12951-023-02044-5
- 67 Saukkonen K, Hemminki A. Tissue-specific promoters for cancer gene therapy. *Expert Opin Biol Ther.* 2004;4:683–96. doi: 10.1517/14712598.4.5.683
- 68 Amara I, Touati W, Beaune P, *et al.* Mesenchymal stem cells as cellular vehicles for prodrug gene therapy against tumors. *Biochimie.* 2014;105:4–11. doi: 10.1016/j.biochi.2014.06.016
- 69 Altaner C. Prodrug cancer gene therapy. *Cancer Lett.* 2008;270:191–201. doi: 10.1016/j.canlet.2008.04.023
- 70 Portsmouth D, Hlavaty J, Renner M. Suicide genes for cancer therapy. *Mol Aspects Med.* 2007;28:4–41. doi: 10.1016/j.mam.2006.12.001
- 71 Shin Ly CY, Kunnath AP. Application of Gene-Directed Enzyme Prodrug Therapy in Cancer Treatment. *Int J Biomed Res Pract.* 2021;1. doi: 10.33425/2769-6294.1004
- 72 Springer CJ, Niculescu-Duvaz I. Prodrug-activating systems in suicide gene therapy. *J Clin Invest.* 2000;105:1161–7.
- 73 Dachs GU, Hunt MA, Syddall S, *et al.* Bystander or No Bystander for Gene Directed Enzyme Prodrug Therapy. *Molecules.* 2009;14:4517–45. doi: 10.3390/molecules14114517
- 74 Sheikh S, Ernst D, Keating A. Prodrugs and prodrug-activated systems in gene therapy. *Mol Ther.* 2021;29:1716–28. doi: 10.1016/j.ymthe.2021.04.006
- 75 Singh V, Khan N, Jayandharan GR. Vector engineering, strategies and targets in cancer gene therapy. *Cancer Gene Ther.* 2022;29:402–17. doi: 10.1038/s41417-021-00331-7
- 76 Chen H, Beardsley GP, Coen DM. Mechanism of ganciclovir-induced chain termination revealed by resistant viral polymerase mutants with reduced exonuclease activity. *Proc Natl Acad Sci.* 2014;111:17462–7. doi: 10.1073/pnas.1405981111
- 77 Tomicic MT, Thust R, Kaina B. Ganciclovir-induced apoptosis in HSV-1 thymidine kinase expressing cells: critical role of DNA breaks, Bcl-2 decline and caspase-9 activation. *Oncogene.* 2002;21:2141–53. doi: 10.1038/sj.onc.1205280
- 78 Fischer U, Steffens S, Frank S, *et al.* Mechanisms of thymidine kinase/ganciclovir and cytosine deaminase/ 5-fluorocytosine suicide

- gene therapy-induced cell death in glioma cells. *Oncogene*. 2005;24:1231–43. doi: 10.1038/sj.onc.1208290
- 79 Aghi M, Hochberg F, Breakefield XO. Prodrug activation enzymes in cancer gene therapy. *J Gene Med*. 2000;2:148–64. doi: 10.1002/(SICI)1521-2254(200005/06)2:3<148::AID-JGM105>3.0.CO;2-Q
- 80 Dey D, Evans GRD, Dey D, *et al*. Suicide Gene Therapy by Herpes Simplex Virus-1 Thymidine Kinase (HSV-TK). *Targets in Gene Therapy*. IntechOpen 2011.
- 81 Bondanza A, Hambach L, Aghai Z, *et al*. IL-7 receptor expression identifies suicide gene-modified allospecific CD8<sup>+</sup> T cells capable of self-renewal and differentiation into antileukemia effectors. *Blood*. 2011;117:6469–78. doi: 10.1182/blood-2010-11-320366
- 82 Kakinoki K, Nakamoto Y, Kagaya T, *et al*. Prevention of intrahepatic metastasis of liver cancer by suicide gene therapy and chemokine ligand 2/monocyte chemoattractant protein-1 delivery in mice. *J Gene Med*. 2010;12:1002–13. doi: 10.1002/jgm.1528
- 83 Ribot EJ, Miraux S, Konsman JP, *et al*. In vivo MR tracking of therapeutic microglia to a human glioma model. *NMR Biomed*. 2011;24:1361–8. doi: 10.1002/nbm.1699
- 84 Pan JG, Zhou X, Luo R, *et al*. The adeno-associated virus-mediated HSV-TK/GCV suicide system: a potential strategy for the treatment of bladder carcinoma. *Med Oncol Northwood Lond Engl*. 2012;29:1938–47. doi: 10.1007/s12032-011-0091-x
- 85 Xu F, Li S, Li X-L, *et al*. Phase I and biodistribution study of recombinant adenovirus vector-mediated herpes simplex virus thymidine kinase gene and ganciclovir administration in patients with head and neck cancer and other malignant tumors. *Cancer Gene Ther*. 2009;16:723–30. doi: 10.1038/cgt.2009.19
- 86 Ji N, Weng D, Liu C, *et al*. Adenovirus-mediated delivery of herpes simplex virus thymidine kinase administration improves outcome of recurrent high-grade glioma. *Oncotarget*. 2015;7:4369–78. doi: 10.18632/oncotarget.6737
- 87 Oraee-Yazdani S, Tavanaei R, Rostami F, *et al*. Suicide gene therapy using allogeneic adipose tissue-derived mesenchymal stem cell gene delivery vehicles in recurrent glioblastoma multiforme: a first-in-human, dose-escalation, phase I clinical trial. *J Transl Med*. 2023;21:350. doi: 10.1186/s12967-023-04213-4
- 88 Aguilar LK, Shirley LA, Chung VM, *et al*. Gene-mediated cytotoxic immunotherapy as adjuvant to surgery or chemoradiation for pancreatic adenocarcinoma. *Cancer Immunol Immunother CII*. 2015;64:727–36. doi: 10.1007/s00262-015-1679-3
- 89 Hasegawa Y, Nishiyama Y, Imaizumi K, *et al*. Avoidance of bone marrow suppression using A-5021 as a nucleoside analog for retrovirus-

- mediated herpes simplex virus type I thymidine kinase gene therapy. *Cancer Gene Ther.* 2000;7:557–62. doi: 10.1038/sj.cgt.7700134
- 90 Zhou M, Zheng M, Zhou X, *et al.* The roles of connexins and gap junctions in the progression of cancer. *Cell Commun Signal CCS.* 2023;21:8. doi: 10.1186/s12964-022-01009-9
- 91 Kokoris MS, Black ME. Characterization of herpes simplex virus type 1 thymidine kinase mutants engineered for improved ganciclovir or acyclovir activity. *Protein Sci Publ Protein Soc.* 2002;11:2267–72. doi: 10.1110/ps.2460102
- 92 Tong XW, Engehausen DG, Kaufman RH, *et al.* Improvement of gene therapy for ovarian cancer by using acyclovir instead of ganciclovir in adenovirus mediated thymidine kinase gene therapy. *Anticancer Res.* 1998;18:713–8.
- 93 MacDougall C, Guglielmo BJ. Pharmacokinetics of valaciclovir. *J Antimicrob Chemother.* 2004;53:899–901. doi: 10.1093/jac/dkh244
- 94 Chiocca EA, Aguilar LK, Bell SD, *et al.* Phase IB study of gene-mediated cytotoxic immunotherapy adjuvant to up-front surgery and intensive timing radiation for malignant glioma. *J Clin Oncol Off J Am Soc Clin Oncol.* 2011;29:3611–9. doi: 10.1200/JCO.2011.35.5222
- 95 Kubo H, Gardner TA, Wada Y, *et al.* Phase I dose escalation clinical trial of adenovirus vector carrying osteocalcin promoter-driven herpes simplex virus thymidine kinase in localized and metastatic hormone-refractory prostate cancer. *Hum Gene Ther.* 2003;14:227–41. doi: 10.1089/10430340360535788
- 96 Senter PD, Su PC, Katsuragi T, *et al.* Generation of 5-fluorouracil from 5-fluorocytosine by monoclonal antibody-cytosine deaminase conjugates. *Bioconjug Chem.* 1991;2:447–51. doi: 10.1021/bc00012a012
- 97 Polk A, Vistisen K, Vaage-Nilsen M, *et al.* A systematic review of the pathophysiology of 5-fluorouracil-induced cardiotoxicity. *BMC Pharmacol Toxicol.* 2014;15:47. doi: 10.1186/2050-6511-15-47
- 98 Longley DB, Harkin DP, Johnston PG. 5-Fluorouracil: mechanisms of action and clinical strategies. *Nat Rev Cancer.* 2003;3:330–8. doi: 10.1038/nrc1074
- 99 Kurozumi K, Tamiya T, Ono Y, *et al.* Apoptosis induction with 5-fluorocytosine/cytosine deaminase gene therapy for human malignant glioma cells mediated by adenovirus. *J Neurooncol.* 2004;66:117–27. doi: 10.1023/b:neon.0000013494.98345.80
- 100 Kuriyama S, Masui K, Sakamoto T, *et al.* Bystander effect caused by cytosine deaminase gene and 5-fluorocytosine in vitro is substantially mediated by generated 5-fluorouracil. *Anticancer Res.* 1998;18:3399–406.
- 101 Formica V, Leary A, Cunningham D, *et al.* 5-Fluorouracil can cross brain–blood barrier and cause encephalopathy: should we expect the same from capecitabine? A case report on capecitabine-induced central

- neurotoxicity progressing to coma. *Cancer Chemother Pharmacol.* 2006;58:276–8. doi: 10.1007/s00280-005-0159-4
- 102 Delma FZ, Al-Hatmi AMS, Brüggemann RJM, *et al.* Molecular Mechanisms of 5-Fluorocytosine Resistance in Yeasts and Filamentous Fungi. *J Fungi.* 2021;7:909. doi: 10.3390/jof7110909
  - 103 Deng L-Y, Wang J-P, Gui Z-F, *et al.* Antitumor activity of mutant bacterial cytosine deaminase gene for colon cancer. *World J Gastroenterol.* 2011;17:2958–64. doi: 10.3748/wjg.v17.i24.2958
  - 104 Wang L, Yuan Y, Lin S, *et al.* Co-delivery of 5-fluorocytosine and cytosine deaminase into glioma cells mediated by an intracellular environment-responsive nanovesicle. *Polym Chem.* 2014;5:4542–52. doi: 10.1039/C4PY00291A
  - 105 Kaliberova LN, Della Manna DL, Krendelchchikova V, *et al.* Molecular chemotherapy of pancreatic cancer using novel mutant bacterial cytosine deaminase gene. *Mol Cancer Ther.* 2008;7:2845–54. doi: 10.1158/1535-7163.MCT-08-0347
  - 106 Gabel M, Kim JH, Kolozsvary A, *et al.* Selective in vivo radiosensitization by 5-fluorocytosine of human colorectal carcinoma cells transduced with the E. coli cytosine deaminase (CD) gene. *Int J Radiat Oncol Biol Phys.* 1998;41:883–7. doi: 10.1016/s0360-3016(98)00125-4
  - 107 Nagy B, Mucsi I, Molnár J, *et al.* Combined effect of cisplatin and 5-fluorouracil with irradiation on tumor cells in vitro. *Anticancer Res.* 2002;22:135–8.
  - 108 Wang F, Zamora G, Sun C-H, *et al.* Increased sensitivity of glioma cells to 5-fluorocytosine following photo-chemical internalization enhanced nonviral transfection of the cytosine deaminase suicide gene. *J Neurooncol.* 2014;118:29–37. doi: 10.1007/s11060-014-1410-9
  - 109 Miyagi T, Koshida K, Hori O, *et al.* Gene therapy for prostate cancer using the cytosine deaminase/uracil phosphoribosyltransferase suicide system. *J Gene Med.* 2003;5:30–7. doi: 10.1002/jgm.317
  - 110 Richard C, Duivenvoorden W, Bourbeau D, *et al.* Sensitivity of 5-fluorouracil-resistant cancer cells to adenovirus suicide gene therapy. *Cancer Gene Ther.* 2007;14:57–65. doi: 10.1038/sj.cgt.7700980
  - 111 Shirakawa T, Gardner TA, Ko SC, *et al.* Cytotoxicity of adenoviral-mediated cytosine deaminase plus 5-fluorocytosine gene therapy is superior to thymidine kinase plus acyclovir in a human renal cell carcinoma model. *J Urol.* 1999;162:949–54. doi: 10.1097/00005392-199909010-00096
  - 112 Rogulski KR, Kim JH, Kim SH, *et al.* Glioma cells transduced with an Escherichia coli CD/HSV-1 TK fusion gene exhibit enhanced metabolic suicide and radiosensitivity. *Hum Gene Ther.* 1997;8:73–85. doi: 10.1089/hum.1997.8.1-73
  - 113 Fuchita M, Ardiani A, Zhao L, *et al.* Bacterial Cytosine Deaminase Mutants Created by Molecular Engineering Demonstrate Improved

- 5FC-Mediated Cell Killing In Vitro and In Vivo. *Cancer Res.* 2009;69:4791–9. doi: 10.1158/0008-5472.CAN-09-0615
- 114 Kazlauskas A, Darinskas A, Meškys R, *et al.* Isocytosine deaminase Vcz as a novel tool for the prodrug cancer therapy. *BMC Cancer.* 2019;19:197. doi: 10.1186/s12885-019-5409-7
- 115 Johnson AJ, Ardiani A, Sanchez-Bonilla M, *et al.* Comparative analysis of enzyme and pathway engineering strategies for 5FC-mediated suicide gene therapy applications. *Cancer Gene Ther.* 2011;18:533–42. doi: 10.1038/cgt.2011.6
- 116 Kaliberov SA, Market JM, Gillespie GY, *et al.* Mutation of Escherichia coli cytosine deaminase significantly enhances molecular chemotherapy of human glioma. *Gene Ther.* 2007;14:1111–9. doi: 10.1038/sj.gt.3302965
- 117 Ortiz de Montellano PR. Cytochrome P450-activated prodrugs. *Future Med Chem.* 2013;5:213–28. doi: 10.4155/fmc.12.197
- 118 Liang J, Huang M, Duan W, *et al.* Design of new oxazaphosphorine anticancer drugs. *Curr Pharm Des.* 2007;13:963–78. doi: 10.2174/138161207780414296
- 119 Roy P, Waxman DJ. Activation of oxazaphosphorines by cytochrome P450: application to gene-directed enzyme prodrug therapy for cancer. *Toxicol Vitro Int J Publ Assoc BIBRA.* 2006;20:176–86. doi: 10.1016/j.tiv.2005.06.046
- 120 Kan O, Griffiths L, Baban D, *et al.* Direct retroviral delivery of human cytochrome P450 2B6 for gene-directed enzyme prodrug therapy of cancer. *Cancer Gene Ther.* 2001;8:473–82. doi: 10.1038/sj.cgt.7700329
- 121 Ramirez DA, Collins KP, Aradi AE, *et al.* Kinetics of Cyclophosphamide Metabolism in Humans, Dogs, Cats, and Mice and Relationship to Cytotoxic Activity and Pharmacokinetics. *Drug Metab Dispos.* 2019;47:257–68. doi: 10.1124/dmd.118.083766
- 122 Giraud B, Hebert G, Deroussent A, *et al.* Oxazaphosphorines: new therapeutic strategies for an old class of drugs. *Expert Opin Drug Metab Toxicol.* 2010;6:919–38. doi: 10.1517/17425255.2010.487861
- 123 Ross AD, Varghese G, Oporto B, *et al.* Effect of propylthiouracil treatment on NADPH-cytochrome P450 reductase levels, oxygen consumption and hydroxyl radical formation in liver microsomes from rats fed ethanol or acetone chronically. *Biochem Pharmacol.* 1995;49:979–89. doi: 10.1016/0006-2952(95)00007-m
- 124 Kumar S. Engineering cytochrome P450 biocatalysts for biotechnology, medicine and bioremediation. *Expert Opin Drug Metab Toxicol.* 2010;6:115–31. doi: 10.1517/17425250903431040
- 125 Roldán MD, Pérez-Reinado E, Castillo F, *et al.* Reduction of polynitroaromatic compounds: the bacterial nitroreductases. *FEMS Microbiol Rev.* 2008;32:474–500. doi: 10.1111/j.1574-6976.2008.00107.x

- 126 Denny WA. Nitroreductase-based GDEPT. *Curr Pharm Des.* 2002;8:1349–61. doi: 10.2174/1381612023394584
- 127 Vass SO, Jarrom D, Wilson WR, *et al.* E. coli NfsA: an alternative nitroreductase for prodrug activation gene therapy in combination with CB1954. *Br J Cancer.* 2009;100:1903–11. doi: 10.1038/sj.bjc.6605094
- 128 Bridgewater JA, Knox RJ, Pitts JD, *et al.* The bystander effect of the nitroreductase/CB1954 enzyme/prodrug system is due to a cell-permeable metabolite. *Hum Gene Ther.* 1997;8:709–17. doi: 10.1089/hum.1997.8.6-709
- 129 Mitchell DJ, Minchin RF. E. coli nitroreductase/CB1954 gene-directed enzyme prodrug therapy: role of arylamine N-acetyltransferase 2. *Cancer Gene Ther.* 2008;15:758–64. doi: 10.1038/cgt.2008.47
- 130 Patel P, Young JG, Mautner V, *et al.* A phase I/II clinical trial in localized prostate cancer of an adenovirus expressing nitroreductase with CB1954 [correction of CB1984]. *Mol Ther J Am Soc Gene Ther.* 2009;17:1292–9. doi: 10.1038/mt.2009.80
- 131 Palmer DH, Mautner V, Mirza D, *et al.* Virus-directed enzyme prodrug therapy: intratumoral administration of a replication-deficient adenovirus encoding nitroreductase to patients with resectable liver cancer. *J Clin Oncol Off J Am Soc Clin Oncol.* 2004;22:1546–52. doi: 10.1200/JCO.2004.10.005
- 132 Prosser GA, Copp JN, Mowday AM, *et al.* Creation and screening of a multi-family bacterial oxidoreductase library to discover novel nitroreductases that efficiently activate the bio-reductive prodrugs CB1954 and PR-104A. *Biochem Pharmacol.* 2013;85:1091–103. doi: 10.1016/j.bcp.2013.01.029
- 133 Green LK, Syddall SP, Carlin KM, *et al.* Pseudomonas aeruginosa NfsB and nitro-CBI-DEI – a promising enzyme/prodrug combination for gene directed enzyme prodrug therapy. *Mol Cancer.* 2013;12:58. doi: 10.1186/1476-4598-12-58
- 134 Parker WB, Allan PW, Shaddix SC, *et al.* Metabolism and Metabolic Actions of 6-Methylpurine and 2-Fluoroadenine in Human Cells. *Biochem Pharmacol.* 1998;55:1673–81. doi: 10.1016/S0006-2952(98)00034-3
- 135 Rosenthal E, Chung T, Parker W, *et al.* Phase I Dose-Escalating Trial of E.coli Purine Nucleoside Phosphorylase and Fludarabine Gene Therapy for Advanced Solid Tumors. *Ann Oncol Off J Eur Soc Med Oncol ESMO.* 2015;26. doi: 10.1093/annonc/mdv196
- 136 Afshar S, Asai T, Morrison SL. Humanized ADEPT comprised of an engineered human purine nucleoside phosphorylase and a tumor targeting peptide for treatment of cancer. *Mol Cancer Ther.* 2009;8:185–93. doi: 10.1158/1535-7163.MCT-08-0652
- 137 Parker WB, Allan PW, Waud WR, *et al.* Effect of expression of adenine phosphoribosyltransferase on the in vivo anti-tumor activity of prodrugs

- activated by *E. coli* purine nucleoside phosphorylase. *Cancer Gene Ther.* 2011;18:390–8. doi: 10.1038/cgt.2011.4
- 138 Pommier Y. Topoisomerase I inhibitors: camptothecins and beyond. *Nat Rev Cancer.* 2006;6:789–802. doi: 10.1038/nrc1977
  - 139 Vanhoefer U, Harstrick A, Achterrath W, *et al.* Irinotecan in the treatment of colorectal cancer: clinical overview. *J Clin Oncol Off J Am Soc Clin Oncol.* 2001;19:1501–18. doi: 10.1200/JCO.2001.19.5.1501
  - 140 Choi SA, Lee YE, Kwak PA, *et al.* Clinically applicable human adipose tissue-derived mesenchymal stem cells delivering therapeutic genes to brainstem gliomas. *Cancer Gene Ther.* 2015;22:302–11. doi: 10.1038/cgt.2015.25
  - 141 Kojima A, Hackett NR, Crystal RG. Reversal of CPT-11 resistance of lung cancer cells by adenovirus-mediated gene transfer of the human carboxylesterase cDNA. *Cancer Res.* 1998;58:4368–74.
  - 142 Capello M, Lee M, Wang H, *et al.* Carboxylesterase 2 as a Determinant of Response to Irinotecan and Neoadjuvant FOLFIRINOX Therapy in Pancreatic Ductal Adenocarcinoma. *JNCI J Natl Cancer Inst.* 2015;107:djv132. doi: 10.1093/jnci/djv132
  - 143 Humerickhouse R, Lohrbach K, Li L, *et al.* Characterization of CPT-11 hydrolysis by human liver carboxylesterase isoforms hCE-1 and hCE-2. *Cancer Res.* 2000;60:1189–92.
  - 144 Sanghani SP, Quinney SK, Fredenburg TB, *et al.* Hydrolysis of irinotecan and its oxidative metabolites, 7-ethyl-10-[4-N-(5-aminopentanoic acid)-1-piperidino] carbonyloxycamptothecin and 7-ethyl-10-[4-(1-piperidino)-1-amino]-carbonyloxycamptothecin, by human carboxylesterases CES1A1, CES2, and a newly expressed carboxylesterase isoenzyme, CES3. *Drug Metab Dispos Biol Fate Chem.* 2004;32:505–11. doi: 10.1124/dmd.32.5.505
  - 145 Danks MK, Morton CL, Krull EJ, *et al.* Comparison of activation of CPT-11 by rabbit and human carboxylesterases for use in enzyme/prodrug therapy. *Clin Cancer Res Off J Am Assoc Cancer Res.* 1999;5:917–24.
  - 146 Wierdl M, Tsurkan L, Hyatt JL, *et al.* An improved human carboxylesterase for enzyme/prodrug therapy with CPT-11. *Cancer Gene Ther.* 2008;15:183–92. doi: 10.1038/sj.cgt.7701112
  - 147 Ozawa S, Miura T, Terashima J, *et al.* Cellular irinotecan resistance in colorectal cancer and overcoming irinotecan refractoriness through various combination trials including DNA methyltransferase inhibitors: a review. *Cancer Drug Resist Alhambra Calif.* 2021;4:946–64. doi: 10.20517/cdr.2021.82
  - 148 Vangara KK, Ali HI, Lu D, *et al.* SN-38-Cyclodextrin Complexation and Its Influence on the Solubility, Stability, and In Vitro Anticancer Activity Against Ovarian Cancer. *AAPS PharmSciTech.* 2014;15:472–82. doi: 10.1208/s12249-013-0068-5



- 149 Oosterhoff D, Pinedo HM, van der Meulen IH, *et al.* Secreted and tumour targeted human carboxylesterase for activation of irinotecan. *Br J Cancer*. 2002;87:659–64. doi: 10.1038/sj.bjc.6600519
- 150 Metz MZ, Gutova M, Lacey SF, *et al.* Neural stem cell-mediated delivery of irinotecan-activating carboxylesterases to glioma: implications for clinical use. *Stem Cells Transl Med*. 2013;2:983–92. doi: 10.5966/sctm.2012-0177
- 151 Seo G-M, Rachakatla RS, Balivada S, *et al.* A self-contained enzyme activating prodrug cytotherapy for preclinical melanoma. *Mol Biol Rep*. 2012;39:157–65. doi: 10.1007/s11033-011-0720-7
- 152 Rainov NG. A phase III clinical evaluation of herpes simplex virus type 1 thymidine kinase and ganciclovir gene therapy as an adjuvant to surgical resection and radiation in adults with previously untreated glioblastoma multiforme. *Hum Gene Ther*. 2000;11:2389–401. doi: 10.1089/104303400750038499
- 153 Huber BE, Austin EA, Richards CA, *et al.* Metabolism of 5-fluorocytosine to 5-fluorouracil in human colorectal tumor cells transduced with the cytosine deaminase gene: significant antitumor effects when only a small percentage of tumor cells express cytosine deaminase. *Proc Natl Acad Sci U S A*. 1994;91:8302–6. doi: 10.1073/pnas.91.17.8302
- 154 Duarte S, Carle G, Faneca H, *et al.* Suicide gene therapy in cancer: where do we stand now? *Cancer Lett*. 2012;324:160–70. doi: 10.1016/j.canlet.2012.05.023
- 155 Garcia-Rodríguez L, Abate-Daga D, Rojas A, *et al.* E-cadherin contributes to the bystander effect of TK/GCV suicide therapy and enhances its antitumoral activity in pancreatic cancer models. *Gene Ther*. 2011;18:73–81. doi: 10.1038/gt.2010.114
- 156 Bi W, Kim YG, Feliciano ES, *et al.* An HSVtk-mediated local and distant antitumor bystander effect in tumors of head and neck origin in athymic mice. *Cancer Gene Ther*. 1997;4:246–52.
- 157 Kianmanesh AR, Perrin H, Panis Y, *et al.* A ‘distant’ bystander effect of suicide gene therapy: regression of nontransduced tumors together with a distant transduced tumor. *Hum Gene Ther*. 1997;8:1807–14. doi: 10.1089/hum.1997.8.15-1807
- 158 Herraiz M, Beraza N, Solano A, *et al.* Liver failure caused by herpes simplex virus thymidine kinase plus ganciclovir therapy is associated with mitochondrial dysfunction and mitochondrial DNA depletion. *Hum Gene Ther*. 2003;14:463–72. doi: 10.1089/104303403321467225
- 159 Pierrefite-Carle V, Baqué P, Gavelli A, *et al.* Cytosine deaminase/5-fluorocytosine-based vaccination against liver tumors: evidence of distant bystander effect. *J Natl Cancer Inst*. 1999;91:2014–9. doi: 10.1093/jnci/91.23.2014

- 160 McConnell MJ, Imperiale MJ. Biology of adenovirus and its use as a vector for gene therapy. *Hum Gene Ther.* 2004;15:1022–33. doi: 10.1089/hum.2004.15.1022
- 161 Bulcha JT, Wang Y, Ma H, *et al.* Viral vector platforms within the gene therapy landscape. *Signal Transduct Target Ther.* 2021;6:1–24. doi: 10.1038/s41392-021-00487-6
- 162 Wold WSM, Toth K. Adenovirus Vectors for Gene Therapy, Vaccination and Cancer Gene Therapy. *Curr Gene Ther.* 2013;13:421–33.
- 163 Bezeljak U. Cancer gene therapy goes viral: viral vector platforms come of age. *Radiol Oncol.* 2022;56:1–13. doi: 10.2478/raon-2022-0002
- 164 Shaw AR, Suzuki M. Immunology of Adenoviral Vectors in Cancer Therapy. *Mol Ther Methods Clin Dev.* 2019;15:418–29. doi: 10.1016/j.omtm.2019.11.001
- 165 Xiao X, Li J, Samulski RJ. Production of high-titer recombinant adeno-associated virus vectors in the absence of helper adenovirus. *J Virol.* 1998;72:2224–32. doi: 10.1128/JVI.72.3.2224-2232.1998
- 166 Samulski RJ, Muzyczka N. AAV-Mediated Gene Therapy for Research and Therapeutic Purposes. *Annu Rev Virol.* 2014;1:427–51. doi: 10.1146/annurev-virology-031413-085355
- 167 Challis RC, Ravindra Kumar S, Chan KY, *et al.* Systemic AAV vectors for widespread and targeted gene delivery in rodents. *Nat Protoc.* 2019;14:379–414. doi: 10.1038/s41596-018-0097-3
- 168 Xu X, Chen W, Zhu W, *et al.* Adeno-associated virus (AAV)-based gene therapy for glioblastoma. *Cancer Cell Int.* 2021;21:76. doi: 10.1186/s12935-021-01776-4
- 169 Santiago-Ortiz JL, Schaffer DV. Adeno-associated virus (AAV) vectors in cancer gene therapy. *J Control Release Off J Control Release Soc.* 2016;240:287–301. doi: 10.1016/j.jconrel.2016.01.001
- 170 Hacker UT, Bentler M, Kaniowska D, *et al.* Towards Clinical Implementation of Adeno-Associated Virus (AAV) Vectors for Cancer Gene Therapy: Current Status and Future Perspectives. *Cancers.* 2020;12:1889. doi: 10.3390/cancers12071889
- 171 Münch RC, Janicki H, Völker I, *et al.* Displaying high-affinity ligands on adeno-associated viral vectors enables tumor cell-specific and safe gene transfer. *Mol Ther J Am Soc Gene Ther.* 2013;21:109–18. doi: 10.1038/mt.2012.186
- 172 Münch RC, Muth A, Muik A, *et al.* Off-target-free gene delivery by affinity-purified receptor-targeted viral vectors. *Nat Commun.* 2015;6:6246. doi: 10.1038/ncomms7246
- 173 Calcedo R, Vandenberghe LH, Gao G, *et al.* Worldwide Epidemiology of Neutralizing Antibodies to Adeno-Associated Viruses. *J Infect Dis.* 2009;199:381–90. doi: 10.1086/595830

- 174 Shirley JL, de Jong YP, Terhorst C, *et al.* Immune Responses to Viral Gene Therapy Vectors. *Mol Ther J Am Soc Gene Ther.* 2020;28:709–22. doi: 10.1016/j.ymthe.2020.01.001
- 175 Cockrell AS, Kafri T. Gene delivery by lentivirus vectors. *Mol Biotechnol.* 2007;36:184–204. doi: 10.1007/s12033-007-0010-8
- 176 Milone MC, O'Doherty U. Clinical use of lentiviral vectors. *Leukemia.* 2018;32:1529–41. doi: 10.1038/s41375-018-0106-0
- 177 Dull T, Zufferey R, Kelly M, *et al.* A third-generation lentivirus vector with a conditional packaging system. *J Virol.* 1998;72:8463–71. doi: 10.1128/JVI.72.11.8463-8471.1998
- 178 Trono D. Lentiviral vectors: turning a deadly foe into a therapeutic agent. *Gene Ther.* 2000;7:20–3. doi: 10.1038/sj.gt.3301105
- 179 Yáñez-Muñoz RJ, Balagán KS, MacNeil A, *et al.* Effective gene therapy with nonintegrating lentiviral vectors. *Nat Med.* 2006;12:348–53. doi: 10.1038/nm1365
- 180 Ostertag D, Amundson KK, Lopez Espinoza F, *et al.* Brain tumor eradication and prolonged survival from intratumoral conversion of 5-fluorocytosine to 5-fluorouracil using a nonlytic retroviral replicating vector. *Neuro-Oncol.* 2012;14:145–59. doi: 10.1093/neuonc/nor199
- 181 Cloughesy TF, Petrecca K, Walbert T, *et al.* Effect of Vocimagene Amiretrorepvec in Combination With Flucytosine vs Standard of Care on Survival Following Tumor Resection in Patients With Recurrent High-Grade Glioma: A Randomized Clinical Trial. *JAMA Oncol.* 2020;6:1939–46. doi: 10.1001/jamaoncol.2020.3161
- 182 Glorioso JC. Herpes Simplex Viral Vectors: Late Bloomers with Big Potential. *Hum Gene Ther.* 2014;25:83–91. doi: 10.1089/hum.2014.2501
- 183 Shen Y, Nemunaitis J. Herpes simplex virus 1 (HSV-1) for cancer treatment. *Cancer Gene Ther.* 2006;13:975–92. doi: 10.1038/sj.cgt.7700946
- 184 Manservigi R, Argnani R, Marconi P. HSV Recombinant Vectors for Gene Therapy. *Open Virol J.* 2010;4:123–56. doi: 10.2174/1874357901004010123
- 185 Argnani R, Lufino M, Manservigi M, *et al.* Replication-competent herpes simplex vectors: design and applications. *Gene Ther.* 2005;12 Suppl 1:S170-177. doi: 10.1038/sj.gt.3302622
- 186 Epstein AL. HSV-1-derived amplicon vectors: recent technological improvements and remaining difficulties--a review. *Mem Inst Oswaldo Cruz.* 2009;104:399–410. doi: 10.1590/s0074-02762009000300002
- 187 de Silva S, Bowers WJ. Herpes Virus Amplicon Vectors. *Viruses.* 2009;1:594–624. doi: 10.3390/v1030594
- 188 Moriuchi S, Glorioso JC, Maruno M, *et al.* Combination gene therapy for glioblastoma involving herpes simplex virus vector-mediated codelivery of mutant IkappaBalpha and HSV thymidine kinase. *Cancer Gene Ther.* 2005;12:487–96. doi: 10.1038/sj.cgt.7700816

- 189 Moriuchi S, Wolfe D, Tamura M, *et al.* Double suicide gene therapy using a replication defective herpes simplex virus vector reveals reciprocal interference in a malignant glioma model. *Gene Ther.* 2002;9:584–91. doi: 10.1038/sj.gt.3301693
- 190 Laurens W, Joussain C, Pierre D, *et al.* Unlocking potential: Herpes Simplex Virus Type 1-based gene therapy in functional urology. *Continence.* 2024;10:101311. doi: 10.1016/j.cont.2024.101311
- 191 Pezzoli D, Kajaste-Rudnitski A, Chiesa R, *et al.* Lipid-based nanoparticles as nonviral gene delivery vectors. *Methods Mol Biol Clifton NJ.* 2013;1025:269–79. doi: 10.1007/978-1-62703-462-3\_21
- 192 Jin L, Zeng X, Liu M, *et al.* Current Progress in Gene Delivery Technology Based on Chemical Methods and Nano-carriers. *Theranostics.* 2014;4:240–55. doi: 10.7150/thno.6914
- 193 Liu Y, Liggitt D, Zhong W, *et al.* Cationic liposome-mediated intravenous gene delivery. *J Biol Chem.* 1995;270:24864–70. doi: 10.1074/jbc.270.42.24864
- 194 Reszka RC, Jacobs A, Voges J. Liposome-mediated suicide gene therapy in humans. *Methods Enzymol.* 2005;391:200–8. doi: 10.1016/S0076-6879(05)91012-4
- 195 Escriou V, Ciolina C, Lacroix F, *et al.* Cationic lipid-mediated gene transfer: effect of serum on cellular uptake and intracellular fate of lipopolyamine/DNA complexes. *Biochim Biophys Acta BBA - Biomembr.* 1998;1368:276–88. doi: 10.1016/S0005-2736(97)00194-6
- 196 Kaneda Y, Tabata Y. Non-viral vectors for cancer therapy. *Cancer Sci.* 2006;97:348–54. doi: 10.1111/j.1349-7006.2006.00189.x
- 197 Nishikawa M, Huang L. Nonviral vectors in the new millennium: delivery barriers in gene transfer. *Hum Gene Ther.* 2001;12:861–70. doi: 10.1089/104303401750195836
- 198 De Laporte L, Cruz Rea J, Shea LD. Design of modular non-viral gene therapy vectors. *Biomaterials.* 2006;27:947–54. doi: 10.1016/j.biomaterials.2005.09.036
- 199 Zhao C, Zhou B. Polyethyleneimine-Based Drug Delivery Systems for Cancer Theranostics. *J Funct Biomater.* 2022;14:12. doi: 10.3390/jfb14010012
- 200 Moradian Tehrani R, Verdi J, Nouredini M, *et al.* Mesenchymal stem cells: A new platform for targeting suicide genes in cancer. *J Cell Physiol.* 2018;233:3831–45. doi: 10.1002/jcp.26094
- 201 Uchibori R, Tsukahara T, Ohmine K, *et al.* Cancer gene therapy using mesenchymal stem cells. *Int J Hematol.* 2014;99:377–82. doi: 10.1007/s12185-014-1537-7
- 202 Long JZ, Cravatt BF. The Metabolic Serine Hydrolases and Their Functions in Mammalian Physiology and Disease. *Chem Rev.* 2011;111:6022–63. doi: 10.1021/cr200075y

- 203 Li S, Yang X, Yang S, *et al.* Technology Prospecting on Enzymes: Application, Marketing and Engineering. *Comput Struct Biotechnol J*. 2012;2:e201209017. doi: 10.5936/csbj.201209017
- 204 Jana S, Mandlekar S, Marathe P. Prodrug Design to Improve Pharmacokinetic and Drug Delivery Properties: Challenges to the Discovery Scientists. *Curr Med Chem*. 2010;17:3874–908. doi: 10.2174/092986710793205426
- 205 Hsieh P-W, Hung C-F, Fang J-Y. Current Prodrug Design for Drug Discovery. *Curr Pharm Des*. 2009;15:2236–50. doi: 10.2174/138161209788682523
- 206 Prabha M. Hydrolytic Enzymes Targeting to Prodrug/Drug Metabolism for Translational Application in Cancer. *J Clin Sci Trans Med* 2019, 1(1): 000102. *Transl Med*. 2019.
- 207 Yang Y, Aloysius H, Inoyama D, *et al.* Enzyme-mediated hydrolytic activation of prodrugs. *Acta Pharm Sin B*. 2011;1:143–59. doi: 10.1016/j.apsb.2011.08.001
- 208 Redinbo MR, Potter PM. Mammalian carboxylesterases: from drug targets to protein therapeutics. *Drug Discov Today*. 2005;10:313–25. doi: 10.1016/S1359-6446(05)03383-0
- 209 Satoh T, Hosokawa M. Structure, function and regulation of carboxylesterases. *Chem Biol Interact*. 2006;162:195–211. doi: 10.1016/j.cbi.2006.07.001
- 210 Yasunari K, Maeda K, Nakamura M, *et al.* Pharmacological and Clinical Studies with Temocapril, an Angiotensin Converting Enzyme Inhibitor that is Excreted in the Bile. *Cardiovasc Drug Rev*. 2004;22:189–98. doi: 10.1111/j.1527-3466.2004.tb00140.x
- 211 Nakamura M, Shirasawa E, Hikida M. Characterization of Esterases Involved in the Hydrolysis of Dipivefrin Hydrochloride. *Ophthalmic Res*. 2009;25:46–51. doi: 10.1159/000267220
- 212 Fleming CD, Bencharit S, Edwards CC, *et al.* Structural Insights into Drug Processing by Human Carboxylesterase 1: Tamoxifen, Mevastatin, and Inhibition by Benzil. *J Mol Biol*. 2005;352:165–77. doi: 10.1016/j.jmb.2005.07.016
- 213 Bencharit S, Morton CL, Howard-Williams EL, *et al.* Structural insights into CPT-11 activation by mammalian carboxylesterases. *Nat Struct Biol*. 2002;9:337–42. doi: 10.1038/nsb790
- 214 Morton CL, Iacono L, Hyatt JL, *et al.* Activation and antitumor activity of CPT-11 in plasma esterase-deficient mice. *Cancer Chemother Pharmacol*. 2005;56:629–36. doi: 10.1007/s00280-005-1027-y
- 215 Lauer-Fields JL, Juska D, Fields GB. Matrix metalloproteinases and collagen catabolism. *Pept Sci*. 2002;66:19–32. doi: 10.1002/bip.10201
- 216 Van Valckenborgh E, Mincher D, Di Salvo A, *et al.* Targeting an MMP-9-activated prodrug to multiple myeloma-diseased bone marrow: a proof of principle in the 5T33MM mouse model. *Leukemia*. 2005;19:1628–33. doi: 10.1038/sj.leu.2403866

- 217 Albright CF, Graciani N, Han W, *et al.* Matrix metalloproteinase-activated doxorubicin prodrugs inhibit HT1080 xenograft growth better than doxorubicin with less toxicity. *Mol Cancer Ther.* 2005;4:751–60. doi: 10.1158/1535-7163.MCT-05-0006
- 218 Rooseboom M, Commandeur JNM, Vermeulen NPE. Enzyme-Catalyzed Activation of Anticancer Prodrugs. *Pharmacol Rev.* 2004;56:53–102. doi: 10.1124/pr.56.1.3
- 219 Graaf M, Boven E, Scheeren HW, *et al.* Beta-Glucuronidase-Mediated Drug Release. *Curr Pharm Des.* 2002;8:1391–403. doi: 10.2174/1381612023394485
- 220 Vogler C, Barker J, Sands MS, *et al.* Murine Mucopolysaccharidosis VII: Impact of Therapies on the Phenotype, Clinical Course, and Pathology in a Model of a Lysosomal Storage Disease. *Pediatr Dev Pathol.* 2001;4:421–33. doi: 10.1007/s10024001-0079-1
- 221 Alaoui AE, Saha N, Schmidt F, *et al.* New Taxol® (paclitaxel) prodrugs designed for ADEPT and PMT strategies in cancer chemotherapy. *Bioorg Med Chem.* 2006;14:5012–9. doi: 10.1016/j.bmc.2006.03.002
- 222 Chen B-M, Chan L-Y, Wang S-M, *et al.* Cure of malignant ascites and generation of protective immunity by monoclonal antibody-targeted activation of a glucuronide prodrug in rats. *Int J Cancer.* 1997;73:392–402. doi: 10.1002/(SICI)1097-0215(19971104)73:3<392::AID-IJC14>3.0.CO;2-F
- 223 Kamal A, Tekumalla V, Raju P, *et al.* Pyrrolo[2,1-c][1,4]benzodiazepine- $\beta$ -glucuronide prodrugs with a potential for selective therapy of solid tumors by PMT and ADEPT strategies. *Bioorg Med Chem Lett.* 2008;18:3769–73. doi: 10.1016/j.bmcl.2008.05.038
- 224 McCormack RT, Wang TJ, Rittenhouse HG, *et al.* Molecular forms of prostate-specific antigen and the human kallikrein gene family: A new era. *Urology.* 1995;45:729–44. doi: 10.1016/S0090-4295(99)80076-4
- 225 Denmeade SR, Lou W, Lövgren J, *et al.* Specific and Efficient Peptide Substrates for Assaying the Proteolytic Activity of Prostate-specific Antigen1. *Cancer Res.* 1997;57:4924–30.
- 226 DiPaola RS, Rinehart J, Nemunaitis J, *et al.* Characterization of a Novel Prostate-Specific Antigen-Activated Peptide-Doxorubicin Conjugate in Patients With Prostate Cancer. *J Clin Oncol.* 2002;20:1874–9. doi: 10.1200/JCO.2002.07.001
- 227 Mhaka A, Denmeade SR, Yao W, *et al.* A 5-fluorodeoxyuridine prodrug as targeted therapy for prostate cancer. *Bioorg Med Chem Lett.* 2002;12:2459–61. doi: 10.1016/S0960-894X(02)00433-X
- 228 Denmeade SR, Jakobsen CM, Janssen S, *et al.* Prostate-Specific Antigen-Activated Thapsigargin Prodrug as Targeted Therapy for Prostate Cancer. *JNCI J Natl Cancer Inst.* 2003;95:990–1000. doi: 10.1093/jnci/95.13.990

- 229 Kumar SK, Williams SA, Isaacs JT, *et al.* Modulating paclitaxel bioavailability for targeting prostate cancer. *Bioorg Med Chem.* 2007;15:4973–84. doi: 10.1016/j.bmc.2007.04.029
- 230 Williams SA, Merchant RF, Garrett-Mayer E, *et al.* A Prostate-Specific Antigen–Activated Channel-Forming Toxin as Therapy for Prostatic Disease. *JNCI J Natl Cancer Inst.* 2007;99:376–85. doi: 10.1093/jnci/djk065
- 231 Dowell RI, Springer CJ, Davies DH, *et al.* New Mustard Prodrugs for Antibody-Directed Enzyme Prodrug Therapy: Alternatives to the Amide Link. *J Med Chem.* 1996;39:1100–5. doi: 10.1021/jm950671i
- 232 Niculescu-Duvaz I, Scanlon I, Niculescu-Duvaz D, *et al.* Significant Differences in Biological Parameters between Prodrugs Cleavable by Carboxypeptidase G2 That Generate 3,5-Difluoro-phenol and -aniline Nitrogen Mustards in Gene-Directed Enzyme Prodrug Therapy Systems. *J Med Chem.* 2004;47:2651–8. doi: 10.1021/jm030966w
- 233 Niculescu-Duvaz D, Niculescu-Duvaz I, Friedlos F, *et al.* Self-Immolative Nitrogen Mustards Prodrugs Cleavable by Carboxypeptidase G2 (CPG2) Showing Large Cytotoxicity Differentials in GDEPT. *J Med Chem.* 2003;46:1690–705. doi: 10.1021/jm020462i
- 234 Moradbeygi F, Ghasemi Y, Farmani AR, *et al.* Glucarpidase (carboxypeptidase G2): Biotechnological production, clinical application as a methotrexate antidote, and placement in targeted cancer therapy. *Biomed Pharmacother Biomedecine Pharmacother.* 2023;166:115292. doi: 10.1016/j.biopha.2023.115292
- 235 Yang Y, Chen Y, Aloysius H, *et al.* Enzymes and Targeted Activation of Prodrugs. *Enzyme Technologies.* John Wiley & Sons, Ltd 2013:163–235.
- 236 Bignami GS, Senter PD, Grothaus PG, *et al.* N-(4'-Hydroxyphenylacetyl)palytoxin: A Palytoxin Prodrug That Can Be Activated by a Monoclonal Antibody-Penicillin G Amidase Conjugate1. *Cancer Res.* 1992;52:5759–64.
- 237 Zawilska JB, Wojcieszak J, Olejniczak AB. Prodrugs: A challenge for the drug development. *Pharmacol Rep.* 2013;65:1–14. doi: 10.1016/S1734-1140(13)70959-9
- 238 Zhao S, Yu N, Han H, *et al.* Advances in acid-degradable and enzyme-cleavable linkers for drug delivery. *Curr Opin Chem Biol.* 2025;84:102552. doi: 10.1016/j.cbpa.2024.102552
- 239 Walther R, Rautio J, Zelikin AN. Prodrugs in medicinal chemistry and enzyme prodrug therapies. *Adv Drug Deliv Rev.* 2017;118:65–77. doi: 10.1016/j.addr.2017.06.013
- 240 Sambrook J. Molecular cloning: a laboratory manual/Joseph Sambrook, David W. Russell. *Q Rev Biol.* 2001;76:348–9.
- 241 Benchling (2024). Benchling. <https://www.benchling.com/academic> (accessed 24 July 2024)

- 242 Davis MW, Jorgensen EM. ApE, A Plasmid Editor: A Freely Available DNA Manipulation and Visualization Program. *Front Bioinforma.* 2022;2:818619. doi: 10.3389/fbinf.2022.818619
- 243 Altschul SF, Gish W, Miller W, *et al.* Basic local alignment search tool. *J Mol Biol.* 1990;215:403–10. doi: 10.1016/S0022-2836(05)80360-2
- 244 Lowry OliverH, Rosebrough NiraJ, Farr AL, *et al.* PROTEIN MEASUREMENT WITH THE FOLIN PHENOL REAGENT. *J Biol Chem.* 1951;193:265–75. doi: 10.1016/S0021-9258(19)52451-6
- 245 Laemmli UK. Cleavage of Structural Proteins during the Assembly of the Head of Bacteriophage T4. *Nature.* 1970;227:680–5. doi: 10.1038/227680a0
- 246 Urbelienė N, Kutanovas S, Meškienė R, *et al.* Application of the uridine auxotrophic host and synthetic nucleosides for a rapid selection of hydrolases from metagenomic libraries. *Microb Biotechnol.* 2019;12:148–60. doi: 10.1111/1751-7915.13316
- 247 Erde J, Loo RRO, Loo JA. Enhanced FASP (eFASP) to increase proteome coverage and sample recovery for quantitative proteomic experiments. *J Proteome Res.* 2014;13:1885–95. doi: 10.1021/pr4010019
- 248 Azwar S, Seow HF, Abdullah M, *et al.* Recent Updates on Mechanisms of Resistance to 5-Fluorouracil and Reversal Strategies in Colon Cancer Treatment. *Biology.* 2021;10:854. doi: 10.3390/biology10090854
- 249 Tabata T, Katoh M, Tokudome S, *et al.* Bioactivation of capecitabine in human liver: involvement of the cytosolic enzyme on 5'-deoxy-5-fluorocytidine formation. *Drug Metab Dispos Biol Fate Chem.* 2004;32:762–7. doi: 10.1124/dmd.32.7.762
- 250 Arshad F, Khan MF, Akhtar W, *et al.* Revealing quinquennial anticancer journey of morpholine: A SAR based review. *Eur J Med Chem.* 2019;167:324–56. doi: 10.1016/j.ejmech.2019.02.015
- 251 Narayanan A, Ananda Baskaran S, Amalaradjou MAR, *et al.* Anticarcinogenic Properties of Medium Chain Fatty Acids on Human Colorectal, Skin and Breast Cancer Cells in Vitro. *Int J Mol Sci.* 2015;16:5014–27. doi: 10.3390/ijms16035014
- 252 Yeh H-C, Su C-C, Wu Y-H, *et al.* Novel insights into the anti-cancer effects of 3-bromopyruvic acid against castration-resistant prostate cancer. *Eur J Pharmacol.* 2022;923:174929. doi: 10.1016/j.ejphar.2022.174929
- 253 Ma Y, Yan X, Du R, *et al.* Synthesis, Anti-cancer Activity and Mechanism Study of 6-Mercapto-purine Derivatives. *Lett Drug Des Discov.* 2016;13:570–6.
- 254 Sadauskas M, Jakutis M, Petkevičius V, *et al.* Biocatalytic synthesis of asymmetric water-soluble indirubin derivatives. *Dyes Pigments.* 2023;219:111585. doi: 10.1016/j.dyepig.2023.111585
- 255 Sári Z, Mikó E, Kovács T, *et al.* Indolepropionic Acid, a Metabolite of the Microbiome, Has Cytostatic Properties in Breast Cancer by



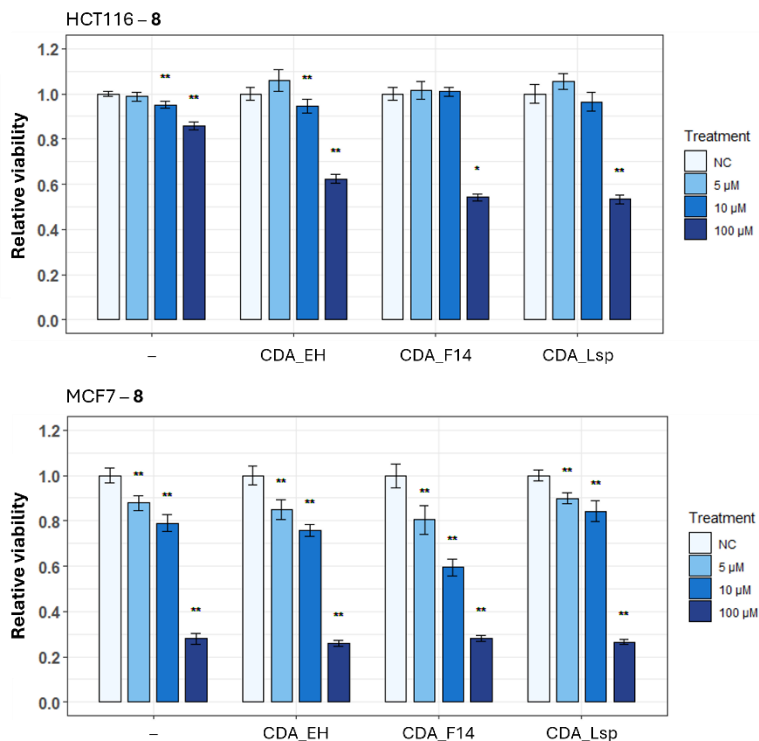
- Activating AHR and PXR Receptors and Inducing Oxidative Stress. *Cancers*. 2020;12:2411. doi: 10.3390/cancers12092411
- 256 Nayerossadat N, Maedeh T, Ali PA. Viral and nonviral delivery systems for gene delivery. *Adv Biomed Res*. 2012;1:27. doi: 10.4103/2277-9175.98152
  - 257 Statkevičiūtė R, Sadauskas M, Rainytė J, *et al*. Comparative Analysis of Mesophilic YqfB-Type Amidohydrolases. *Biomolecules*. 2022;12:1492. doi: 10.3390/biom12101492
  - 258 Cheng X, Wang G, Liao Y, *et al*. Chronic exposure to the gibberellin derivative GA-13315 sensitizes breast cancer MCF-7 cells but not colon cancer HCT116 cells to irinotecan. *Oncol Lett*. 2020;20:281. doi: 10.3892/ol.2020.12144
  - 259 de Jonge ME, Huitema ADR, Rodenhuis S, *et al*. Clinical pharmacokinetics of cyclophosphamide. *Clin Pharmacokinet*. 2005;44:1135–64. doi: 10.2165/00003088-200544110-00003
  - 260 Ciaffaglione V, Modica MN, Pittalà V, *et al*. Mutual Prodrugs of 5-Fluorouracil: From a Classic Chemotherapeutic Agent to Novel Potential Anticancer Drugs. *ChemMedChem*. 2021;16:3496–512. doi: 10.1002/cmdc.202100473
  - 261 Zhang N, Yin Y, Xu S-J, *et al*. 5-Fluorouracil: Mechanisms of Resistance and Reversal Strategies. *Molecules*. 2008;13:1551–69. doi: 10.3390/molecules13081551
  - 262 Lam SW, Guchelaar HJ, Boven E. The role of pharmacogenetics in capecitabine efficacy and toxicity. *Cancer Treat Rev*. 2016;50:9–22. doi: 10.1016/j.ctrv.2016.08.001
  - 263 Preitakaitė V, Barasa P, Aučynaitė A, *et al*. Bacterial amidohydrolases and modified 5-fluorocytidine compounds: Novel enzyme-prodrug pairs. *PLOS ONE*. 2023;18:e0294696. doi: 10.1371/journal.pone.0294696
  - 264 Serdžebi C, Milano G, Ciccolini J. Role of cytidine deaminase in toxicity and efficacy of nucleosidic analogs. *Expert Opin Drug Metab Toxicol*. 2015;11:665–72. doi: 10.1517/17425255.2015.985648
  - 265 Frances A, Cordelier P. The Emerging Role of Cytidine Deaminase in Human Diseases: A New Opportunity for Therapy? *Mol Ther J Am Soc Gene Ther*. 2020;28:357–66. doi: 10.1016/j.ymthe.2019.11.026
  - 266 Cacciamani T, Vita A, Cristalli G, *et al*. Purification of human cytidine deaminase: Molecular and enzymatic characterization and inhibition by synthetic pyrimidine analogs. *Arch Biochem Biophys*. 1991;290:285–92. doi: 10.1016/0003-9861(91)90543-R
  - 267 Xie F, Zhao H, Zhao L, *et al*. Synthesis and biological evaluation of novel 2,4,5-substituted pyrimidine derivatives for anticancer activity. *Bioorg Med Chem Lett*. 2009;19:275–8. doi: 10.1016/j.bmcl.2008.09.067

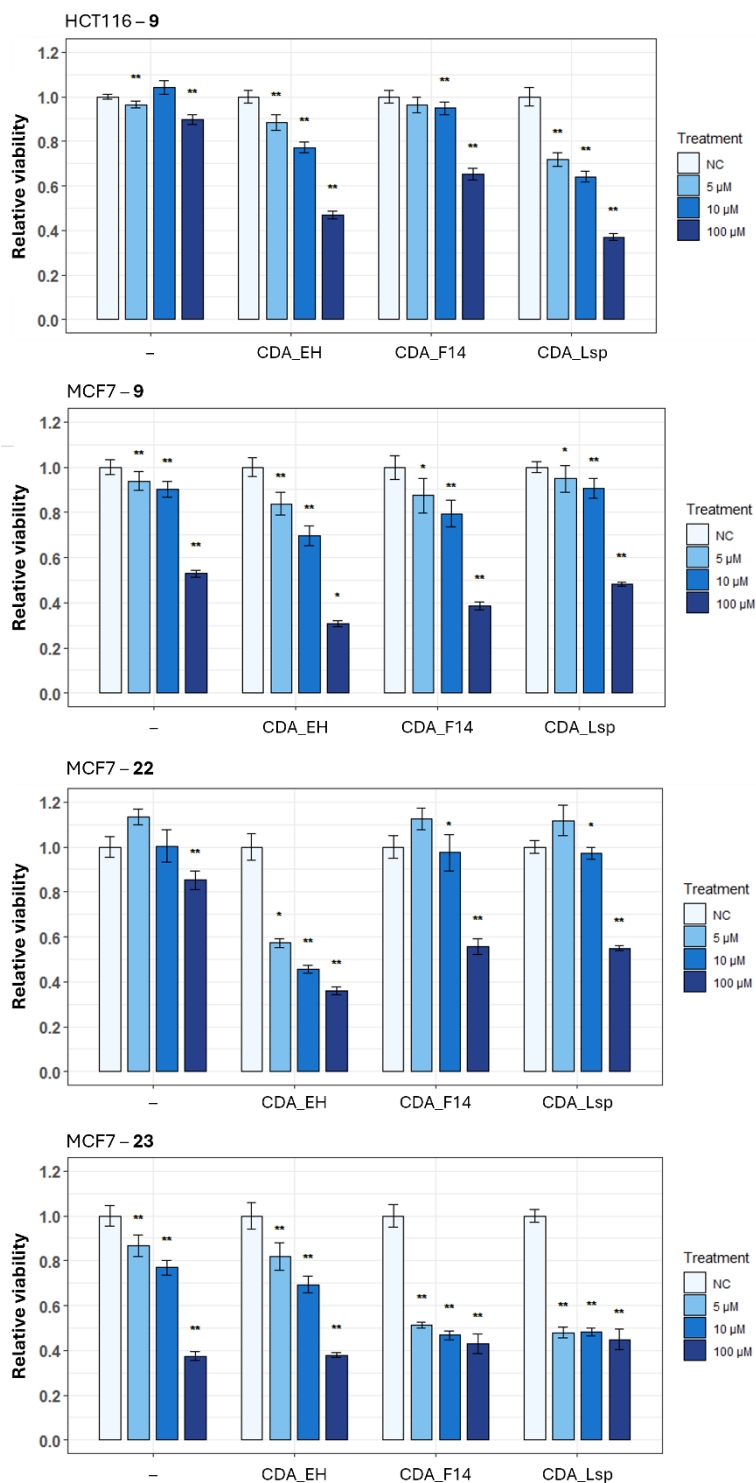
- 268 Matsuda A, Sasaki T. Antitumor activity of sugar-modified cytosine nucleosides. *Cancer Sci.* 2004;95:105–11. doi: 10.1111/j.1349-7006.2004.tb03189.x
- 269 Mohamed MM, Khalil AK, Abbass EM, *et al.* Design, synthesis of new pyrimidine derivatives as anticancer and antimicrobial agents. *Synth Commun.* 2017;47:1441–57. doi: 10.1080/00397911.2017.1332223
- 270 Testa B. Prodrugs: bridging pharmacodynamic/pharmacokinetic gaps. *Curr Opin Chem Biol.* 2009;13:338–44. doi: 10.1016/j.cbpa.2009.04.620
- 271 Mathijssen RHJ, Sparreboom A, Verweij J. Determining the optimal dose in the development of anticancer agents. *Nat Rev Clin Oncol.* 2014;11:272–81. doi: 10.1038/nrclinonc.2014.40
- 272 Parvathy ST, Udayasuriyan V, Bhadana V. Codon usage bias. *Mol Biol Rep.* 2022;49:539–65. doi: 10.1007/s11033-021-06749-4
- 273 Mauro VP. Codon Optimization in the Production of Recombinant Biotherapeutics: Potential Risks and Considerations. *BioDrugs.* 2018;32:69–81. doi: 10.1007/s40259-018-0261-x
- 274 Inouye S, Sahara-Miura Y, Sato J, *et al.* Codon optimization of genes for efficient protein expression in mammalian cells by selection of only preferred human codons. *Protein Expr Purif.* 2015;109:47–54. doi: 10.1016/j.pep.2015.02.002
- 275 Cano-Soldado P, Pastor-Anglada M. Transporters that translocate nucleosides and structural similar drugs: structural requirements for substrate recognition. *Med Res Rev.* 2012;32:428–57. doi: 10.1002/med.20221
- 276 Fukami T, Yokoi T. The Emerging Role of Human Esterases. *Drug Metab Pharmacokinet.* 2012;27:466–77. doi: 10.2133/dmpk.DMPK-12-RV-042
- 277 Grabbe C, Cai L. Regioselective Deacetylation in Nucleosides and Derivatives. *ChemBioChem.* 2024;25:e202400360. doi: 10.1002/cbic.202400360
- 278 Yalamarty SSK, Filipczak N, Li X, *et al.* Mechanisms of Resistance and Current Treatment Options for Glioblastoma Multiforme (GBM). *Cancers.* 2023;15:2116. doi: 10.3390/cancers15072116

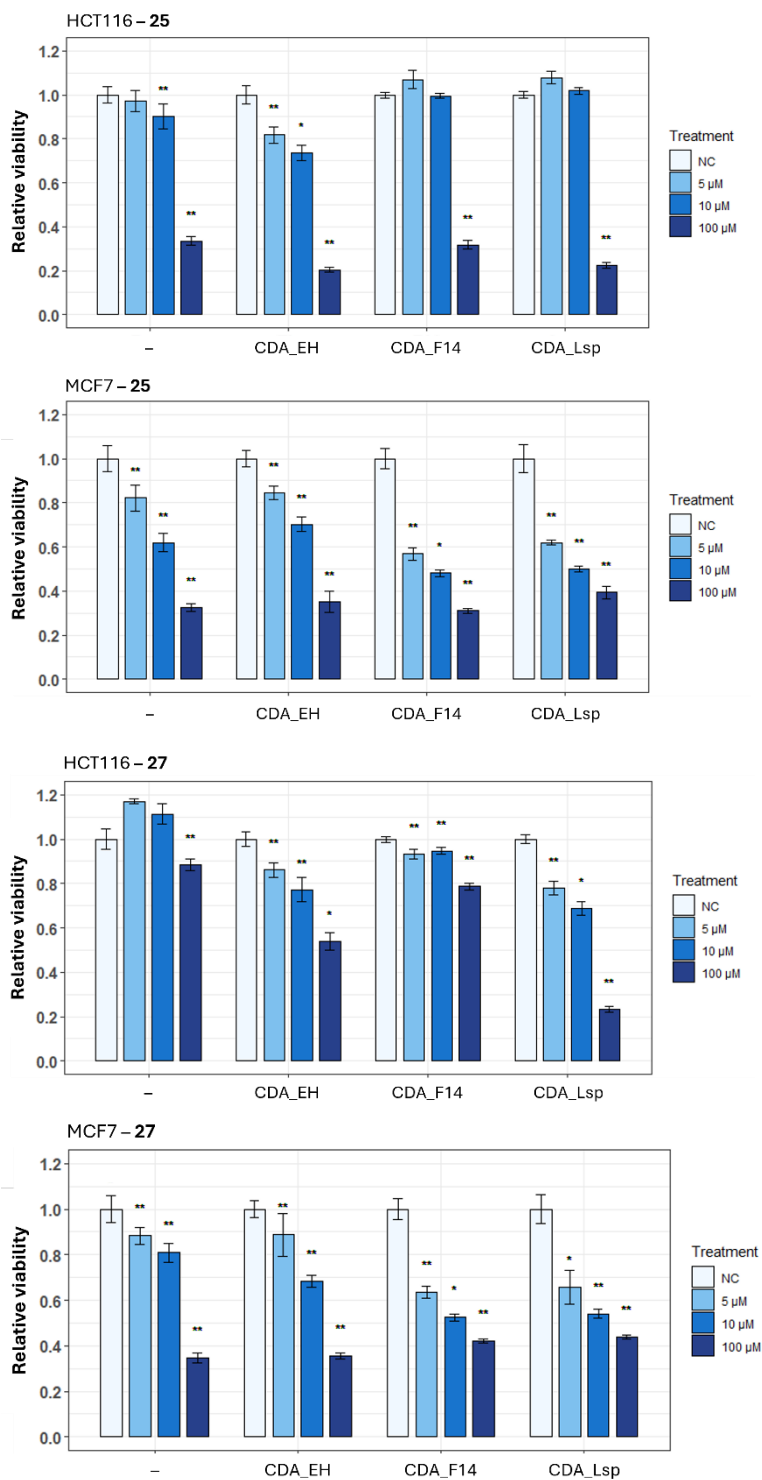
## SUPPLEMENT

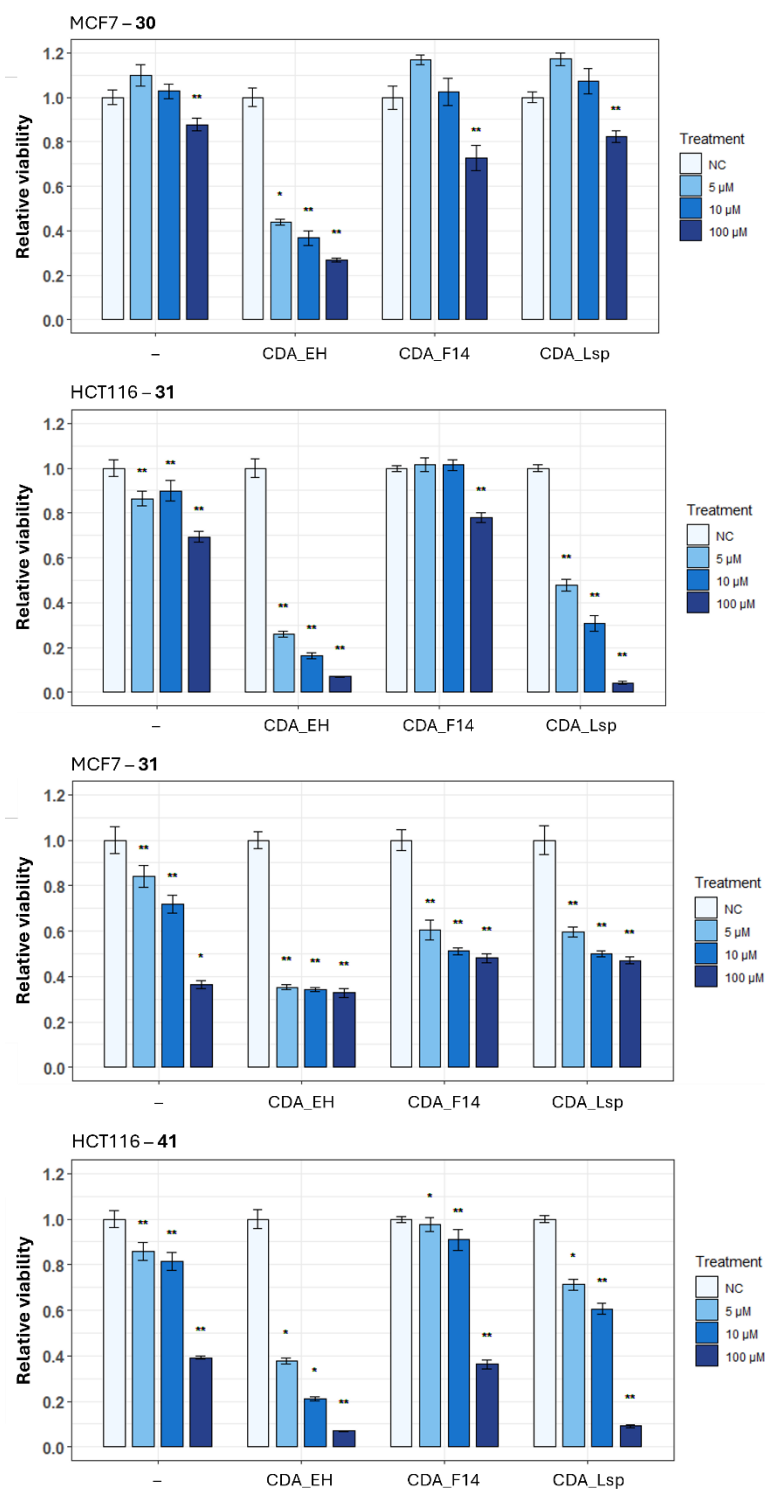
**Section S1.** Evaluation of cell viability in bacterial CDA\_EH, CDA\_F14, and CDA\_Lsp-expressing cells following prodrug treatment.

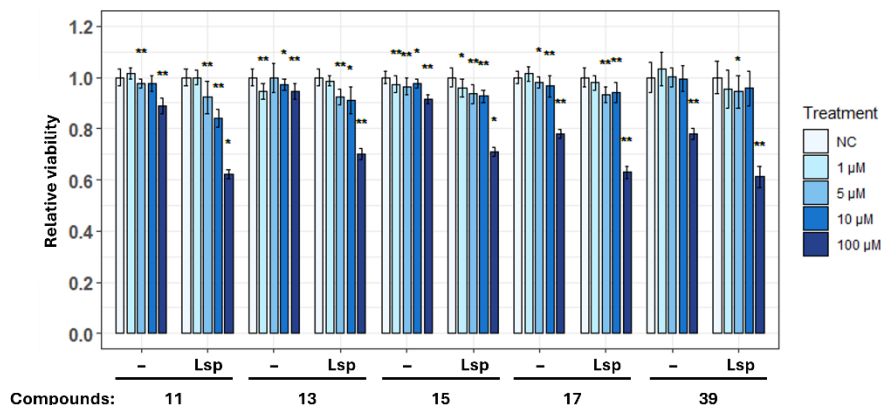
Detailed graphs illustrating the changes in cell viability of HCT116 and MCF7 cells expressing bacterial CDA\_EH, CDA\_F14, and CDA\_Lsp after exposure to **8, 9, 22, 23, 25, 27, 30, 31, and 41** are presented below. Cell lines transduced with CDA\_EH-encoding vector pBABE-CDA\_EH (designated as CDA\_EH), CDA\_F14-encoding vector pBABE-CDA\_F14 (designated as CDA\_F14), CDA\_Lsp-encoding vector pBABE-CDA\_Lsp (designated as CDA\_Lsp) or control vector pBABE-Puro (designated as symbol “–”) were exposed to 5  $\mu$ M, 10  $\mu$ M, and 100  $\mu$ M concentrations of compounds for the 48 hours. Statistical significance is indicated by *p*-values, where the symbol \* designates  $p < 0.05$ , whereas the symbol \*\* designates  $p < 0.01$  with respect to untreated cells (negative control (NC)).







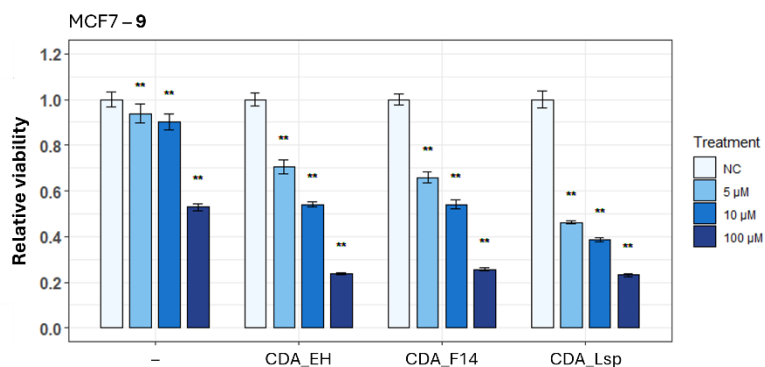
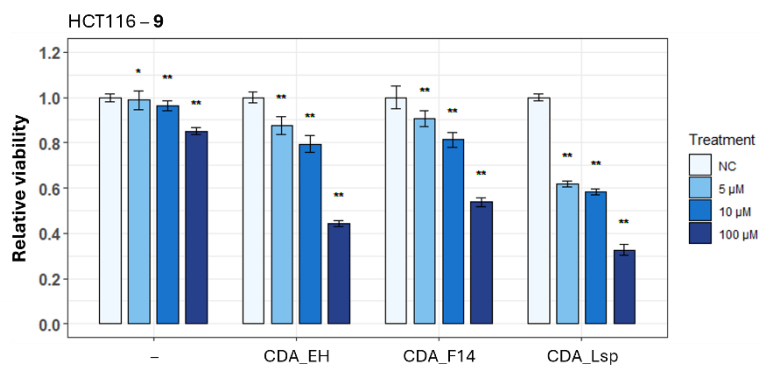
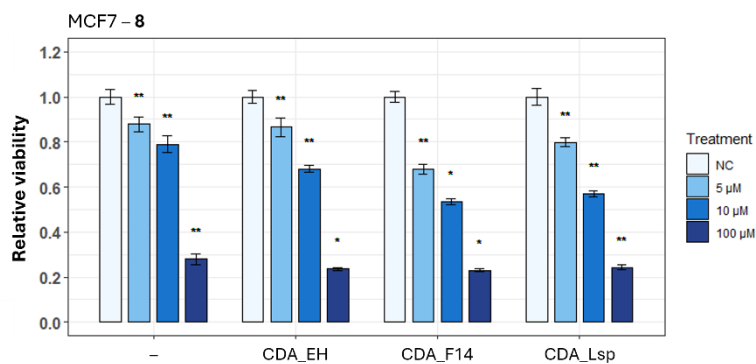
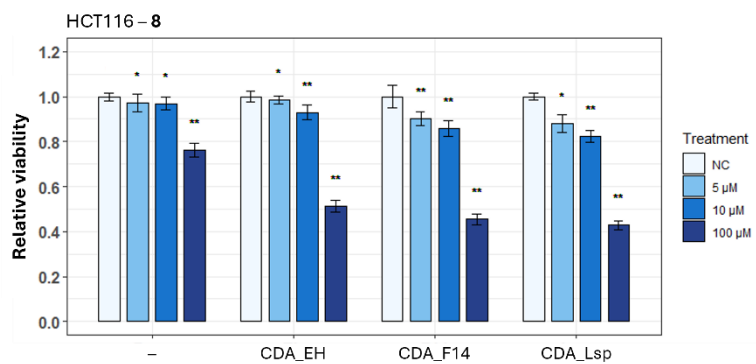




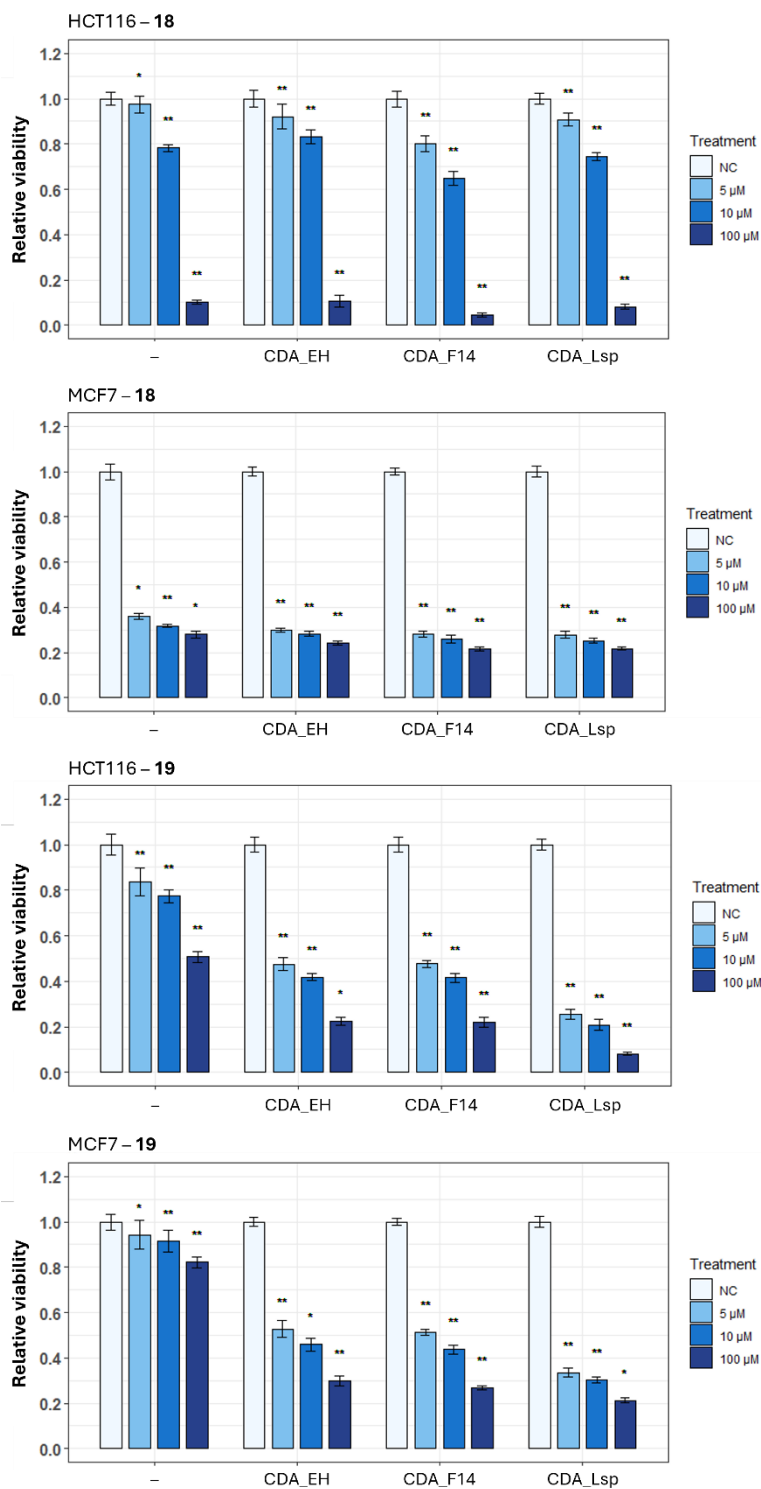
**Figure S1.** MTT assay of HCT116 cell line expressing CDA\_Lsp following treatment of **11**, **13**, **15**, **17**, and **39**. Cell lines transduced with CDA\_Lsp-encoding vector pBABE-CDA\_Lsp (designated as Lsp) or control vector pBABE-Puro (designated as symbol –) were exposed to several different concentrations (1–100  $\mu$ M) of compounds for the 24 hours. Statistical significance is indicated by *p*-values, where the symbol \* designates  $p < 0.05$ , whereas the symbol \*\* designates  $p < 0.01$  with respect to untreated cells (negative control (NC)).

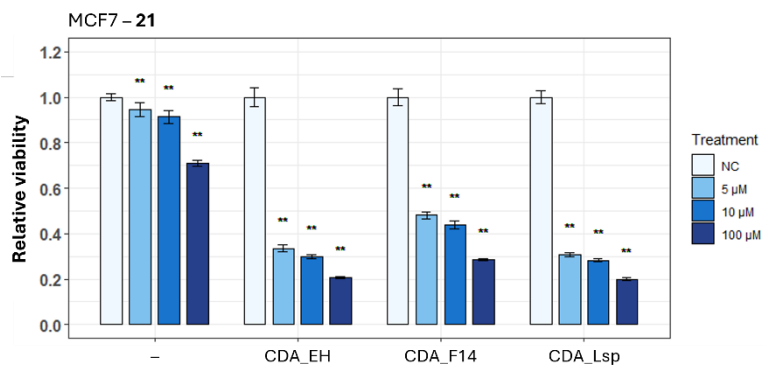
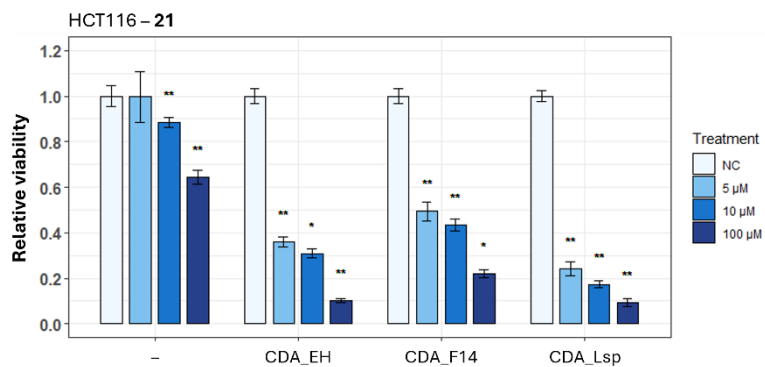
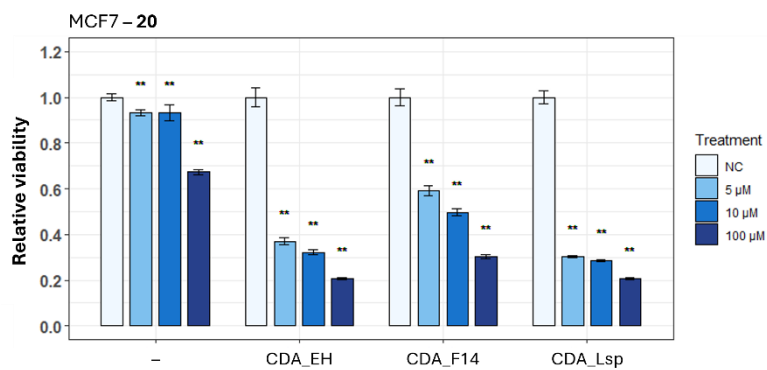
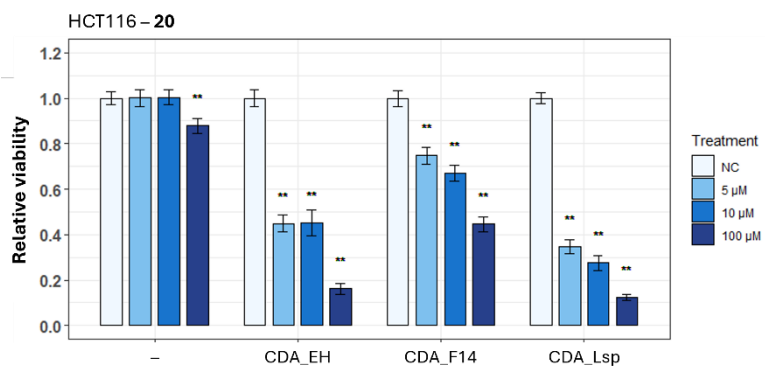
**Section S2.** Evaluation of cell viability in human codon-optimized CDA\_EH, CDA\_F14, and CDA\_Lsp-expressing cells following prodrug treatment.

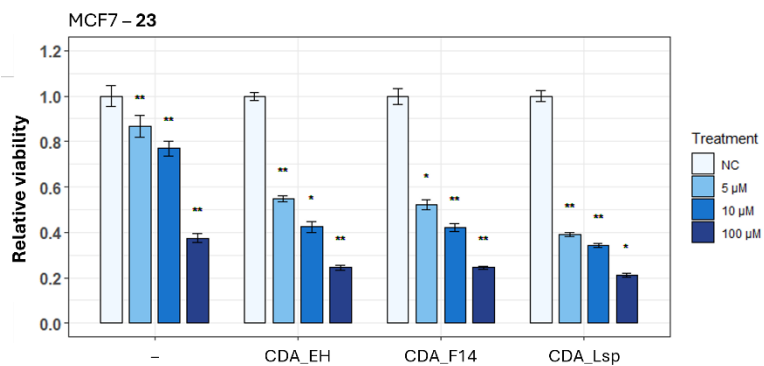
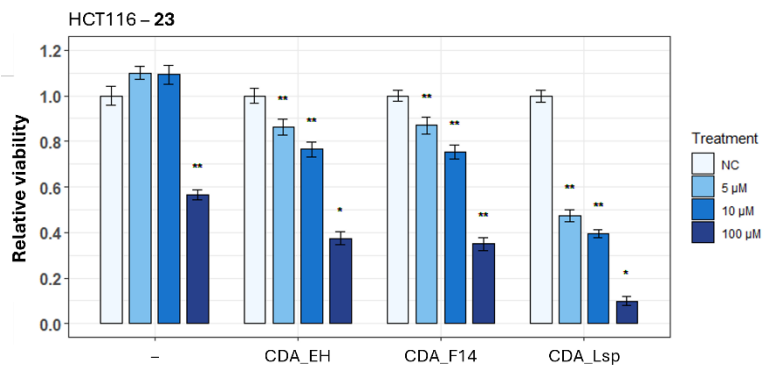
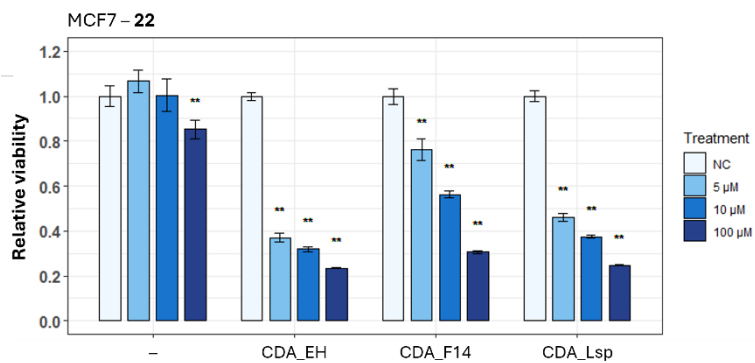
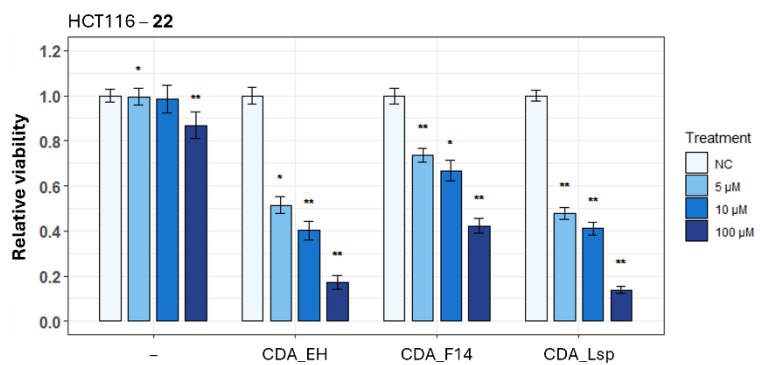
Detailed graphs illustrating the changes in cell viability of HCT116 and MCF7 cells expressing human codon-optimized CDA\_EH, CDA\_F14, and CDA\_Lsp after exposure to **8**, **9**, **18–25**, **27**, **28**, **30–32**, **34**, **36**, **40–42**, **44**, **46**, and **48** are presented below. Cell lines transduced with CDA\_EH-encoding vector pBABE-CDA\_EH (designated as CDA\_EH), CDA\_F14-encoding vector pBABE-CDA\_F14 (designated as CDA\_F14), CDA\_Lsp-encoding vector pBABE-CDA\_Lsp (designated as CDA\_Lsp) or control vector pBABE-Puro (designated as symbol “–”) were exposed to 5  $\mu$ M, 10  $\mu$ M, and 100  $\mu$ M concentrations of compounds for the 48 hours. Statistical significance is indicated by *p*-values, where the symbol \* designates  $p < 0.05$ , whereas the symbol \*\* designates  $p < 0.01$  with respect to untreated cells (negative control (NC)).

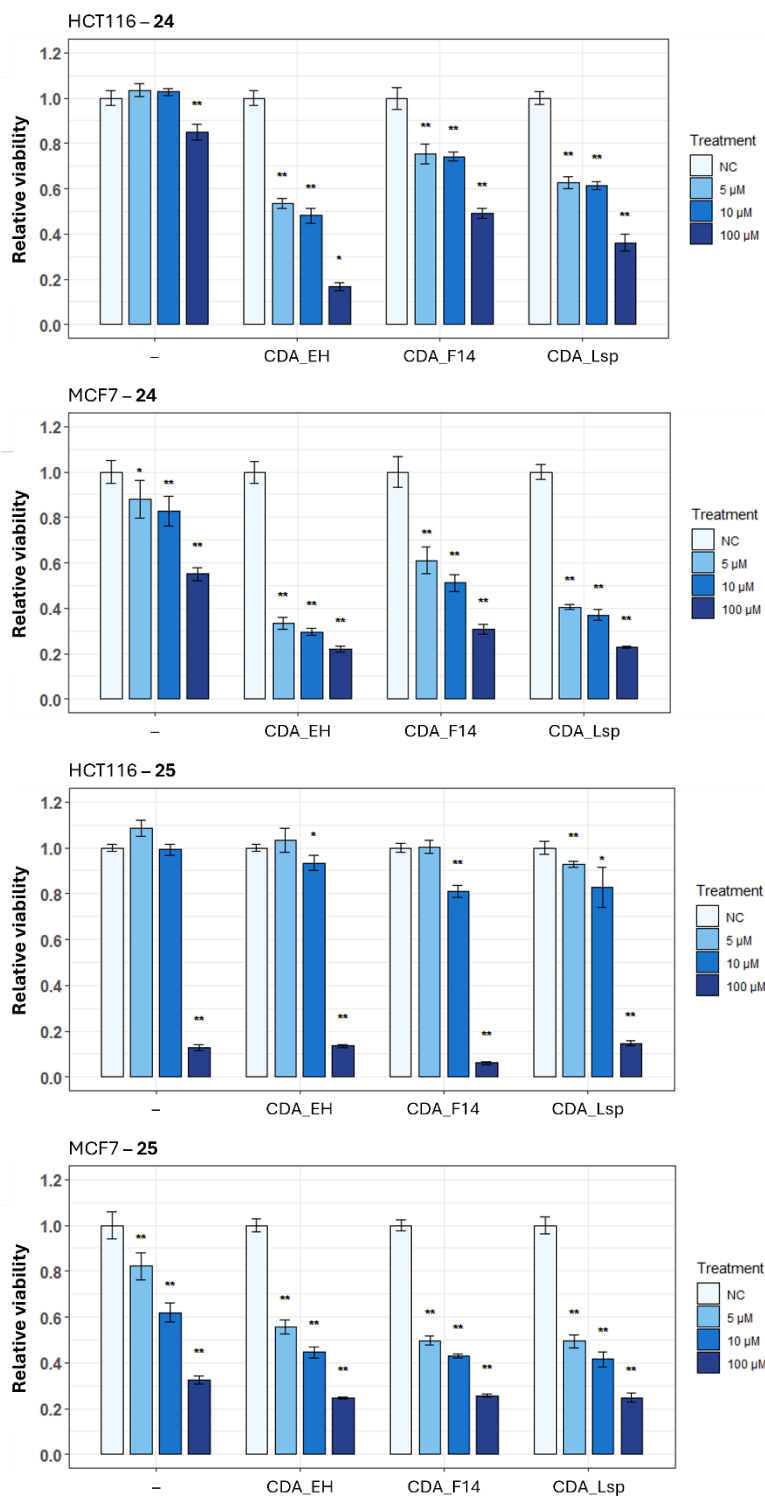


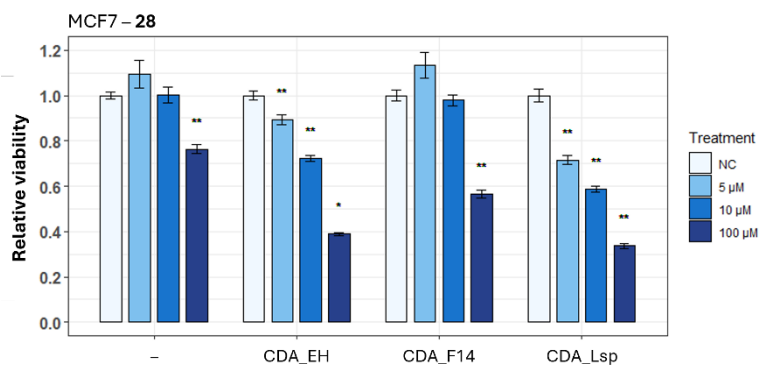
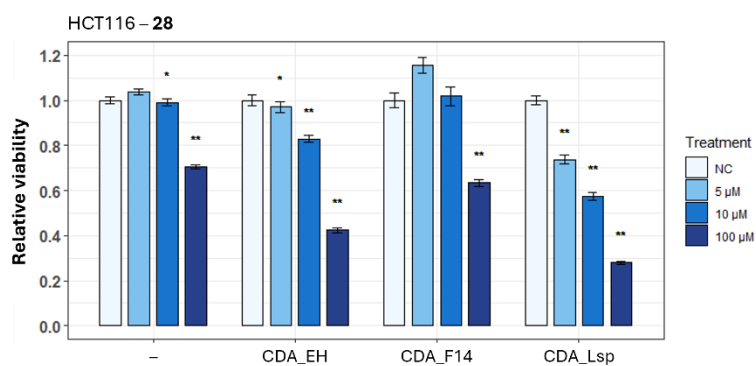
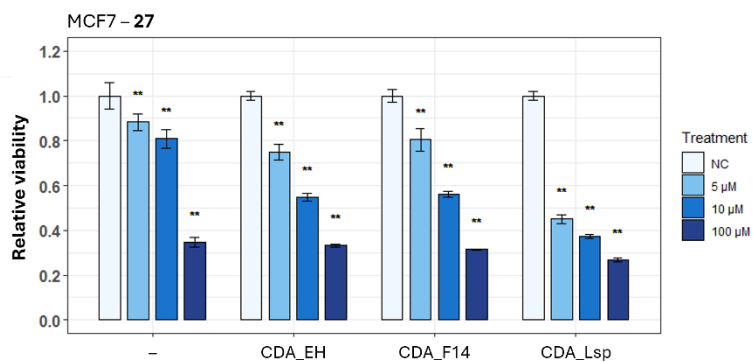
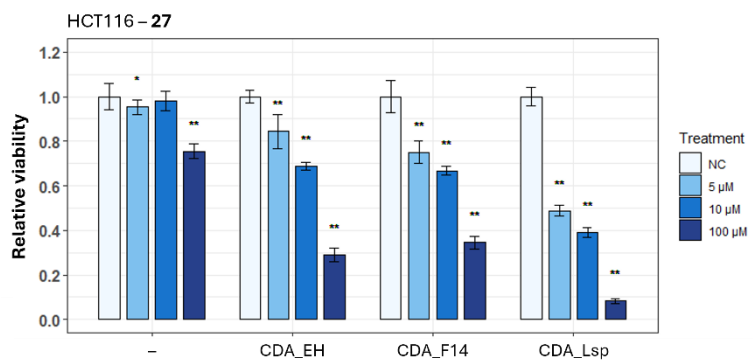


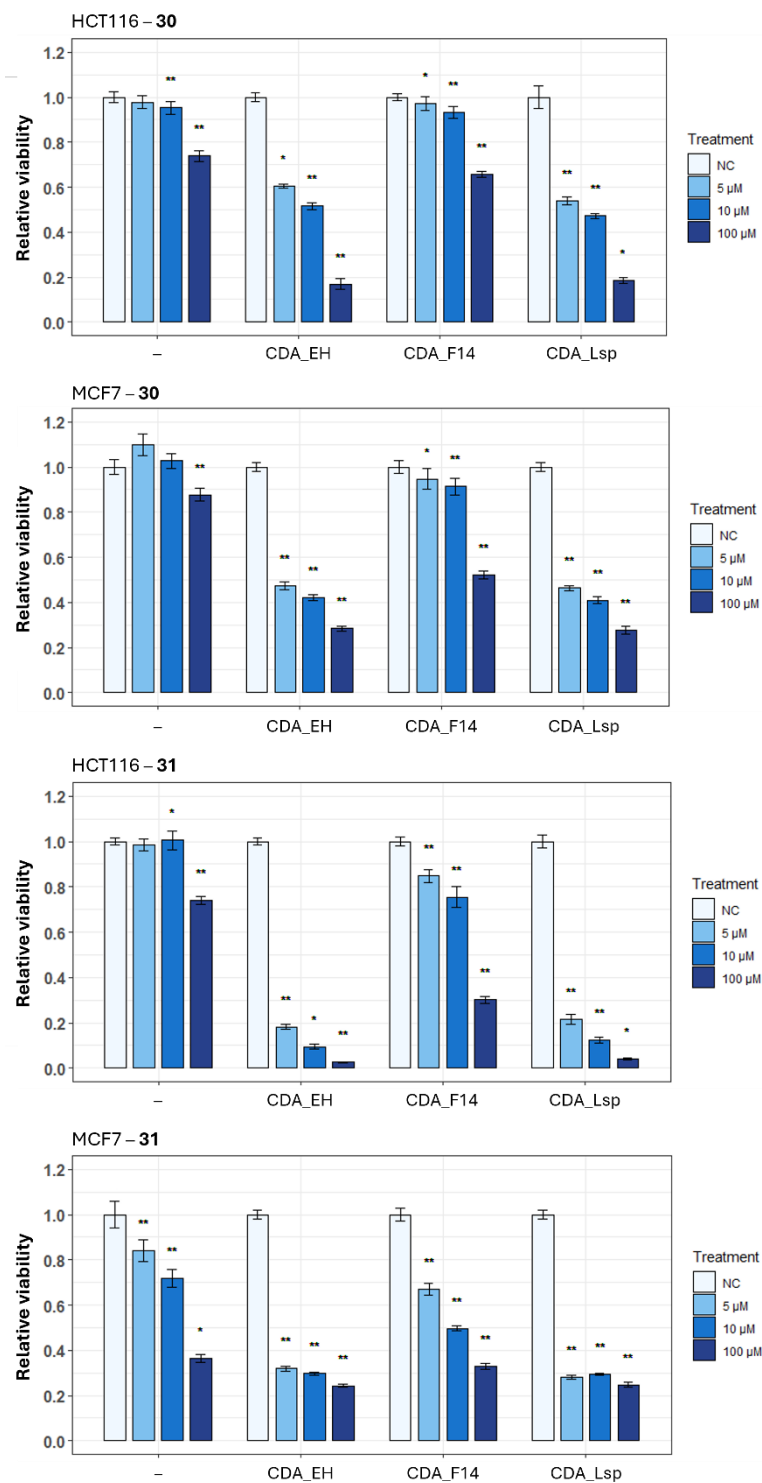


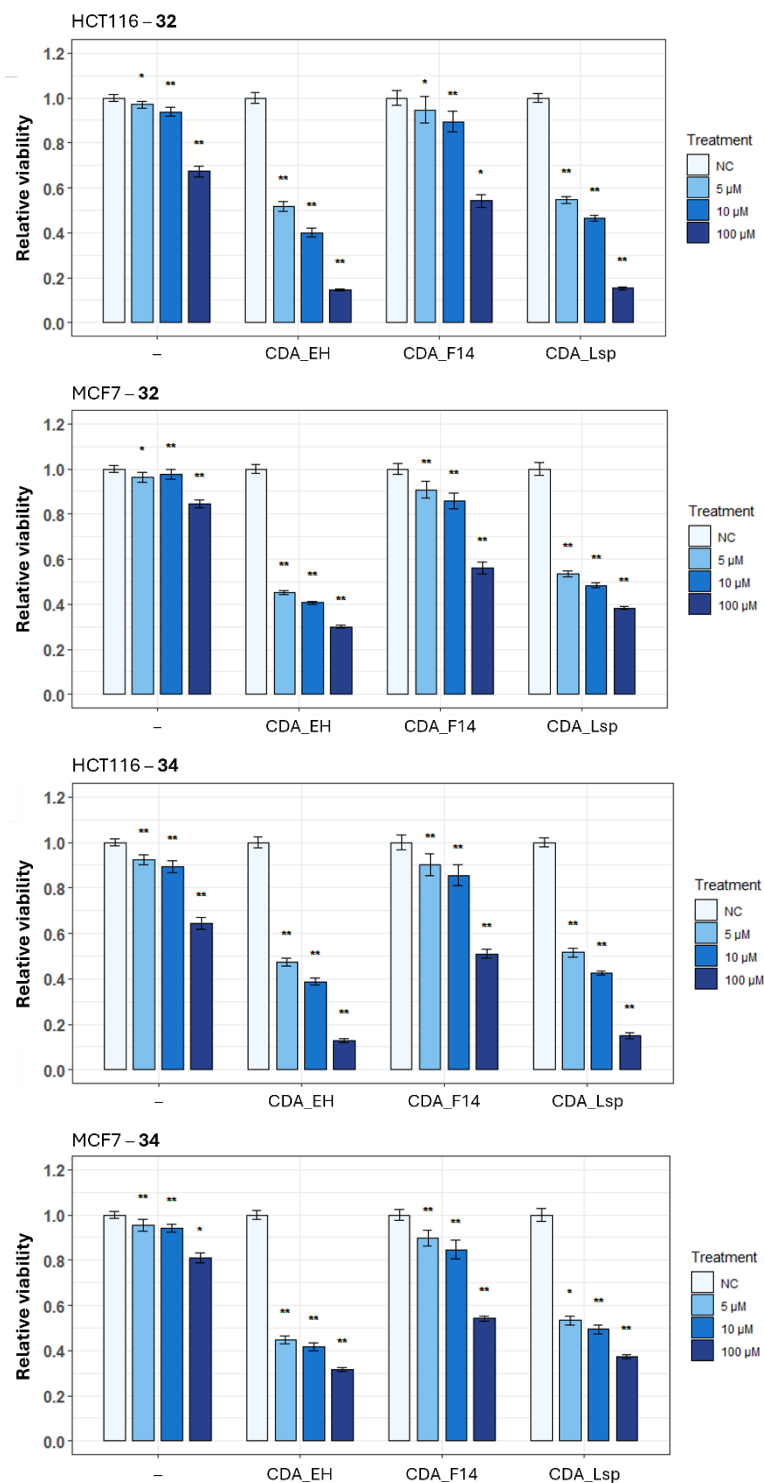


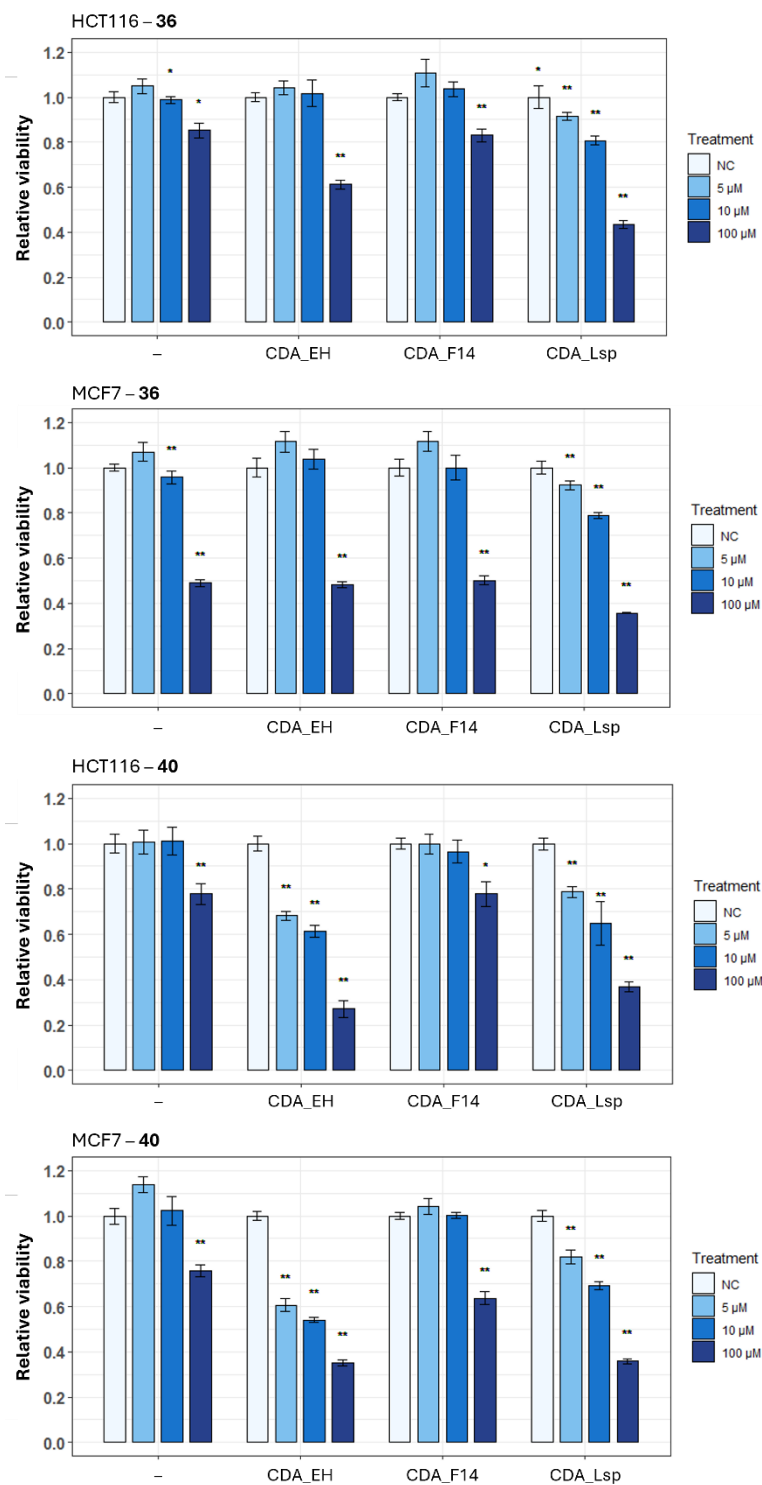




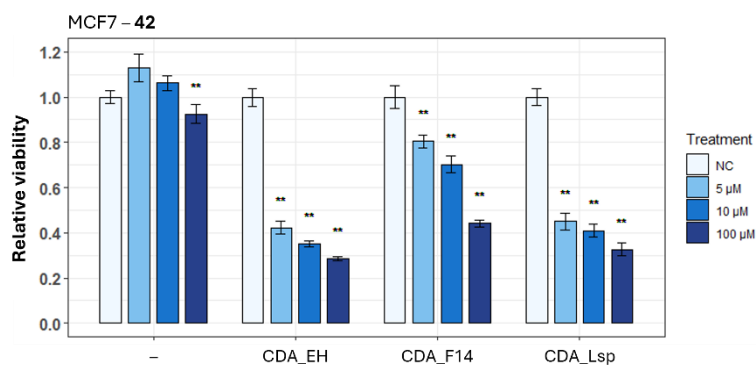
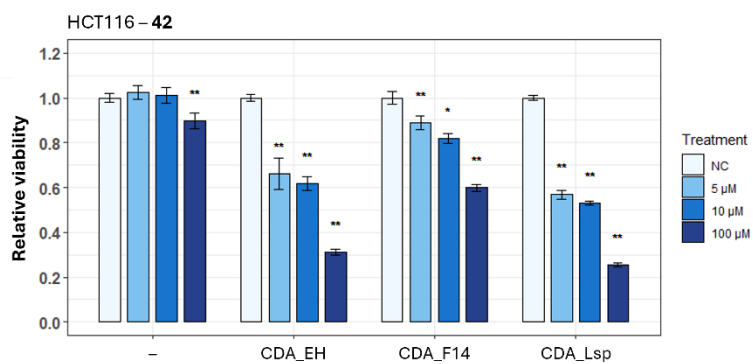
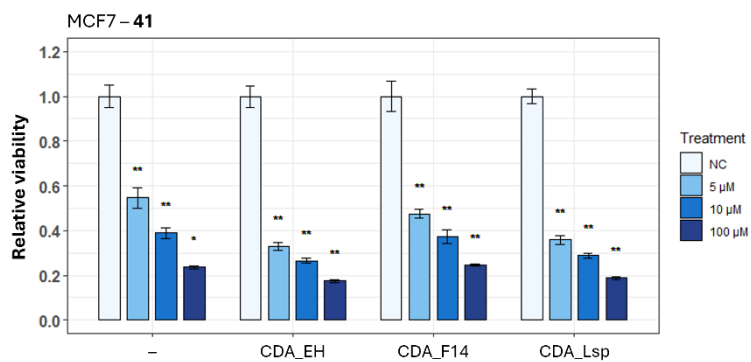
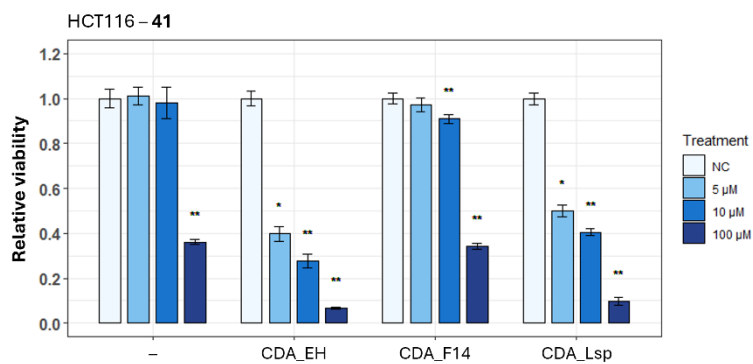


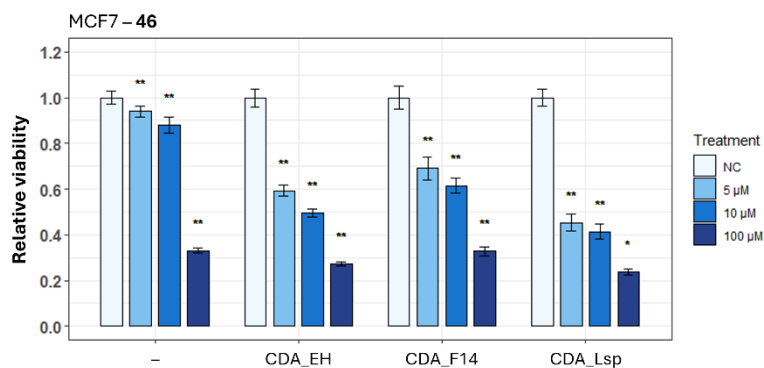
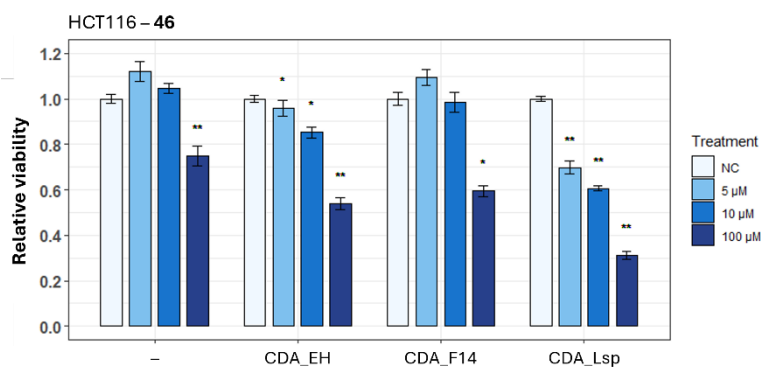
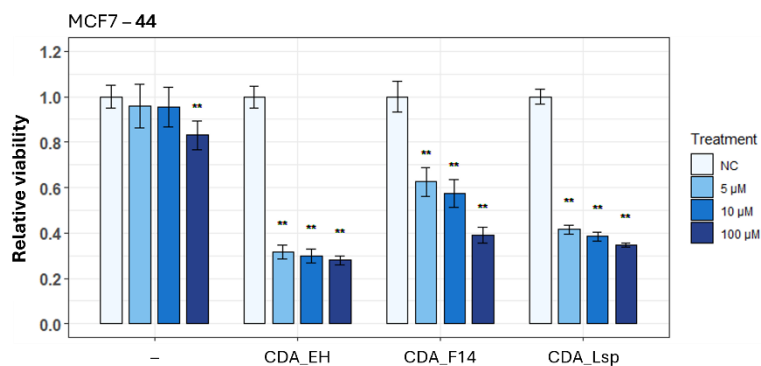
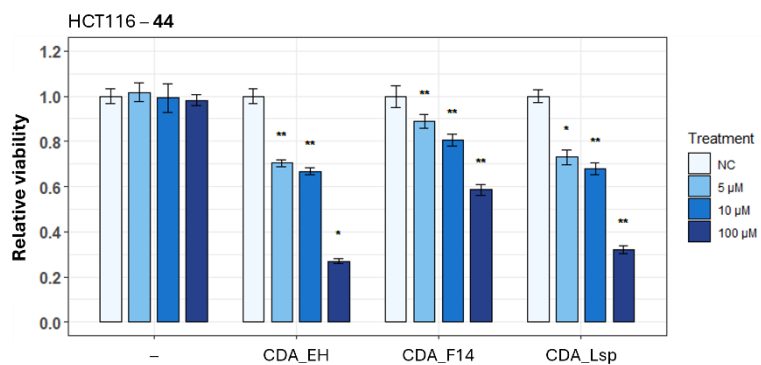












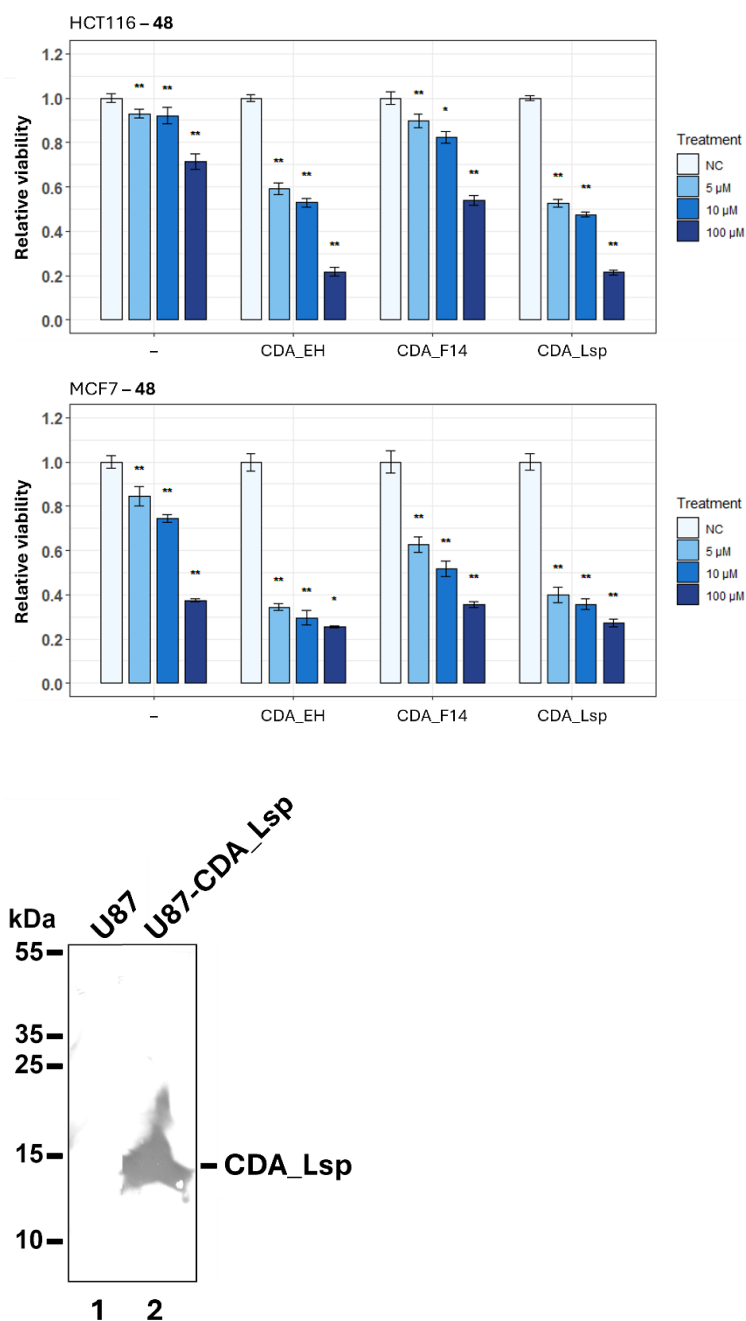


**Figure S2.** Expression of CDA\_Lsp in the U87MG cells. The expression of FLAG-tagged protein in U87MG (negative control, lane 1) and U87-CDA\_Lsp cells was detected by Western blot analysis, using FLAG-specific antibodies. The positions of the molecular mass standards (in kDa) and FLAG-tagged protein CDA\_Lsp are indicated.

## SANTRAUKA

### 1. SANTRUMPOS

3BrPyrA	3-brompiruvo rūgštis
5FaCyd	5-fluor- <i>N</i> <sup>4</sup> -acetilcitidinas
5FbCyd	5-fluor- <i>N</i> <sup>4</sup> -benzoilcitidinas
5FCyd	5-fluorcitidinas
5FdCyd	5-fluor-2'-deoksicitidinas
5FdCyd-Hex	5-fluor- <i>N</i> <sup>4</sup> -heksanoil-2'-deoksicitidinas
5FipCyd	5-fluor- <i>N</i> <sup>4</sup> -[3-indolepropionil]citidinas
5FpCyd	5-fluor- <i>N</i> <sup>4</sup> -pivaloilcitidinas
5FU	5-fluoruracilas
5FUDR	5-fluor-2'-deoksiuridinas
5FUDR-Mo	5-fluor-4-(4-morfolinil)-2'-deoksiuridinas
5FUR	5-fluoruridinas
6MP	6-merkaptopurinas
GDEPT	tikslinė fermento-provaisto terapija (angl. <i>Gene-directed enzyme prodrug therapy</i> )
MTT	3-(4,5-dimetil-2-tiazolil)-2,5-difenil-2-H-tetrazolio bromidas

## 2. ĮVADAS

Vėžiniai susirgimai vis dar išlieka viena pagrindinių mirties priežasčių pasaulyje. Nors dabartiniai gydymo metodai – radioterapija, chirurgija ir chemoterapija – yra gerokai pažengę, dalies jų ilgalaikis veiksmingumas dažnai yra apribotas dėl vėžinių ląstelių atsparumo vaistams ir sisteminio vaistų toksiškumo organizmui. Šie trūkumai pabrėžia naujų priešvėžinių vaistų, pasižyminčių didesniu veiksmingumu ir selektyvumu, paieškos poreikį. Tarp naujai atsirandančių priešvėžinių aktyvumu pasižyminčių junginių daug dėmesio sulaukė indirubinas ir jo dariniai. Nepaisant didelio šių junginių potencialo, klinikinis jų pritaikymas yra ribotas dėl prasto tirpumo vandenyje, nepalankių farmakokinetinių savybių ir riboto terapinio efektyvumo. Siekiant išspręsti šias problemas buvo susintetinta keletas indirubino darinių, pasižyminčių stipresniu priešvėžiniu poveikiu bei palankesnėmis farmakokinetinėmis savybėmis. Tolimesni tyrimai, skirti naujų indirubino pagrindu sukurtų junginių kūrimui, gali atverti kelią efektyvesnių ir selektyvesnių vėžinių susirgimų gydymo galimybių plėtrai.

Tikslinio vaistų pristatymo ir aktyvavimo strategijos vis labiau domina kaip būdas pagerinti priešvėžinių junginių selektyvumą ir terapinį indeksą. Vienas iš perspektyviausių metodų šioje srityje yra tikslinė fermento-provaisto terapija (angl. *Gene-directed enzyme prodrug therapy, GDEPT*). Tai naujai besiformuojanti vėžio gydymo strategija, panaudojanti transgeną, kuris koduoja fermentą, gebantį netoksišką provaistą paversti į aktyvų terapinį metabolitą, veikiantį vėžinių ląstelių gyvybingumą. Ši terapija turi keletą aiškių privalumų lyginant su tradiciniais vėžinių susirgimų gydymo metodais: aktyvus citotoksinis vaistas susidaro tik naviko audinyje, todėl ne tik padidėja gydymo efektyvumas, bet ir sumažėja šalutinių poveikių tikimybė; taip pat provaistą galima skirti pakartotinai, kol aktyvuojantis fermentas vis dar išlieka lokalizuotas navike, taip sunaikinant visas terapijos vietoje esančias vėžines ląsteles. Egzogeninio fermento panaudojimas leidžia pritaikyti provaistus, kurių žmogaus fermentai neatpažįsta, taip sumažinant nepageidaujamą aktyvumą sveikuose audiniuose ir maksimaliai padidinant toksiškumą naviko aplinkoje. Iki šiol buvo sukurta keletas fermento ir provaisto kombinacijų, kurios parodė didelį potencialą tiek ikiklinikiniuose tyrimuose, tiek ankstyvose klinikinėse studijose, tačiau nė viena iš jų dar nepasiekė klinikos dėl tam tikrų trūkumų. Daugelį strategijų riboja žemas fermentų specifiskumas tiksliniams junginiams, didelis afiniškumas natūraliems substratams, ribotas provaistų patekimas į terapinę vietą, nepalankios farmakokinetinės savybės bei nepageidaujamas provaistų aktyvavimas

natūraliai organizme esančių fermentų. Dėl šių priežasčių naujų fermento ir provaisto kombinacijų, kurios pasižymėtų dideliu specifiskumu, kūrimas yra būtinas siekiant GDEPT pritaikyti klinikinėje praktikoje.

Vienas iš perspektyvių fermentų variantų, kuriuos būtų galima panaudoti GDEPT strategijoje, yra hidrolazės. Tai gausi fermentų klasė, kuri katalizuoja cheminių ryšių hidrolizę biomolekulėse naudojant vandenį kaip hidroksilo grupės donorą. Dėl didelio stereo- ir regioselektivumo hidrolazės yra plačiai taikomos cheminėje sintezėje, maisto ir kosmetikos pramonėje bei farmacijoje. Šiame darbe siekiama parodyti, kad hidrolazės gali būti panaudojamos terapiniais tikslais kaip provaistus aktyvuojantys fermentai. Ankstesniuose tyrimuose YqfB ir D8\_RL baltymai buvo aprašyti kaip mažos amidohidrolazės, aktyvios  $N^4$ -acilintų citidinių atžvilgiu. Taip pat buvo identifikuoti CDA\_EH, CDA\_F14 ir CDA\_Lsp fermentai – citidino deaminazės, aktyvios  $S^4$ -/ $N^4$ -/ $O^4$ -modifikuotų pirimidino nukleozidų atžvilgiu. Visi šie fermentai turi keletą reikšmingų privalumų, tokių kaip platus sintetinių substratų spektras, didelis katalizinis aktyvumas, mažas molekulių dydis ir kitos savybės, kurios dažnai akcentuojamos kuriant terapinius įrankius. Tai leido iškelti hipotezę, kad būtent šios hidrolazės yra daug žadantis tyrimų objektas fermento-provaisto sistemų kūrime.

Šio darbo tikslas buvo sukurti ir ištirti naujus priešvėžinius junginius, ypatingą dėmesį skiriant fermentų rinkinio 5-fluorpirimidinų provaistams aktyvuoti kūrimui. Siekiant šio tikslo, buvo keliami šie uždaviniai:

1. Identifikuoti citotoksiniu poveikiu vėžinėms ląstelių linijoms pasižyminčius indirubino darinius.
2. Įvertinti modifikuotų 5-fluorpirimidino nukleozidų kaip provaistų tinkamumą panaudojimui fermento-provaisto terapijoje.
3. Ištirti YqfB ir D8\_RL amidohidrolazių pritaikomumą 5-fluorpirimidino pagrindu sukurtų provaistų aktyvavimui.
4. Įvertinti CDA\_EH, CDA\_F14 ir CDA\_Lsp citidino deaminazių gebėjimą aktyvuoti 5-fluorpirimidinų provaistus.

## **Mokslinis naujumas**

Nepaisant reikšmingos pažangos vėžinių susirgimų gydymo srityje, dabartinių terapijų veiksmingumą vis dar riboja vaistams atsparių navikinių ląstelių atsiradimas ir sisteminis vaistų toksiškumas, todėl išlieka poreikis kurti naujus priešvėžinius junginius, pasižyminčius didesniu veiksmingumu ir selektyvumu. Indirubinas ir jo dariniai išryškėjo kaip perspektyvūs kandidatai dėl turimų priešvėžinių savybių; vis dėlto jų klinikinį pritaikymą riboja prastas

tirpumas vandenyje. Šiame darbe buvo išanalizuotas mūsų tyrimų grupės neseniai susintetintų, geru tirpumu vandenyje pasižyminčių monokarboksindirubino darinių galimas toksiškumas, siekiant įvertinti jų tinkamumą tolesniam vystymui. Nustatyti keli junginiai, turintys citotoksiinį poveikį vėžinėms ląstelėms, kurie ne tik praplėtė žinias apie indirubino darinių savybes, bet ir išryškino jų potencialą terapiniam pritaikymui. Taip pat provaistų technologija jau daugelį metų yra vertinama kaip veiksmingas tikslinės vėžio terapijos metodas. Nors ši sritis yra gana pažengusi, provaistų taikymą vis dar riboja daugybė veiksnių, tokių kaip ribotas provaistų pateikimas į ląsteles, prasti farmakokinetiniai rodikliai, nespecifinis aktyvavimas ir kiti apribojimai, kurie mažina jų efektyvumą *in vivo*. Šiame darbe buvo pasiūlyta plati kolekcija modifikuotų 5-fluoropirimidinių, kurie gali veikti kaip potencialūs provaistai. Šie junginiai buvo pateikti kartu su fermentais, galinčiais juos specifiskai aktyvuoti, taip padidinant jų pritaikymo galimybes tolimesniuose tyrimuose. Nors jau yra žinomi keli chemoterapinio vaisto 5-fluoruracilo pagrindu sukurti provaistų variantai, šiame darbe pristatytos struktūrinės modifikacijos iki šiol nebuvo aprašytos. Ankstesni tyrimai rodo, kad įvairios amidohidrolazės dėl savo fizikocheminių savybių yra patrauklūs objektai daugelyje sričių ir gali būti pritaikytos maisto, farmacijos pramonėje bei biotechnologijoje. Šiame darbe parodyta, kad amidohidrolazės gali būti taikomos GDEPT strategijoje ir naudojamos terapiniais tikslais. Anksčiau buvo identifikuotos dvi mažos amidohidrolazės – YqfB ir D8\_RL – pasižyminčios aktyvumu prieš  $N^4$ -acilцитidinus. Šiame darbe parodyta, kad YqfB ir D8\_RL taip pat gali katalizuoti  $N^4$ -acilintų 5-fluorцитidinių konversiją į priešvėžinį junginį 5-fluorцитidiną. Keturi nauji sintetiniai junginiai buvo pasiūlyti kaip tinkami substratai YqfB ir D8\_RL fermentiniam hidrolizavimui. Taip pat CDA\_EH, CDA\_F14 ir CDA\_Lsp fermentai anksčiau buvo identifikuoti kaip citidino deaminazės, hidrolizuojančios  $S^4$ -/ $N^4$ -/ $O^4$ -modifikuotus pirimidino nukleozidus. Šiame darbe parodyta, kad CDA\_EH, CDA\_F14 ir CDA\_Lsp taip pat gali aktyvuoti  $N^4$ -acilintus/alkilintus 5-fluorцитidinus, 4-alkiltio-5-fluoruridinus, 4-alkoksi-5-fluoruridinus ir 4-alkoksi-5-fluor-2'-deoksiuridinus, kurių konversijos produktai yra priešvėžiniai junginiai 5-fluoruridinas arba 5-fluor-2'-deoksiuridinas. Keletas iki šiol niekur kitur neaprašytų provaistų buvo pasiūlyti kaip tinkami substratai CDA\_EH, CDA\_F14 ir CDA\_Lsp fermentams. Apibendrinant, šio darbo rezultatai leido pasiūlyti kelias skirtingas fermento-provaisto kombinacijas, paremtas penkiomis hidrolazėmis ir įvairiais 5-fluorpirimidino analogais. Kadangi nė viena iš šių sistemų iki šiol nebuvo išsamiai ištirta, padidėja tikimybė, kad bent viena iš jų gali būti tinkama tolesniam vystymui ir klinikiniam pritaikymui.

## Ginamieji disertacijos teiginiai

1. Indirubino karboksirūgšties ir 2-indolinono dariniai yra perspektyvūs kandidatai kuriant priešvėžinius vaistus.
2. Modifikuoti 5-fluorpirimidino nukleozidai yra perspektyvūs provaistų kandidatai tikslinei vėžio terapijai.
3. YqfB ir D8\_RL amidohidrolazės, kartu su  $N^4$ -acilintais 5-fluorцитидино dariniais, gali būti taikomos kaip naujos fermento-provaisto sistemos GDEPT strategijoje.
4. CDA\_EH, CDA\_F14 ir CDA\_Lsp citidino deaminazės kartu su  $N^4$ -acilintais/alkilintais 5-fluorцитидинаis, 4-alkiltio-5-fluoruridinais, 4-alkoksi-5-fluoruridinais ir 4-alkoksi-5-fluor-2'-deoksiuridinais turi potencialo būti naudojamos fermento-provaisto terapijoje.



### 3. METODAI

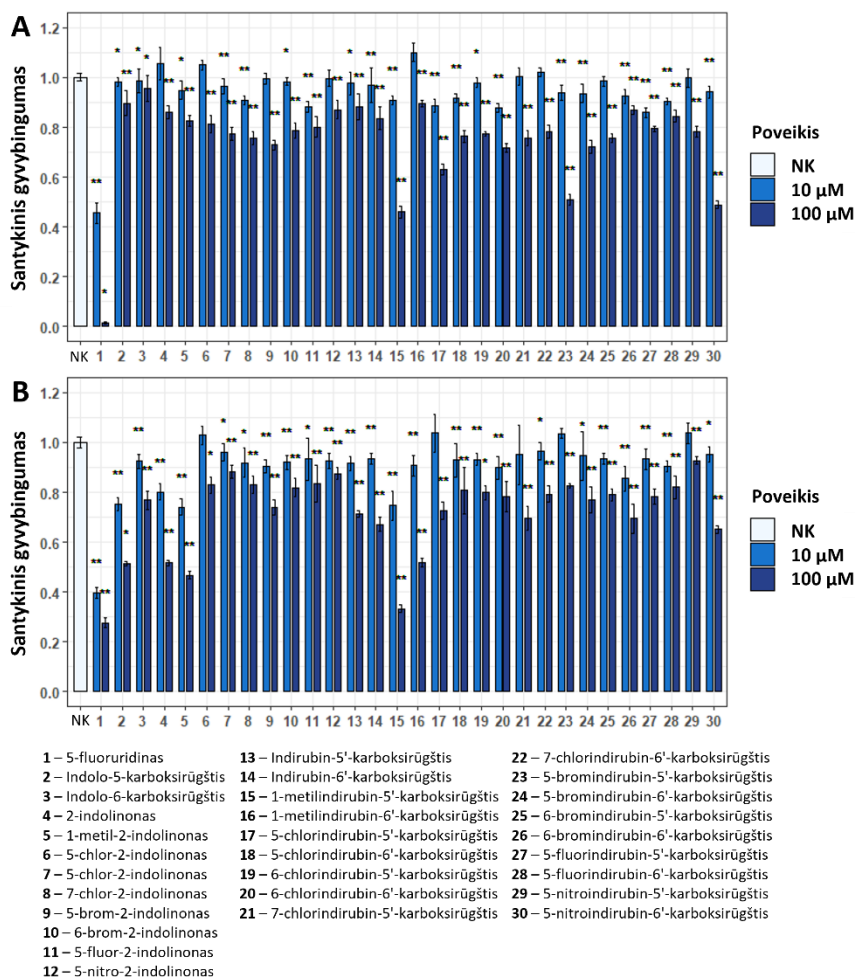
Plazmidiniai vektoriai buvo konstruojami standartiniais molekulinės biologijos metodais, naudojantis komerciniais rinkiniais. Bakterinių ir žinduolinių ląstelių auginimas buvo vykdomas standartinėmis sąlygomis parenkant tinkamas terpes, kurių sudėtis detaliai nurodyta šioje disertacijoje. Tyrimams naudoti rekombinantiniai baltymai buvo išreikšti įvairiuose *E. coli* kamienuose naudojant indukuojamas baltymų sintezės sistemas ir išgryninti metalų afininės chromatografijos metodu. Fermentų gebėjimas katalizuoti skirtingų substratų konversiją buvo įvertintas taikant skysčių chromatografiją-tandeminę masių spektrometriją. Tiriamuosius rekombinantinius fermentus koduojantys genai į vėžinių ląstelių linijas buvo įterpti retrovirusinės transdukcijos būdu. Ląstelių linijų su stabiliai integruotais konstruktais atranka vykdyta naudojant antibiotines medžiagas. Tikslinių baltymų raiška ir biosintezė vėžinių ląstelių linijose buvo įvertinta atliekant realaus laiko PGR ir *Western Blot* metodus (išimtyms nurodytos disertacijoje ir publikacijose). Vėžinių ląstelių gyvybingumas po poveikio tiriamaisiais provaistais buvo vertinamas MTT metodu. Gautų duomenų analizei taikyti statistiniai kriterijai detalizuoti šioje disertacijoje bei publikacijose.

## 4. REZULTATAI

### 4.1. Potencialių priešvėžinių junginių ir provaistų atranka

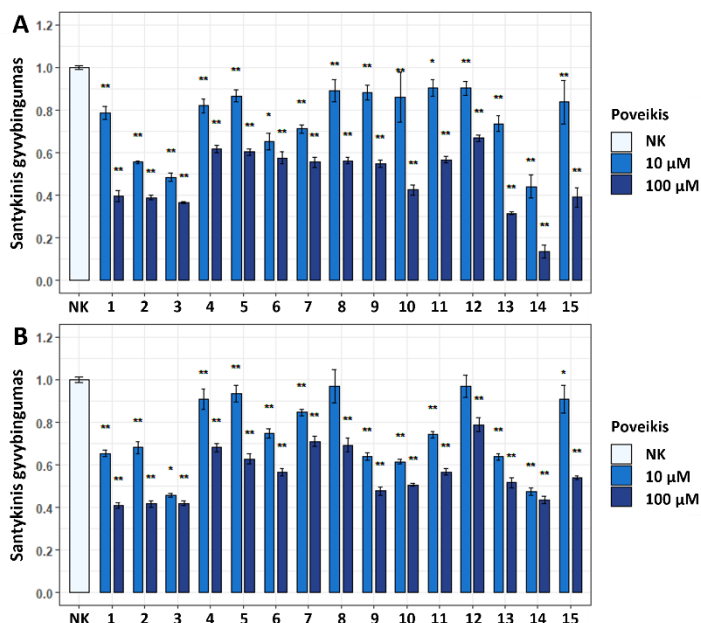
#### 4.1.1. Vandenyje tirpių asimetrinių indirubino karboksirūgščių poveikis vėžinių ląstelių gyvybingumui

Literatūros duomenimis indirubinas pasižymi priešvėžiniu aktyvumu ir tai priklauso nuo jo tirpumo vandenyje. Buvo nuspręsta patikrinti, ar dideliu tirpumu vandenyje pasižymintys 2-indolinono ir indirubino karboksirūgštys dariniai taip pat turi citotoksinių savybių. HCT116 ir MCF7 ląstelių linijos 48 val. buvo veikiamos skirtingomis monokarboksiindirubinų koncentracijomis ir jų gyvybingumas įvertintas MTT metodu (1 pav.). Visi tirti junginiai pasižymėjo statistiškai reikšmingu citotoksiniu aktyvumu. Didžiausiu aktyvumu abiejose ląstelių linijose pasižymėjo 1-metilindirubin-5'-karboksirūgštis, tuo tarpu 5-bromindirubin-5'-karboksirūgštis ir 5-nitroindirubin-6'-karboksirūgštis – tik HCT116 ląstelių linijoje. Įdomu tai, kad monokarboksiindirubinų sintezės substratai (indolo-5-karboksirūgštis, indolo-6-karboksirūgštis ir 2-indolinonas) pasižymėjo stipriu poveikiu MCF7 ląstelių linijai, bet ne HCT116 ląstelėms.



**1 pav.** 2-indolinono ir indirubino karboksirūgšties darinių citotoksinis aktyvumas ląstelių linijose: A – HCT116 ląstelių linija, B – MCF7 ląstelių linija. Abi ląstelių linijos 48 val. buvo veikiamos 10  $\mu$ M ir 100  $\mu$ M indirubino karboksirūgščių koncentracijomis. 5-fluoruridinas naudotas kaip teigiama kontrolė. Statistiškai reikšmingi skirtumai pažymėti  $p$  reikšmėmis: simbolis \* reiškia  $p < 0,05$ , o simbolis \*\* reiškia  $p < 0,01$ , lyginant su nepaveiktomis ląstelėmis (neigiama kontrolė (NK)).

Gauti rezultatai parodė, kad 1-metilindirubin-5'-karboksirūgštis yra tinkamas pradinis junginys provaistų kūrimui. Dėl šios priežasties buvo susintetinti ir išbandyti keli analogiški junginiai – modifikuoti 1-metilindirubino-5'-karboksirūgšties dariniai bei kelios naujos giminingos medžiagos. HCT116 ir MCF7 ląstelių linijos buvo veikiamos šiais junginiais ir praėjus 48 valandoms jų gyvybingumas įvertintas MTT metodu (2 pav.).



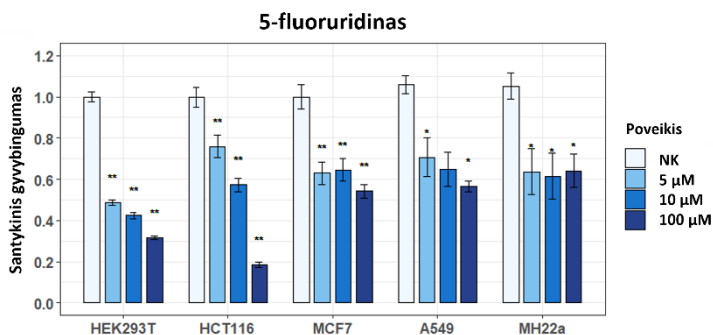
- |   |  |
|---|--|
| 1 – 1-metilindirubin-5'-karboksirūgštis         | 9 – 6-chlor-1-metil-2-indolinonas                |
| 2 – 6-brom-1-metilindirubin-6'-karboksirūgštis  | 10 – 6-brom-1-metil-2-indolinonas                |
| 3 – 6'-etilindirubin-5-karboksirūgštis          | 11 – 6-brom-2-indolinon-4-karboksirūgštis        |
| 4 – 6-fluor-1-metilindirubin-6'-karboksirūgštis | 12 – 6-jodindirubin-6'-karboksirūgštis           |
| 5 – 1-etilindirubin-6'-karboksirūgštis          | 13 – 6-chlor-1-metilindirubin-5'-karboksirūgštis |
| 6 – 1-etilindirubin-5'-karboksirūgštis          | 14 – 6-chlor-1-metilindirubin-6'-karboksirūgštis |
| 7 – 6-fluor-1-metilindirubin-5'-karboksirūgštis | 15 – 6-brom-1-metilindirubin-5'-karboksirūgštis  |
| 8 – 6-jod-2-indolinonas                         |  |

**2 pav.** Modifikuotų 2-indolinonų ir indirubino karboksirūgščių citotoksinis aktyvumas vėžinių ląstelių linijoms: A – HCT116 ląstelių linija, B – MCF7 ląstelių linija. Abi ląstelių linijos 48 val. buvo veikiamos 10  $\mu$ M ir 100  $\mu$ M junginių koncentracijomis. Statistiškai reikšmingi skirtumai pažymėti *p* reikšmėmis: simbolis \* reiškia  $p < 0,05$ , o simbolis \*\* reiškia  $p < 0,01$ , lyginant su nepaveiktomis ląstelėmis (neigiama kontrolė (NK)).

Visi tirti junginiai statistiškai reikšmingai sumažino ląstelių gyvybingumą. Didžiausią toksiškumą abiem tirtoms ląstelių linijoms parodė 6-brom-1-metilindirubin-6'-karboksirūgštis, 6-chlor-1-metilindirubin-5'-karboksirūgštis ir 6-chlor-1-metilindirubin-6'-karboksirūgštis. Tai rodo, kad ne tik 1-metilindirubin-5'-karboksirūgštis, bet ir įvairūs jos dariniai arba 1-metilindirubin-6'-karboksirūgšties dariniai gali panašiai ar net toksiškiau veikti vėžines ląsteles. Kitas perspektyvus junginys buvo 6'-etilindirubin-5-karboksirūgštis, kuri buvo toksiška abiem ląstelių linijoms net ir veikiant mažesnei koncentracijai. Gauti duomenys dar kartą įrodė, kad monokarboksiindirubinais yra perspektyvūs junginiai priešvėžiniams preparatams kurti.

#### 4.1.2. Terapijai tinkamų ląstelių linijų atranka

Vėžinės ląstelės gali pasižymėti įgimtu arba įgytu atsparumu 5-fluoruracilui (5FU) ar jo metabolitams (5-fluoruridinui (5FUR) bei 5-fluor-2'-deoksiuridinui (5FUDR)). Siekiant identifikuoti tinkamus modelius tolimesniems tyrimams buvo pasirinktos kelios ląstelių linijos ir patikrintos dėl jų galimo atsparumo 5FUR. HEK293T, HCT116, MCF7, A549 ir MH22a ląstelių linijos buvo veikiamos keliomis skirtingomis 5FUR koncentracijomis 24 valandas, po to ląstelių gyvybingumas buvo įvertintas MTT metodu (3 pav.).

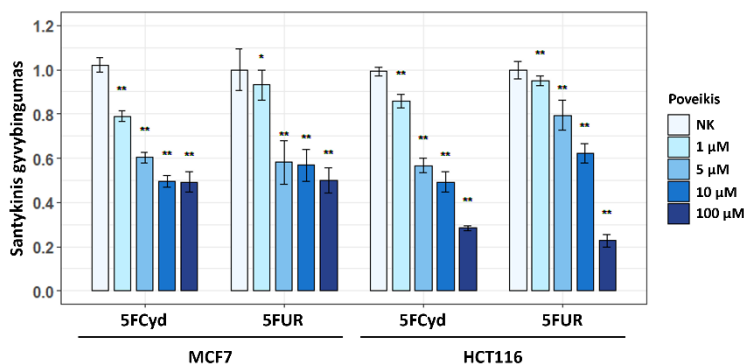


**3 pav.** MTT tyrimas skirtingoms ląstelių linijoms po poveikio 5-fluoruridinu (5FUR). Visos ląstelių linijos buvo veikiamos 5 μM, 10 μM ir 100 μM 5FUR koncentracijomis 24 valandas. Statistiškai reikšmingi skirtumai nurodyti *p* reikšmėmis: simbolis \* žymi  $p < 0,05$ , o simbolis \*\* –  $p < 0,01$ , lyginant su nepaveiktomis ląstelėmis (neigiama kontrolė (NK)).

Poveikis mažesnėmis 5FUR koncentracijomis (5 μM ir 10 μM) reikšmingai sumažino HEK293T ląstelių gyvybingumą. Tai parodė didelį šių ląstelių potencialą vertinant provaistų stabilumą ląstelinėje aplinkoje, kadangi net ir atsitiktinė provaisto konversija į toksišką vaistą turėtų būti lengvai aptinkama. Vis dėlto, šios ląstelės nėra optimalus įrankis MTT tyrimui, nes buvo pastebėta silpna jų sąveika su kultivavimo plokštelės šulinėlių paviršiumi. Reikšmingi rezultatai buvo gauti vertinant 5FUR poveikį HCT116 ląstelių linijai, kur buvo stebėtas nuo koncentracijos priklausomas gyvybingumo mažėjimas. Kitos ląstelių linijos į 5FUR reagavo panašiai, visų tirtų koncentracijų atveju gyvybingumo lygis buvo apie 60%. Atsižvelgiant į gautus rezultatus, buvo nuspręsta neatmesti nė vienos iš šių ląstelių linijų kaip potencialių įrankių provaistų atrankai. Vis dėlto, siekiant supaprastinti eksperimentų dizainą, tolimesniems tyrimams buvo pasirinktos HCT116 ir MCF7 ląstelių linijos.

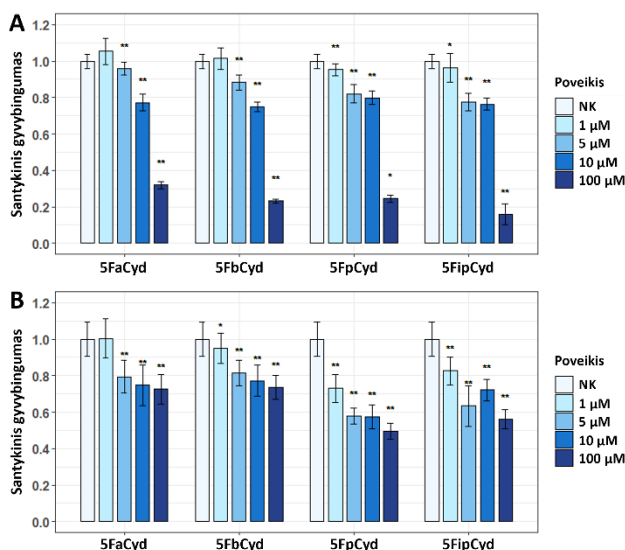
#### 4.1.3. Modifikuotų nukleozidų poveikis vėžinių ląstelių gyvybingumui

Toliau buvo identifikuojami junginiai, kaip galimi provaistai, kurie idealiau atveju būtų pakankamai stabilūs ląstelinėje aplinkoje, kad būtų išvengta toksiško vaisto susidarymo nepageidaujamoje vietoje ar netinkamu metu. Norint išplėsti tiriamų junginių imtį, buvo nuspręsta analizuoti ne tik 5FUR, bet ir 5-fluorцитидино (5FCyd) darinius. Ši idėja buvo paremta tuo, kad žmogaus ląstelės sintetina citidino deaminazę, kuri katalizuoja 5FCyd vartimą į 5FUR. Siekiant nustatyti, ar 5FCyd daro panašų poveikį vėžinėms ląstelėms kaip ir 5FUR, HCT116 ir MCF7 ląstelių linijos buvo veikiamos šiais junginiais 24 valandas ir ląstelių gyvybingumas įvertintas MTT metodu (4 pav.).



**4 pav.** MTT tyrimas MCF7 ir HCT116 ląstelių linijoms po poveikio 5-fluorцитидinu (5FCyd) ir 5-fluoruridinu (5FUR). Abi ląstelių linijos buvo veikiamos tiriamųjų junginių 1–100 μM koncentracijomis 24 valandas. Statistiškai reikšmingi skirtumai pažymėti *p* reikšmėmis: simbolis \* reiškia  $p < 0,05$ , o simbolis \*\* reiškia  $p < 0,01$ , lyginant su nepaveiktomis ląstelėmis (neigiama kontrolė (NK)).

Rezultatai parodė, kad 5FCyd ir 5FUR poveikis ląstelių gyvybingumui buvo labai panašus abiejose tirtose ląstelių linijose. Tolimesniems tyrimams buvo pasirinkti  $N^4$  padėtyje modifikuoti 5FCyd dariniai: 5-fluor- $N^4$ -acetilцитидinas (5FaCyd), 5-fluor- $N^4$ -benzoilцитидinas (5FbCyd), 5-fluor- $N^4$ -pivaloilцитидinas (5FpCyd) ir 5-fluor- $N^4$ -[3-indolepropionil]цитидinas (5FipCyd). Norint ištirti, ar šie junginiai nėra toksiški eukariotinėms ląstelėms prieš juos aktyvuojant, HCT116 ir MCF7 vėžinių ląstelių linijos 24 valandas buvo veikiamos keliomis skirtingomis junginių koncentracijomis, po ko įvertintas ląstelių gyvybingumas (5 pav.).

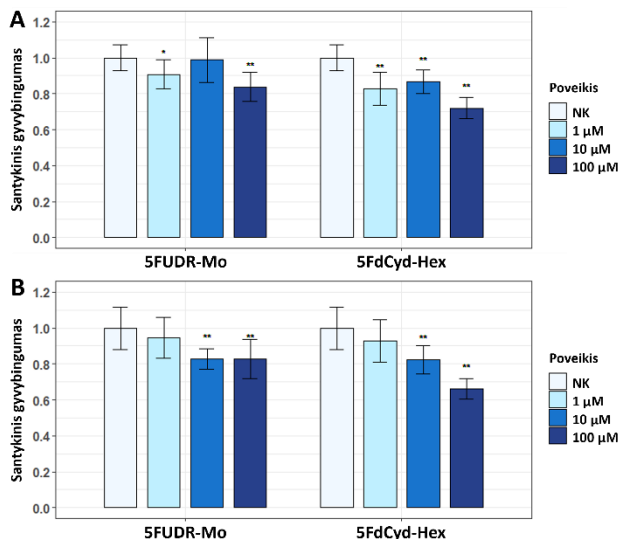


**5 pav.** MTT tyrimas HCT116 (A) ir MCF7 (B) ląstelių linijoms po poveikio provaistais. Abi ląstelių linijos buvo veikiamos 1–100  $\mu\text{M}$  junginių koncentracijomis 24 valandas. 5FaCyd – 5-fluor- $N^4$ -acetilcitidinas, 5FbCyd – 5-fluor- $N^4$ -benzoilcitidinas, 5FpCyd – 5-fluor- $N^4$ -pivaloilcitidinas, 5FipCyd – 5-fluor- $N^4$ -[3-indolepropionil]citidinas. Statistiškai reikšmingi skirtumai pažymėti  $p$  reikšmėmis: simbolis \* reiškia  $p < 0,05$ , o simbolis \*\* reiškia  $p < 0,01$ , lyginant su nepaveiktomis ląstelėmis (neigiama kontrolė (NK)).

Po poveikio mažesnėmis visų tirtų provaistų koncentracijomis (1–10  $\mu\text{M}$ ) HCT116 ląstelių gyvybingumas biologiškai reikšmingai nesiskyrė nuo kontrolinių ląstelių. Tuo tarpu 100  $\mu\text{M}$  koncentracija ląstelių gyvybingumą reikšmingai sumažino, todėl tolesniuose tyrimuose šiai ląstelių linijai reikėtų vengti koncentracijų, viršijančių 10  $\mu\text{M}$ . MCF7 ląstelėse kiekvienas provaistas atskirai nulėmė panašų gyvybingumo sumažėjimą visame tirtų koncentracijų diapazone. 5FpCyd ir 5FipCyd buvo toksiškesni MCF7 ląstelėms lyginant su 5FaCyd ir 5FbCyd. Vis dėlto, varijuojantys rezultatai skirtingose ląstelių linijose tolimesniems tyrimams leido neatmesti nei vieno iš tirtų provaistų.

Toliau buvo tiriami modifikuoti 5-fluor-2'-deoksicitidinais/uridinais – 5-fluor-4-(4-morfolinil)-2'-deoksiridinas (5FUDR-Mo) ir 5-fluor- $N^4$ -heksanoil-2'-deoksicitidinas (5FdCyd-Hex) – kuriuos hidrolizuojant susidaro ne tik 5FUDR ar 5-fluor-2'-deoksicitidinas (5FdCyd), bet ir papildomi priešvėžiniai aktyvumu pasižymintys produktai – morfolinas ir kaprono rūgštis. HCT116 ir MCF7 ląstelių linijos buvo paveiktos šiais junginiais ir po 24 valandų jų gyvybingumas buvo įvertintas MTT metodu (6 pav.). 5FUDR-Mo pasižymėjo

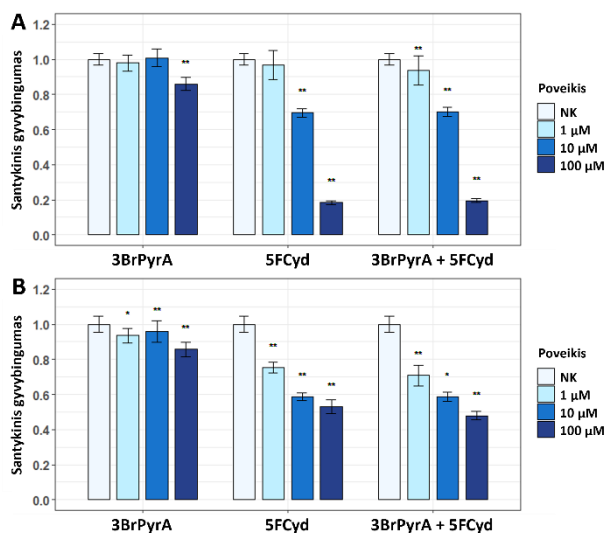
šiek tiek mažesniu toksiškumu abiem ląstelių linijoms lyginant su 5FdCyd-Hex. Esant didžiausiai tirtai 5FUDR-Mo ir 5FdCyd-Hex koncentracijai (100  $\mu$ M), ląstelių gyvybingumas siekė atitinkamai apie 85 % ir 70 %. Šie junginiai buvo laikomi tinkamais kandidatais tolimesniems tyrimams, tačiau išliko poreikis ieškoti ir kitų alternatyvų.



**6 pav.** MTT tyrimas HCT116 (A) ir MCF7 (B) ląstelių linijoms po poveikio 5-fluor-4-(4-morfolinil)-2'-deoksiuridinu (5FUDR-Mo) ir 5-fluor-*N*<sup>4</sup>-heksanoil-2'-deoksicitidinu (5FdCyd-Hex). Abi ląstelių linijos buvo veikiamos 1  $\mu$ M, 10  $\mu$ M ir 100  $\mu$ M tiriamųjų provaistų koncentracijomis 24 valandas. Statistiškai reikšmingi skirtumai pažymėti *p* reikšmėmis: simbolis \* reiškia  $p < 0,05$ , o simbolis \*\* reiškia  $p < 0,01$ , lyginant su nepaveiktomis ląstelėmis (neigiamą kontrolę (NK)).

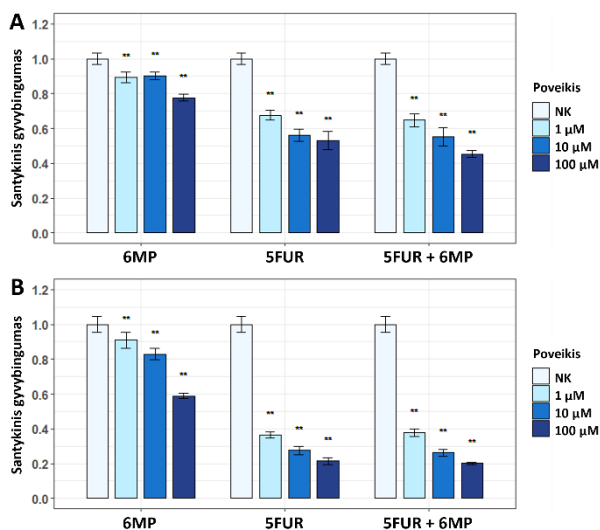
Tęsiant idėją naudoti provaistą, kurio hidrolizė lemtų dviejų toksiškų vaistų susidarymą, toliau buvo tirtos kelios toksiškų junginių kombinacijos – 5FCyd su 3-brompiruvo rūgštimi (3BrPyrA) ir 5FUR su 6-merkaptopurinu (6MP). Pirmiausia HCT116 ir MCF7 ląstelių linijos buvo paveiktos 5FCyd, 3BrPyrA bei šių junginių kombinacija. Praėjus 24 valandoms, ląstelių gyvybingumas buvo įvertintas MTT metodu (7 pav.). Pastebėta, kad 3BrPyrA šiek tiek sumažino abiejų tirtų ląstelių linijų gyvybingumą. Vis dėlto, vertinant 5FCyd poveikį atskirai ir kartu su 3BrPyrA, reikšmingų pokyčių nepastebėta.





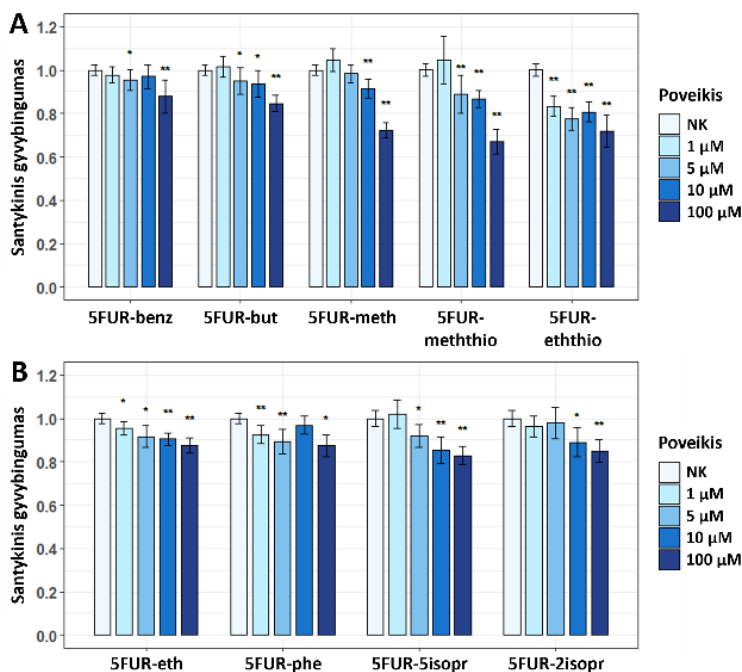
**7 pav.** MTT tyrimas HCT116 (A) ir MCF7 (B) ląstelių linijoms po poveikio 3-brompiruvo rūgštimi (3BrPyrA), 5-fluorocitidinu (5FCyd) ir šių dviejų junginių kombinacija. Abi ląstelių linijos buvo veikiamos 1–100  $\mu$ M tiriamųjų junginių koncentracijomis 24 valandas. Statistiškai reikšmingi skirtumai pažymėti *p* reikšmėmis: simbolis \* reiškia  $p < 0,05$ , o simbolis \*\* reiškia  $p < 0,01$ , lyginant su nepaveiktomis ląstelėmis (neigiama kontrolė (NK)).

Vėliau MCF7 ląstelių linija buvo paveikta 5FUR, 6MP ir šių junginių kombinacija. Ląstelių gyvybingumas buvo įvertintas MTT metodu po 24 ir 48 valandų (8 pav.). Nors 6MP reikšmingai sumažino MCF7 ląstelių gyvybingumą, akivaizdžių skirtumų tarp 5FUR poveikio ir 5FUR poveikio kartu su 6MP nepastebėta.



**8 pav.** MTT tyrimas MCF7 ląstelių linijai po poveikio 6-merkaptopurinu (6MP), 5-fluoruridinu (5FUR) ir šių dviejų junginių kombinacija. Ląstelės buvo veikiamos 1–100  $\mu$ M tiriamųjų junginių koncentracijomis 24 (A) ir 48 (B) valandas. Statistiškai reikšmingi skirtumai pažymėti  $p$  reikšmėmis: simbolis \* reiškia  $p < 0,05$ , o simbolis \*\* reiškia  $p < 0,01$ , lyginant su nepaveiktomis ląstelėmis (neigiama kontrolė (NK)).

Galiausiai buvo analizuoti modifikuoti 5-fluoruridinai. HCT116 ląstelių linija buvo paveikta įvairiomis junginių koncentracijomis (1–100  $\mu$ M) ir po 24 valandų ląstelių gyvybingumas buvo įvertintas MTT metodu (9 pav.). Rezultatai parodė, kad 5-fluor-4-benziloksiuridinas ir 5-fluor-4-butoksiuridinas neturėjo reikšmingo toksiško poveikio HCT116 ląstelėms nė vienoje iš tirtų koncentracijų. 5-Fluor-4-metoksiuridinas sumažino ląstelių gyvybingumą iki maždaug 75% tik veikiant didžiausiai tirtai koncentracijai (100  $\mu$ M). 5-Fluor-4-metiltiouridinas ir 5-fluor-4-etiltiouridinas parodė šiek tiek didesnę toksiškumą tiriamoms ląstelėms, tačiau jų naudojimas tolimesniuose tyrimuose nebuvo atmestas. 5-Fluor-4-etoksiuridinas, 5-fluor-4-fenoksiuridinas, 5-fluor-4-(5-izopropil-2-metilfenoksi)-uridinas ir 5-fluor-4-(2-izopropil-5-metilfenoksi)-uridinas neturėjo biologiniu požiūriu reikšmingo toksiško poveikio HCT116 ląstelėms.



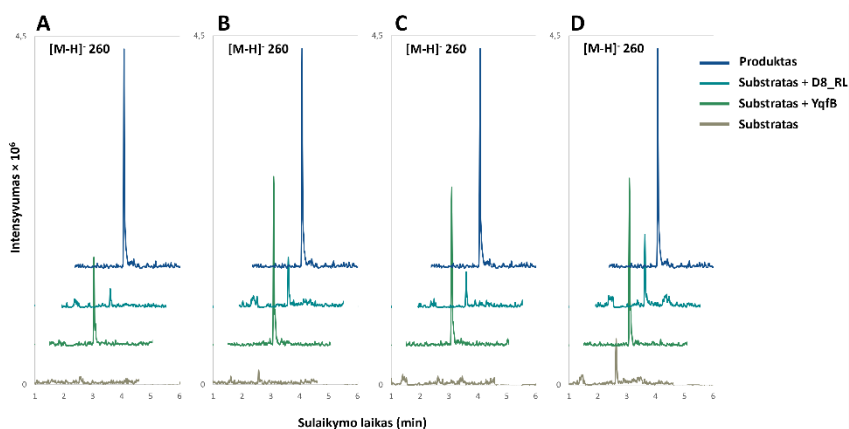
**9 pav.** MTT tyrimas HCT116 ląstelių linijai po poveikio (A) 5-fluor-4-benziloksiuridinu (5FUR-benz), 5-fluor-4-butoksiuridinu (5FUR-but), 5-fluor-4-metoksiuridinu (5FUR-meth), 5-fluor-4-metiltiouridinu (5FUR-meththio) ir 5-fluor-4-etiltiouridinu (5FUR-eththio), bei (B) 5-fluor-4-etoksiuridinu (5FUR-eth), 5-fluor-4-fenoksiuridinu (5FUR-phe), 5-fluor-4-(5-izopropil-2-metilfenoksi)-uridinu (5FUR-5isopr) ir 5-fluor-4-(2-izopropil-5-metilfenoksi)-uridinu (5FUR-2isopr). Ląstelės buvo veikiamos 1–100 μM tiriamųjų junginių koncentracijomis 24 valandas. Statistiškai reikšmingi skirtumai pažymėti *p* reikšmėmis: simbolis \* reiškia  $p < 0,05$ , o simbolis \*\* reiškia  $p < 0,01$ , lyginant su nepaveiktomis ląstelėmis (neigiama kontrolė (NK)).

Apibendrinant rezultatus, dauguma ištirtų modifikuotų 5-fluorpirimidino nukleozidų parodė minimalų arba visiškai neturėjo citotoksinio poveikio vėžinėms ląstelių linijoms. Nors kol kas nebuvo aišku, ar visiems junginiams pavyks parinkti juos specifiskai aktyvuojantį fermentą, lyginamoji skirtingų cheminių medžiagų analizė suteikė vertingų įžvalgų, kuria linkme toliau sintetinti junginius norint atrinkti tinkamiausius kandidatus terapijai.

## 4.2. YqfB ir D8\_RL amidohidrolazės kaip provaistus aktyvuojantys fermentai

### 4.2.1. Potencialių substratų YqfB ir D8\_RL amidohidrolazėms atranka *in vitro*

Pirmiausiai buvo tiriama, kurie provaistai yra tinkami substratai YqfB ir D8\_RL amidohidrolazėms. Keletas  $N^4$ -acilintų 5-fluorцитидино darinių, įskaitant 5-fluor- $N^4$ -acetilцитидiną, 5-fluor- $N^4$ -benzoilцитидiną, 5-fluor- $N^4$ -pivaloilцитидiną ir 5-fluor- $N^4$ -[3-indolepropionil]цитидiną, buvo inkubuoti su išgrynintais fermentais ir po 12 valandų inkubacijos mėginiai buvo tiriami LC-MS metodu. Kaip ir tikėtasi, tiek YqfB, tiek D8\_RL amidohidrolazės galėjo hidrolizuoti 5-fluor- $N^4$ -acetilцитидiną iki 5-fluorцитидино (10 pav.), nes  $N^4$ -acetilцитидinas yra pagrindinis jų substratas. Be to, fermentai buvo aktyvūs visų kitų tirtų substratų atžvilgiu.

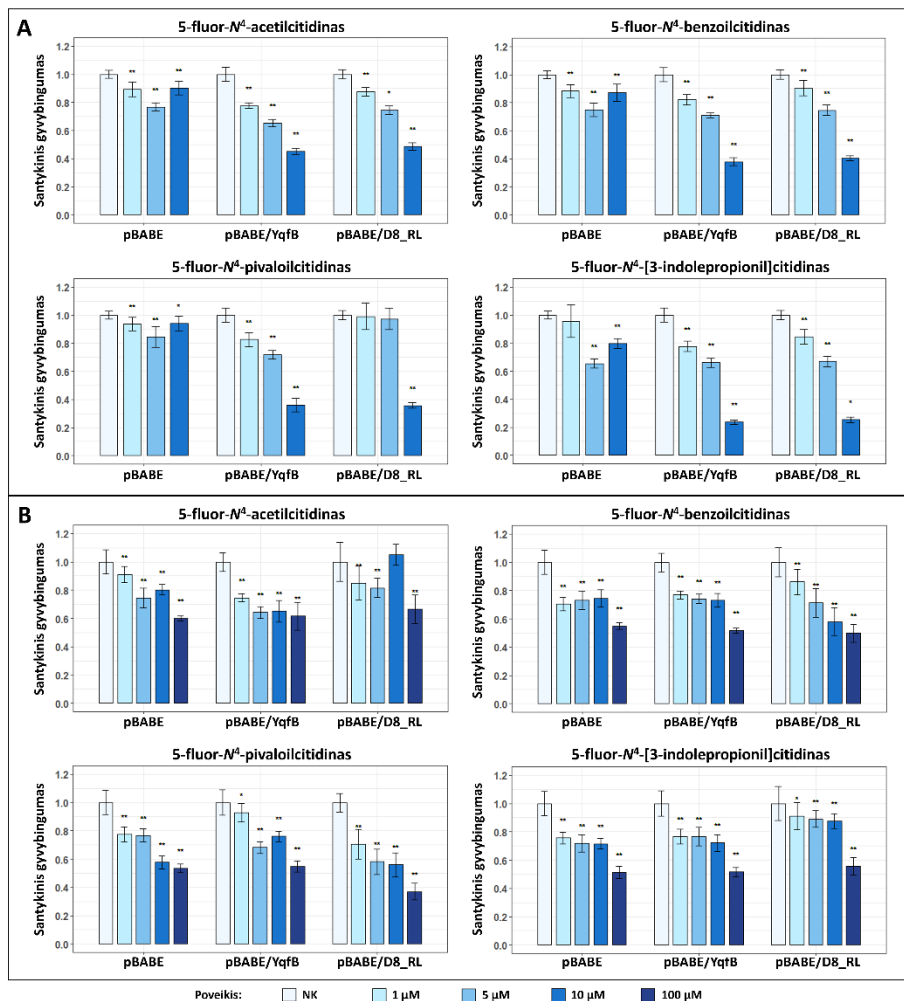


**10 pav.** YqfB ir D8\_RL amidohidrolazių substratinis specifiškumas. Grafikuose pavaizduoti 5-fluorцитидино ( $m/z$  [M-H]<sup>-</sup> 260) masės pėdsakai fermentinių reakcijų mėginiuose. YqfB ir D8\_RL amidohidrolazės buvo inkubuojamos su (A) 5-fluor- $N^4$ -acetilцитидinu, (B) 5-fluor- $N^4$ -benzoilцитидinu, (C) 5-fluor- $N^4$ -pivaloilцитидinu ir (D) 5-fluor- $N^4$ -[3-indolepropionil]цитидinu. Kaip teigiama kontrolė naudotas produktas 5-fluorцитидinas (pažymėtas tamsiai mėlyna spalva).

### 4.2.2. YqfB ir D8\_RL fermentų vykdoma provaistų hidrolizė eukariotinėse ląstelėse

Toliau siekėme nustatyti, ar bakterinės amidohidrolazės gali aktyvuoti provaistus eukariotinėse ląstelėse. Šiam tikslui buvo sukurtos ląstelių linijos, stabiliai vykdančios YqfB arba D8\_RL amidohidrolazes koduojančių genų raišką. HCT116 ir MCF7 ląstelių linijos, turinčios YqfB arba D8\_RL amidohidrolazes, buvo veikiamos keliomis skirtingomis pasirinktų provaistų

koncentracijomis. Ląstelių gyvybingumas buvo įvertintas MTT metodu praėjus 24 valandoms po poveikio ir palygintas su kontrolinėmis ląstelėmis, transdukuotomis vektoriumi, neturinčiu jokio įterpto geno (11 pav.).



**11 pav.** Ląstelių linijų, turinčių YqfB ir D8\_RL, MTT tyrimas po poveikio provaistais. HCT116 (A) ir MCF7 (B) ląstelių linijos, transdukuotos YqfB koduojančiu vektoriumi pBAGE/YqfB, D8\_RL koduojančiu vektoriumi pBAGE/D8\_RL arba kontroliniu vektoriumi pBAGE-Puro (žymimas pBAGE), buvo veikiamos skirtingomis 5-fluor-*N*<sup>4</sup>-acetilcitidino, 5-fluor-*N*<sup>4</sup>-benzoilcitidino, 5-fluor-*N*<sup>4</sup>-pivaloilcitidino ir 5-fluor-*N*<sup>4</sup>-[3-indolepropionil]citidino koncentracijomis 24 val. Statistiškai reikšmingi skirtumai pažymėti *p* reikšmėmis: simbolis \* reiškia *p* < 0,05, o simbolis \*\* reiškia *p* < 0,01, lyginant su nepaveiktomis ląstelėmis (neigiama kontrolė (NK)).

HCT116 ląstelių linijų, vykdančių YqfB arba D8\_RL amidohidrolazės koduojančių genų raišką, gyvybingumas reikšmingai sumažėjo po poveikio visais tirtais provaistais. Šie rezultatai rodo, kad bakterinės amidohidrolazės, veikdamos kartu su ląsteline citidino deaminaze, HCT116 ląstelių linijoje paverčia netoksiškus provaistus į toksišką 5FUR. Tuo tarpu MCF7 ląstelių linijų su įterptais YqfB arba D8\_RL koduojančiais genais gyvybingumas nesiskyrė nuo kontrolinių ląstelių gyvybingumo visų tirtų provaistų atveju. Tai rodo, kad nors YqfB ir D8\_RL amidohidrolazės kartu su modifikuotų 5-fluorocitidinių pagrindu sukurtais provaistais galėtų veikti kaip naujos fermentų-provaistų sistemos, terapijos sėkmė gali priklausyti nuo vėžinių ląstelių tipo ir/arba kilmės.

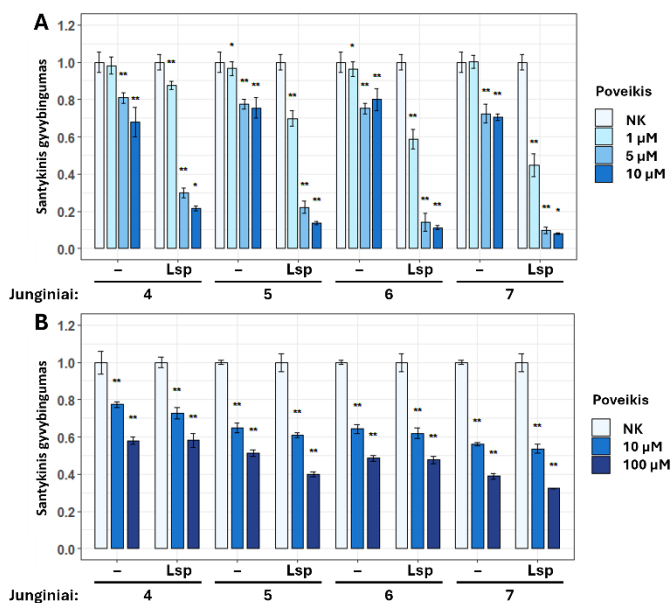
#### 4.3. CDA\_EH, CDA\_F14 ir CDA\_Lsp citidino deaminazės kaip provaistus aktyvuojantys fermentai

##### 4.3.1. CDA aktyvuoja įvairius modifikuotus 5-fluorpirimidino nukleozidus

Siekiant ištirti, ar modifikuoti 5-fluorpirimidino nukleozidai gali veikti kaip fermentais aktyvuojami provaistai, buvo susintetinta substratų kolekcija (12 pav.), kurią sudarė kontroliniai toksiški junginiai (**1–3**),  $N^4$ -acil-5-fluorocitidinais (**4–7**), 4-alkiltio-5-fluoruridinais (**8–17**) (tiek acetilintos, tiek deacetilintos formos),  $N^4$ -alkil-5-fluorocitidinais (**18–24**), 4-alkoksi- ir 4-ariloksi-5-fluoruridinais (**25–41**) (tiek acetilintos, tiek deacetilintos formos) bei 4-alkoksi-5-fluor-2'-deoksiuridinais (**42–49**) (tiek acetilintos, tiek deacetilintos formos).

Susintetinti substratai buvo įvertinti, ar aktyvuojami fermentų *in vitro* jie virsta toksiškais junginiais. Šiai analizei buvo pasirinktos trys citidino deaminazės (CDA): CDA\_EH, CDA\_F14 ir CDA\_Lsp. Acetilintų substratų (**10, 12, 14, 16, 26, 28, 32, 34, 36, 38, 42, 44, 46, 48**) konversija nebuvo aptikta, o tai rodo, kad CDA\_EH, CDA\_F14 ir CDA\_Lsp nepriima acetilintų junginių kaip substratų. Priešingai, fermentai galėjo konvertuoti deacetilintus substratus (**11, 13, 15, 17–24, 27, 29, 33, 35, 37, 39, 43, 45, 47, 49**). Šie rezultatai išryškino įvertintų CDA gebėjimą aktyvuoti skirtingas modifikacijas turinčius 5-fluorpirimidinus ir leido toliau tirti naujas fermento-provaisto sistemas vėžinių ląstelių linijose.





**13 pav.** HCT116 (A) ir MCF7 (B) ląstelių linijų, vykdančių CDA\_Lsp koduojančio geno raišką, MTT tyrimas po poveikio junginiais 4–7. Ląstelių linijos, transdukuotos CDA\_Lsp koduojančiu vektoriumi pBABE-CDA\_Lsp (žymimas Lsp) arba kontroliniu vektoriumi pBABE-Puro (žymimas simboliu –), 24 val. buvo veikiamos keliomis skirtingomis junginių koncentracijomis (HCT116 – 1  $\mu$ M, 5  $\mu$ M ir 10  $\mu$ M; MCF7 – 10  $\mu$ M ir 100  $\mu$ M). Statistiškai reikšmingi skirtumai pažymėti  $p$  reikšmėmis: simbolis \* reiškia  $p < 0,05$ , o simbolis \*\* reiškia  $p < 0,01$ , lyginant su nepaveiktomis ląstelėmis (neigiama kontrolė (NK)).

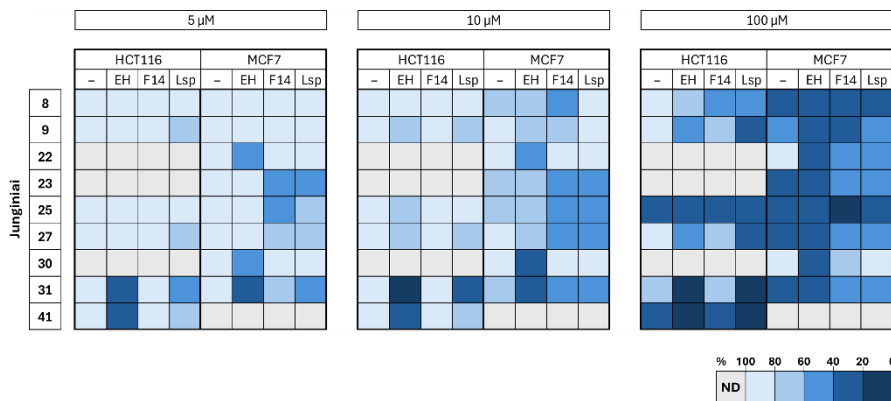
HCT116 ląstelių, vykdančių CDA\_Lsp koduojančio geno raišką, gyvybingumas reikšmingai sumažėjo po visų tirtų  $N^4$ -acil-5-fluorocitidinių poveikio. Šie rezultatai rodo, kad CDA\_Lsp vėžinėse ląstelėse veiksmingai aktyvuoja  $N^4$ -acil-5-fluorocitidinus, susidarant toksiškam metabolitui, kuris mažina ląstelių gyvybingumą. Priešingai, tarp kontrolinių ir CDA\_Lsp turinčių MCF7 ląstelių gyvybingumas reikšmingai nesiskyrė, o tai rodo, kad atsakas į  $N^4$ -acil-5-fluorocitidinus yra ląstelių linijai specifinis. Be to, šio tyrimo metu buvo pastebėta problemų, susijusių su junginių stabilumu, o tai galėjo turėti įtakos rezultatams.

#### 4.3.3. Bakterinės CDA\_EH, CDA\_F14 ir CDA\_Lsp aktyvuoja $S^4/O^4/N^4$ pakeistus 5-fluorpirimidinus vėžinių ląstelių linijose

Toliau buvo tiriamas bakterinių CDA fermentinis aktyvumas katalizuojant  $S^4/O^4/N^4$  pakeistų 5-fluorpirimidinų konversiją vėžinėse ląstelėse. HCT116 ir



MCF7 ląstelių linijos, vykdančios bakterines CDA\_EH, CDA\_F14 ir CDA\_Lsp koduojančių genų raišką, buvo veikiamos 4-alkiltio-5-fluoruridinais (**8**, **9**),  $N^4$ -alkil-5-fluorocitidinais (**22**, **23**) ir 4-alkoksi-5-fluoruridinais (**25**, **27**, **30**, **31**, **41**) 48 valandas, po ko ląstelių gyvybingumas buvo įvertintas MTT metodu (14 pav.).



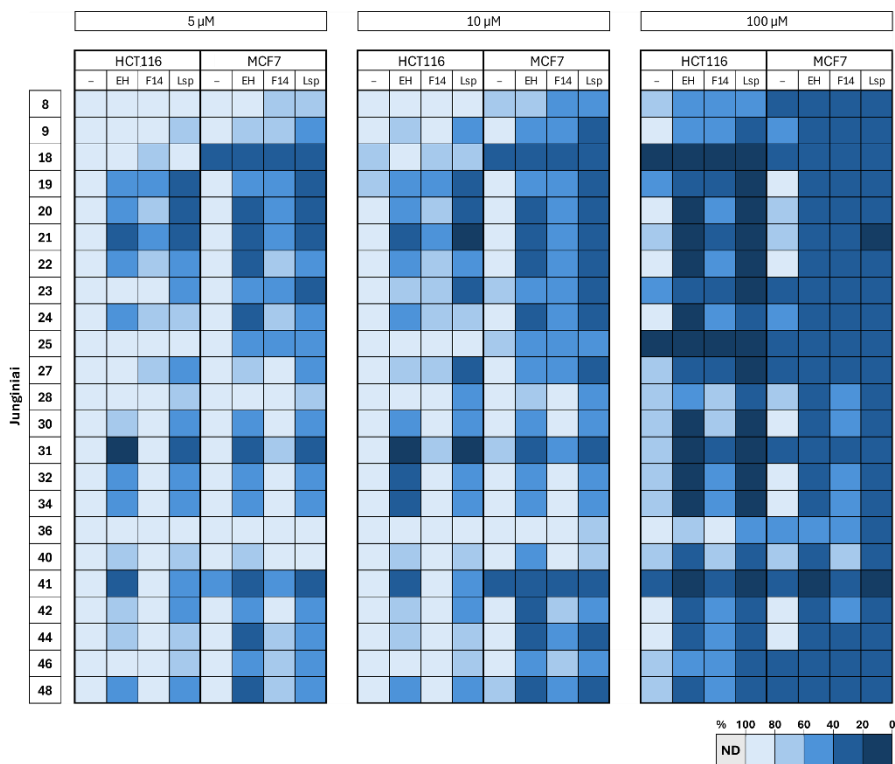
**14 pav.** HCT116 ir MCF7 ląstelių linijų, vykdančių bakterines CDA\_EH, CDA\_F14 ir CDA\_Lsp koduojančių genų raišką, gyvybingumo pokyčių po poveikio  $S^4/O^4/N^4$  pakeistais 5-fluorpirimidinais grafinis atvaizdavimas. Ląstelių linijos, transdukuotos CDA\_EH koduojančiu vektoriumi pBABE-CDA\_EH (žymimas EH), CDA\_F14 koduojančiu vektoriumi pBABE-CDA\_F14 (žymimas F14), CDA\_Lsp koduojančiu vektoriumi pBABE-CDA\_Lsp (žymimas Lsp) arba kontroliniu vektoriumi pBABE-Puro (žymimas simboliu –), 48 valandas buvo veikiamos 5 μM, 10 μM ir 100 μM junginių koncentracijomis. ND – nenustatyta.

Ląstelių gyvybingumo rezultatai atskleidė reikšmingus skirtumus tarp provaistų aktyvuojančių fermentų ir ląstelių linijų. 4-metiltio-5-fluoruridinas (**8**) veikiant 100 μM koncentracijai sumažino HCT116 ląstelių gyvybingumą efektyviausiai konversiją vykdant CDA\_F14 ir CDA\_Lsp fermentams. 4-Etiltio-5-fluoruridinas (**9**) veiksmingiausiai sumažino CDA\_Lsp turinčių HCT116 ląstelių gyvybingumą. MCF7 ląstelėse CDA\_EH ir CDA\_F14 buvo efektyvesni, tačiau didesnės junginio **9** koncentracijos buvo toksiškos kontrolinėms ląstelėms.  $N^4$ -heksil- ir  $N^4$ -propargil-5-fluorocitidinais (**22** ir **23**) reikšmingai sumažino CDA turinčių MCF7 ląstelių gyvybingumą net ir veikiant mažiausiai (5 μM) koncentracijai. **22** junginį veiksmingiau aktyvavo CDA\_EH, o **23** – CDA\_F14 ir CDA\_Lsp. 4-Metoksi-5-fluoruridinas (**25**) buvo toksiškas HCT116 ir MCF7 ląstelėms, o 4-etoksi-5-fluoruridinas (**27**) reikšmingai sumažino ląstelių gyvybingumą CDA\_EH ir CDA\_Lsp turinčiose HCT116 ląstelėse bei CDA\_F14 ir CDA\_Lsp turinčiose MCF7 ląstelėse. 5-fluorpirimidinais su 4-butoksi grupe **30** ir **31** reikšmingai sumažino CDA\_EH

turinčių MCF7 ląstelių gyvybingumą net esant 5  $\mu$ M koncentracijai. Junginys **30**, priešingai nei **31**, nebuvo toksiškas kontrolinėms ląstelėms. Kadangi **30** yra acetilintas **31** darinys, šie rezultatai rodo, kad acetilintus junginius ląstelės lengviau toleruoja, o CDA turinčiose ląstelių linijose jų hidrolizė vis tiek vyksta. 4-Benziloksi-5-fluoruridinas (**41**) veiksmingai sumažino CDA\_EH turinčių HCT116 ląstelių gyvybingumą (5  $\mu$ M ir 10  $\mu$ M), tačiau didesnė koncentracija buvo toksiška kontrolinėms ląstelėms. Apibendrinant galima teigti, kad bakterinės CDA\_EH, CDA\_F14 ir CDA\_Lsp gebėjo aktyvuoti pasirinktus 4-alkiltio-5-fluoruridinus, *N*<sup>4</sup>-alkil-5-fluorocitidinus ir 4-alkoksi-5-fluoruridinus HCT116 ir MCF7 vėžinėse ląstelėse. Nors šios bakterinės CDA pasižymi panašiu fermentiniu aktyvumu, ląstelių gyvybingumas po poveikio provaistais skyrėsi priklausomai nuo turimos konkrečios CDA.

#### 4.3.4. Žmogui optimizuotos CDA\_EH, CDA\_F14 ir CDA\_Lsp versijos efektyviau hidrolizuoja modifikuotus 5-fluorpirimidinus vėžinėse ląstelėse

Analizuojant bakterinių CDA gebėjimą aktyvuoti modifikuotus 5-fluorpirimidinus vėžinių ląstelių linijose, gauti nevienareikšmiški rezultatai. Šį kintamumą galima paaiškinti ribota bakterinių fermentų biosinteze eukariotinėse ląstelėse. Dėl šios priežasties buvo sukurti ir į HCT116 ir MCF7 ląstelių genomus integruoti žmogaus kodonams optimizuoti CDA\_EH, CDA\_F14 ir CDA\_Lsp variantai. HCT116 ir MCF7 ląstelės, turinčios žmogui optimizuotas CDA\_EH, CDA\_F14 ir CDA\_Lsp versijas, buvo veikiamos 4-alkiltio-5-fluoruridinais (**8**, **9**), *N*<sup>4</sup>-alkil-5-fluorocitidinais (**18–24**), 4-alkoksi-5-fluoruridinais (**25**, **27**, **28**, **30**, **31**, **32**, **34**, **36**, **40**, **41**) ir 4-alkoksi-5-fluor-2'-deoksiuridinais (**42**, **44**, **46**, **48**). Ląstelių gyvybingumas buvo įvertintas MTT metodu praėjus 48 valandoms nuo poveikio pradžios (15 pav.).



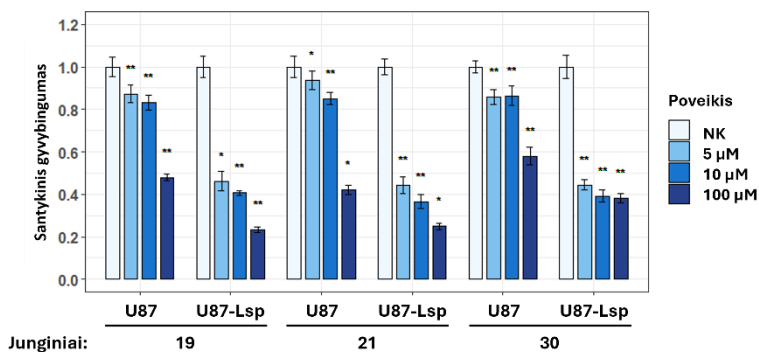
**15 pav.** HCT116 ir MCF7 ląstelių linijų, turinčių žmogaus kodonams optimizuotus CDA\_EH, CDA\_F14 ir CDA\_Lsp variantus, gyvybingumo pokyčių po  $S^4/O^4/N^4$  pakeistų 5-fluorpirimidinų poveikio grafinis atvaizdavimas. Ląstelių linijos buvo transdukuotos vektoriais, koduojančiais žmogui optimizuotus CDA variantus: pBABE-CDA\_EH (žymimas EH), pBABE-CDA\_F14 (žymimas F14), pBABE-CDA\_Lsp (žymimas Lsp) arba kontrolinį vektorių pBABE-Puro (žymimas simboliu –). Ląstelės 48 valandas buvo veikiamos 5 μM, 10 μM ir 100 μM pasirinktų junginių koncentracijomis. ND – nenustatyta.

Nei vienas iš tirtų potencialių provaistų nebuvo toksiškas kontrolinėms HCT116 ląstelėms, kai jų koncentracija buvo 5 μM ir 10 μM (išskyrus minimaliai toksiška 10 μM  $N^4$ -metil- ir  $N^4$ -propil-5-fluorcitidinų (18 ir 19) koncentracija). Mažiausios tirtų junginių koncentracijos taip pat nesukėlė toksiškumo kontrolinėms MCF7 ląstelėms, išskyrus 18 ir 41 (4-benziloksi-5-fluoruridinas). Vis dėlto, 41 reikšmingai sumažino CDA\_EH ir CDA\_Lsp turinčių HCT116 ląstelių gyvybingumą. Ryškesnis poveikis ląstelių gyvybingumui buvo pastebėtas su 4-etiltio pakeistu uridinu (9) nei su 4-metiltio grupę turinčiu junginiu (8). Ilgesnę alkilo grupę turintys 5-fluorcitidinais (20, 21, 22 ir 24) reikšmingai sumažino CDA turinčių HCT116 ir MCF7 ląstelių linijų gyvybingumą.  $N^4$ -propil-5-fluorcitidinas (19) taip pat

reikšmingai veikė CDA turinčias MCF7 ląsteles. Pažymėtina, kad **22** ir **23** junginiai efektyviau veikė žmogui optimizuotas CDA turinčiose ląstelių linijose lyginant su bakterinės CDA turinčiomis ląstelių linijomis. Vis dėlto, nepaisant kodonų optimizavimo, ląstelių gyvybingumo skirtumai po poveikio provaistais tarp CDA\_EH, CDA\_F14 arba CDA\_Lsp turinčių ląstelių linijų išliko. 4-Alkoksi-5-fluoruridiai (**27**, **30**, **31**, **32**, **34** ir **41**) reikšmingai sumažino CDA turinčių HCT116 ląstelių gyvybingumą net veikiant mažiausiomis tirtomis koncentracijomis, taip pat panašus šių junginių bei **25** junginio poveikis stebėtas ir MCF7 ląstelių linijose. Acetilintus 4-butoksi- ir 4-benziloksi-5-fluoruridinus **30** ir **40** kontrolinės ląstelės geriau toleravo esant didesnei jų koncentracijai nei deacetilintus jų analogus (atitinkamai **31** ir **41**). Vis dėlto, mažesnės **31** ir **41** koncentracijos efektyviau slopino CDA turinčių ląstelių gyvybingumą. Daug žadančių rezultatų davė ląstelių poveikis acetilintais 4-alkoksi-5-fluor-2'-deoksiuridinais (**42**, **44**, **46**, **48**). Veikiant ląsteles 5  $\mu$ M koncentracija reikšmingai sumažėjo CDA\_EH ir CDA\_Lsp turinčių MCF7 ląstelių linijų gyvybingumas, panašus 2'-deoksiuridinių **42** ir **48** poveikis pastebėtas ir HCT116 ląstelių linijose. Taip pat pastebėtas ryškus CDA turinčių ląstelių gyvybingumo sumažėjimas veikiant 100  $\mu$ M **42** ir **44** koncentracijomis, tuo tarpu kontrolinių ląstelių gyvybingumas išliko nepakitęs. Apibendrinant galima teigti, kad gauti rezultatai išryškino keletą junginių, pasižyminčių cheminiu stabilumu ir veiksmingumu mažinant CDA raišką vykdančių vėžinių ląstelių gyvybingumą, kurie gali būti naudojami fermento-provaisto strategijoje.

#### 4.3.5. CDA\_Lsp aktyvuoja $N^4/O^4$ pakeistus 5-fluorpirimidino nukleozidus U87MG žmogaus glioblastomos ląstelių linijoje

Žmogaus glioblastomos U87MG ląstelių linija buvo pasirinkta siekiant įvertinti CDA ir modifikuotų 5-fluorpirimidinų fermento-provaisto sistemos universalumą. Į U87MG ląstelių genomą buvo integruotas genas, koduojantis žmogaus kodonams optimizuotą CDA\_Lsp variantą. CDA\_Lsp biosintezė sukurtoje ląstelių linijoje buvo patvirtinta *Western blot* metodu. Toliau buvo tiriamas CDA\_Lsp gebėjimas aktyvuoti provaistus U87MG ląstelėse. Šiam tikslui buvo pasirinkti  $N^4$ -propil- ir  $N^4$ -pentil-5-fluorцитidinais (**19**, **21**) bei acetilintas 4-butoksi-5-fluoruridinas (**30**), kurie ankstesniuose eksperimentuose pasižymėjo dideliu veiksmingumu. CDA\_Lsp turinčios U87MG ląstelės 72 valandas buvo veikiamos **19**, **21** bei **30** ir ląstelių gyvybingumas buvo įvertintas MTT metodu (16 pav.).



**16 pav.** U87MG ląstelių linijos, vykdančios CDA\_Lsp koduojančio geno raišką, MTT tyrimas po poveikio  $N^4/O^4$  pakeistais 5-fluorpirimidiniais. U87MG ląstelių linija, turinti CDA\_Lsp (pažymėta U87-Lsp), ir kontrolinė ląstelių linija (pažymėta U87) 72 valandas buvo veikiamos trimis skirtingomis **19, 21 ir 30** junginių koncentracijomis (5  $\mu$ M, 10  $\mu$ M ir 100  $\mu$ M). Statistiškai reikšmingi skirtumai pažymėti  $p$  reikšmėmis: simbolis \* reiškia  $p < 0,05$ , o simbolis \*\* reiškia  $p < 0,01$ , lyginant su nepaveiktomis ląstelėmis (neigiama kontrolė (NK)).

Gauti rezultatai parodė, kad po visų tirtų provaistų poveikio CDA\_Lsp turinčių U87MG ląstelių gyvybingumas reikšmingai sumažėjo. Nors 100  $\mu$ M junginių koncentracija buvo toksiška kontrolinėms ląstelėms, ryškūs skirtumai tarp kontrolinių ir CDA\_Lsp turinčių ląstelių buvo matomi veikiant 5  $\mu$ M ir 10  $\mu$ M provaistų koncentracijoms, dėl ko nebelieka poreikio naudoti didesnes koncentracijas. Šie rezultatai patvirtina, kad CDA\_Lsp-19/21/30 fermento-provaisto sistemos yra veiksmingos mažinant U87MG vėžinių ląstelių gyvybingumą, ir pabrėžia sistemos universalumą įvairiose vėžinių ląstelių linijose.

## 5. IŠVADOS

1. Indirubino karboksirūgšties ir 2-indolinono dariniai parodė reikšmingą citotoksinį aktyvumą HCT116 ir MCF7 vėžinių ląstelių linijoms, pagrindžiantį jų potencialą tolesniam priešvėžinių vaistų kūrimui.
2. Modifikuoti 5-fluorpirimidino nukleozidai pasižymėjo minimaliu toksiškumu vėžinėms ląstelių linijoms, kas patvirtina jų, kaip provaistų, tinkamumą taikymui fermento-provaisto terapijoje.
3. Bakterinės amidohidrolazės YqfB ir D8\_RL efektyviai aktyvavo  $N^4$ -acilintų 5-fluorцитидинų pagrindu sukurtus provaistus, kas reikšmingai sumažino vėžinių ląstelių gyvybingumą ir patvirtino šių fermentų potencialą terapiniam pritaikymui.
4. Bakterinės citidino deaminazės CDA\_EH, CDA\_F14 ir CDA\_Lsp gebėjo aktyvuoti įvairius 5-fluorpirimidinų pagrindu sukurtus provaistus, iš kurių  $N^4$ -alkil-5-fluorцитидинаi ir 4-alkoksi-5-fluoruridinai pasižymėjo reikšmingu selektyviu citotoksiškumu CDA turinčioms vėžinėms ląstelėms, taip pabrėžiant šių fermentų pritaikymo galimybes tikslinėje vėžio terapijoje.

## ACKNOWLEDGEMENTS

I express my deepest gratitude to my supervisor, Prof. Dr. Rolandas Meškys, for his invaluable guidance, continuous support, and inspiring mentorship throughout this doctoral research. His expertise and encouragement have been vital in developing and completing this work.

I am sincerely grateful to all my colleagues from the Department of Molecular Microbiology and Biotechnology for their assistance with this thesis's experimental part and constant support and collaboration. Their insight and friendship have greatly enriched my research experience.

I extend my warmest thanks to my colleagues from the Department of Biological Models for their kind welcome and full assistance with the cellular experiments. Their openness and generosity have made my time in their lab productive and enjoyable.

I owe my deepest gratitude to my family. To Arnas, thank you for your constant support, patience, and understanding. To my wonderful mother, whose love, encouragement, and sacrifices have made this journey possible. And to my beloved father and grandmother, who waited even more than I did for this stage to come to an end, and who gifted me with their unconditional love, support, and trust. I hope they see me now and rejoice with me in this achievement.

## LIST OF PUBLICATIONS

This dissertation is based on the following original publications:

- Sadauskas, M., Jakutis, M., Petkevičius, V., Malikėnas, M., **Preitakaitė, V.**, Vaitekūnas, J., & Meškys, R. (2023). Biocatalytic synthesis of asymmetric water-soluble indirubin derivatives. *Dyes and Pigments*, 219, 111585. DOI: 10.1016/j.dyepig.2023.111585

Personal contributions: selected methodology and performed experiments on cancer cell lines, investigated the effect of all compounds presented in the publication on cell viability, visualised the results obtained from these experiments, and described the part of the publication related to the cellular investigations.

- **Preitakaitė, V.**, Barasa, P., Aučynaitė, A., Plakys, G., Koplūnaitė, M., Zubavičiūtė, S., & Meškys, R. (2023). Bacterial amidohydrolases and modified 5-fluorocytidine compounds: Novel enzyme-prodrug pairs. *Plos ONE*, 18(11), e0294696. DOI: 10.1371/journal.pone.0294696

Personal contributions: decided on the idea of what the publication should look like, selected the methodology and carried out most of the experiments, visualised the results and other figures, wrote the original manuscript, submitted the publication to the journal, and answered the reviewers' questions.

- **Preitakaitė, V.**, Kazlauskas, A., Aučynaitė, A., Butkutė, K., Lapinskaitė, R., Urbelienė, N., Laurynėnas, A., & Meškys, R. (2025). Bacterial cytidine deaminases as versatile activators of fluoropyrimidine nucleoside prodrugs. *European Journal of Medicinal Chemistry*, 117860. DOI: 10.1016/j.ejmech.2025.117860

Personal contributions: decided on the idea of what the publication should look like, selected the methodology and carried out most of the experiments, visualised the results and other figures, wrote the original manuscript, submitted the publication to the journal, and answered the reviewers' questions.



## PATENT APPLICATIONS AND PATENTS

- Meškys, R., Urbelienė, N., Tauraitė, D., Tiškus, M., **Preitakaitė, V.** Hydrolases and uses thereof. LT 7046.
- Meškys, R., Urbelienė, N., Tauraitė, D., Tiškus, M., **Preitakaitė, V.** Hydrolases and uses thereof. EP23168045.

## CONFERENCE PRESENTATIONS

- **Preitakaitė, V.**, Barasa, P., Koplūnaitė, M., Meškys, R. Bacterial amidohydrolases and modified 5-fluorocytidine compounds: novel enzyme-prodrug pairs. The 5th Congress of Baltic Microbiologists “CBM2023”, 11-13 October 2023, Vilnius, Lithuania (Poster).
- **Preitakaitė, V.**, Barasa, P., Koplūnaitė, M., Meškys, R. Bacterial amidohydrolases in cancer therapy: a useful tool for selective activation of prodrugs. The 47th FEBS Congress „Together in bioscience for a better future“, 8-12 July 2023, Tours, France (Poster).
- **Preitakaitė, V.**, Barasa, P., Koplūnaitė, M., Meškys, R. Bacterial amidohydrolases in cancer therapy: a useful tool for selective activation of prodrugs. The 22nd FEBS Young Scientists‘ Forum, 6-8 July 2023, Tours, France (Poster).
- **Preitakaitė, V.**, Stanislauskienė, R., Urbelienė, N., Meškys, R. Activation of modified cytidine-based prodrugs by bacterial amidohydrolases: application to gene-directed enzyme prodrug therapy. IUBMB-FEBS-PABMB 2022 Congress „The Biochemistry Global Summit“, 9-14 July 2022, Lisbon, Portugal (Poster).
- **Preitakaitė, V.**, Stanislauskienė, R., Urbelienė, N., Meškys, R. Bacterial amidohydrolases for gene-directed enzyme prodrug therapy: a potential advance in geriatric oncology. Arqus Research Focus Forum „Healthy Aging from a Multidisciplinary Perspective“, 27-29 June 2022, Vilnius, Lithuania (Poster).

- **Preitakaitė, V.,** Zubavičiūtė, S., Stanislauskienė, R., Urbelienė, N., Meškys, R. The potential of bacterial amidohydrolases as an activating enzymes in gene-directed enzyme prodrug therapy. Conference of Lithuanian Microbiological Society „Microbiology 2022“, 28-29 April 2022, Birštonas, Lithuania (Poster).
- **Preitakaitė, V.,** Stanislauskienė, R., Urbelienė, N., Meškys, R. Bacterial amidohydrolases YqfB and RL\_D8: a novel tool for gene-directed enzyme prodrug therapy. International Conference of Life Sciences „The Coins 2022“, 28 February – 3 March 2022, Virtual Conference (Poster).

## CURRICULUM VITAE

### **Viktorija PREITAKAITĖ**

---

PhD student at the Department of Molecular Microbiology and Biotechnology, Institute of Biochemistry, Life Science Centre, Vilnius University

Sauletekio ave. 7, Vilnius, Lithuania

+37069667803

viktorija.preitakaite@gmc.vu.lt

### **EDUCATION**

---

**2020–Present    PhD in Biochemistry**

Vilnius University

Construction and characterization of prodrug-activating enzymes. Supervisor Prof. dr. Rolandas Meškys

**2018–2020    MSc in Molecular Biology, *magna cum laude***

Vilnius University

Analysis of bacterial isocytosine deaminases. Supervisor dr. Agota Aučynaitė

**2014–2018    BSc in Medical and Veterinary Genetics, *cum laude***

Lithuanian University of Health Sciences

*In vitro* study of Sema3C effects on angiogenesis and generation of U87 cell line coding inducible Sema3C expression system. Supervisor dr. Arūnas Kazlauskas

### **SCIENTIFIC INTERESTS & SKILLS**

---

Enzyme-prodrug systems and their effects on cancer cells; strategies for identification and characterization of novel bacterial enzymes. Knowledge of common laboratory techniques in fields of biochemistry, genetic engineering, molecular biology, microbiology, cell technology.

## **EMPLOYMENT**

---

**October 2022–Present**

**Junior Assistant**

Laboratory work and lectures for undergraduate students: enzymology, genetic engineering, microbiology. Institute of Biochemistry, Life Sciences Center, Vilnius University.

**September 2024–Present**

**Junior Researcher**

Identification and characterisation of novel enzymes for selective activation of prodrugs. Department of Molecular Microbiology and Biotechnology, Institute of Biochemistry, Life Sciences Center, Vilnius University.

**September 2024–December2024** **Junior Researcher**

Rational design of new prodrug and enzyme pairs for gene-directed prodrug therapy. Institute of Biochemistry, Life Sciences Center, Vilnius University.

**November 2022–August 2023**

**Project Expert**

Digital guides for practical activities in biology modules developed to improve the quality of pedagogical studies. Department of Development, Vilnius University.

**February 2020–August 2023**

**Junior Researcher**

Identification and characterisation of novel enzymes for selective activation of prodrugs. Department of Molecular Microbiology and Biotechnology, Institute of Biochemistry, Life Sciences Center, Vilnius University.

## PUBLICATIONS

---

1. **Preitakaitė, V.**, Kazlauskas, A., Aučynaitė, A., Butkutė, K., Lapinskaitė, R., Urbelienė, N., Laurynėnas, A., & Meškys, R. (2025). Bacterial cytidine deaminases as versatile activators of fluoropyrimidine nucleoside prodrugs. *European Journal of Medicinal Chemistry*, 117860.
2. **Preitakaitė, V.**, Barasa, P., Aučynaitė, A., Plakys, G., Koplūnaitė, M., Zubavičiūtė, S., & Meškys, R. (2023). Bacterial amidohydrolases and modified 5-fluorocytidine compounds: Novel enzyme-prodrug pairs. *Plos ONE*, 18(11), e0294696.
3. Sadauskas, M., Jakutis, M., Petkevičius, V., Malikėnas, M., **Preitakaitė, V.**, Vaitekūnas, J., & Meškys, R. (2023). Biocatalytic synthesis of asymmetric water-soluble indirubin derivatives. *Dyes and Pigments*, 219, 111585.
4. Vidal, S., El Motiam, A., Seoane, R., **Preitakaite, V.**, Bouzaher, Y. H., Gómez-Medina, S., ... & Rivas, C. (2019). Regulation of the Ebola virus VP24 protein by SUMO. *Journal of Virology*, 94(1), 10-1128.
5. Valiulyte, I., **Preitakaite, V.**, Tamasauskas, A., & Kazlauskas, A. (2018). Importance of the putative furin recognition site 742 RNRR 745 for antiangiogenic Sema3C activity in vitro. *Brazilian Journal of Medical and Biological Research*, 51.

## PATENT APPLICATIONS AND PATENTS

---

- Meškys, R., Urbelienė, N., Tauraitė, D., Tiškus, M., **Preitakaitė, V.** Hydrolases and uses thereof. LT 7046.
- Meškys, R., Urbelienė, N., Tauraitė, D., Tiškus, M., **Preitakaitė, V.** Hydrolases and uses thereof. EP23168045.

## PROJECTS

---

1. 2024 Rational design of new prodrug and enzyme pairs for gene-directed enzyme-prodrug therapy. Research Council of Lithuania (No. S-MIP-24-114). Junior researcher.
2. 2020–2023 Selective enzymatic system for prodrug activation. Research Council of Lithuania (No. 01.2.2-LMT-K-718-03-0082). Junior researcher.
3. 2020–2023 Optimization of the network of higher education institutions and improvement of the quality of studies by merging Šiauliai University and Vilnius University. European Social Fund (No. 09.3.1-ESFA-V-738-03-0001). Project expert.

## GRANTS

---

- Federation of European Biochemical Societies awarded a grant to attend the Young Scientists' Forum 2023 (YSF 2023) in Tours, France, 6–8 July 2023.
- On 26 April 2024, the Life Sciences Center of Vilnius University awarded a nominal scholarship for excellent scientific results, active scientific, science popularizing and organizational activities.

## ORGANIZATION OF SCIENTIFIC CONGRESSES

---

1. Conference of Lithuanian Microbiological Society „Microbiology 2022“, 28-29 April 2022, Birštonas, Lithuania. Communications manager, press design specialist, abstract book layout.
2. The 5th Congress of Baltic Microbiologists “CBM2023”, 11-13 October 2023, Vilnius, Lithuania. Communications manager, press design specialist, abstract book layout.

## CONGRESSES

---

1. **Preitakaitė, V.**, Barasa, P., Koplūnaitė, M., Meškys, R. Bacterial amidohydrolases and modified 5-fluorocytidine compounds: novel enzyme-prodrug pairs. The 5th Congress of Baltic Microbiologists “CBM2023”, 11-13 October 2023, Vilnius, Lithuania (Poster).
2. **Preitakaitė, V.**, Barasa, P., Koplūnaitė, M., Meškys, R. Bacterial amidohydrolases in cancer therapy: a useful tool for selective activation of prodrugs. The 47th FEBS Congress „Together in bioscience for a better future“, 8-12 July 2023, Tours, France (Poster).
3. **Preitakaitė, V.**, Barasa, P., Koplūnaitė, M., Meškys, R. Bacterial amidohydrolases in cancer therapy: a useful tool for selective activation of prodrugs. The 22nd FEBS Young Scientists' Forum, 6-8 July 2023, Tours, France (Poster).
4. **Preitakaitė, V.**, Stanislauskienė, R., Urbelienė, N., Meškys, R. Activation of modified cytidine-based prodrugs by bacterial amidohydrolases: application to gene-directed enzyme prodrug therapy. IUBMB-FEBS-PABMB 2022 Congress „The Biochemistry Global Summit“, 9-14 July 2022, Lisbon, Portugal (Poster).
5. **Preitakaitė, V.**, Stanislauskienė, R., Urbelienė, N., Meškys, R. Bacterial amidohydrolases for gene-directed enzyme prodrug therapy: a potential advance in geriatric oncology. Arqus Research Focus Forum „Healthy Aging from a Multidisciplinary Perspective“, 27-29 June 2022, Vilnius, Lithuania (Poster).

6. **Preitakaitė, V.**, Zubavičiūtė, S., Stanislauskienė, R., Urbelienė, N., Meškys, R. The potential of bacterial amidohydrolases as an activating enzymes in gene-directed enzyme prodrug therapy. Conference of Lithuanian Microbiological Society „Microbiology 2022“, 28-29 April 2022, Birštonas, Lithuania (Poster).
7. **Preitakaitė, V.**, Stanislauskienė, R., Urbelienė, N., Meškys, R. Bacterial amidohydrolases YqfB and RL\_D8: a novel tool for gene-directed enzyme prodrug therapy. International Conference of Life Sciences „The Coins 2022“, 28 February – 3 March 2022, Virtual Conference (Poster).
8. Valiulytė, I., **Preitakaitė, V.**, Steponaitis, G., Kazlauskas, A. The Role of Sema3C and R745A mutant on cell motility and microcapillary formation. XVth International Conference of the Lithuanian Biochemical Society, 26-29 June 2018, Dubingiai, Lithuania (Poster).
9. Valiulytė, I., Kazlauskas, A., **Preitakaitė, V.**, Steponaitis, G., Marčiulionytė, A. An in vitro study of Sema3C effects on microcapillary formation and cell motility. 1st International doctoral students' conference “Science for Health”, 13 April 2018, Kaunas, Lithuania (Poster).
10. Valiulyte, I., **Preitakaite, V.**, Steponaitis, G., Marciulionyte, A., Tamasauskas, A., Kazlauskas, A. The Role of Sema3c Protein in vitro Angiogenesis. 9th International Conference of Lithuanian Neuroscience Association „Neurodiversity: From Theory to Clinics“, 1 December 2017, Kaunas, Lithuania (Poster).

## **INTERNSHIPS**

**February 2018–May 2018**

**Center for Research in Molecular Medicine and Chronic Diseases (CiMUS), Santiago de Compostela, Spain**

Investigating mechanism by which Ebola virus exploits the ubiquitin and SUMO pathways.

**August 2017–September 2017**

**UAB “Aconitum”**

Investigating process of manufacturing pharmaceutical agents.

<b>September 2016– December 2016</b>	<b>Laboratory of Neurooncology and Genetics, Neuroscience Institute, Lithuanian University of Health Sciences</b>  Performing cell transfection and generation of stable selects, molecular cloning and protein detection using Western blot analysis.
<b>August 2016–September 2016</b>	<b>The Hospital of Lithuanian University of Health Sciences Kauno klinikos, Clinic of Laboratory Medicine</b>  Performing a complete blood count (CBC), blood chemistry tests, platelet aggregation test.
<b>August 2016–September 2016</b>	<b>The Hospital of Lithuanian University of Health Sciences Kauno klinikos, Clinic of Genetics and Molecular Medicine</b>  Performing DNA extraction, RNA extraction, PCR, RT-PCR.

## **MEMBERSHIPS**

- 2022–Present** Member of Lithuanian Biochemical Society.
- 2022–Present** Member of Lithuanian Microbiological Society.

## **MENTORSHIPS**

- 2020–2021** Supervising undergraduate student Augustas Šeporaitis. Bachelor thesis topic – Construction and characterisation of vectors encoding bifunctional deaminases.
- 2023–2025** Supervising undergraduate student Kamilė Dzisevič. Bachelor thesis topic – Optimisation of YqfB amidohydrolase for targeted enzyme-prodrug therapy.



## NOTES

## NOTES

## NOTES

Vilniaus universiteto leidykla  
Saulėtekio al. 9, III rūmai, LT-10222 Vilnius  
El. p. [info@leidykla.vu.lt](mailto:info@leidykla.vu.lt), [www.leidykla.vu.lt](http://www.leidykla.vu.lt)  
[bookshop.vu.lt](http://bookshop.vu.lt), [journals.vu.lt](http://journals.vu.lt)  
Tiražas 15 egz.